UNIVERSITE DES SCIENCES ET TECHNIQUES DE LILLE (LILLE I)
U.F.R. DES SCIENCES DE LA TERRE

THESE

pour obtenir le grade de

DOCTEUR DE L'UNIVERSITE DE LILLE I

Discipline: Géologie marine, Paléocéanographie

Présentée et soutenue publiquement

Par

Hélène JACOT DES COMBES

Le 18 décembre 1998

Reconstruction des variations paléocéanographiques et de la paléoproductivité dans l'Océan Indien du nord-ouest durant les 300 000 dernières années : la réponse géochimique comparée à l'enregistrement biologique

Directeur de Thèse : Nicolas Tribovillard

JURY

M. Hervé CHAMLEY,	**Président**
Mme Liselotte DIESTER-HAASS,	**Rapporteur**
M. Philippe BERTRAND,	**Rapporteur**
M. Nicolas TRIBOVILLARD,	**Directeur de Thèse**
Mme Anne-Marie KARPOFF,	**Examinateur**
M. Jean Pierre CAULET,	**Examinateur**

AVANT-PROPOS

Je suis très reconnaissante à Monsieur le professeur Hervé Chamley, directeur du Laboratoire de sédimentologie et géodynamique de l'université de Lille de faire partie de mon jury de thèse.

Je remercie vivement d'avoir accepté d'être rapporteurs de cette thèse

* Madame le professeur Liselotte Diester-Haass. Ses remarques m'ont été très utiles pour améliorer ce manuscrit.

* Monsieur le professeur Philippe Bertrand. Les discussions scientifiques que j'ai pu avoir avec lui lors de nos différentes rencontres ont toujours été très constructives.

Je remercie Madame Anne-Marie Karpoff d'avoir accepté de juger ce travail.

Je suis extrêmement reconnaissante

- envers Jean Pierre Caulet pour m'avoir soutenu et encadré durant ces trois années de thèse. Par ses encouragements, ses conseils, sa disponibilité, pour les discussions paléocéanographiques que nous avons eues ensemble, en un mot par sa participation active à l'élaboration de cette thèse, en particulier durant la dernière année, il peut en être considéré comme le co-directeur. De plus, je n'oublie pas qu'il m'a permis d'effectuer ma première mission océanographique à bord du *Marion-Dufresne* en 1997, me permettant ainsi de réaliser un rêve ancien. Pour cela, toute ma gratitude lui est acquise.

- envers Nicolas Tribovillard qui a bien voulu diriger cette thèse. Sa gentillesse et sa patience, en particulier au début de ces travaux m'ont permis de me familiariser avec la géochimie sédimentaire, domaine qui m'était quasiment inconnu auparavant. Il m'a été d'un grand soutien lors des périodes difficiles pendant lesquelles les analyses chimiques n'étaient plus faisables au laboratoire d'Orsay. Il a également fait en sorte que ce travail se déroule bien et ne subisse pas de retard lorsqu'il a quitté Orsay pour être nommé professeur à l'Université de Lille.

Travailler durant ces trois années en totale collaboration avec Nicolas Tribovillard et Jean Pierre Caulet fut pour moi une véritable chance. Leurs champs de compétences différents mais complémentaires m'ont permis d'avoir une vision très large de la géologie marine (géochimie et minéralogie avec Nicolas Tribovillard, paléontologie et paléocéanographie avec Jean Pierre Caulet). Ce large éventail de connaissances, de concepts et de méthodes a rendu ce travail de recherche passionnant. Dernier point que je veux souligner, les relations humaines instaurées avec Nicolas et Jean Pierre durant ces trois années ont été excellentes et enrichissantes. Nous n'étions pas toujours d'accord sur tout, en particulier sur le thé, mais des goûts musicaux et littéraires communs nous ont permis d'établir des échanges de livres et de CD très agréables et toujours enrichissants.

Cette thèse présente la particularité de s'être déroulée dans trois laboratoires différents : le laboratoire de Géologie du Muséum National d'Histoire Naturelle à Paris, le laboratoire de Géochimie des roches sédimentaires à Orsay, et le laboratoire de Sédimentologie et Géodynamique à Lille. Mon accueil dans ces trois structures a toujours été excellent et je tiens à remercier tous les membres de ces laboratoires.

Au Muséum, mes remerciements vont tout d'abord à Monsieur le professeur Patrick De Wever, directeur du laboratoire de géologie, qui m'a autorisé à terminer ma thèse dans ses locaux

alors que je dépendais d'une autre unité. Sa convivialité, sa bonne humeur, son dynamisme ont été très motivants et très agréables.

Je remercie également Monsieur le professeur Alain Foucault qui m'a encadré durant mon stage de DEA lors de mon arrivée au laboratoire. Ce stage a ainsi été l'occasion de faire connaissance avec les membres du laboratoire, principalement Madame Denise Trauth-Badaut, Messieurs Pierre-Jean Giannesini et Pierre Clément avec lesquels j'ai étroitement travaillé et qui m'ont enseigné les méthodes de recherche sur les carottes sédimentaires. Leur patience et leurs conseils furent précieux et les relations qu'ils ont établies avec moi chaleureuses.

Durant ma thèse, Maurice Tamby m'a été d'une grande aide en m'apprenant à préparer les lames pour l'observation et le comptage des radiolaires. Sa compétence et sa gentillesse ont été très agréables, de plus je garde un souvenir ému des plats indiens qu'il préparait parfois. Le dynamisme de Marie-Madeleine Blanc-Valleron, sa disponibilité, ainsi que ses connaissances géologiques ont constitué un apport important tant au cours du DEA que de la thèse. Je tiens également à remercier Michelle Destarac pour ses conseils avisés lors de la préparation des posters et des transparents pour les congrès. Sa bonne humeur et sa gentillesse sont réconfortantes.

Je remercie également les autres membres du laboratoire : Jean-Marie Rouchy, Frédéric Mélières, François Frölich, Simone Servant, Emmanuelle Vennin, Annie Maurs, Annie Cornée, Agathe Cambreleng, Michèle Baconat, Anne Marie Brunet et Maud Pallas, toujours disposés à rendre service ou à répondre à mes questions, avec lesquels les relations bien que moins étroites furent toujours très agréables.

Je remercie :

Nicole Moureau et Seng Phetman, du laboratoire de Géochimie sédimentaire d'Orsay pour leur collaboration lors de la préparation et de l'analyse des échantillons par ICP, et des analyses en diffraction X,

Olivier Dufaure pour son aide lors de la préparation de pastilles pour la microscopie électronique,

Pierre Tremblay pour sa disponibilité à venir régler tous les petits problèmes qui se sont posés en informatique et en électronique,

Philippe Pradel pour son aide technique et pour les discussions non scientifiques que nous avons eues ensemble, ainsi que pour sa tentative, infructueuse, de m'apprendre à jouer au Go,

Roberte Coquelle a toujours été là pour m'aider à résoudre les questions administratives, je lui en suis reconnaissante.

Je remercie également Monsieur le professeur Michel Steinberg, qui m'a chaleureusement accueillie au laboratoire, et tous les membres du laboratoire : Fabienne Orzag, Alain Desprairies, Pierre Massard, Alain Perruchot, et Marc Rivière, qui étaient toujours prêts à partager leurs connaissances scientifiques.

Mes remerciements vont aussi à tous les membres du laboratoire de Sédimentologie et Géodynamique de Lille, en particulier Jean-François Deconinck et Alain Trentesaux, avec qui mes rencontres furent épisodiques, mais toujours chaleureuses.

Ce travail de thèse m'a également permis de travailler avec Catherine Pierre et Jean-François Salièges du LODYC pour toutes les datations isotopiques. Leurs connaissances en ce domaine, et leurs conseils ont été d'une aide inestimable lors de ces travaux. Le dosage de la matière organique dans mes échantillons a été réalisé au laboratoire de Stratigraphie de

l'Université de Paris VI (Jussieu) en collaboration avec François Baudin, qui s'est montré patient, chaleureux et peu avare de son temps lors de nos discussions, qu'il en soit remercié.

Les deux missions océanographiques que j'ai effectuées sur le *Marion-Dufresne* ont été l'occasion de rencontrer d'autres paléocéanographes avertis, avec lesquels les échanges ont été à la fois scientifiquement stimulants et humainement chaleureux. Je remercie tout particulièrement Luc Beaufort, du CEREGE, qui m'a permis d'embarquer pour ma seconde mission, Franck Bassinot et Jean-Pierre Peypouquet pour les discussions scientifiques que nous avons eus ainsi que pour leur gentillesse et leur humour. Sophie Bieda, Nicole Page, Michel Decobert, Laurent Londeix et Jean-Claude Relexans ont été des compagnons de quart formidables, dans les périodes de travail intense comme dans les moments plus calmes où leur bonne humeur faisait merveille. Je n'oublie pas les autres scientifiques du bord, et les étudiants avec lesquels j'ai passé des moments mémorables, ainsi que les officiers et membres d'équipage du *Marion-Dufresne* toujours à l'écoute. Ils ont tous fait de ces missions des périodes inoubliables.

Toutes ces missions n'auraient pas pu être réalisées sans le soutien logistique et financier de l'IFRTP, affreteur du *Marion-Dufresne*. La communauté paléocéanographique possède en ce navire un outil formidable pour la récolte d'échantillons. Tous les échantillons étudiés durant cette thèse proviennent de carottes prélevées sur le *Marion-Dufresne*. Je suis donc très reconnaissante à cet organisme et en particulier à Yvon Balut pour leur aide et leur soutien.

Cet avant-propos serait incomplet si je n'évoquais pas les autres étudiants rencontrés durant ces trois années de thèse. Les bons moments passés avec les amis (es) Emmanuelle Lambert au Muséum, Sylvie Ogier, Séverine Penon, Jessica Vizinet, Marianne Rihoual, Jérôme Lombardi, Thierry Mongenot, Lionel Moutier et Hyacinthe Tongban à Orsay ont été riches en plaisanteries et autres bavardages non scientifiques, mais aussi en encouragements, échanges de vues et d'informations. Je leur suis très reconnaissante à tous.

Je terminerais cet avant–propos en remerciant ma famille, et plus particulièrement mes parents, pour leur soutien sans faille pendant toutes ces années. Ils m'ont toujours encouragée et aidée de leur mieux, je leur dois énormément.

TABLES DES MATIÈRES

Reconstruction des variations paléocéanographiques et de la paléoproductivité dans l'Océan Indien du nord-ouest durant les 300 000 dernières années : la réponse géochimique comparée à l'enregistrement biologique.

INTRODUCTION GENERALE

Problématique

L'existence de faibles teneurs atmosphériques en CO_2 lors du dernier maximum glaciaire (environ un tiers plus basses qu'au cours de l'Holocène) constitue l'une des découvertes les plus stimulantes faites ces dernières années (Delmas et al., 1980; Barnola et al., 1987). L'amplitude et la rapidité des variations de ces teneurs, qui ont accompagné les altérations thermiques de la dernière déglaciation, suggèrent que les variations de la composition chimique des océans sont le principal facteur de ces changements. L'océan mondial contient, en effet, 60 fois plus de carbone que l'atmosphère et toute modification mineure de sa chimie peut provoquer des variations importantes dans la composition du réservoir atmosphérique avec lequel il communique. Il apparaît ainsi comme un réservoir et un régulateur dans le cycle du CO_2 à l'échelle globale (Tans et al., 1990; Siegenthaler et Sarmiento, 1993). C'est par les fluctuations de la productivité que l'océan semble reguler le plus facilement sa composition chimique (Broecker et Peng, 1986). La photosynthèse, suivie d'un export vers le fond de matière organique à partir de la zone euphotique, agit comme une "pompe biologique" qui diminue la pression partielle de CO_2 dans les eaux de surface. La majorité des eaux chaudes oligotrophiques de surface sont ainsi pauvres en CO_2 tandis que les valeurs les plus élevées sont mesurées dans les zones eutrophiques relativement restreintes aux upwellings ou aux aires présentant une couche de mélange profonde (Walsh et al., 1985; Martin et al., 1987; Wollast, 1991).

La nécessité de comprendre les relations entre la productivité, la chimie de l'océan, le cycle du carbone et les variations du climat, s'est accrue depuis que la Terre est entrée dans une période de réchauffement qui serait liée à l'accroissement des émissions de gaz à effet de serre (Jones et al., 1987). Le plus sûr moyen de comprendre les variations du système serait de savoir comment fonctionne la pompe biologique. Mais les biologistes sont loin d'être d'accord sur la question et, dans le contexte actuel, les reconstitutions paléocéanographiques qui intègrent une information climatique à plus grande échelle permettent de mieux comprendre les résultats du fonctionnement de cette pompe biologique en mettant en valeur ses caractéristiques principales (Berger et al., 1989). La reconstruction des variations paléocéanographiques, particulièrement de la paléoproductivité, dans les zones océaniques à

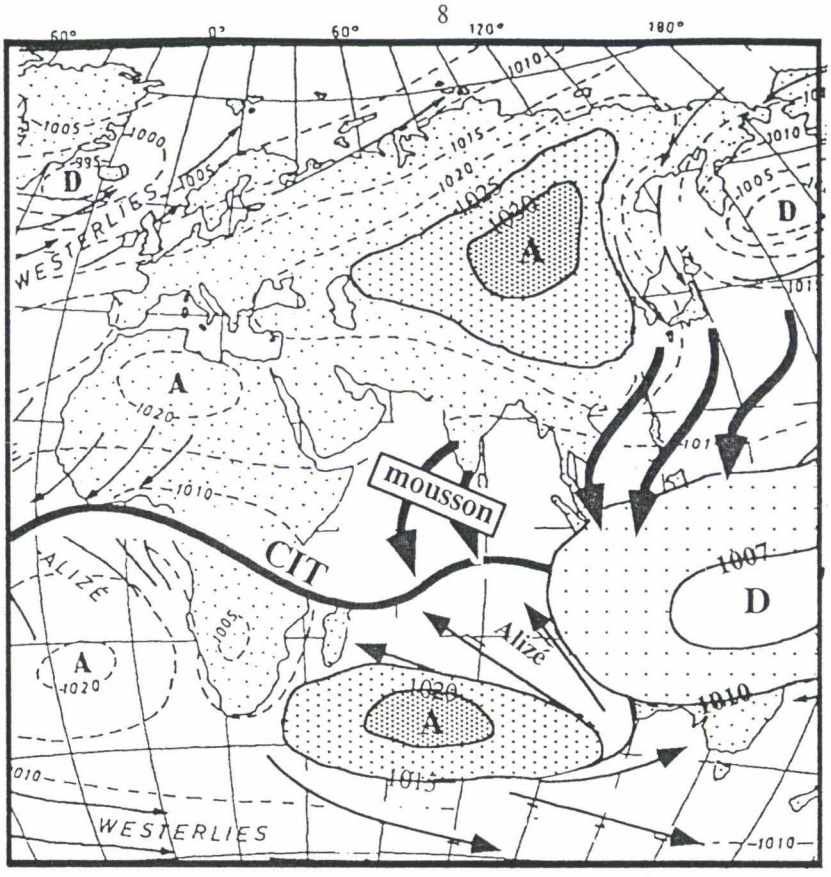

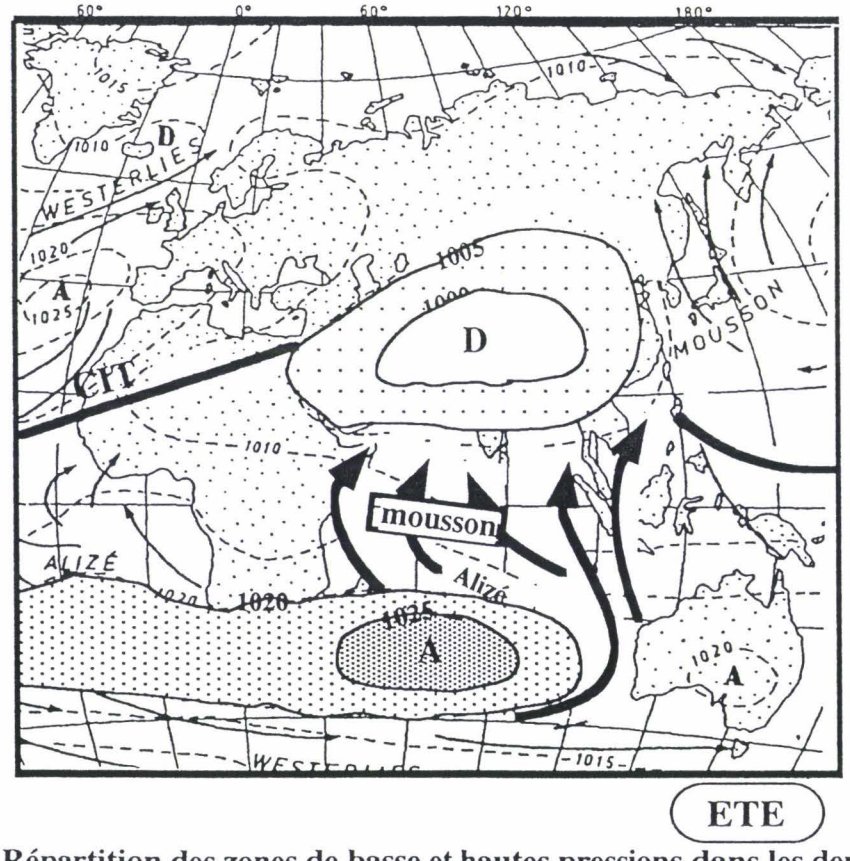

Figure 1: Répartition des zones de basse et hautes pressions dans les deux hémisphères.

CIT = zone de convergence intertropicale.
(D'après Estienne et Godard, 1970 et Pedelaborde, 1958).

forte productivité actuelle, et les relations avec les grands changements climatiques, sont donc devenues un des principaux objectifs de recherche dans le domaine de la géologie marine. Les résultats obtenus permettent de décrire des "scénarios d'évolution climatique" utiles pour tester les prévisions fournies par les grands modèles climatiques mis en place aujourd'hui.

La principale difficulté des reconstructions paléocéanographiques réside dans l'utilisation de nouveaux concepts et de nouveaux outils permettant de déchiffrer le message sédimentaire qui constitue la seule mémoire disponible des variations chimiques de l'océan (Berger et al., 1989; Berger et Herguera, 1992). Les outils mis en œuvre sont à la fois de nature "directe", tels que la teneur en carbone organique total (COT), ou "indirecte", tels que la composition des associations de microfossiles ou de certains éléments chimiques. Le contenu en matière organique du sédiment et sa composition sont généralement considérés comme de bons indicateurs de la production de surface (Romankevitch, 1984; Pedersen et Calvert, 1990; Calvert and Pedersen, 1992). Ils présentent toutefois l'inconvénient d'être très sensibles à la dégradation dans la colonne d'eau puis au sein même du sédiment. Le message porté par la matière organique peut donc être perturbé par un certain nombre de processus majoritairement liés à la diagenèse et un débat existe toujours pour déterminer si l'accumulation de COT dans le sédiment est contrôlée par la production ou par la préservation (Pedersen et Calvert, 1990; Demaison; 1991; Calvert et Pedersen, 1992; Bertrand et Lallier-Vergès, 1993). Un autre moyen d'estimer la paléoproductivité est l'analyse de marqueurs "indirects" tels que les microfossiles, soit par l'intermédiaire de fonctions de transfert à partir de bases de données actuelles sur la distribution et l'abondance des espèces planctoniques en fonction de la productivité (Pujos, 1992; Sarnthein et al., 1992), soit par des analyses statistiques portant sur des associations à caractéristiques écologiques connues (Prell, 1984; Caulet et al., 1992; Vénec-Peyré et al., 1995). Les marqueurs géochimiques sont aussi des marqueurs indirects de la paléoproductivité. Certains métaux, comme le phosphore et le baryum, sont en effet connus pour être liés à la matière organique et les variations de leur teneur dans le sédiment peuvent donc refléter les variations de la paléoproductivité (Shimmield et Mowbray, 1991; Dymond et al., 1992; Shimmield, 1992; Gingele et Dahmke, 1994; Shimmield et al., 1994; Francois et al., 1995; Paytan et Kastner, 1996). Par ailleurs, les différents métaux peuvent être représentés par des formes minéralogiques sensibles aux modifications diagénétiques induites par les conditions chimiques lors du dépôt et dans le

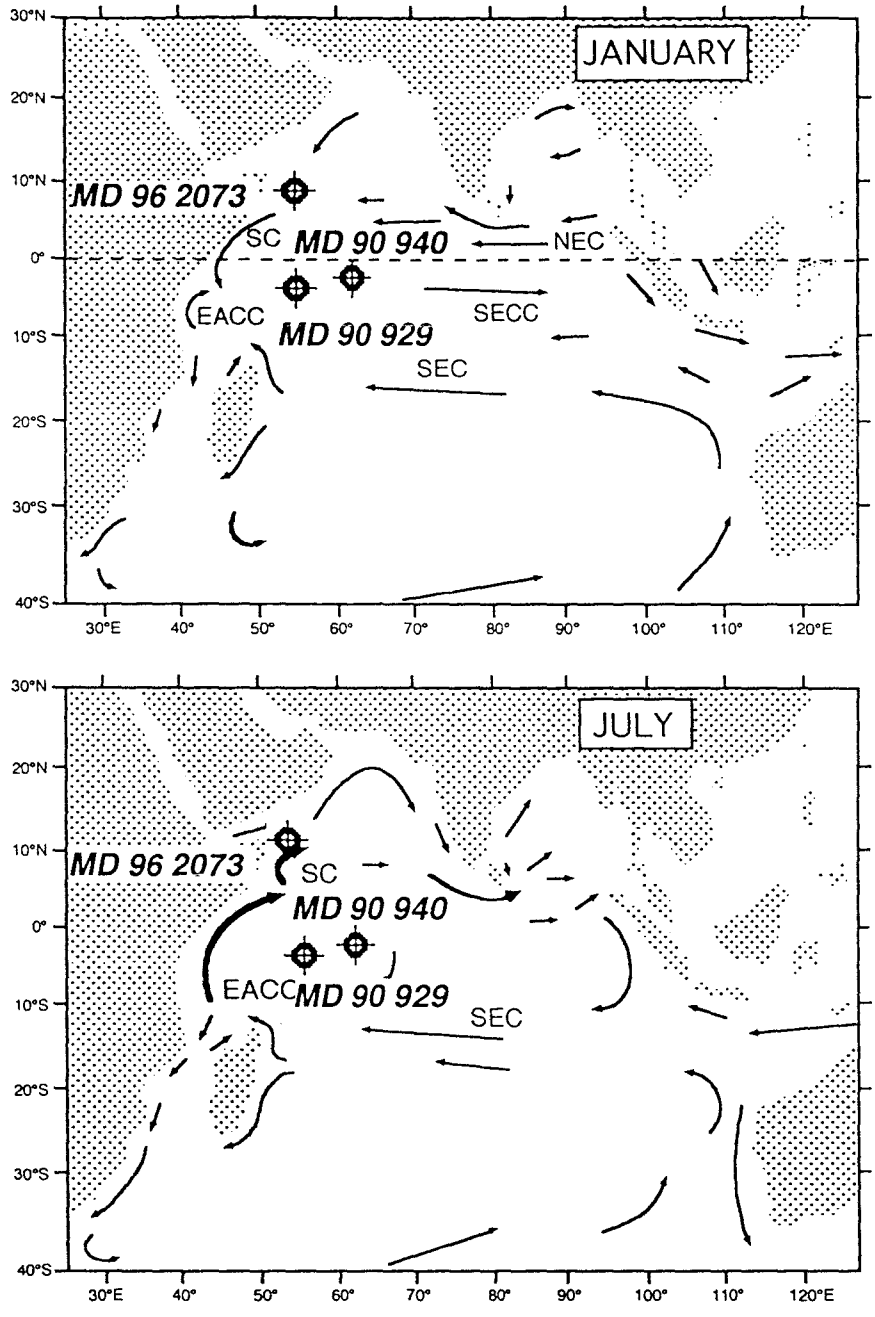

Figure 2. Localisation des Carottes analysées et Courants marins
(Carte des courants d'après Yasuda et al. 1990 et Vanney, 1991)

NEC: courant nord équatorial
SEC: courant sud-équatorial
SECC: contre-courant équatorial
SC: courant de Somalie
EACC: contre-courant est-africain
(Abréviations en anglais).

sédiment et sont donc susceptibles de représenter les variations de ces conditions plutôt que celles de la productivité (Van Os et al., 1991; Thomson et al., 1993; 1995; De Lange et al., 1994; Van Santvoort et al. 1996). Le baryum offre un bon exemple de ce type de comportement. De nombreuses études ont montré que l'enrichissement du sédiment en baryum, en particulier lorsque ce baryum est présent sous forme de barytine, peut correspondre à une augmentation de la production de surface, spécialement à partir du plancton siliceux (diatomées et radiolaires) (Dehairs et al., 1980, 1987, 1991; Bishop, 1988). Mais la barytine peut toutefois avoir une origine hydrothermale (Dymond et al., 1992), et le baryum peut également être présent dans le sédiment sous d'autres formes : incorporé dans les feldspaths (Shimmield et al., 1994; Shimmield et Jahnke, 1995), sous forme de carbonate de baryum (Boyle, 1981; Lea et Boyle, 1989; Lea et Spero, 1994), et/ou incorporés aux oxy-hydroxydes de manganèse et de fer (Van Santvoort et al., 1996). Toutes les études montrent qu'en fait aucun des différents marqueurs, directs ou indirects, est totalement représentatif des variations de la paléoproductivité ou des conditions paléocéanographiques, c'est-à-dire reflétant uniquement les variables souhaitées. La validité des marqueurs est également modifiée selon les domaines géographiques considérés. Certaines espèces de foraminifères sont ainsi caractéristiques de conditions d'upwelling dans l'océan Pacifique mais indicatives de productivité semi-profonde dans l'océan Indien (Vergnaud Grazzini et al., 1995). La nécessité d'études combinant l'utilisation simultanée et l'intercomparaison de plusieurs marqueurs est récemment apparue comme un palliatif aux problèmes rencontrés, de même que la comparaison (quand c'est possible) des données nouvellement obtenues avec celles déjà publiées (Peterson et al., 1995).

C'est dans cette perspective qu'a été conçu et réalisé ce travail de thèse sur la reconstruction des variations paléocéanographiques et de la paléoproductivité dans la partie équatoriale de l'océan Indien du NW au cours des derniers 300 000 ans. La démarche consiste d'abord à reconstituer pour chaque période climatique (stade isotopique) et site géographique les conditions à l'interface eau/sédiment, l'apport terrigène continental, les caractéristiques des masses d'eaux locales et la productivité. Pour aboutir à cette première reconstruction partielle, une combinaison d'outils géochimiques permet de définir une signature géochimique globale qui est ensuite interprétée et comparée aux données résultant de l'analyse statistique de marqueurs biologiques, tels que les foraminifères et les radiolaires. L'intégration des résultats site par site conduit finalement à une synthèse des variations paléocéanographiques

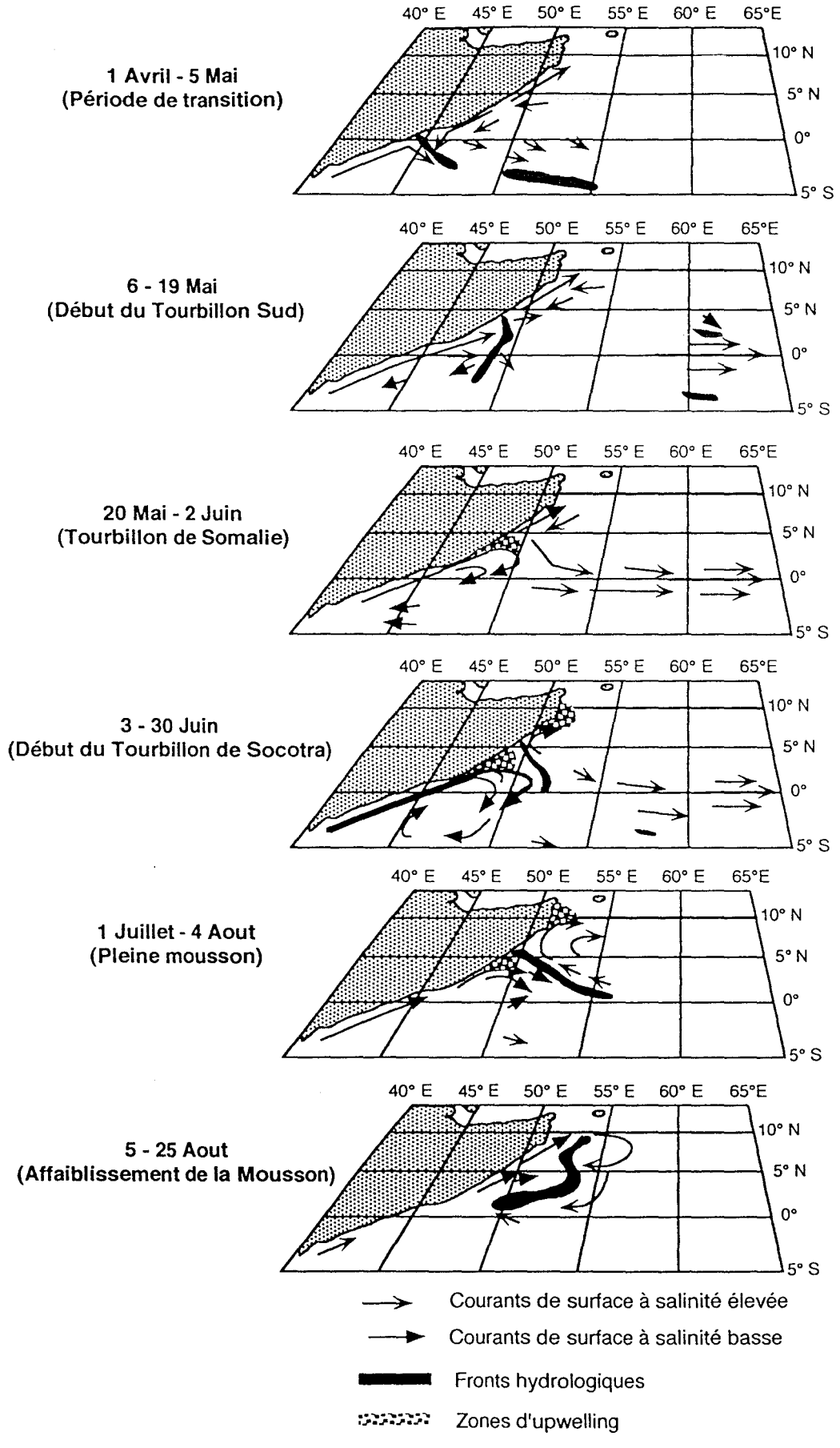

Figure 3 : Courant de Somalie,
Evolution de la circulation de surface en 1979
(d'après M. Fieux, 1987)

intervenues dans chacune des zones étudiées. L'ensemble des résultats doit permettre de répondre aux principales interrogations posées par:

- la pertinence et la fiabilité des marqueurs utilisés ;
- l'existence, la durée et l'extension des apports continentaux résultant de l'érosion ;
- les conditions de dépôt ;
- la réponse hydrologique de l'océan Indien du NW aux grandes variations climatiques ;
- les variations d'intensité de la paléoproductivité dans la ceinture équatoriale et sous les zones à upwelling au cours des 4 derniers cycles climatiques.

Cadre et présentation générale

Cadre géographique et océanographique.

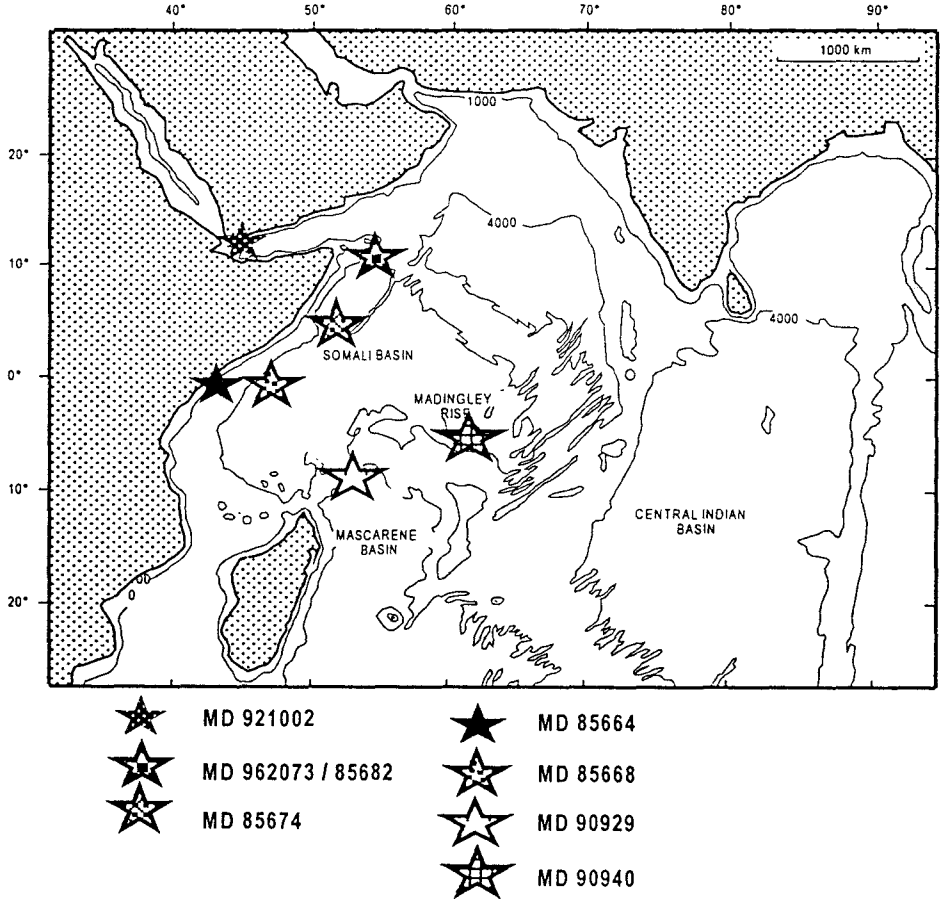

Figure 4 : Localisation des sites étudiés lors de ce travail.
La bathymetrie de l'Océan Indien est indiquée en m.

Le domaine étudié englobe l'océan Indien occidental, surtout représenté par le bassin de Somalie et la ceinture équatoriale voisine, de 6°S à 11°N et de 45° à 60° E. Cette région a été choisie comme zone d'étude parce que s'y trouvent juxtaposés des systèmes hydrologiques caractérisés par des productivités variables, mais significatives : upwellings océaniques et côtiers, milieux pélagiques avec ou sans apports terrigènes...

Cette région de l'océan Indien a pour caractéristique particulière d'être soumise à une alternance climatique et hydrologique saisonnière très marquée du fait de sa localisation dans la zone d'action de la mousson indienne. D'une façon générale, la mousson est un système de vents dont le sens s'inverse selon les saisons et qui affecte les basses couches de l'atmosphère dans certaines régions intertropicales.Ce système se met en place en réponse à un fort gradient de pression atmosphérique entre les deux hémisphères (fig. 1). Dans le cas de la mousson indienne, le moteur est la différence de pression existant entre l'océan Indien et le continent asiatique (résumé in : Clemens et al., 1991). Durant l'été boréal, le continent asiatique se réchauffe plus vite que l'océan et des cellules de basse pression s'y développent. Un flux d'air maritime venant des anticyclones de l'océan Indien et de l'océan Pacifique occidental va s'écouler sur le continent, ce qui provoque de fortes précipitations sur l'Inde et le sud de la Chine. On parle alors de mousson du sud-ouest. Pendant l'hiver boréal, la situation atmosphérique s'inverse avec une circulation d'air des hautes pressions situées sur le continent vers les basses pressions localisées sur l'océan et on parle de mousson du nord-est (résumé in : Sirocko, 1991).

Une telle modification du régime des vents a des implications profondes sur la circulation des eaux de surface, qui est fortement liée à la circulation atmosphérique. Entre les deux saisons de la mousson, on observe un renversement des courants de surface. Durant l'été boréal, la partie nord de l'océan Indien est sous l'influence de la mousson du sud-ouest (Yasuda et al., 1990; Vanney, 1991). Les vents soufflant depuis le sud-ouest induisent un grand mouvement de dérive vers l'est, appelé le courant de mousson. Au large de Sumatra, ce courant prend une direction sud à sud-est et rejoint le courant sud équatorial (SEC), qui s'écoule vers l'ouest entre 8°S et 20°S et qui est très intense en cette saison (fig. 2). Pendant l'hiver boréal, les eaux de surface forment, dans la partie nord de l'océan indien une dérive vers l'ouest, appelée courant nord équatorial (NEC), depuis Sumatra jusqu'à la côte africaine, qu'elle longe vers le sud pour ensuite alimenter le contre-courant équatorial (ECC). Ce contre-courant s'affaiblit à mesure qu'il progresse vers l'est et se scinde en deux branches. La plus

importante va rejoindre au sud le courant sud équatorial, et la seconde va fusionner avec le courant nord équatorial (Tchernia, 1978). Au sud de l'équateur, le courant sud équatorial entraîne les eaux depuis la côte occidentale de l'Australie jusqu'à la côte de Madagascar où il se sépare en deux branches, l'une partant vers le nord, et la seconde rejoignant au sud le courant des Aiguilles.

Pendant la période de transition entre les deux saisons de la mousson, les eaux sont entraînées vers l'est le long de l'équateur et forment le jet de Wyrtki (Leetma et al., 1980). Un des aspects les plus marquants de cette alternance entre mousson du sud-ouest et mousson du nord-est est la mise en place d'un système d'upwelling durant l'été boréal en relation avec le courant de Somalie (fig. 3). Pendant l'hiver boréal, ce courant suit la côte africaine du nord vers le sud depuis l'hémisphère nord jusqu'à 6°S. Pendant l'été boréal, ce courant change de sens et longe la côte africaine vers le nord (Swallow, 1980). Il se sépare alors en deux branches : la branche sud va tourner vers l'est et former un tourbillon à 4°N (tourbillon de Somalie) tandis que la branche nord continue le long de la côte pour former une autre boucle centrée vers 8°N (tourbillon de Socotra) (Swallow et Bruce, 1966; Philander et Delecluse, 1983; Currie, 1992). Les bordures nord des deux tourbillons engendrent des zones d'upwelling intense. A l'automne, ces deux boucles fusionnent pour ne plus former qu'un seul tourbillon (Bruce et Beatty, 1985).

La situation particulière de l'océan Indien, fermé au nord par la péninsule arabique et le sous-continent indien, va induire une circulation particulière des eaux intermédiaires et de fond. L'eau de fond entre dans le bassin de Somalie par le passage des Amirantes, qui est la seule communication du bassin située à plus de 4000 m de profondeur. Cette eau de fond, relativement peu salée et riche en oxygène s'écoule le long de la pente continentale africaine entre 2500 m de profondeur et le fond (Warren, 1981; Warren et al., 1966; 1974). A une profondeur intermédiaire sur cette même pente (750-2000 m), une eau plus chaude, plus salée et plus pauvre en oxygène s'écoule vers le sud-ouest (Warren et al., 1966). Cette eau, dite de la mer Rouge, résulte d'un mélange entre des masses d'eaux venues de la mer Rouge et de la mer d'Arabie (Tchernia, 1978). L'étagement de faciès sédimentaires réduits dans des sédiments quaternaires provenant de différents niveaux de la pente continentale africaine montre que l'individualisation de cette eau de la mer Rouge serait intervenue il y a moins de 800 000 ans et que sa profondeur aurait varié dans le temps, avec une remontée rapide dans les derniers 400 000 ans (Caulet et al., 1988).

Les sédiments analysés.

Les sédiments ramenés par les missions "MD 44-INDUSOM", "MD 65-SEYMAMA" et "MD104-PEGASOM" du Marion-Dufresne donnent, malgré un maillage relativement faible, une bonne idée de la sédimentation quaternaire dans le bassin de Somalie et ses abords immédiats (Caulet, et al., 1987; Bassinot, 1993; Giannesini et al., en prép.). Les principales caractéristiques lithologiques et les vitesses d'accumulation de ces sédiments peuvent être ainsi résumées :

Sur la pente continentale est-africaine, les sédiments rencontrés de 880 à 1 000 m de fond sont généralement des sables et des boues carbonatées à foraminifères (30 à 70%) avec des débris détritiques grossiers (20 à 40 %). De nombreuses passées de sables granoclassés, des fragments de calcaires bioclastiques et des niveaux riches en glauconie témoignent d'apports turbides en milieu agité et de remaniements intenses. Les taux de sédimentation demeurent très faibles (en moyenne : 1,6 cm/1 000 ans pour le Pléistocène).

De 2 000 à 2 600 m, la pente du talus est-africain est très forte avec de nombreux ravinements. Les sédiments sont des boues calcaires à coccolithes (25 à 50%), riches en foraminifères (10 à 20%). Les débris biosiliceux (jusqu'à 10%), de même que les foraminifères, sont beaucoup plus abondants dans les sédiments situés sous les deux tourbillons de Somalie et Socotra. Les vitesses de sédimentation sont plus fortes (en moyenne : 2 à 4 cm/1000 ans) pour le Pléistocène supérieur. Des niveaux "réduits" plus riches en pyrite et débris organiques non dégradés se situent dans les sédiments Pléistocène moyen-supérieur de la zone équatoriale.

De 3 000 à 4 000 m, la pente continentale est interrompue par plusieurs ressauts qui se prolongent vers la plaine abyssale par des talus raides. La couverture est constituée de boues calcaires à coccolithes, mais avec une plus forte proportion de diatomées et moins de 5% de débris détritiques, sauf dans quelques passées turbides (surtout sous l'Equateur). Le Pléistocène supérieur est bien développé (3,5 à 5 cm/1 000 ans). Le Pléistocène moyen et inférieur sont en revanche très condensés (moins de 1 cm/1 000 ans).

Les grands fonds du bassin de Somalie sont tapissés de boues carbonatées à coccolithes, qui prolongent au delà de 4 500 m les dépôts de bas de pente du précontinent africain. L'existence de ces boues carbonatées profondes résulte à la fois d'une productivité de surface intense dans les zones à upwelling proches, ainsi qu'au niveau de la ceinture de productivité

équatoriale, et d'apports turbides en provenance de la pente continentale est-africaine (Leclaire, 1974).

Les reliefs mous profonds (3 000 à 4 000 m) de la ride de Madingley et du bassin des Amirantes, respectivement au nord des Seychelles et au sud des Seychelles, sont recouverts de boues calcaires à coccolithes, relativement riches en débris biosiliceux. Les vitesses de sédimentation estimées sont beaucoup plus faibles, de l'ordre de 2 à 4 cm/1000 ans).

Pour les besoins de cette étude, trois sites, de domaines océaniques différents (fig. 2), mais de compositions lithologiques et de profondeurs équivalents, ont été étudiés en détail pour la première fois :

- Dépôts pélagiques de la Madingley Rise :

Carotte MD 90940, 05°33,53 S – 61°40,12 E, profondeur : 3 190 m.

- Dépôts pélagiques du passage des Amirantes :

Carotte MD 90929, 6°59 S – 52°03 E, profondeur : 3 070 m.

- Dépôts de l'upwelling de Socotra :

Carotte MD 962073, 10.936° N - 52.616° E, profondeur : 3 142 m.

Les données de plusieurs autres sites de l'océan Indien du NW (bassin de Somalie, upwelling de Somalie et golfe d'Aden, fig. 4) ont été réutilisées ou complétées pour comparaison. Leur liste est donnée dans chacune des parties concernées de ce travail.

Les outils.

La majeure partie des marqueurs géochimiques classiquement employés dans ce genre d'études a été utilisée pour les reconstructions paléocéanographiques et de la paléoproductivité : COT, teneurs en carbonates, éléments majeurs, mineurs, et en traces des sédiments. L'étude du baryum, qui est généralement considéré comme un bon marqueur de la productivité, a été particulièrement détaillée. L'utilisation du protocole d'extraction mis au point par Robbins et al. (1984) et adapté par Lyle et al. (1984) permet, en effet, de mettre en solution successivement les fractions du stock de baryum liées soit aux carbonates, soit aux oxydes et hydroxydes, soit à la matière organique, soit aux aluminosilicates, soit enfin à la barytine, seule phase en relation avec les processus biogènes, et donc utilisable pour les reconstructions de paléoproductivité. Les résultats obtenus devraient aboutir à une meilleure connaissance de la distribution du baryum sous ses diverses formes minéralogiques et affiner

l'interprétation du signal porté par le baryum. Pour chaque site étudié, les marqueurs retenus et leur techniques d'extraction seront précisés.

Les données géochimiques ont été comparées à des résultats, déjà publiés ou originaux, obtenus grâce à des marqueurs biologiques, en particulier les radiolaires et les foraminifères :

- analyses statistiques combinées de populations de foraminifères et radiolaires (Vénec-Peyré et al., 1995)

- index à radiolaires dont l'upwelling radiolarian index (URI) pour la mise en évidence des variations d'intensité des systèmes à upwelling (Caulet et al., 1992), et l'index des variations d'abondance des formes de la thermocline par rapport à celles des formes de surface pour interpréter les modifications de la productivité de surface (Jacot Des Combes et al., in press). Pour chaque site étudié seront caractérisés les marqueurs biologiques retenus.

Organisation générale

Ce travail est présenté en quatre chapitres. Le premier va concerner l'étude géochimique de sédiments prélevés en domaine pélagique. Il est composé de deux notes, l'une sous presse, et l'autre acceptée, portant sur des carottes prélevées sur la ride de Madingley, dans le bassin de Somalie et dans le passage des Amirantes. Le second chapitre traitera de l'enregistrement géochimique dans la boucle nord du système d'upwelling de Somalie, appelée tourbillon de Socotra, et de la comparaison de ces données avec des données déjà publiées sur la boucle sud, ou tourbillon de Somalie. La troisième partie comparera les résultats obtenus lors de ces nouvelles études avec des résultats précédents provenant d'autres sites de façon à établir une synthèse de l'enregistrement géochimique à l'échelle régionale. Enfin, le dernier chapitre, qui correspondra à la conclusion générale, s'appuiera sur les résultats de ce travail pour proposer une nouvelle interprétation des variations de la paléocéanographie et de la productivité dans l'océan Indien du NW.

Bibliographie

Barnola, J.M., Raynaud, D., Korotkevich, Y.S., and Lorius, C., 1987. Vostok ice core provides 160,000-year record of atmospheric CO_2. *Nature*, 329 : 408-414.

Bassinot, F., 1993. Analyse paléocéanographique à haute résolution des carbonates pélagiques des océans Indien et Pacifique en région tropicale. Thesis : 1-220.

Berger, W.H., Smetacek, V.S. and Wefer, G., 1989. Ocean productivity and paleoproductivity. An overview. In : W.H. Berger et al. (Editors), Production of the ocean : Present and past, Life Science Research Report 44, Wiley and Sons : 1-34.

Berger, W.H. and Herguera, J.C., 1992. Reading the sedimentary record of the ocean's productivity. In : P.G. Falkowski and A.D. Woodhead (Editors), Primary productivity and biochemical cycles in the sea, Plenum Press, New York : 455-486.

Bertrand, P., and Lallier-verges, E., 1993. Past sedimentary organic matter accumulation and degradation controlled by productivity. *Nature*, 364 : 786-788.

Bishop, J.K.B., 1988. The barite-opal-organic carbon association in oceanic particulate matter. *Nature*, 332 : 341-343.

Boyle, E.A., 1981. Cadmium, zinc, copper and barium in foraminifera tests. *Earth Planet. Sci. Lett.*, 53 : 11-35.

Broecker, W. S., and Peng, T.H., 1986. Carbon cycle : 1985. Glacial to interglacial changes in the operation of the global carbon cycle. *Radiocarbon* 28 (2A) : 309-327.

Bruce, J.G. and Beatty, W.H., 1985. Some observations of the coalescing of Somali eddies and description of the Socotra eddy. *Oceanol. Acta*, 8 : 207-209.

Calvert, S.E., and Pedersen, T.F., 1992. Organic carbon accumulation and preservation in marine sediments : How important is anoxia? In : J.K. Whelan and J.W. Farrington (Editors), Productivity, accumulation and preservation of organic matter in recent and ancient sediments, New York : Columbia Univ. Press : 231-263.

Caulet, J.P., 1987. MD 44/INDUSOM, Rapports des Campagnes à la Mer, TAAF Report 85-04 : 1-109.

Caulet, J.P., Debrabant, P. and Fieux, M., 1988. Dynamique des masses d'eaux océaniques et sédiment quaternaire sur la marge d'Afrique de l'est et dans le bassin de Somalie. Résultats préliminaires de la mission MD 44-INDUSOM du Marion-Dufresne. *C.R. Acad. Sci.*, Paris, 307 (2) : 281-288.

Caulet, J.P. Vénec-Peyré, M.-T., Vergnaud Grazzini, C., and Nigrini, C., 1992. Variation of South Somalian upwelling during the last 160 ka : radiolarian and foraminifera records in core MD 85674. In : Summerhayes, C.P., Prell, W.L., and Emeis, K.C. (Eds), Upwelling systems : evolution since the Early Miocene, *Geol. Soc. Sp. Pub.*, 64 : 360-379.

Clemens, S., Prell, W., Murray, D., Shimmield, G.B., and Weedon, G., 1991. Forcing mechanisms of the Indian ocean monsoon. *Nature*, 353 : 720-725.

Currie, R.J., 1992. Circulation and upwelling off the coast of south-east Arabia. *Oceanol. Acta*, 15 : 43-60.

De Lange, G.J., Van Os, B., Pruysers, P.A., Middelburg, J.J., Castadori, D., Van Santvoort P., Muller, P.J., Eggenkamp, H., and Prahl, F.G., 1994. Possible early diagenetic alteration of paleo-proxies. In : Iahn et al. (Editors), Carbon cycling in the glacial ocean : constraints on the ocean role on global change. Quantitative approaches in paleoceanography. NATO ASI Series, serie 1, Global Environment Changes, 17 :225-258.

Dehairs, F., Chesselet, R. and Jedwab, J., 1980. Discrete suspended particles of barite and barium cycle in the open ocean. *Earth Planet. Sci. Lett.*, 49 : 528-550.

Dehairs, F., Lambert, C.E., Chesselet, R., and Risler, N., 1987. The biological production of marine suspended barite and the baryum cycle in the Western Mediterranean Sea. *Biogeochemistry*, 4 : 119-139.

Dehairs, F., Stroobants, N., and Goeyens, L., 1991. Suspended barite as tracer of biological activity in the Southern Ocean. *Mar. Chem.*, 35 : 399-410.

Delmas, R.J., Ascencio, J.-M., and Legrand M, 1980. Polar ice evidence that atmospheric CO_2 20,000 years BP was 50% of present. *Nature*, 284 : 155-157.

Demaison, G.J., 1991. Anoxia vs. productivity : What controls the formation of organic-carbon-rich sediments and sedimentary rocks? discussion. *Amer. Asso. Petrol. Geolog. Bull.*, 75 : 499.

Dymond, J., Suess, E. and Lyle, M., 1992. Barium in deep-sea sediment : A geochemical proxy for paleoproductivity. *Paleoceanography*, 7 : 163-181.

Francois, R., Honjo, S., Manganini, S.J., and Ravizza, G.E., 1995. Biogenic barium fluxes to the deep sea : Implications for paleoproductivity reconstruction. *Global Biogeochem. Cycles*, 9 : 289-303.

Giannesini, P-J., Clément, P., and Caulet, J. P., in prep. Campagne MD 104-PEGASOM IFRTP Report.

Gingele, F., and Dahmke, A., 1994. Discrete barite particles and barium as tracers of paleoproductivity in south Atlantic sediments. *Paleoceanography*, 9 : 151-168.

Jacot Des Combes, H., Caulet, J.P., and Tribovillard, N.P., in press. Pelagic productivity changes in the equatorial area of the NW Indian Ocean during the last 400 000 years. *Mar. Geol.*

Jones, P.D., Wigley, T.M.L., and Raper, S.C.B., 1987. The rapidity of CO_2-induced climatic change : observations, model results and palaeoclimatic implications. In : Abrupt climatic change, W.H. Berger, and L.D. Labeyrie (Eds), Riedel : 47-55.

Lea, D.W. and Spero, H.J., 1994. Assessing the reliability of paleochemical tracers : Barium uptake in the shells of planktonic foraminifera. Paleoceanography, 9 : 445-452.

Lea, D.W and Boyle, E.A., 1989. Barium content of benthic foraminifera controlled by bottom water composition. *Nature*, 338 : 751-753.

Leclaire, L., 1974. Late Cretaceous and Cenozoic pelagic deposits. Paleoenvironnement and paleoceanography of the central western Indian Ocean. In : Simpson, E.S.W. and Schlich, R., DSDP, Init. Repts, 25 : 481-513.

Leetma, A., Rossby, H.T., Saunders, P.M., and Wilson, P., 1980. Subsurface circulation in the Somali Current. *Science*, 209 : 590-592.

Lyle, M., Heath, G.R., and Robbins, J.M., 1984. Transport and release of transition elements during early diagenesis : Sequential leaching from MANOP sites M and H. Part I : pH 5 acetic acid leach. *Geochim. Cosmochim. Acta*, 48 : 1705-1715.

Martin, J.H., Knauer, G.A., Karl, M.D., and Broenkow, W.W., 1987. VERTEX : carbon cycling in the northeast Pacific. *Deep Sea Res.*, 34 : 267-285.

Paytan, A. and Kastner, M., 1996. Benthic Ba fluxes in the Central Equatorial Pacific, implications for the oceanic Ba cycle. *Earth Planet. Sci. Lett.*, 142 : 439-450.

Pedersen, T.F. and Calvert, S.E., 1990. Anoxia vs productivity? What controls the formation of organic-carbon-rich sediments and sedimentary rocks? *Amer. Asso. Petrol. Geolog. Bull.*, 74 : 454-466.

Peterson, L.C., Abbott, M.R., Anderson, D.M., Caulet, J.P., Conté, M.H., Emeis, K.-C., Kemp, A.E.S., and Summerhayes, C.P., 1995. How do upwelling systems vary through time? In : C.P. Summerhayes, K.-C. Emeis, M.V. Angel, R.L. Smith, and B. Zeitzchel

(Eds), Upwelling in the ocean : modern processes and ancient records, Wiley and Sons : 285-311.

Philander, S.G.H. and Delecluse, P., 1983. Coastal current in low latitudes (with application to the Somali and El Niño currents). *Deep-Sea Res.*, 30 : 887-902.

Prell, W.L., 1984. Monsoonal climate of the Arabian Sea during the late Quaternary : a response to changing solar radiation. In : A.L. Berger et al., (Eds), Milankovitch and Climate, Riedel, part 1 : 349-366.

Pujos, A., 1992. Calcareous nanofossils of Plio-Pleistocene sediments from the northwestern margin of tropical Africa. In : Summerhayes, C.P., Prell, W.L., and Emeis, K.C. (Eds), Upwelling systems : evolution since the Early Miocene, *Geol. Soc. Sp. Pub.*, 64 : 332-343.

Robbins, J.M., Lyle, M., and Heath, G.R., 1984. A sequential extraction procedure for partitioning elements among co-existing phases in marine sediments. Rep. College Oceanography, Oregon State Univ. 45p.

Romankevitch, E.A., 1984. Geochemistry of organic matter in the ocean. Springer-Verlag, 335 pp.

Sarnthein, M., Pflaumann, U. Ross, R., Tiedemann, R, and Winn, K., 1992. Transfer functions to reconstruct ocean paleoproductivity : a comparison. In : Summerhayes, C.P., Prell, W.L., and Emeis, K.C. (Eds), Upwelling systems : evolution since the Early Miocene, *Geol. Soc. Sp. Pub.*, 64 : 411-427.

Shimmield, G.B., 1992. Can sediment geochemistry record changes in coastal upwelling paleoproductivity ? Evidence from Northwest Africa and the Arabian Sea. In : Summerhayes, C.P., Prell, W.L., and Emeis, K.C. (Eds), Upwelling systems : evolution since the Early Miocene, *Geol. Soc. Sp. Pub.*, 64 : 9-46.

Shimmield, G.B. and Mowbrays, R., 1991. The inorganic geochemical record of Northwestern Arabian Sea : A history of productivity variation over the last 4,000 ky from sites 722A and 724. In : Prell W.L. et al., Proc. ODP, Sci. Res., 117 : 409-429.

Shimmield, G.B., Derrick, S., Mackensen, A., Grobe, H., and Pudsey, C., 1994. The history of barium, biogenic silica and organic carbon accumulation in the Weddel Sea and the Antarctic Ocean during the last 150,000 years. In : R. Iahn et al. (Editors), Carbon cycling in the glacial ocean : constraints on the ocean role in global change. Quantitative

approaches in paleoceanography. NATO ASI Series (1) : Global environmental changes, 17 : 555-574.

Shimmield, G.B. and Jahnke, R.A., 1995. Particle flux and its conversion to the sediment record : Open ocean upwelling systems. In : Summerhayes, C.P., Prell, W.L., and Emeis, K.C. (Eds), Upwelling systems : evolution since the Early Miocene, *Geol. Soc. Sp. Pub.*, 64 : 172-191.

Siegenthaler, U., and Sarmiento, J.L., 1993. Atmospheric carbon dioxide and the ocean. *Nature*, 365 : 119-125.

Sirocko, F., 1991. Deep Sea sediments of the Arabian sea : a paleoclimatic record of the southwest Asian summer monsoon. *Geologische Rundschau*, 80/3, Stuttgart : 557-566.

Swallow, J.C., 1980. The Indian Ocean Experiment : Introduction. *Science*, 209 : 588-589.

Swallow, J.C. and Bruce, J.G., 1966. Current measurements off the Somali coast during the southwest monsoon of 1964. *Deep-Sea Res.*, 13 : 861-888.

Tans, P.P., Fung, L.Y., and Takahashi T., 1990. Observational constraints on the global atmospheric CO_2 budget. *Science*, 247 : 1431-1438.

Tchernia, P., 1978. Océanographie Régionale : Description physique des océans et des mers. ENSTA. 19 pl, 1-275.

Thomson, J., Higgs, N.C., Croudace, I.W., Colley, S. and Hydes, D.J., 1993. Redox zonation of elements at an oxic/post-oxic boundary in deep-sea sediments. *Geochim. Cosmochim. Acta*, 57 : 579-595.

Thomson, J., Higgs, N.C., Wilson, T.R.S., Croudace, I.W., De Lange, G.J., and Van Santvoort, P.J.M. , 1995. Redistribution and geochemical behaviour of redox sensitive elements around S1, the most recent eastern Mediterranean sapropel. *Geochim. Cosmochim. Acta*, 59 : 3487-3501.

Van Os, B.J.H., Middelburg, J.J., and De Lange, G.J., 1991. Possible diagenetic mobilization of barium in sapropelic sediment from the eastern Mediterranean. *Mar. Geol.*, 100 : 125-136.

Van Santvoort, P.J.M., De Lange, G.J., Thomson, J., Cussen, H., Wilson, T.R.S., Krom, M.D., and Ströhle, K., 1996. Active post-depositional oxidation of the most recent sapropel (S1) in sediments of the eastern Mediterranean sea. *Geochim. et Cosmochim. Acta*, 60 : 4007-4024.

Vanney, J.R., 1991. L'Océan indien. *Oceanis*, 17 : 179-193.

Vénec-Peyré, M.-T., Caulet, J.P., and Vergnaud Grazzini, C., 1995. Paleohydrographic changes in the Somali Basin (5°N upwelling and equatorial areas) during the last 160 kyr, based on correspondence analysis of foraminiferal and radiolarian assemblages. *Paleoceanography*, 10 (3) : 473-491.

Vénec-Peyré, M.T., and Caulet, J.P., in press. Paleoproductivity changes during the last 72,000 years in the upwelling system of Socotra (Somali Basin, N.W. Indian Ocean) : Biological signatures. *Mar. Micropal.*

Vergnaud Grazzini, C., Caulet, J.P., and Vénec-Peyré, M.-T., 1995. Index de fertilité et mousson dans le bassin de Somalie. Evolution au Quaternaire supérieur. *Bull. Soc. Géol. Fr.*, 166 (3) : 259-270.

Walsh, J.J., Rowe, G.T., Iverson, R.L., and McRoy, C.P., 1981. biological export of shelf carbon is a sink of the global CO_2 cycle. *Nature*, 291 : 196-201.

Walsh, J.J., Premuzic, E.T., Gaffney, J.S., Rowe, G.T., Hartbottle, G., Stoenner, R.W., Balsam, W.L., Betzer, P.R., and Macko, S.A., 1985.Organic storage of CO_2 on continental slope off the mid-Atlantic Bight, the southern Bering Sea and the Peru coast. *Deep Sea Res.*, 37 : 853-883.

Warren, B.A., 1974. Deep flow in the Madagascar and Mascarene basins. *Deep Sea Res.*, 21 : 1-21.

Warren, B.A., 1981. Transindian hydrographic section at 188° : Property distributions and circulation in the South Indian Ocean. *Deep-Sea Res.*, 13 : 759-788.

Warren, B.A., Stommel, H., and Swallow, J.C., 1966. Water masses and patterns of flow in the Somali Basin during the southwest monsoon of 1964. *Deep-Sea Res.*, 28 : 825-860.

Wollast, R., 1991. The coastal organic carbon cycles : fluxes, sources and sinks. In : R.F.C. Mantoura, J.M. Martin and R. Wollast (Editors) Ocean margin processes in the global change. 356-381.

Yasuda, Y., Amano, K., and Yamanoi, T., 1990. Pleistocene climatic changes as deduced from a pollen analysis of site 717 cores. In : J.R. Cochran et al., Proc. ODP., Sci., Res., 116:249-261.

1ère PARTIE

PALEOCEANOGRAPHIE ET PALEOPRODUCTIVITEDANS LE DOMAINE PELAGIQUE DE L'OCEAN INDIEN DU NORD-OUEST.

Les variations de la paléocéanographie et de la paléoproductivité dans la ceinture équatoriale de l'océan Indien sont étudiées par l'intermédiaire de l'enregistrement géochimique (avec une attention particulière pour le baryum) contenu dans les sédiments de trois sites localisés à des profondeurs similaires dans le domaine pélagique de l'océan Indien équatorial. La première carotte (MD 90940) est située sur la ride de Madingley (au nord des Seychelles) la seconde (MD 85668) dans le bassin de Somalie et la troisième (MD 90929) dans le passage des Amirantes, entre Madagascar et les Seychelles (Fig. 1).

Le sédiment de ces carottes est analysé selon le même protocole : datation par la méthode des isotopes de l'oxygène mesurés sur le sédiment total (ou bulk), mesure des teneurs en carbonates par calcimétrie Bernard, dosage des teneurs en éléments majeurs et en traces par ICP-OES (carottes MD 90940 et 85668) et ICP-MS pour la carotte MD 90929, mesure du taux de carbone organique total par LECO (MD 90929) ou Rock-Eval (MD 90940 et 85668). Des échantillons ont été choisis dans ces trois carottes pour être analysés selon le protocole d'attaques chimiques séquentielles proposé par Robbins et al. (1984) et modifié par Lyle et al. (1984) afin de déterminer la distribution du baryum dans les différentes phases du sédiment. Dans les carottes MD 90940 et 90929, les abondances de 3 espèces de radiolaires vivant à la surface (moins de 20 m de fond) et de 6 espèces vivant au niveau, ou au dessous de la thermocline (au dessous de 250 m), ont été comptées afin d'établir un index de productivité qui soit indépendant de l'enregistrement géochimique. Cet index consiste dans le rapport des formes de la thermocline aux formes de surface. Il augmente quand les apports nutritifs en provenance de la surface s'accroissent suffisamment pour qu'il y ait un export important au dessous de la zone euphotique, c'est-à-dire quand la productivité de surface est suffisamment forte pour excéder le recyclage dans les eaux de surface.

Les résultats de l'étude du signal géochimique comparé avec le signal biologique sont présentés sous la forme de deux articles. Le premier concerne la ride de Madingley et le bassin de Somalie, le second le passage des Amirantes accompagné d'une comparaison avec les autres sites.

En résumé, la comparaison du signal géochimique enregistré dans ces trois carottes durant les derniers 400 ka montre de grandes différences entre les trois sites. Le bassin de Somalie enregistre classiquement des taux d'accumulation (bulk MAR, comme mass accumulation rate) plus élevés pendant les périodes glaciaires. C'est également le cas de la ride de Madingley, avec toutefois une exception notable : une période d'accumulation maximale durant un stade interglaciaire (stade isotopique 9). Ce pic d'accumulation est également enregistré dans le passage des Amirantes, mais avec une plus faible amplitude. L'événement le plus marquant dans l'enregistrement des variations du taux d'accumulation à ce site est la période comprise entre la transition isotopique 8/7 et le stade isotopique 2 qui est anormalement caractérisée par des valeurs constantes et faibles du bulk MAR. A ce site, les pics de productivité sont surtout localisés aux transitions climatiques et durant les stades glaciaires. Dans les carottes MD 90940 et 90929, la bonne corrélation entre les variations du taux d'accumulation et celles de l'index à radiolaires indique que les variations du bulk MAR résultent de celles de la productivité de surface.

Le comportement des éléments majeurs et en traces présente des différences entre les sites étudiés. Le site localisé sur la ride de Madingley peut être considéré comme étant en domaine purement pélagique, avec des apports terrigènes très faibles à négligeables (rapport Ti/Al faible), des variations des éléments en traces (Ba, P, Cu, et Ni) plutôt liées à la productivité de surface, et un dépôt s'effectuant sous conditions oxiques (teneurs en V faible et en Mn élevée). A ce site, le baryum est presque exclusivement déposé sous forme de barytine. Dans le bassin de Somalie, les apports terrigènes sont plus importants et les conditions sont légèrement plus réductrices. De telles conditions ont modifié l'enregistrement des éléments en trace, notamment Ba, Cu et Ni qui paraissent moins directement liés à la productivité de surface. Dans la carotte étudiée, la teneur en barytine est négligeable et le baryum est majoritairement lié à la phase terrigène détritique. Dans le passage des Amirantes, les variations des teneurs en éléments terrigènes (Al, Fe, Mg et K) sont assez comparables à celles observées dans le bassin de Somalie, mais le comportement des éléments en trace diffère fortement. Le sédiment révèle ainsi des teneurs en Ti très importantes et l'enrichissement du

sédiment en Cu, Ni, Zn, Mn, et V par rapport à Al est très fortement corrélé à l'enrichissement du sédiment en Ti comparé à Al. Le baryum est également lié au titane, mais se présente à 30% sous forme de barytine. Dans le passage des Amirantes, les conditions de dépôt semblent être demeurées oxiques au cours de l'intervalle de temps considéré.

D'une façon générale, les différences observées dans la réponse géochimique enregistrée à chaque site peuvent être attribuées à des variations de la productivité de surface en raison des faibles apports terrigènes. Les variations du rapport radiolaires de la thermocline /radiolaires de surface montrent que ces variations sont dues à des modifications de la circulation des eaux de surface dans la région. Les alternances cycliques des valeurs du bulk MAR dans le bassin de Somalie, avec de fortes valeurs durant les intervalles glaciaires (à l'exception du stade isotopique 8) et de plus faibles pendant les interglaciaires, indiquent que les variations de la productivité de surface ont été liées à des modifications de la circulation de surface induites par les changements climatiques globaux. La situation est peu différente sur la ride de Madingley où les forts taux d'accumulation, et donc les fortes paléoproductivités, sont majoritairement enregistrés pendant les stades glaciaires, à l'exception notable de la période à bulk MAR maximal pendant le stade isotopique interglaciaire 9. Ce pic de productivité est interprété comme un affaiblissement du déplacement vers le nord du contre-courant équatorial lors des alternances climatiques. Dans le passage des Amirantes, le message géochimique indique clairement une période de faible taux de sédimentation entre la transition 8/7 et le stade 2. Ce taux de sédimentation est interprété comme le produit d'une productivité de surface diminuée. L'enrichissement en titane et autre métaux en traces suggère un apport détritique différent de celui observé dans les autres sites du bassin de Somalie, qui doit être originaire des bassins du sud de l'océan Indien. La très faible productivité de surface enregistrée à ce site est interprétée comme résultant d'une stagnation à ce niveau de la zone oligotrophique qui s'étend entre le courant sud équatorial et le contre-courant équatorial. Les facteurs climatiques de cette immobilité du système sud-équatorial de fronts et ceintures de productivité pendant une période relativement prolongée ne sont pas encore connus.

Pelagic productivity changes in the equatorial area of the NW Indian Ocean during the last 400 kyr.

Hélène Jacot Des Combes[a, b], Jean-Pierre Caulet[b] and Nicolas P. Tribovillard[a].

a Laboratoire de Géochimie des Roches Sédimentaires, URA 723 CNRS, Université de Paris Sud, bât 504, 91405 ORSAY CEDEX (FRANCE).

b Laboratoire de Géologie, MNHN, 43 rue Buffon 75005 PARIS (FRANCE).

Sous presse à Marine Geology.

Keywords: NW Indian Ocean, pelagic sedimentation, paleoproductivity, geochemical proxies, barium, sequential leaching.

Abstract

Major and selected trace element (Al, Fe, Mg, K, Ba, P, Mn, V, Cu, Ni, and Ti) records were analyzed in two cores recovered from the Northwestern Indian Ocean (core MD 90940 on the Madingley Rise and core MD 85668 in the Somali Basin) in order to monitor the sedimentary response to pelagic productivity in this area during the last 400 kyr. Geochemical proxies such as bulk Mass Accumulation Rate (MAR), Al-normalized major and trace element contents, major and trace element MARs were compared to biologic markers of paleoproductivity: a new radiolarian index (rad ratio), and the variations of foraminiferal and radiolarian assemblages. A special attention being paid to the barium record, a sequential leaching procedure determined the main Ba-carrier fraction in the sediment, and, thus, the amount of biogenic barium. The "blue ocean" sedimentation on the Madingley Rise (core MD 90940) is characterized by a low MAR and an insignificant terrigenous input. The bulk MAR variations are directly related to the variations of the rad ratio, reflecting a direct link between surface productivity and pelagic sedimentation at this site. In this sediment, barium is mainly found as barite and can be considered as a paleoproductivity proxy. In the Somali Basin (core MD 85668), the terrigenous inputs are relatively higher, but the bulk MAR variations are still related to the variations of surface productivity. No barite was found and barium is mainly linked to the terrigenous input. Comparing the two pelagic sites of the Madingley Rise and the Somali Basin points out the differences between the barium records at both sites. Despite the location of both cores in the pelagic domain, the geochemical record, and especially the barium one, is different from one core to the other. The comparison of the variations of the bulk MAR, which reflects the variations of the surface productivity, presents significant discrepancies between both sites. In the "blue ocean" (core MD 90940), the productivity peak values are mainly recorded during glacial intervals, but their maximum values are observed during interglacial isotope stage 9. In the Somali Basin (core MD 85668), high bulk MAR periods occurred during glacial isotope stages. The interglacial episode of high productivity recorded on the Madingley Rise, the absence of significant variations of productivity at the 8/7 transition in the Somali basin, as well as the absence of a time lag between both records indicate that the surface productivity is, in this area, controlled more by the local variations of the paleoceanographic patterns than the global climatic changes, e.g. the glacial/interglacial alternations.

1. Introduction

Variations in oceanic surface productivity are the response of living organisms to climate-induced chemical and physical changes affecting the oceanic domain. Through photosynthesis and export of organic matter to the bottom, primary productivity is an important factor in the carbon cycle. The study of paleoproductivity recorded in sediments can, thus, provide complementary information on carbon budget variations. Paleoproductivity can be estimated using different proxies: biological ones such as abundance and diversity of foraminifers, coccolithophorids, radiolarians and diatoms, and geochemical markers such as total organic carbon (TOC) and trace elements. Inorganic geochemistry of sediments and, particularly, trace element studies are useful tools for paleoceanographic and paleoproductivity reconstructions (Arrhenius, 1952; Brongersma et al., 1980; Calvert and Pedersen, 1993; Collier and Edmond, 1984; Francois et al., 1995; Lea and Spero, 1994; McManus et al., 1994; Paytan, 1995; Shimmield, 1992). Barium is considered a potentially good paleoproductivity marker when carefully used, but its interpretation depends on its multiple origins (Dymond et al., 1992; Ouahdi, 1997), its sensitivity to changes in redox conditions within the sediment (Pruysers et al., 1993; Thomson et al., 1993, 1995; Van Os et al., 1991; Van Santvoort et al., 1996) and water depth (Dymond et al., 1992; Von Breymann et al., 1992). Multiple interpretations for the origin of the barium fraction must be discussed when barium is extracted from the bulk sediment. To reduce the uncertainties about the origin of the barium, some sequential leaching procedures were established to measure the barium content in different fractions of the sediment (Lyle et al., 1984; Robbins et al., 1984). Few published works are, however, based upon this method, and they are mostly restricted to high productivity environments, such as the Mediterranean sapropels, or upwelling-influenced areas, e.g. the Peru margin or the southwestern African margin (Pruysers et al., 1993; Shimmield, 1992; Thomson et al., 1993, 1995; Van Os et al., 1991; Van Santvoort et al., 1996; Von Breymann et al., 1992). In the Indian Ocean, geochemical studies of paleoproductivity have mostly been focused on the Oman Margin (Murray and Prell, 1992; Shimmield, 1992; Shimmield and Mowbray, 1991; Weedon and Shimmield, 1991). The results of these inorganic-geochemistry studies point out the marked influence of eaolian dust

input upon sedimentary records in the NW Arabian Sea. In this area, productivity maxima occurred during interglacial stages.

The goal of this paper is to study the inorganic geochemical signal of the paleoproductivity recorded in the pelagic sediments of the Somali Basin (Northwestern Indian Ocean), with a special focus on barium using the protocol proposed by Lyle et al. (1984). The variations in the major and trace element contents and mass accumulation rates will also be compared to a productivity index based on the composition of the radiolarian assemblages. This region is interesting because it is close to the two upwelling areas (Somali and Socotra upwelling systems) that are controlled by the Southwest Indian Monsoon.

Two cores, recovered in the equatorial area of the western Indian Ocean during two oceanographic cruises of the R/V "*Marion-Dufresne*", were studied to constrain the productivity response of the pelagic realm (Fig. 1).

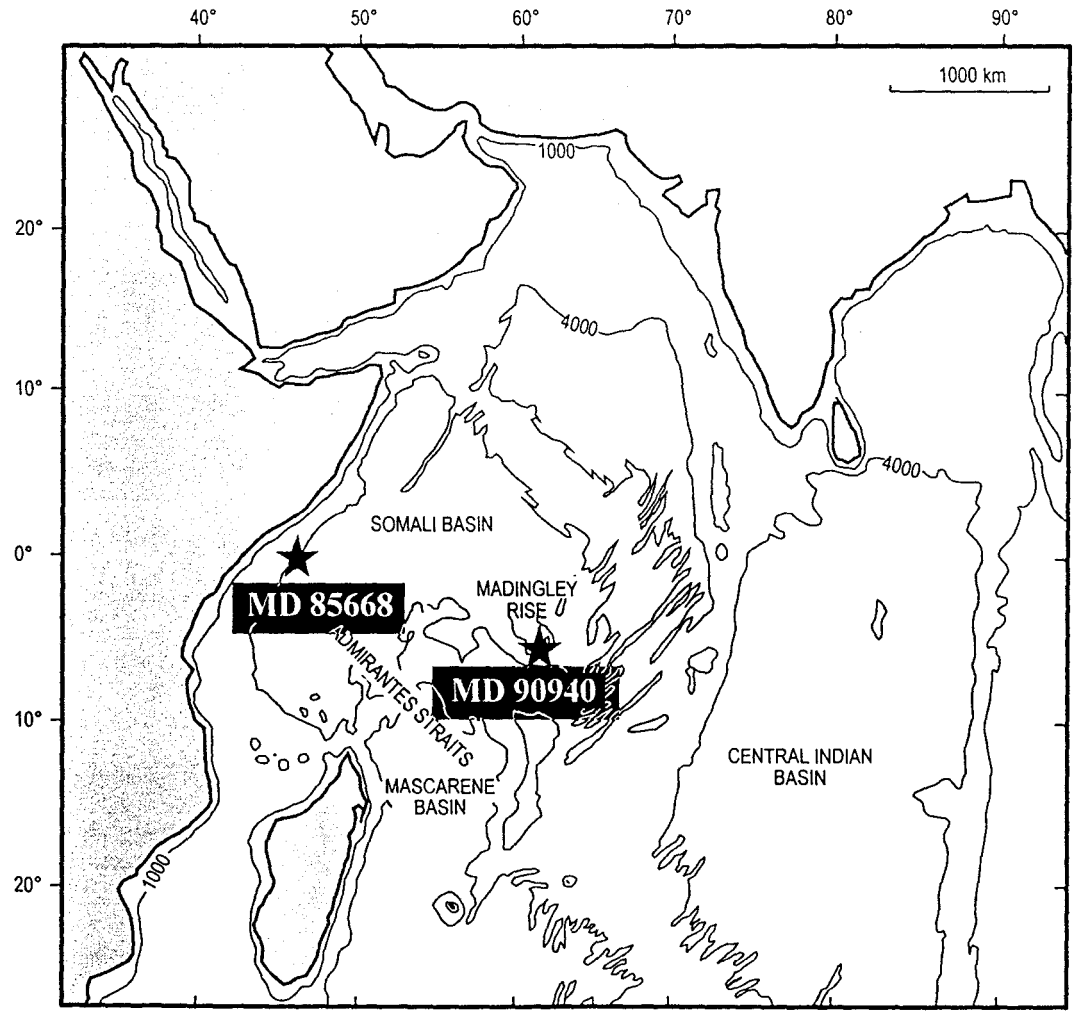

Figure 1. Location of Cores MD 85668 and MD 90940. Isobaths in meters.

One core (MD 90940) is characteristic of the "blue ocean", the pelagic realm where the surface productivity is very low, and the other one (MD 85668) is located closer to the continent and contains limited terrestrial input. A comparison between the results obtained from these two cores allows the monitoring of the sedimentation in a fertile area for the last 400,000 years, and to establish a geochemical record for typical pelagic sedimentation of the Equatorial Northwestern Indian Ocean. A precise pelagic record of paleoproductivity will be useful for further comparison with sediments deposited under monsoon-induced upwelling. Sediments located under these monsoon-induced upwellings generally comprise a mixing of upwelling-induced deposition during the summer monsoon and pelagic sedimentation during the winter. An estimation of the pelagic signal is, thus, essential in order to isolate and monitor the upwelling signal. Therefore, this study should be a suitable benchmark for further studies about inorganic proxies in this part of the Northwestern Indian Ocean.

Water masses of different origins characterize the equatorial belt of the Northwestern Indian Ocean and surface circulation patterns are mostly linked to the Indian monsoon (Fig. 2).

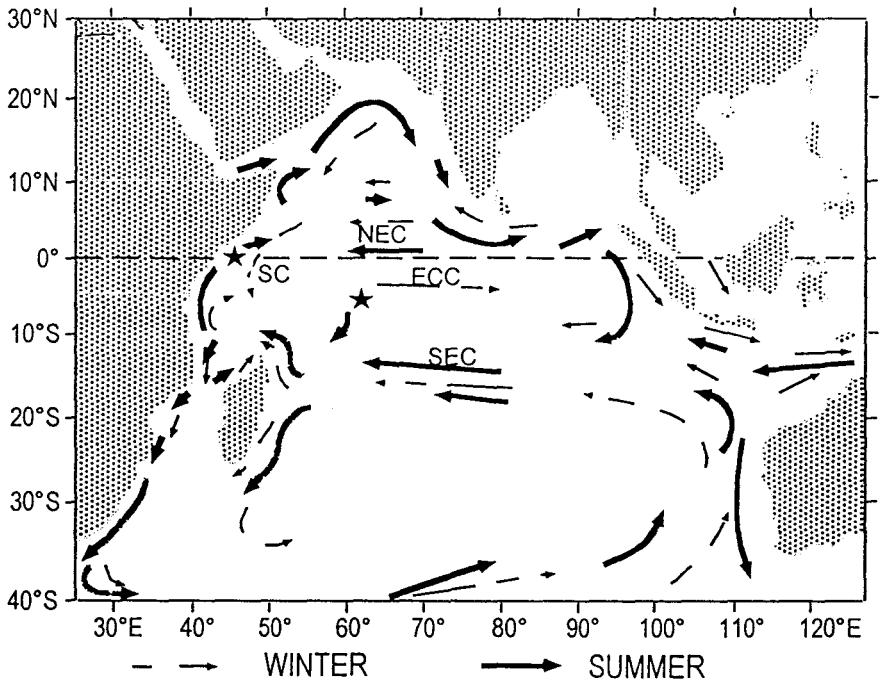

Figure 2a: Oceanic circulation in the surface layer in the Northwestern Indian Ocean.

NEC: North Equatorial Current. SEC: South Equatorial Current. ECC: Equatorial Counter Current. SC: Somali Current.

Locations of both cores are indicated by two black stars.

During Arctic winters, the South Equatorial Current (SEC) flows westward from the Indonesian Straits to the African Coast at 10°S. Before reaching the coast, it divides into 2 branches. The south branch flows southward through the Mozambique Channel. The north branch merges with the North Equatorial Current (NEC), flowing westward at 5°N, and forms the Equatorial Counter Current (ECC) flowing eastward at 5°S. During Arctic summers, the NEC and ECC both disappear. Off the African Coast, the SEC turns northward to become the Somali Current which flows northeastward along the coast (Swallow, 1980; Tchernia et al., 1978; Yasuda et al., 1990).

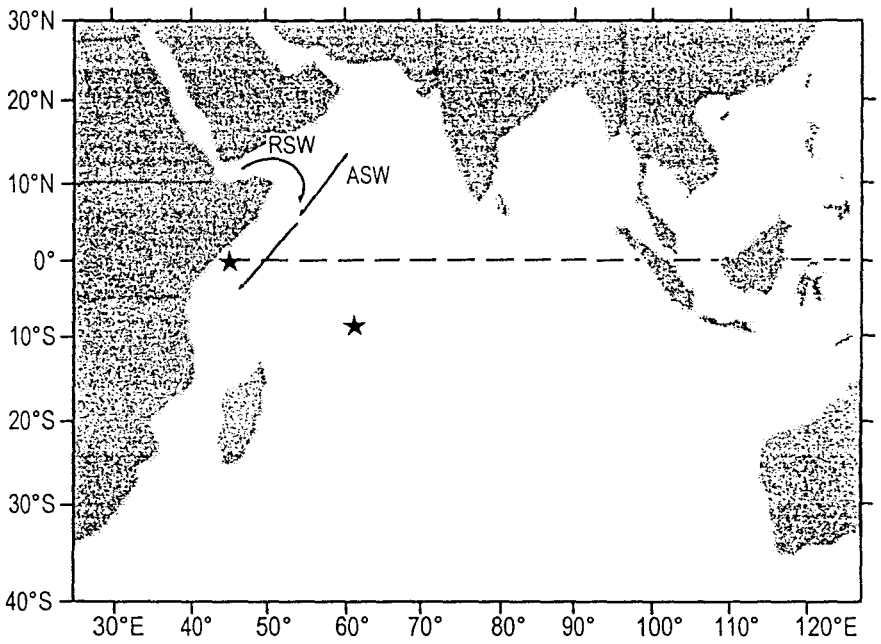

Figure 2b: Oceanic circulation at intermediate depth in the Northwestern Indian Ocean.
RSW: Red Sea Water. ASW: Arabian Sea Water.
Location of both cores are indicated by two black stars.

At intermediate depths (fig. 2b) a warm, salt-rich and oxygen-poor water mass flows southward (Warren et al., 1966). This intermediate water results from a mixing of the Red Sea water and the Arabian Sea water (Tchernia et al., 1978). Suboxic sediments, deposited during the last 0.4 Myr, can be found on the continental slope at various depths suggesting that the thickness and the depth of this intermediate water mass changed rapidly during this period (Caulet et al., 1988). Below 2500 m, bottom water masses are composed of cold, salt-poor and oxygen-rich water flowing from the Mascarene basin through the Amirantes Strait (Warren,

1974, 1981; Warren et al., 1966). Off Somalia, the Somali Current creates two gyres resulting in two upwelling systems: one at 5°N (the Somali upwelling) and one at 10°N (the Socotra upwelling) (Bruce and Beatty, 1985; Currie, 1992; Düing et al., 1980; Philander and Delecluse, 1983; Swallow and Bruce, 1966 and references therein). During Arctic winters, the Somali Current flow reverses and the upwelling systems stop.

2. Material and methods

The "blue ocean" piston core (MD 90940), dominated by open ocean processes, was recovered from a water depth of 3875 m on the Madingley Rise (5°20'6"S, 61°24'36"E) during the MD65 SEYMAMA-SHIVA cruise of the R/V *"Marion-Dufresne"*. The core MD 85668, with a relative stronger continental influence, was recovered from a water depth of 4020 m in the Somali Basin (0°0'36"S, 46°13'48"E) during the MD44 INDUSOM cruise of the R/V *"Marion-Dufresne"*(Fig. 1). Both cores are located within the equatorial productivity belt but not in areas of direct upwelling. The sediment of both cores is a very light yellow-gray coccolithophorid calcareous ooze with some planktic foraminifers and radiolarians (47.5% to 90% of $CaCO_3$). The < 36 μm fraction is dominant and mainly composed of coccolithophorids and fragmented tests of foraminifers. In the coarser fraction, foraminifers are well preserved. The carbonate fraction is partially dissolved, but the intensity of dissolution does not change between glacial and interglacial stages (Tribovillard et al., 1996; Vénec-Peyré et al., 1997). The sediment contains terrigenous debris such as quartz, feldspars and clay minerals. No turbidites, or reworked levels, were recognized.

The age model for the "blue ocean" core (MD 90940) is based on a high-resolution oxygen-isotope analysis of 120 bulk sediment samples retrieved every 5 cm. Previous work has shown that oxygen-isotope analysis of bulk sediment provides good ages in this area (Shackleton et al., 1993). The $\delta^{18}O$ content of bulk carbonate was measured by a mass-spectrometer (OPTIMA). The $\delta^{18}O$ was calculated relative to the PDB and a graphic correlation was done by peak to peak adjustment to the SPECMAP stack record (Fig. 3.A).

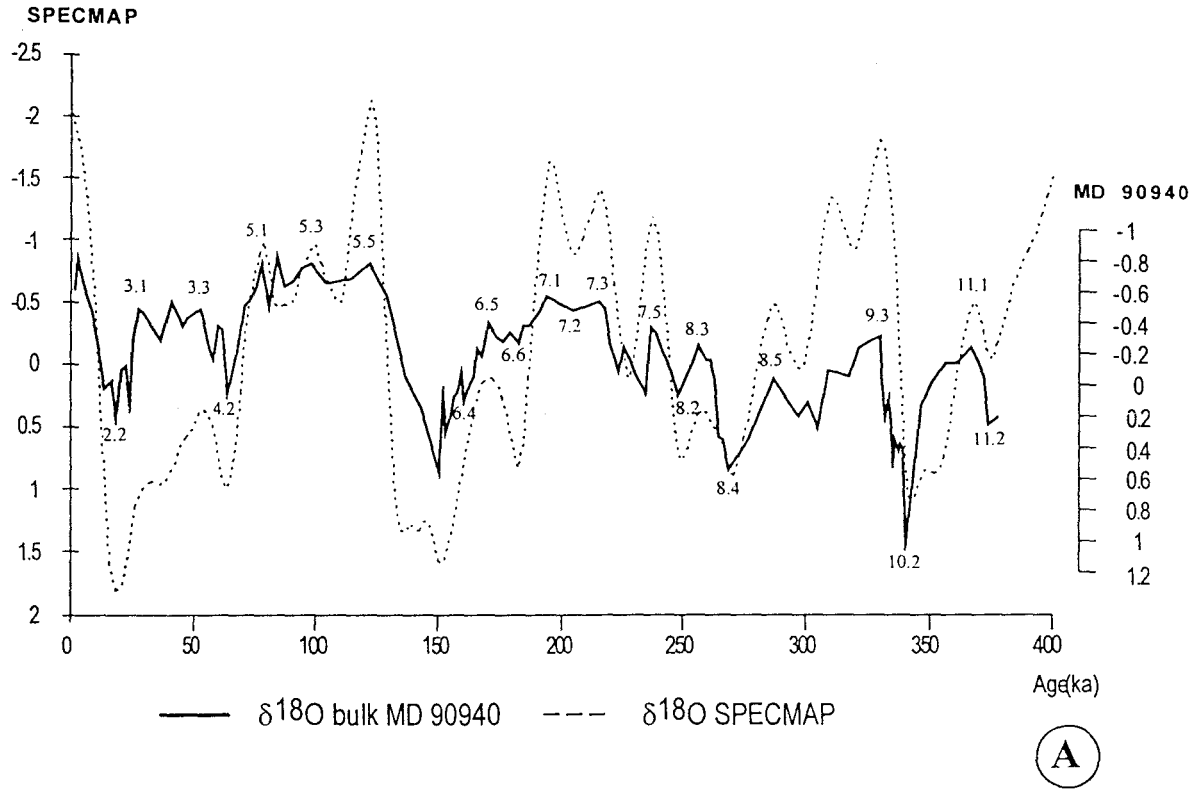

Figure 3.A. Oxygen isotope record for the bulk carbonate of Core MD 90940 (solid line) with indication of the major isotopic events identified in this core compared to the SPECMAP ^{18}O stack (dashed line).

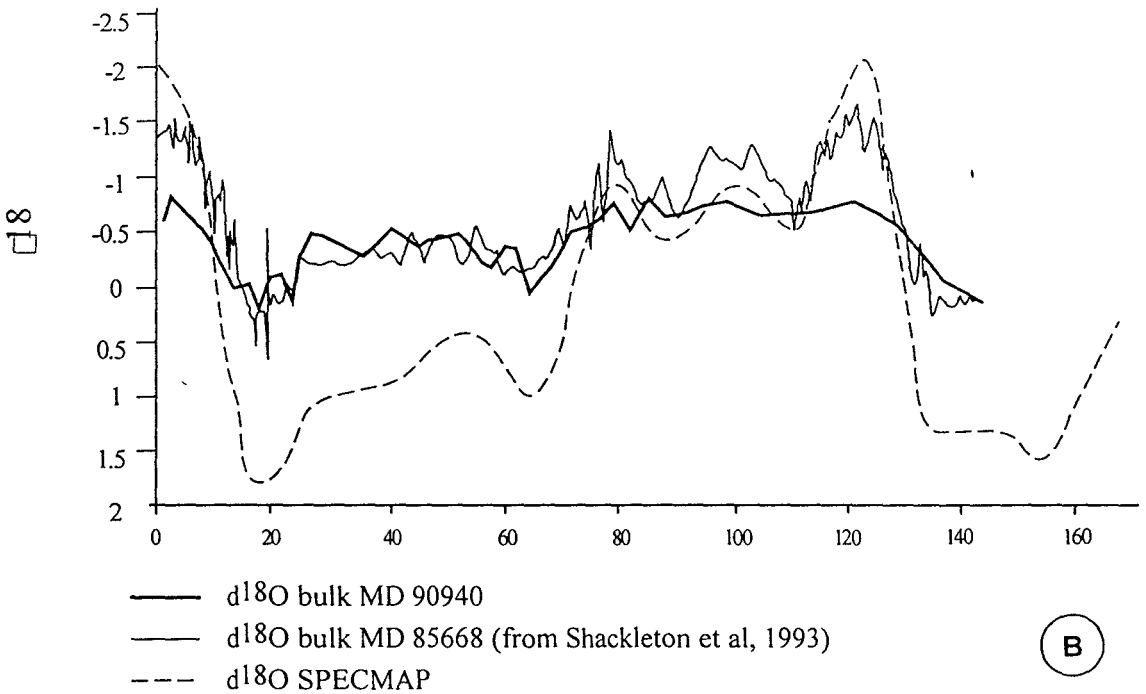

Figure 3.B. Comparison of the oxygen isotope record for the bulk sediment of Core MD 90940 (this study) and for the bulk sediment of Core MD 85668 (Shackleton et al., 1994) with the SPECMAP ^{18}O stack.

In core MD 90940, 22 major isotopic events were determined (Table 1). The oldest sample (5.86 mbsf) is dated 381 kyr. Data about the age model of the Somali Basin core (MD 85668) were published in VÈnec-PeyrÈ et al. (1997).

Isotopic event	Age of control point (ka)	epth (cmbsf)
2.2	19	36
3.1	28	62
3.3	53	92
4.2	65	122
5.1	80	142
5.3	99	171
5.5	122	186
6.4	151	206
6.5	171	271
6.6	183	292
7.1	194	316
7.2	205	321
7.3	216	326
7.5	238	365
8.2	249	386
8.3	257	394
8.4	269	427
8.5	287	436
9.3	331	488
10.2	341	538
11.1	368	563
11.2	375	577

Table 1. Age and depth of the control points used to established the age of Core MD 90 940.

Major and trace elements such as Ca, Al, Fe, Mg, K, Ba, P, Mn, V, Ni, Cu, and Ti are commonly used as markers of deposition and accumulation patterns. Aluminium, Fe, K, Mg, and Ti are mostly linked to terrigenous debris such as quartz, feldspars and clays minerals.

Carbonate content is generally related to surface productivity and dissolution processes. Manganese and V are strongly dependent on changes in redox conditions within the sediment. Barium, P, and, to a lesser degree Ni and Cu, are primarily related to biogenic activity, but they can be dependent on diagenesis through changes in redox conditions (Calvert and Pedersen, 1993). Nickel and Cu can be linked with organic matter through metal-organic complexes (Calvert and Pedersen, 1993).

Barium is generally considered as a reliable paleoproductivity proxy when it is present as barite (Calvert and Pedersen, 1993; Dymond et al., 1992; Francois et al., 1995; Gingele and Dahmke, 1994; Lea and Spero, 1994; Shimmield, 1992; Shimmield and Mowbray, 1991; Shimmield et al., 1994). Formation of barite in living organisms, or in microenvironments of decaying organic matter through sulfate oversaturation, suggests that biogenetic barium

content can be used as an indicator of surface biologic productivity (Dehairs et al., 1980, 1987, 1991; Dymond et al., 1992; Gingele and Dahmke, 1994; Goldberg and Arrhenius, 1958; Stroobants et al., 1991). Such a process is supposed to occur preferentially within siliceous-organism debris, such as diatoms and, possibly, radiolarians (Bishop, 1988; Dehairs et al., 1980, 1987, 1991). Barium can also be remobilized under reducing conditions (Francois et al. 1995; Torres et al. 1996). Thus, high productivity areas are often characterized by environmental conditions of low Ba preservation (Von Breymann et al., 1992).

Geochemical analyses were made on sediment samples with a 10 cm sampling step. This regular sampling step was chosen because the sediment color and texture are homogeneous all along the cores (El Foukali, 1995). This sampling step was also chosen to provide one sample approximately every 5 kyr (between 2 and 6 kyr).

Carbonate content was measured in both cores with a Bernard calcimeter, which measures the volume of CO_2 released by the dissolution of carbonates with 8N HCl.

Rock-Eval pyrolysis was performed on the bulk sediment. The pyrolysis cycle was adapted for young and immature organic matter (Espitalié et al., 1985). The amount of major and significant trace elements (Ba, P, Ti, Mn, V, Cu and Ni) was measured in the following way: 100 mg of bulk sediment were dried at 105°C for 24 hours and thoroughly ground in an agate mortar mill prior to a $HClO_4$, HNO_3 and HF acid digestion. The final residue was taken up in HCl 1M. The elements were measured with a ICP-spectrometer (Varian Liberty 20 ICP-EOS). The analytical precision and accuracy of the results were both found to be equal to, or better than, 5% for all elements. Data were checked by comparison with international standards and with the help of replicate samples.

Eight samples scattered along the upper half of the Madingley Rise core (MD 90940) were submitted to a sequential leaching procedure to determine the main carrier-phases of Ba in the sediment. These samples were chosen because their bulk barium contents are contrasted. The protocol used in this study is derived from that described by Lyle et al. (1984) and Robbins et al.(1984), and was already applied to samples from the Somali Basin core (MD 85668; Tribovillard et al., 1996). The dried and ground samples were subjected to a pH 5 acetic acid extraction to remove adsorbed and calcite-bound elements, and then to a treatment with a pH 5 hydroxyl amine hydrochloride solution to remove elements adsorbed on poorly crystalline Fe-Mn oxyhydroxides. The pH 9 sodium sulfate extraction of the organic matter was not carried out as organic matter content in Core MD 90940 is insignificant. In Core MD

85668, this extraction was performed, but since no barium was found, the data were omitted in the tables of results. An extra treatment with HF was added for sediments from Core MD 85668 to dissolve the silicate-bound barium (HF alone does not dissolve barite). Residual elements were determined from the difference between the total content (from the bulk analysis) and the sum of the three partial extractions. After each step, element concentrations were measured by ICP spectrometry. Due to an insignificant detrital fraction (average 0.78% Al), the final HF extraction was omitted in Core MD 90940. In this case, barite content was calculated from MD 85668 values, for which the additional HF step have been carried on:

$$\text{mean \% barite}_{90940} = \%\ Ba_{res.90940} - (\%\ Ba_{det.} / \%\ Al)_{85668} \times \%\ Al_{90940}.$$

where:

mean % $barite_{90940}$ is the mean percent of barium as barite in Core MD 90940.

% $Ba_{res.90940}$ is the percent of barium in the residual fraction (barite + terrestrial) in Core MD 90940.

(% $Ba_{det.}$ / % $Al)_{85668}$ is the ratio of the percent of barium in the terrestrial fraction to Al percent in Core MD 85668.

Al_{90940} is the Al percent in Core MD 90940.

Bulk sediment mass accumulation rates (MAR) were calculated by multiplying the linear sedimentation rate (LSR) derived from the age model and the dry bulk density (DBD). The DBD was obtained by the ratio: g dry weight / cm^3 wet volume.

Elements fluxes were calculated from the formula:

$$\text{Flux} = \text{element concentration (ppm)} \times \text{MAR} \times 10^{-6}.$$

Tables 2, 3, 4, and 5 summarize Core MD 90940 results. Core MD 85668 data were published by Tribovillard et al. (1996).

Depth (cmbsf)	Age (ka)	Rad ratio	CaCO3 (%)	Al (%)	Fe (%)	Mg (%)	K (%)	Ba (ppm)	P (ppm)	Mn (ppm)	V (ppm)	Ni (ppm)	Cu (ppm)	Ti (ppm)
7	3.7		83.0	0.53	0.39	0.37	0.23	1147	399	458	10	19	40	276
17	8.9	0.21	83.4	0.47	0.34	0.38	0.21	969	378	343	9	15	32	251
27	14.2	0.12	82.6	0.75	0.60	0.43	0.33	1185	284	546	16	25	37	481
36	19.0	0.18	82.4	0.69	0.55	0.40	0.30	1069	294	338	14	18	33	431
47	22.8	0.19	83.8	0.61	0.49	0.37	0.27	980	281	412	13	18	26	382
56	25.9	0.57	84.0	0.55	0.43	0.35	0.24	963	312	499	11	18	28	338
64	29.7	0.46	83.9	0.56	0.44	0.35	0.25	955	721	316	10	14	24	351
78	41.3	0.13	83.2	0.56	0.44	0.36	0.25	906	333	249	11	13	24	349
85	47.2	0.19	83.2	0.61	0.48	0.37	0.27	938	307	422	12	17	31	380
95	54.2	0.31	78.8	0.83	0.65	0.45	0.36	1121	319	894	16	21	48	521
106	58.6	0.46	78.6	0.82	0.64	0.44	0.36	1152	343	250	16	17	30	511
116	62.6	0.70	76.5	1.02	0.80	0.47	0.44	1624	355	418	19	22	45	617
127	68.8	1.16	75.0	0.98	0.78	0.45	0.42	1560	336	314	18	18	42	589
135	74.8	0.50	79.5	0.76	0.60	0.37	0.32	1373	289	282	13	15	37	439
146	82.6	0.13	83.2	0.79	0.63	0.38	0.34	1342	301	530	15	17	47	466
156	89.2	1.07	81.5	0.76	0.61	0.37	0.32	1454	307	844	14	22	55	450
166	95.7	0.85	75.2	0.91	0.73	0.43	0.38	1796	313	742	16	25	56	548
175	105.1	0.93	71.2	1.09	0.88	0.51	0.46	2198	398	1030	20	32	69	679
186	122.0	0.65	71.0	1.10	0.89	0.52	0.47	2238	383	515	20	24	53	675
196	136.5	0.74	74.5	0.99	0.79	0.56	0.45	1218	336	1747	23	63	92	663
206	151.0	0.89	76.6	0.91	0.71	0.55	0.44	1502	298	1112	21	53	60	640
216	154.1	2.05	74.1	0.94	0.75	0.56	0.45	1401	283	1008	21	41	47	647
226	157.2	1.07	75.4	0.90	0.69	0.53	0.43	1174	260	693	18	28	42	596
236	160.2	1.07	73.3	0.95	0.74	0.56	0.46	1263	264	230	19	27	34	629
246	163.3	1.39	71.4	0.95	0.74	0.56	0.46	1380	266	244	19	25	38	627
256	166.4	1.26	76.7	0.90	0.71	0.54	0.43	1357	257	598	19	35	49	608
266	169.5	2.40	79.6	0.79	0.62	0.45	0.37	1199	238	1586	18	22	43	504
276	173.9	0.73	80.5	0.78	0.58	0.44	0.36	1224	261	503	16	18	38	496
286	179.6	0.88	77.2	0.93	0.75	0.50	0.43	1638	300	154	19	24	45	603
296	184.8	1.09	71.7	1.07	0.87	0.53	0.49	2210	354	148	19	23	54	680
306	189.4	0.64	76.7	0.92	0.79	0.46	0.42	1767	369	144	15	18	59	558
316	194.0	0.37	82.1	0.67	0.52	0.35	0.30	1477	333	196	11	12	41	392
326	216.0	0.59	81.9	0.68	0.52	0.37	0.31	1162	296	200	11	13	38	409
335	221.1	0.32	80.2	0.80	0.61	0.42	0.37	1188	297	239	14	14	43	503
345	226.7	0.98	78.0	0.88	0.68	0.44	0.40	1567	320	321	16	17	47	548
354	231.8	0.89	79.8	0.75	0.61	0.42	0.33	1380	318	365	13	16	42	452
365	238.0	0.40	82.1	0.67	0.54	0.41	0.31	845	265	479	12	26	40	410
374	242.7	0.81	83.1	0.58	0.47	0.39	0.27	978	230	757	12	26	43	366
386	249.0	0.54	84.0	0.52	0.41	0.35	0.25	1155	221	483	10	16	30	320
394	257.0	0.58	84.6	0.51	0.40	0.34	0.24	1006	226	438	10	16	29	313
406	261.4	1.25	81.1	0.72	0.57	0.43	0.33	1166	269	408	13	21	33	448
416	265.0	1.27	74.5	0.99	0.80	0.54	0.46	1505	328	379	19	23	46	622
427	269.0	0.88	68.2	1.23	1.04	0.64	0.58	2030	354	548	24	33	62	795
436	287.0	0.66	81.3	0.67	0.55	0.36	0.30	1266	299	388	10	15	38	387
448	297.2	0.43	82.9	0.61	0.49	0.33	0.28	1169	303	335	10	13	34	347
458	305.6	0.61	83.4	0.61	0.49	0.33	0.27	1224	304	309	9	12	34	347
468	314.1	0.49	78.0	0.80	0.66	0.41	0.36	1613	372	475	13	17	49	454
478	322.5	1.11	78.2	0.76	0.64	0.40	0.35	1722	395	497	13	21	48	434
488	331.0	1.49	80.4	0.66	0.52	0.36	0.29	1104	334	511	11	18	41	376
497	332.8	1.64	81.3	0.72	0.57	0.43	0.33	972	287	847	14	26	48	439
508	335.0	2.19	79.0	0.73	0.60	0.43	0.34	1383	280	1189	16	33	58	448
517	336.8	1.15	80.0	0.69	0.57	0.41	0.33	1374	329	748	13	25	43	417
528	339.0	1.24	77.2	0.83	0.68	0.46	0.39	1333	284	537	16	22	42	508
538	341.0	0.93	77.9	0.84	0.69	0.45	0.39	1438	310	462	15	20	43	525
548	351.8	0.64	76.3	0.87	0.72	0.44	0.40	1630	385	248	14	17	46	547
557	361.5	0.70	71.3	1.07	0.88	0.52	0.48	2137	497	275	17	20	56	652
568	370.5	0.53	61.8	0.38	1.15	0.67	0.63	3217	685	618	24	33	79	867
577	375.0	0.42	79.2	0.75	0.59	0.46	0.35	1210	359	637	15	21	43	483
586	380.8		78.8	0.68	0.52	0.41	0.31	1511	416	735	12	20	43	399

Table 2. Element contents and rad ratio in Core MD 90940. Element concentrations are given in %, or in ppm (mg/g).

Depth (cmbsf)	Age (ka)	Mg/Ca	Ti/Al	Fe/Al	Mg/Al	K/Al	Ba/Al (x10⁴)	P/Al (x10⁴)	Mn/Al (x10⁴)	V/Al (x10⁴)	Cu/Al (x10⁴)	Ni/Al (x10⁴)
7	3.7	0.011	0.052	0.736	0.698	0.434	2 164	753	864	01 9	07 5	03 6
17	8.9	0.011	0.053	0.723	0.809	0.447	2 062	804	730	01 9	06 8	03 2
27	14.2	0.013	0.064	0.800	0.573	0.440	1 580	379	728	02 1	04 9	03 3
36	19.0	0.012	0.062	0.797	0.580	0.435	1 549	426	490	02 0	04 8	02 6
47	22.8	0.011	0.063	0.803	0.607	0.443	1 607	461	675	02 1	04 3	03 0
56	25.9	0.010	0.061	0.782	0.636	0.436	1 751	567	907	02 0	05 1	03 3
64	29.7	0.010	0.063	0.786	0.625	0.446	1 705	1 288	564	01 8	04 3	02 5
78	41.3	0.011	0.062	0.786	0.643	0.446	1 618	595	445	02 0	04 3	02 3
85	47.2	0.011	0.062	0.787	0.607	0.443	1 538	503	692	02 0	05 1	02 8
95	54.2	0.014	0.063	0.783	0.542	0.434	1 351	384	1 077	01 9	05 8	02 5
106	58.6	0.014	0.062	0.780	0.537	0.439	1 405	418	305	02 0	03 7	02 1
116	62.6	0.015	0.060	0.784	0.461	0.431	1 592	348	410	01 9	04 4	02 2
127	68.8	0.015	0.060	0.796	0.459	0.429	1 592	343	320	01 8	04 3	01 8
135	74.8	0.012	0.058	0.789	0.487	0.421	1 807	380	371	01 7	04 9	02 0
146	82.6	0.011	0.059	0.797	0.481	0.430	1 699	381	671	01 9	05 9	02 2
156	89.2	0.011	0.059	0.803	0.487	0.421	1 913	404	1 111	01 8	07 2	02 9
166	95.7	0.014	0.060	0.802	0.473	0.418	1 974	344	815	01 8	06 2	02 7
175	105.1	0.018	0.062	0.807	0.468	0.422	2 017	365	945	01 8	06 3	02 9
186	122.0	0.018	0.061	0.809	0.473	0.427	2 035	348	468	01 8	04 8	02 2
196	136.5	0.019	0.067	0.798	0.566	0.455	1 230	339	1 765	02 3	09 3	06 4
206	151.0	0.018	0.070	0.780	0.604	0.484	1 651	327	1 222	02 3	06 6	05 8
216	154.1	0.019	0.069	0.798	0.596	0.479	1 490	301	1 072	02 2	05 0	04 4
226	157.2	0.018	0.066	0.767	0.589	0.478	1 304	289	770	02 0	04 7	03 1
236	160.2	0.019	0.066	0.779	0.589	0.484	1 329	278	242	02 0	03 6	02 8
246	163.3	0.020	0.066	0.779	0.589	0.484	1 453	280	257	02 0	04 0	02 6
256	166.4	0.018	0.068	0.789	0.600	0.478	1 508	286	664	02 1	05 4	03 9
266	169.5	0.014	0.064	0.785	0.570	0.468	1 518	301	2 008	02 3	05 4	02 8
276	173.9	0.014	0.064	0.744	0.564	0.462	1 569	335	645	02 1	04 9	02 3
286	179.6	0.016	0.065	0.806	0.538	0.462	1 761	323	166	02 0	04 8	02 6
296	184.8	0.018	0.064	0.813	0.495	0.458	2 065	331	138	01 8	05 0	02 1
306	189.4	0.015	0.061	0.859	0.500	0.457	1 921	401	157	01 6	06 4	02 0
316	194.0	0.011	0.059	0.776	0.522	0.448	2 204	497	293	01 6	06 1	01 8
326	216.0	0.011	0.060	0.765	0.544	0.456	1 709	435	294	01 6	05 6	01 9
335	221.1	0.013	0.063	0.763	0.525	0.463	1 485	371	299	01 8	05 4	01 8
345	226.7	0.014	0.062	0.773	0.500	0.455	1 781	364	365	01 8	05 3	01 9
354	231.8	0.013	0.060	0.813	0.560	0.440	1 840	424	487	01 7	05 6	02 1
365	238.0	0.012	0.061	0.806	0.612	0.463	1 261	396	715	01 8	06 0	03 9
374	242.7	0.012	0.063	0.810	0.672	0.466	1 686	397	1 305	02 1	07 4	04 5
386	249.0	0.010	0.062	0.788	0.673	0.481	2 221	425	929	01 9	05 8	03 1
394	257.0	0.010	0.061	0.784	0.667	0.471	1 973	443	859	02 0	05 7	03 1
406	261.4	0.013	0.062	0.792	0.597	0.458	1 619	374	567	01 8	04 6	02 9
416	265.0	0.018	0.063	0.808	0.545	0.465	1 520	331	383	01 9	04 6	02 3
427	269.0	0.023	0.065	0.846	0.520	0.472	1 650	288	446	02 0	05 0	02 7
436	287.0	0.011	0.058	0.821	0.537	0.448	1 890	446	579	01 5	05 7	02 2
448	297.2	0.010	0.057	0.803	0.541	0.459	1 916	497	549	01 6	05 6	02 1
458	305.6	0.010	0.057	0.803	0.541	0.443	2 007	498	507	01 5	05 6	02 0
468	314.1	0.013	0.057	0.825	0.513	0.450	2 016	465	594	01 6	06 1	02 1
478	322.5	0.013	0.057	0.842	0.526	0.461	2 266	520	654	01 7	06 3	02 8
488	331.0	0.011	0.057	0.788	0.545	0.439	1 673	506	774	01 7	06 2	02 7
497	332.8	0.013	0.061	0.792	0.597	0.458	1 350	399	1 176	01 9	06 7	03 6
508	335.0	0.014	0.061	0.822	0.589	0.466	1 895	384	1 629	02 2	07 9	04 5
517	336.8	0.013	0.060	0.826	0.594	0.478	1 991	477	1 084	01 9	06 2	03 6
528	339.0	0.015	0.061	0.819	0.554	0.470	1 606	342	647	01 9	05 1	02 7
538	341.0	0.014	0.062	0.821	0.536	0.464	1 712	369	550	01 8	05 1	02 4
548	351.8	0.014	0.063	0.828	0.506	0.460	1 874	443	285	01 6	05 3	02 0
557	361.5	0.018	0.061	0.822	0.486	0.449	1 997	464	257	01 6	05 2	01 9
568	370.5	0.027	0.064	3.026	1.763	1.658	8 466	1 803	1 626	06 3	208	08 7
577	375.0	0.015	0.059	0.787	0.613	0.467	1 613	479	849	02 0	05 7	02 8
586	380.8	0.013	0.027	0.7647	0.603	0.456	2 222	612	1 081	01 8	06 3	02 9

Table 3. Al normalized elements in Core MD 90940.

Depth (cmbsf)	Age (ka)	bulk MAR	CaCO3 MAR	Al MAR	Fe MAR	Mg MAR	K MAR	Ba MAR	P MAR	Mn MAR	V MAR	Ni MAR	Cu MAR	Ti MAR
0.38	3.7	1.37	1.13	7.24	5.32	5.05	3.14	1.57	0.54	0.63	0.01	0.03	0.05	0.38
0.35	8.9	1.39	1.16	6.51	4.71	5.26	2.91	1.34	0.52	0.48	0.01	0.02	0.04	0.35
0.66	14.2	1.37	1.13	10.28	8.22	5.89	4.52	1.62	0.39	0.75	0.02	0.03	0.05	0.66
0.78	19.0	1.82	1.50	12.53	9.99	7.26	5.45	1.94	0.53	0.61	0.03	0.03	0.06	0.78
0.81	22.8	2.11	1.77	12.88	10.35	7.81	5.70	2.07	0.59	0.87	0.03	0.04	0.05	0.81
0.72	25.9	2.14	1.80	11.80	9.22	7.51	5.15	2.07	0.67	1.07	0.02	0.04	0.06	0.72
0.30	29.7	0.87	0.73	4.86	3.82	3.04	2.17	0.83	0.63	0.27	0.01	0.01	0.02	0.30
0.31	41.3	0.89	0.74	4.96	3.90	3.19	2.21	0.80	0.29	0.22	0.01	0.01	0.02	0.31
0.33	47.2	0.87	0.72	5.31	4.18	3.22	2.35	0.82	0.27	0.37	0.01	0.01	0.03	0.33
0.93	54.2	1.78	1.40	14.79	11.58	8.02	6.42	2.00	0.57	1.59	0.03	0.04	0.09	0.93
0.88	58.6	1.71	1.35	14.06	10.97	7.54	6.17	1.98	0.59	0.43	0.03	0.03	0.05	0.88
1.06	62.6	1.72	1.32	17.56	13.77	8.09	7.58	2.80	0.61	0.72	0.03	0.04	0.08	1.06
0.55	68.8	0.94	0.70	9.19	7.31	4.22	3.94	1.46	0.31	0.29	0.02	0.02	0.04	0.55
0.43	74.8	0.98	0.78	7.44	5.87	3.62	3.13	1.34	0.28	0.28	0.01	0.01	0.04	0.43
0.54	82.6	1.15	0.96	9.07	7.23	4.36	3.90	1.54	0.35	0.61	0.02	0.02	0.05	0.54
0.52	89.2	1.15	0.94	8.75	7.02	4.26	3.68	1.67	0.35	0.97	0.02	0.03	0.06	0.52
0.55	95.7	1.01	0.76	9.18	7.36	4.34	3.83	1.81	0.32	0.75	0.02	0.03	0.06	0.55
0.28	105.1	0.41	0.29	4.51	3.64	2.11	1.90	0.91	0.16	0.43	0.01	0.01	0.03	0.28
0.27	122.0	0.40	0.29	4.42	3.57	2.09	1.89	0.90	0.15	0.21	0.01	0.01	0.02	0.27
0.30	136.5	0.46	0.34	4.55	3.63	2.57	2.07	0.56	0.15	0.80	0.01	0.03	0.04	0.30
0.50	151.0	0.78	0.60	7.12	5.56	4.31	3.44	1.18	0.23	0.87	0.02	0.04	0.05	0.50
1.42	154.1	2.19	1.63	20.63	16.46	12.29	9.87	3.07	0.62	2.21	0.05	0.09	0.10	1.42
1.29	157.2	2.17	1.63	19.51	14.95	11.49	9.32	2.54	0.56	1.50	0.04	0.06	0.09	1.29
1.28	160.2	2.03	1.49	19.28	15.02	11.36	9.33	2.56	0.54	0.47	0.04	0.05	0.07	1.28
1.23	163.3	1.96	1.40	18.65	14.52	10.99	9.03	2.71	0.52	0.48	0.04	0.05	0.07	1.23
1.31	166.4	2.15	1.65	19.39	15.30	11.64	9.27	2.92	0.55	1.29	0.04	0.08	0.11	1.31
1.18	169.5	2.34	1.86	18.45	14.48	10.51	8.64	2.80	0.56	3.70	0.04	0.05	0.10	1.18
0.61	173.9	1.23	0.99	9.60	7.14	5.41	4.43	1.51	0.32	0.62	0.02	0.02	0.05	0.61
0.75	179.6	1.24	0.96	11.55	9.31	6.21	5.34	2.03	0.37	0.19	0.02	0.03	0.06	0.75
0.96	184.8	1.41	1.01	15.09	12.27	7.48	6.91	3.12	0.50	0.21	0.03	0.03	0.08	0.96
0.82	189.4	1.47	1.13	13.54	11.63	6.77	6.18	2.60	0.54	0.21	0.02	0.03	0.09	0.82
0.22	194.0	0.57	0.47	3.84	2.98	2.01	1.72	0.85	0.19	0.11	0.01	0.01	0.02	0.22
0.22	216.0	0.55	0.45	3.71	2.84	2.02	1.69	0.63	0.16	0.11	0.01	0.01	0.02	0.22
0.65	221.1	1.29	1.03	10.30	7.86	5.41	4.76	1.53	0.38	0.31	0.02	0.02	0.06	0.65
345	226.7	1.27	0.99	11.21	8.66	5.61	5.10	2.00	0.41	0.41	0.02	0.02	0.06	0.70
354	231.8	1.29	1.03	9.65	7.85	5.41	4.25	1.78	0.41	0.47	0.02	0.02	0.05	0.58
365	238.0	1.42	1.16	9.48	7.64	5.80	4.39	1.20	0.38	0.68	0.02	0.04	0.06	0.58
374	242.7	1.46	1.21	8.46	6.86	5.69	3.94	1.43	0.34	1.10	0.02	0.04	0.06	0.53
386	249.0	1.00	0.84	5.20	4.10	3.50	2.50	1.16	0.22	0.48	0.01	0.02	0.03	0.32
394	257.0	1.36	1.15	6.96	5.46	4.64	3.27	1.37	0.31	0.60	0.01	0.02	0.04	0.43
406	261.4	2.03	1.64	14.59	11.55	8.71	6.69	2.36	0.55	0.83	0.03	0.04	0.07	0.91
416	265.0	1.88	1.40	18.61	15.04	10.15	8.65	2.83	0.62	0.71	0.04	0.04	0.09	1.17
427	269.0	0.61	0.42	7.50	6.34	3.90	3.54	1.24	0.22	0.33	0.01	0.02	0.04	0.48
436	287.0	0.63	0.51	4.21	3.45	2.26	1.88	0.79	0.19	0.24	0.01	0.01	0.02	0.24
448	297.2	0.95	0.78	5.77	4.64	3.12	2.65	1.11	0.29	0.32	0.01	0.01	0.03	0.33
458	305.6	0.97	0.81	5.91	4.75	3.20	2.62	1.19	0.29	0.30	0.01	0.01	0.03	0.34
468	314.1	0.88	0.68	7.02	5.79	3.60	3.16	1.42	0.33	0.42	0.01	0.01	0.04	0.40
478	322.5	0.85	0.67	6.47	5.45	3.40	2.98	1.47	0.34	0.42	0.01	0.02	0.04	0.37
488	331.0	3.74	3.01	24.70	19.46	13.47	10.85	4.13	1.25	1.91	0.04	0.07	0.15	1.41
497	332.8	3.69	3.00	26.55	21.02	15.86	12.17	3.58	1.06	3.12	0.05	0.10	0.18	1.62
508	335.0	3.65	2.88	26.63	21.89	15.69	12.40	5.05	1.02	4.34	0.06	0.12	0.21	1.63
517	336.8	3.65	2.92	25.20	20.82	14.97	12.05	5.02	1.20	2.73	0.05	0.09	0.16	1.52
528	339.0	3.53	2.72	29.27	23.98	16.22	13.75	4.70	1.00	1.89	0.06	0.08	0.15	1.79
538	341.0	1.02	0.80	8.59	7.06	4.60	3.99	1.47	0.32	0.47	0.02	0.02	0.04	0.54
548	351.8	0.64	0.49	5.56	4.60	2.81	2.56	1.04	0.25	0.16	0.01	0.01	0.03	0.35
557	361.5	0.61	0.43	6.52	5.36	3.17	2.92	1.30	0.30	0.17	0.01	0.01	0.03	0.40
568	370.5	1.12	0.69	4.27	12.93	7.53	7.08	3.62	0.77	0.69	0.03	0.04	0.09	0.98
577	375.0	1.27	1.01	9.53	7.50	5.85	4.45	1.54	0.46	0.81	0.02	0.03	0.05	0.61

Table 4 : Bulk MAR and element MARs in Core MD90 940. Bulk MAR and major element MARs are given in g/cm^2/kyr, and trace elements MARs in mg/cm^2/kyr.

Depth (cmbsf)		7	56	95	116	146	186	296	316
Age (ka)		3.7	25.9	54.2	62.6	82.6	122	184.8	194
Carbonate-linked fraction	ppm Ba	30	15	7	23	23	29	21	33
	% Ba	2.6	1.6	0.6	1.4	1.7	1.3	1.0	2.2
Oxyhydroxide-bound fraction	ppm Ba	140	115	143	130	114	169	126	176
	% Ba	12.2	11.9	12.7	8.0	8.3	7.6	5.7	11.9
Terrigenous fraction	ppm Ba	73	76	116	141	109	152	148	93
	% Ba	6.4	7.9	10.3	8.7	7.9	6.8	6.7	6.3
Residual = barite fraction	ppm Ba	904	757	856	1330	1127	1888	1915	1175
	% Ba	78.8	78.6	76.3	81.9	82.1	84.4	86.7	79.6

Table 5a. Core MD 90940. Distribution of barium within the different fractions of the sediment: carbonates, oxy-hydroxides, aluminosilicates, and residual (barite) fractions.

Based upon the observations of Kling and Boltovskoy (1995) on the vertical distribution of the plankton in the eastern Pacific, the abundance of some radiolarian species characteristic of the surface layer (*Heliodiscus asteriscus*, *Lithopera bacca*, and *Siphonosphaera polysiphonia*), and of the thermocline layer (*Cycladophora d. davisiana*, *Cycladophora d. cornutoïdes*, *Cyrtolagena laguncula*, *Eucyrtidium calvertense*, *Larcopyle bütschli* and *Spongopyle osculosa*) were counted for each level, and a ratio of the total of the individuals of the thermocline population versus the total of the individuals of the surface population was calculated. This radiolarian index (called rad ratio) can be used as an indicator of the fertility of the upper layers of the ocean: when the food supply in the surface layer increases, the surficial planktic populations, including the radiolarians, are thriving. Resulting increase in fecal pellets and food transport towards the deeper water masses allows the thermocline populations to grow. As a result, the thermocline/surface ratio calculated for the exported populations of radiolarians increases.

Depth (cmbsf)		16	79	355	872	1296	1450
Age (ka)		4.64	14.68	71.47	192.5	301.1	348
Carbonate-linked fraction	ppm Ba	57	38	38	36	51	42
	% Ba	7	7	4	5	10	9
Oxyhydroxide-bound fraction	ppm Ba	110	118	191	220	85	83
	% Ba	14	22	22	28	17	18
Terrigenous fraction	ppm Ba	623	377	615	530	372	328
	% Ba	79	71	72	66	73	72
Residual = barite fraction	ppm Ba	1	1	6	11		
	% Ba			1	1		

Table 5b: Core MD 85668. Distribution of barium within the different fractions of the sediment: carbonates, oxy-hydroxydes, aluminosilicates, and residual (barite) fractions. (Data from Tribovillard et al., 1996).

Radiolarians are sensible to the intensity of dissolution during the settling of particles through the water column and within the sediment. Changes in opal dissolution can, thus modify the resulting composition of fossil radiolarian assemblages. Siliceous skeletons are submitted to dissolution, but sea water is Si-undersaturated from the surface layer to the bottom of the ocean, and variations of sedimented radiolarian populations can be considered as linked to variations in the surface productivity rather than to variations of the dissolution strength (Berger, 1968). Within the sediment, it is known that opal dissolution occurs within the first centimeters under the water/sediment interface (Johnson, 1974; 1976), but in areas submitted to a significant export of siliceous debris, this dissolution leads to a Si saturation of the interstitial water and the dissolution stops at nearly 20/30 cm under the interface. Under fertile water masses, the variations of the radiolarian content in the sediment can, thus, be considered as representative of the surface productivity changes.

Radiolarian slides were prepared following the next procedure: first, the sediment was dispersed, using a water softener; second the organic matter was removed by boiling the residue in 20% concentrated H_2O_2. After clearing, the residue was treated with hot HCl (8N). The residual fraction was rinsed with distilled water and sieved at 50 μm. Occurrences of representatives of selected radiolarian species were counted on a microscopic slide and the ratio of specimens characteristic of the thermocline *versus* the total of specimens living at the surface was calculated. Rad ratio values calculated for the Madingley Rise (Core MD 90940) are summarized in Table 2.

In the Somali Basin (Core MD 85668), such a rad ratio was not calculated because a statistical analysis of foraminiferal and radiolarian assemblages was already carried out (Vénec-Peyré et al., 1997).

3. Results and interpretations

3.1. Chronological framework

For the Somali Basin Core (MD 85668), the age model was established through the $\delta^{18}O$ isotope stratigraphy from one part upon hand-picked foraminifers by Vénec-Peyré et al.

(1995, 1997), and from the other part upon bulk sediment by Shackelton et al. (1993). Both methods give consistent results.

For the Madingley Rise Core (MD 90940), the age model is established through the $\delta^{18}O$ isotope stratigraphy upon bulk sediment. The Core MD 90940 age model is confirmed by the datation of the first appearance of the radiolarian *Buccinosphaera invaginata* at 189 ka (previously dated at 170 $\pm$ 10 ka by Johnson et al., 1989).

Comparison of the $\delta^{18}O$ record of the bulk sediment for the last 140 kyr in Core MD 90940 and in Core MD 85668 shows a good correlation (Fig. 3.b). During isotope stages 1 and 5 (especially substage 5.5), $\delta^{18}O$ values in Core MD 85668 are more negative than in Core MD 90940. This may reflect a stronger carbonate dissolution in core MD 90940 during these intervals. No comparison was established for the record of samples from 140 to 380 ka B.P., but the correlation between both bulk $\delta^{18}O$ records for the last 140 kyr permits the establishment of a chronological framework for Core MD 90940 based on the bulk $\delta^{18}O$ record for the last 380 kyr. The radiolarian species assemblage of the lowest samples in Core MD 90940 reveals, however, that the sediment older than 352 ka B.P. is strongly reworked. Samples from below 549 cm contain about 20% reworked Eocene material. The oldest part of the isotope curve cannot, thus, be used in the chronological framework. Above this sample, no reworked material was observed. This lack of reworked fauna and the good correlation with the results of Shackleton et al. (1993) based on the bulk sediment of Core MD 85668, indicate that the chronological framework established for the last 350 kyr in Core MD 90940 is reliable. The rad ratio defined above is a means to test the validity of the age model. The good correlation between the bulk MAR and the rad ratio (Fig. 12) shows the coherency of the two signals, which are completely independent. As the bulk MAR depends directly on the age model, the validity of the age model is thus reinforced.

3.2. Geochemical markers in core MD 90940

3.2.1. Bulk Mass Accumulation Rate (MAR)

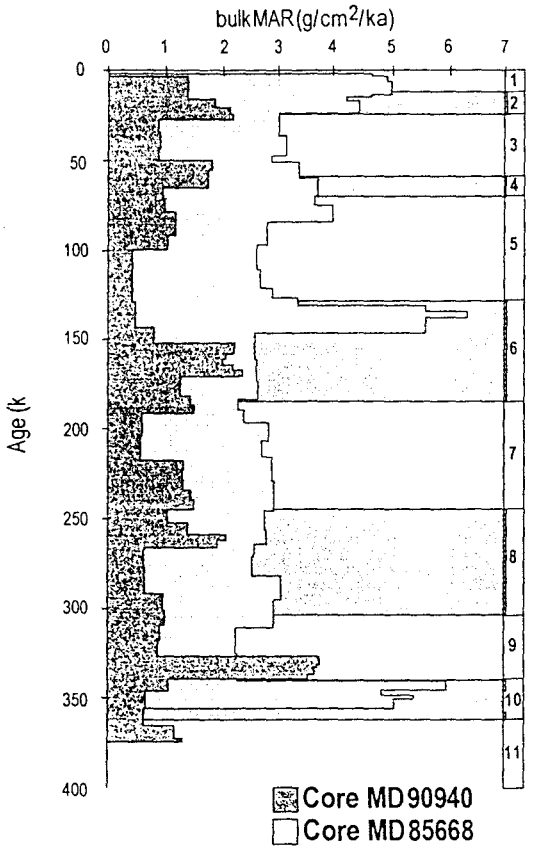

Figure 4. Variations of bulk MAR versus age in Cores MD 90940 (shaded area) and MD 85668 (light area).

Bulk MAR values calculated for the Madingley Rise core (MD 90940) during the last 400 kyr range from 0.5 to 3.5 g/cm^2/kyr (Fig. 4). Significant increases in MAR values are recorded during isotope stage 6 (2.3 g/cm^2/kyr), between 260 and 270 ka B.P. (2 g/cm^2/kyr), and for the interval between 330 and 340 ka B.P., i.e., from the 10/9 transition to the lower part of isotope stage 9 (3.5 g/cm^2/kyr). In this latter interval, MAR variations exhibit a peak value (3.5 g/cm^2/kyr), which can be considered as the most significant event at this site.

3.2.2. Geochemical proxies

Carbonate content in the Madingley Rise core (MD 90940) varies between 62% and 85% (Fig. 5). Carbonate fractions are composed of planktic foraminifers and coccolithophorids. During the last 400 kyr, the carbonate content distribution has changed as shown in Fig. 5. Lithogenic elements are not abundant: e.g. Al: 0.4 to 1.25% and Ti: 251 to 867 ppm (Fig. 5). These elements show a rather regular distribution throughout the core, with relatively higher values recorded at transition intervals 2/1 and 7/6, during isotope stages 4, 8, and in the lower part of isotope stage 11. Vanadium content correlates well with the lithogenic elements (Figs. 6 and 8). Thus, no diagenetical enrichment relative to the terrigenous supply is inferred. Barium content is high (from 845 to 3217 ppm) at all levels in the core, relative to deep-sea carbonate average values (Turekian and Wedepohl, 1961; Fig. 5). Barium-aluminium

relationship suggests some Ba enrichment compared to the land-derived Ba input (Figs. 6 and 7). Phosphorus content varies between 250 and 400 ppm with low values occurring during isotope stages 2 and 6, the earlier part of stages 5 and 8, and isotope stage 9. Barium peak values

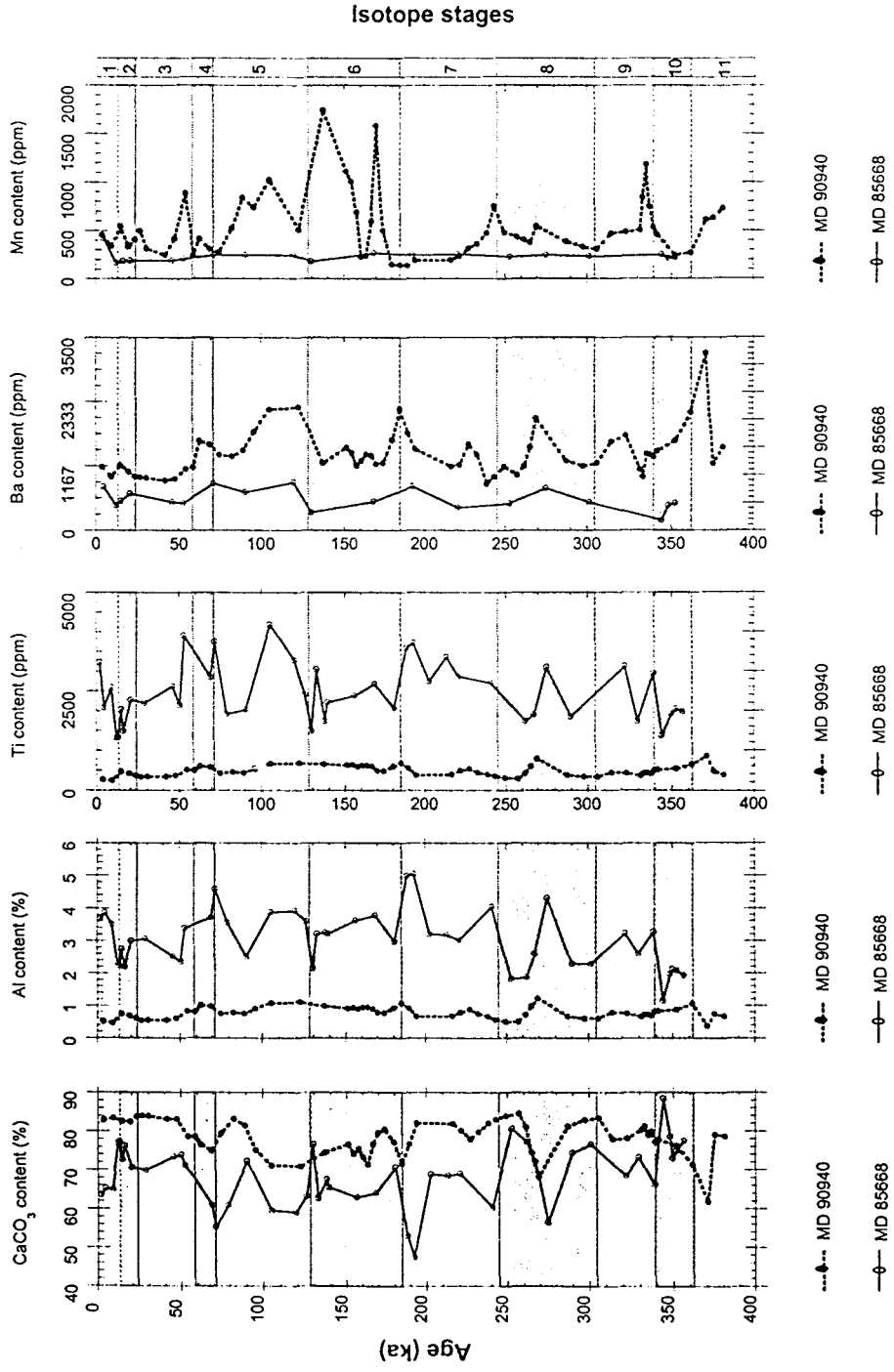

Figure 5: Variations of $CaCO_3$, Al, Ti, Baand Mn contents versus ages in cores MD 90940 and MD 85668.
Glacial isotope stages are identified as shaded areas.

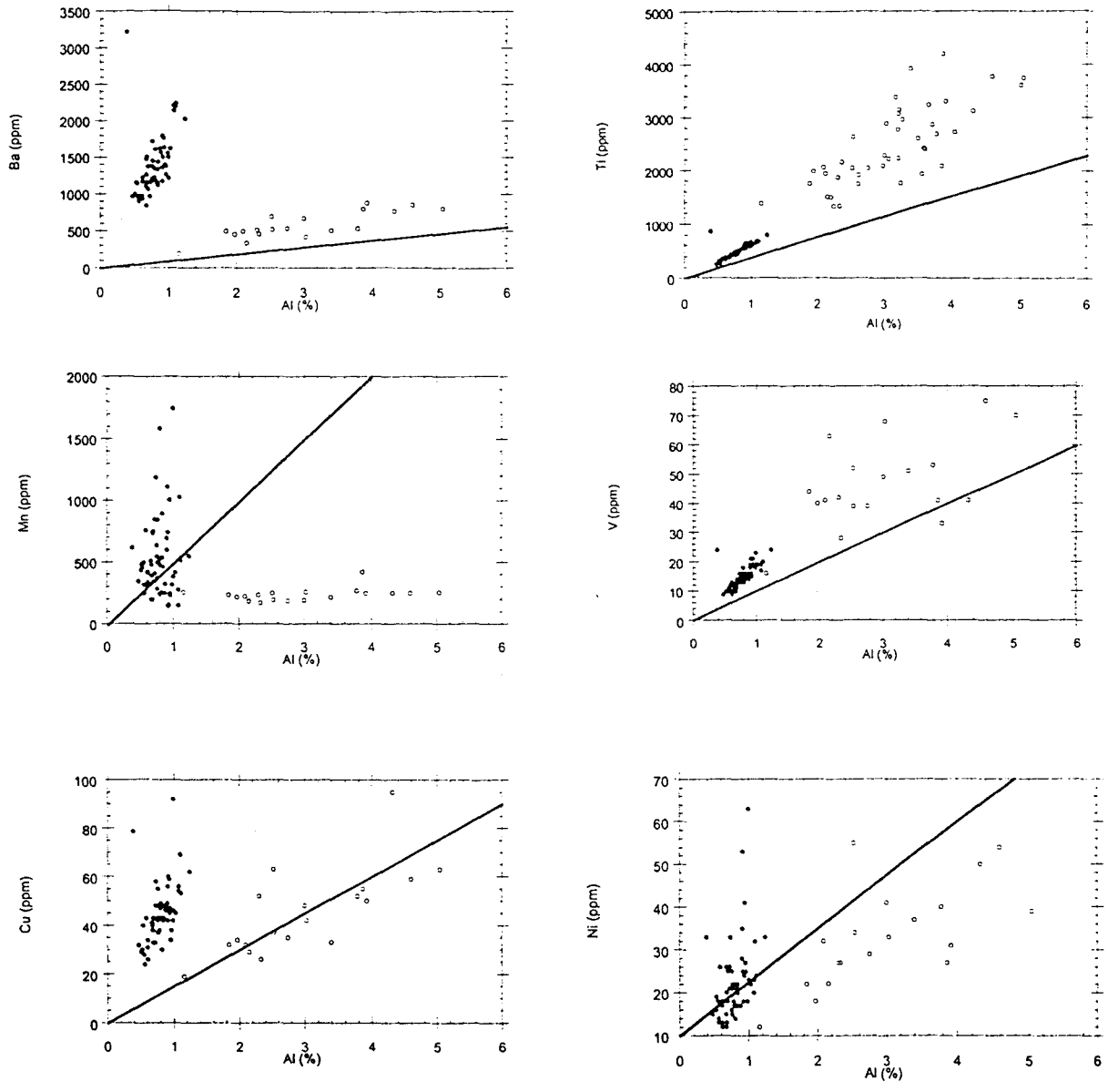

Figure 6: Variations trace element contents: Ba, Ti, Mn, V, Cu and Ni versus Al content in cores MD 90940 (black dots), and MD 85668 (light dots). Bold line represents the average value of each trace element in deep sea carbonates (data from Turekian & Wedepohl, 1961)

correlate with peak values of terrigenous elements. In the Madingley Rise core (MD 90940), Mn/Al, Cu/Al and Ni/Al variations exhibit coeval changes (Fig. 8). Rock-Eval pyrolysis indicates that the organic carbon content is always below 0.2 wt %.

3.2.3. Results of sequential leaching

Sequential leaching of the samples from the Madingley rise core (MD 90940) shows that barium is mainly accumulated as barite (81%), but it is also found within the aluminosilicate phase (7.5%) and adsorbed on the ferromanganese oxides (10%). The rest of the barium (1.5%) is linked to the carbonates (Fig. 9a). Without further analyses of barite (e.g. REE content measurements, or isotopic Sr ratios), biogenetic barite cannot be directly distinguished from diagenetically formed barite. Nevertheless, in the case of Core MD 90940, the disconnection between the distributions of Ba and Mn, which is very sensitive to diagenetical remobilization, indicates that barite must originate primarily from surface productivity rather than from diagenesis, and that barium content can be considered as a paleoproductivity proxy. Small contents of barium in oxyhydroxides phases of the sediment (10%) may result from a weak dissolution of barite (Van Santvoort et al. 1996) or come directly from organic matter.

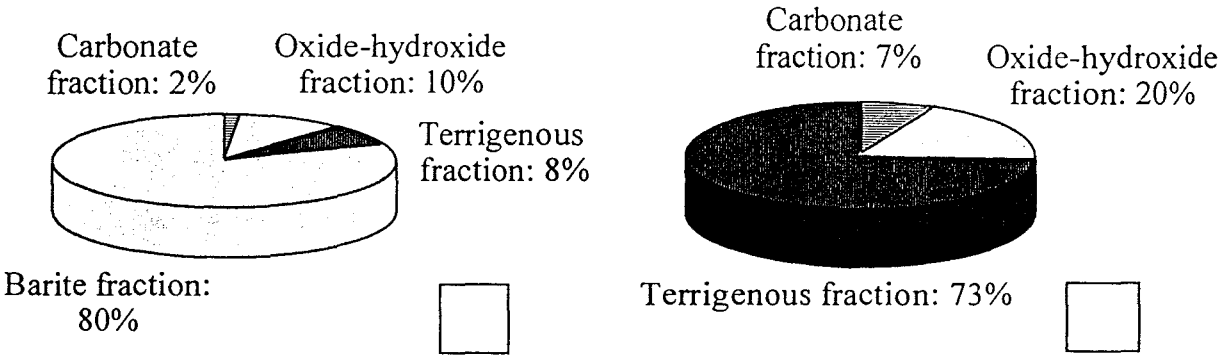

Figure 9. Mean distribution of barium bound to the different fractions of the sediment: carbonates, oxy-hydroxides, aluminosilicates, and residual (barite) fractions.
A = Madingley Rise Core MD 90940
B = Somali Basin Core MD 85668 (data from Tribovillard et al., 1996).

3.2.4. Element Mass Accumulation Rate

Changes in carbonate MAR monitor bulk MAR variations. $CaCO_3$ MAR varies from 0.3 to 3 g/cm^2/kyr (Fig. 10). The maximum Al MAR peaks at only 0.05 g/cm^2/kyr (Fig. 10). Barium MAR shows two well-defined peaks within isotope stage 9 (at 330 ka B.P. and between 335 and 340 ka B.P.). As for barium content, barium MAR is always high (2 to 6 mg/cm^2/kyr) (Fig. 10). Manganese MAR values are usually low (0.2 mg/cm^2/kyr). Peak values

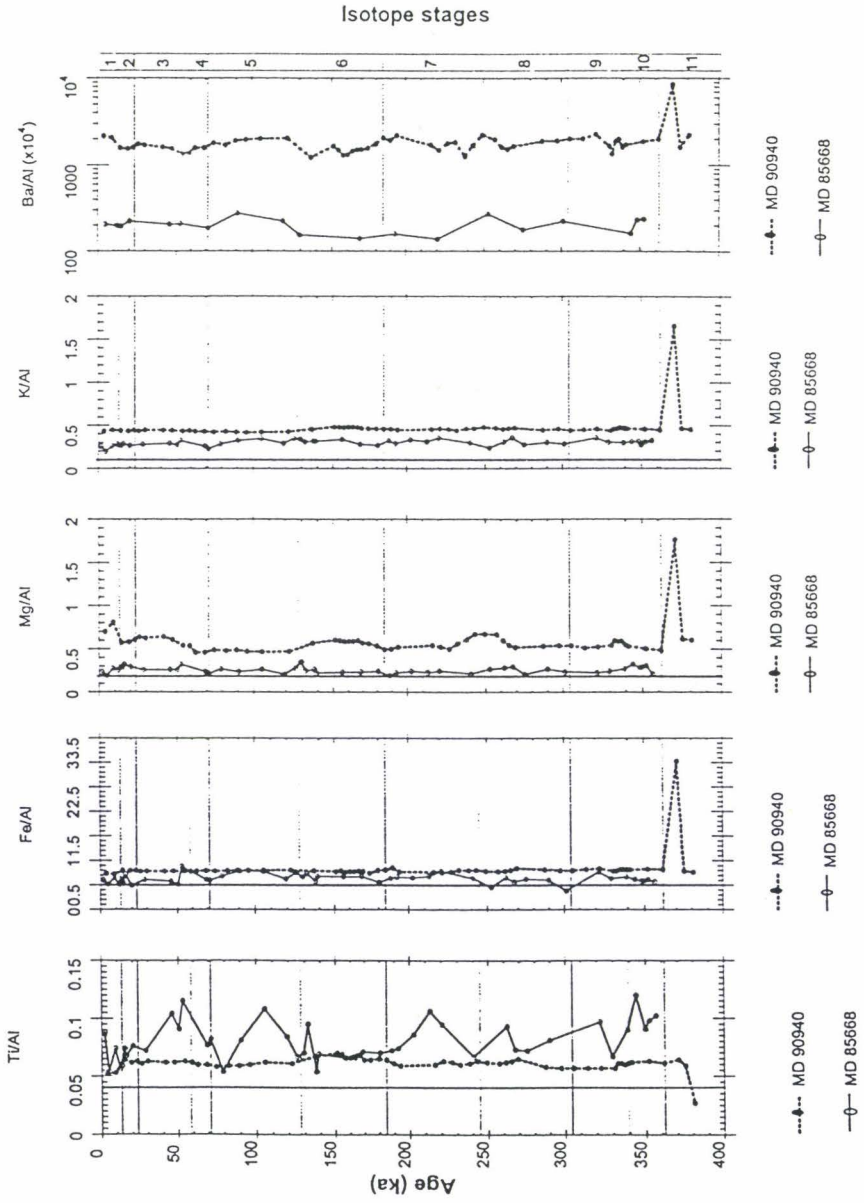

Figure 7: Variations of the Ti/Al, Fe/Al, K/Al, and Ba/Al ratios versus ages in Cores MD 90940 and 85668. The Ba/Al ratio is expressed with a logarithmic scale

Solid line = average value of the ratio in deep sea carbonates (after Turekian & Wedepohl, 1961)

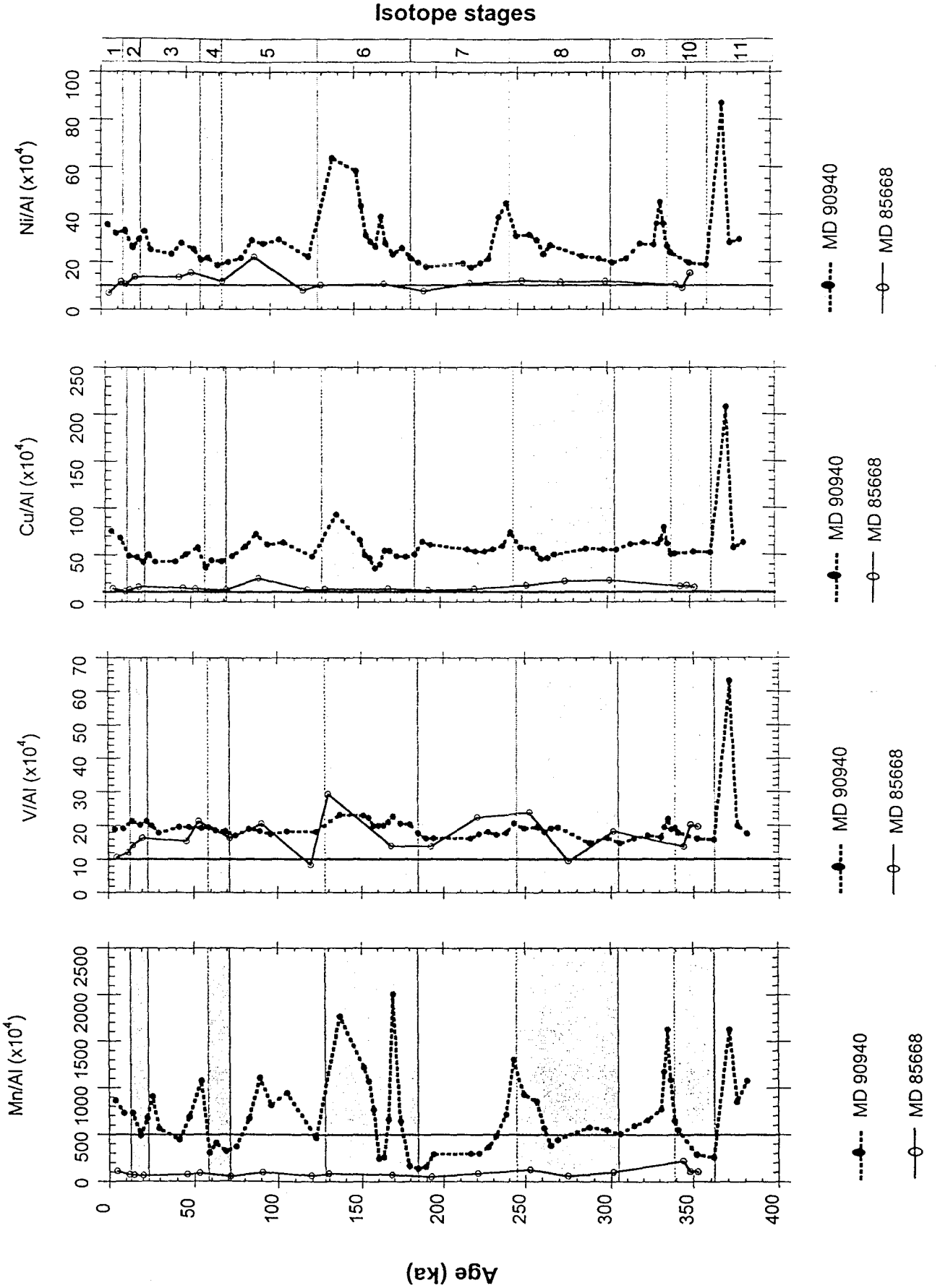

ure 8: Variations of the Mn/Al, V/Al, Cu/Al and Ni/Al ratios versus ages in Cores MD 90940 and 85668. The Ba/Al ratio is expressed with a logarithmic scale

Solid line = average value of the ratio in deep sea carbonates (after Turekian & Wedepohl, 1961)

(3.7 mg/cm^2/kyr) are recorded within isotope stage 6 (170 ka B.P.), where a double-spike occurs, and in early isotope stage 9. Lower intensity peaks (around 1 mg/cm^2/kyr) are related with maximum abundances in terrigenous elements (Fig. 11).

Copper and Ni MAR exhibits variations similar to the Mn MAR, despite minor discrepancies (Fig. 11).

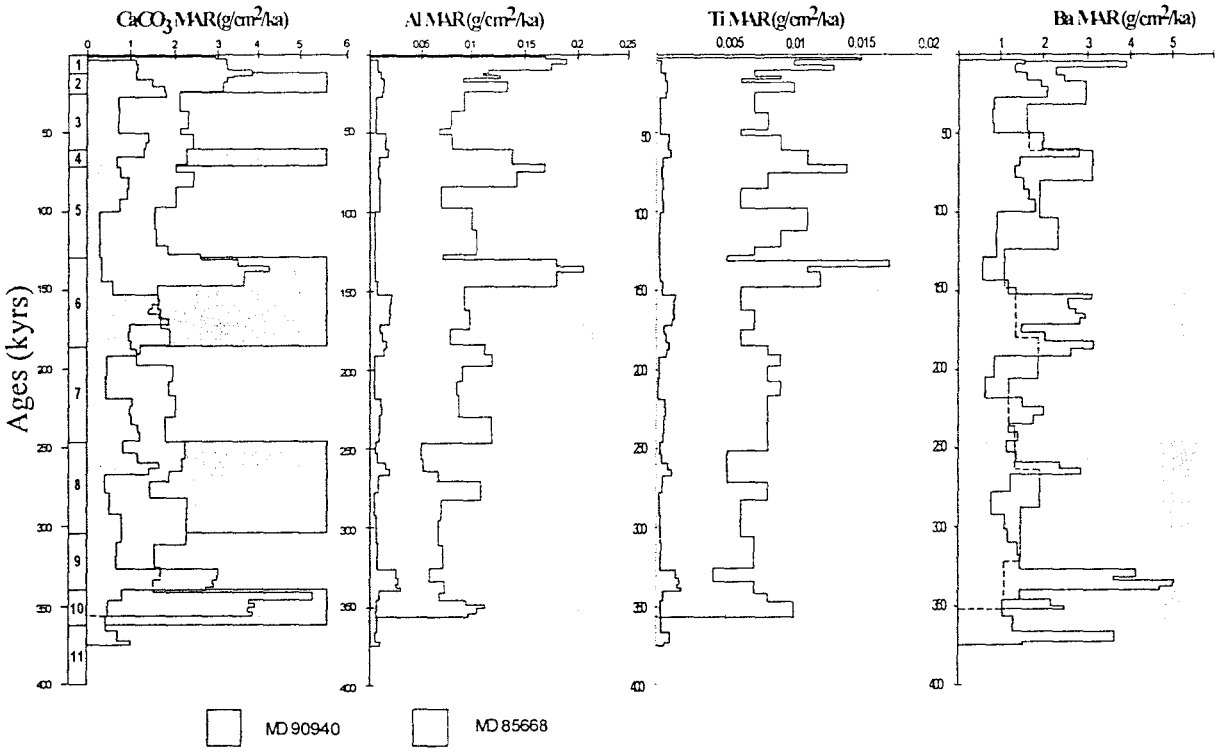

Figure 10. Variations of element MARs: Mn, V, Ni, and Cu, versus age in Cores MD 90940 (shaded areas) and MD 85668 (ligth areas).
Isotope stages are identified as light shaded areas.

3.2.5. The radiolarian Index (rad ratio)

In the Madingley Rise core (MD 90940), the rad ratio varies from 0.2 to 2.4. High rad ratio values are recorded at 155, 170, and 335 ka (Fig. 12). The variations of the rad ratio along the core correlate well with the variations of the bulk MAR, and thus with element MARs, despite some discrepancies, e.g.:150 to 105 ka (Fig. 12). Such a correlation indicates

that the bulk MAR variations are directly induced by the variations of surface productivity, and the discrepancies could be related to stronger carbonate dissolution periods.

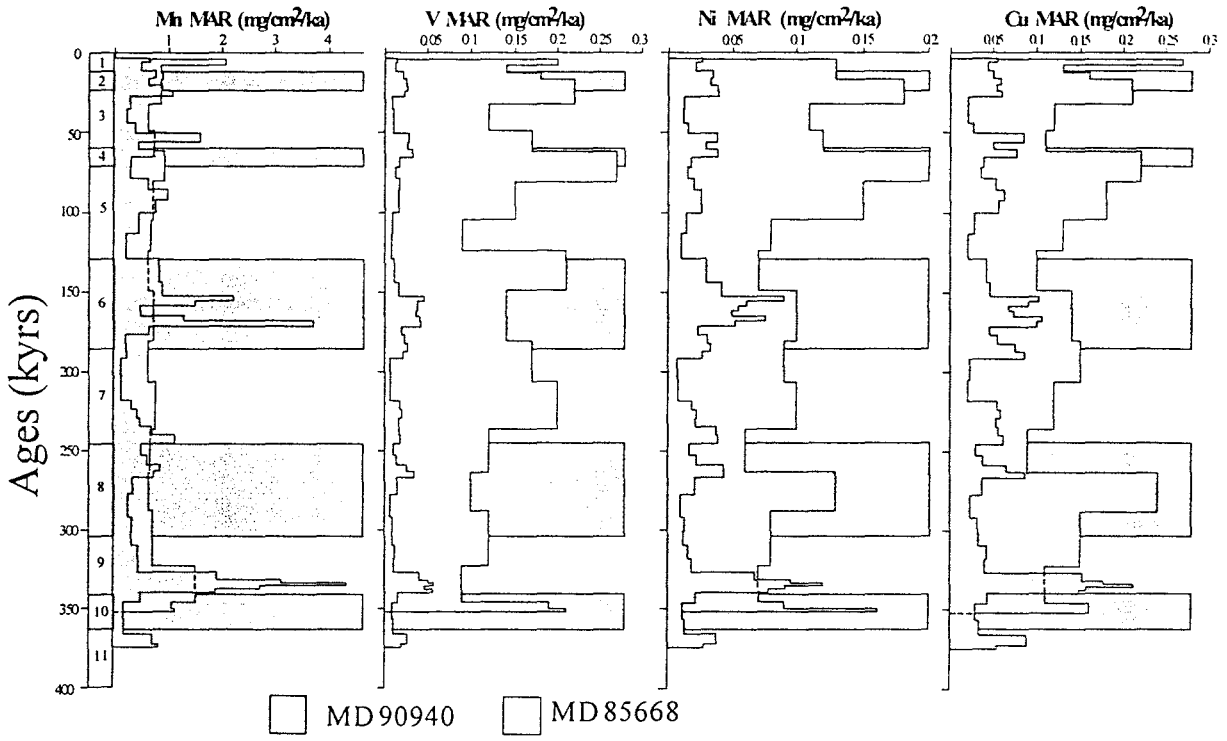

Figure 11. Variations of trace elements MARs: Mn, V, Ni, and Cu, versus age in Cores MD 90940 (shaded areas) and MD 85668 (light areas).
Isotope stages are identified as light shaded areas.

3.3. Geochemical markers in the Somali Basin core (MD 85668)

3.3.1. Bulk Mass Accumulation Rate (MAR)

In the Somali Basin core, bulk MAR records exhibit, for the last 360 kyr, strong alternations between high (4 to 6 g/cm^2/kyr) and low values (2 to 3 g/cm^2/kyr). All bulk MAR peaks correspond to glacial stages (Fig. 4).

3.3.2. Geochemical proxies

In the Somali Basin core, carbonate content can be relatively high, from 47.5 to 88.5% (Fig. 5). Large cyclic variations are, however, recorded with maximum values located during isotope stages 1 and 2, and 2/1 transition, and in the late part of glacial isotope stages 6, 8, and 10. Minimum values are found in the lower intervals of interglacial isotope stages 5 and 7. As well as bulk MAR, strong variations in carbonate content distinguish glacial from interglacial stages. Carbonate content variations are negatively correlated with changes in the terrigenous elements such as Al. All terrigenous elements, i.e. Al, Fe, Mg, K and Ti, exhibit similar downcore distributions (Fig. 5). In this core, the sediment contains a relatively high Ti-fraction compared to Al content (Ti/Al: 0.054 to 0.120) (Figs. 6 and 7). Bulk barium variations are similar to those of the terrigenous elements, suggesting that this element is mainly terrestrial in origin at this site (Fig. 5). Cu/Al and Ni/Al ratios also exhibit the same variations as the terrigenous elements (Fig. 8). Furthermore, Cu and Ni contents correlate well with the Al content (Fig. 6), testifying of the land-derived origin of both elements. Palynofacies analyses performed on selected samples, show that organic matter is uniquely composed of vascular plant debris. TOC content remains low along the core, and no marine organic matter was found (Tribovillard et al., 1996). From 400 ka B.P. to early isotope stage 1, Mn content values are relatively constant rating between 180 ppm and 240 ppm. During isotope stage 1, the Mn content values increase to a maximum of 421 ppm (Tribovillard et al., 1996). The values of the Mn/Al ratio ($50x10^{-4}$-$219x10^{-4}$) indicate a loss of Mn in this sediment compared to the average value of deep-sea carbonates (Turekian and Wedepohl, 1961) (Figs. 6 and 8). The P/Al ratio exhibits variations similar to those of the Mn/Al ratio. The V/Al ratio is generally above the average value of deep-sea carbonate (Figs. 6 and 7). Variations do not correlate with the record of any other element, be it diagenesis influenced, terrigenous or productivity-induced. Together with the low Mn/Al ratio, the high V/Al ratio could indicate that the sediment was dysoxic or slightly reducing.

3.3.3. Results of the sequential leaching

In the Somali Basin core, sequential leaching results show that 73% of the barium is linked to the terrigenous phase, 20% is oxyhydroxide-adsorbed, 7% is carbonate-bound and 0.3% is barite-Ba (Table 5). At this site, barium is, thus, essentially terrestrial in origin, even though a significant amount of barium is presently adsorbed on the Fe-Mn oxyhydroxides,

possibly resulting from barite dissolution (Thomson et al., 1993, 1995). Consequently, barium cannot be used as a paleoproductivity proxy at this site (Fig. 9.b).

3.3.4. Element Mass Accumulation Rate

Bulk MAR variations are primarily related to carbonate MAR variations. In this equatorial part of the Indian Ocean, carbonate MAR is higher during glacial stages than during interglacial ones (Fig. 10). Terrigenous element MARs (Al, Fe, Mg, K and Ti) exhibit peak values during isotope stages 6, 4, 2 and 1. Copper and Ni MARs show peak values during isotope stages 8, 4, 2 and 1 (Figs. 10 and 11). The barium MAR record does not correlate very well with the terrigenous element MARs, despite its detrital origin (Fig. 10). This suggests a diagenetical constraint, possibly related to a redox front in the core between a reducing layer and more oxic sediments laying above. Phosphorus and Mn MARs exhibit two strong peak values (2 $mg/cm^2/kyr$), around 10 ka B.P., and at the 10/9 transition (Fig. 11). Between these peak values, Mn MAR is roughly constant, and P MAR records little variations (0.75 to 1.25 $mg/cm^2/kyr$), with a higher value (1.4 $mg/cm^2/kyr$) at the 5/4 transition. This can be interpreted as more reducing conditions within the sediment, as further evidenced by a relatively higher V content. Changes in the V MAR record are correlated with changes in Cu, Ni and Ba MAR records down to 120 ka B.P. (Fig. 10 and 11). In older sediments, a peak value is recorded at the 6/5 transition, during isotope stage 7 (210 to 240 ka B.P.) and in late isotope stage 10.

3.4. Biological proxies

The statistical analysis carried out upon foraminiferal and radiolarian assemblages by Vénec-Peyré et al. (1997) indicates that high productivity periods are recorded during the glacial intervals, and are followed by a sharp decrease during the glacial/interglacial transitions. This classical pattern is, however, not observed at the 8/7 transition, but is recorded later in isotope stage 7 (218 ka B.P.).

4. Discussion of the geochemical proxies for both cores

The comparison between the major and trace elements, and the biological markers of surface productivity recorded in both cores allow us to determine the reliability of the geochemical markers of the paleoproductivity in the pelagic equatorial belt of the Northwestern Indian Ocean, in order to use them for a reconstruction of the variations of the paleoproductivity.

Due to their locations far off the African Continent and at depths greater than 3,500 m, the sediments deposited at both sites can be considered as pelagic. Lithologic and geochemical analyses show, however, that the expected sedimentary response is dissimilar at each location. Core MD 90940 recovered from the Madingley Rise, north of the Seychelles Plateau, is made of pure carbonate ooze with no terrigenous fraction (mean Al content = 0.8 wt %). Core MD 85668, recovered from the Somali Basin, contains calcareous oozes mixed with a small fraction (mean Al content = 3 wt %) of terrigenous debris originating from the Somalian Peninsula (El Foukali, 1995). Both sites are, however, located under the fertile equatorial productivity belt where present surface productivity is roughly estimated to be from 60 to 90 g $C/cm^2/y$ (Berger and Herguera, 1992).

Organic carbon contents measured in sediments from both cores do not reflect any paleoproductivity of such an order since TOC values of the Somali Basin (core MD 85668) do not exceed 0.4 % and are only of terrestrial origin (Tribovillard et al.,1996) while organic carbon is almost absent (TOC <0.2%) from the Madingley Rise core (MD 90940). This lack of marine organic matter can be related to different processes. First, according to the composition of the microfossil assemblages, coccolithophorids are abundant in this area and the organic matter they produce is known to be poorly preserved within the sediment. Second, due to the depth at which both cores were recovered, extensive remineralization of the organic matter can occur during settling through the water column. Third, low accumulation rates allow a more extensive remineralization at the water/sediment interface.

Bulk MAR values integrate biogenic component MARs as well as terrigenous debris MAR values. In the Madingley Rise core (MD 90940), sedimentation patterns can be considered as typical of pelagic sedimentation because its location on the inner levels of the Madingley Rise strongly limits any input of terrigenous debris from the Seychelles Plateau (less than 1.5% of Al). Bulk sediment MAR is low (1.53 $g/cm^2/kyr$ on average) but may be considered as a paleoproductivity proxy because it correlates well with the rad ratio (Fig. 12).

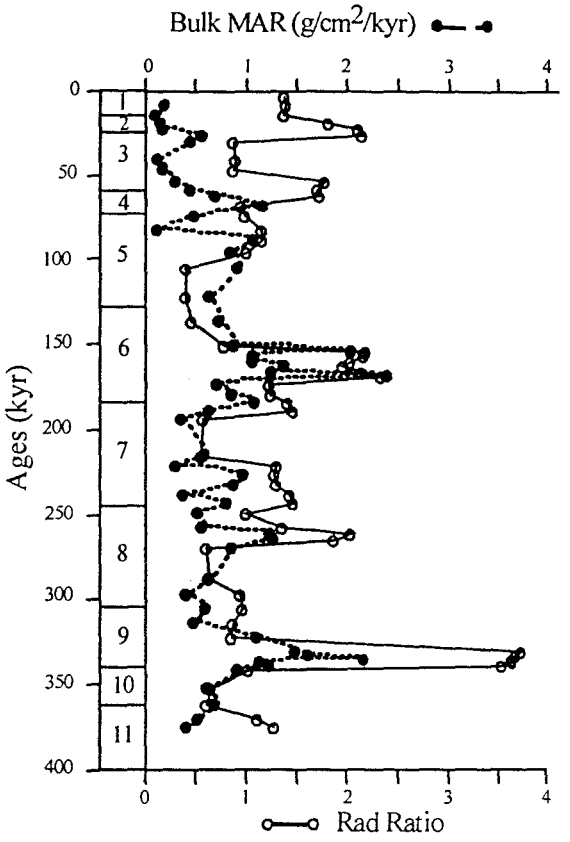

Figure 12. Variations of the bulk MAR (solid line) and the Rad ratio (dashed line) versus age in Core MD 90940.

Periods of high surface productivity with high sedimentation rates (1 to 4 g/cm^2/kyr) are recognized during time intervals comprised between 340 and 330 ka B.P., 270 and 220 ka B.P., 170 and 150 ka B.P., and at transition intervals between isotope stages 4/3 (59 ka B.P.) and 3/2 (24 ka B.P.). These periods including both glacial and interglacial stages, this pattern suggests that paleoproductivity at this site was not closely linked to global climatic changes. In the Somali Basin core (MD 85668), bulk MAR is almost three times higher (4 to 6 g/cm^2/kyr) than in core MD 90940.

This high bulk MAR can be related to the terrigenous supply, which is relatively higher at this site, although mean Al content is only 3 wt %. Biogenic carbonate is by far the main component of the sediment (from 48 to 89 %), and bulk MAR peak values correlate well with high carbonate content events during late isotope stage 6 (138 to 132 ka B.P.), early isotope stage 8 (301 to 289 ka B.P.), and stage 10 (350 to 344 ka B.P.). In the Somali Basin, as well as on the Madingley Rise, the bulk MAR variations can, thus, be linked with changes in surface productivity. The high productivity periods recognized through the biological proxies during glacial intervals, especially isotope stages 6 and 10 (Vénec-Peyré et al., 1997) are also recognized trough the bulk MAR and the element MARs, but Mn and P records. These results are in agreement with a climatic control, which induces high surface productivity (due to a stronger water mixing) during glacial intervals. Bulk MAR variations in core MD 90940 and core MD 85668 do not correlate, however, suggesting that sedimentation patterns, or paleoceanographic conditions, were different at both locations. This discrepancy may results from two factors: a disturbance of the surface signal by the terrigenous input, and/or a difference

in the surface productivity cycles between both sites. The lithogenic input is neglectible in Core MD 90940. The Ti/Al ratio is also very low (0.057 to 0.070). This ratio being considered as a wind strength proxy (Shimmield, 1992; Weedon and Shimmield, 1991), those low values, rating, however, above the deep-sea carbonates average values (Figs. 6 and 7), indicate that the Madingley Rise was subjected to a very low and constant aeolian input, with no variation between glacial and interglacial stages. We can, thus, consider that at this site the bulk MAR is directly linked to the surface productivity. In Core MD 85668, the terrigenous fraction is slightly more abundant and can, somehow, disturb the record of the surface productivity. The Ti/Al ratio is higher (0.054 to 0.120), suggesting an aeolian origin for a part of the terrigenous debris. Two detrital sources may be involved: a direct continental input (rivers and soil weathering), and an aeolian fraction originating from the Arabian Peninsula (El Foukali, 1995). According to the good correlation on the Madingley Rise between the rad ratio and the bulk MAR, and to the correspondence between the high surface paleoproductivity periods recognized in the Somali Basin by the biological markers and the bulk MAR, we can consider that bulk MAR variations are mostly related to the variations of the surface productivity at both locations. The differences between importance of the terrigenous inputs at both sites limit, however, the use of bulk MAR records for correlations between the two sites.

To avoid these uncertainties and to make use of the most abundant biological fraction of the sediment to track paleoproductivity changes, carbonate MAR can be used instead of bulk MAR because both cores are high in carbonate content. In both cores, bulk MAR and carbonate MAR exhibit almost the same variations (Figs. 4 and 10). Carbonate MAR of both cores, as well as bulk MAR, do not correlate. In Core MD 90940, carbonate MAR peak values are recorded during glacial and interglacial isotope stages, and the $CaCO_3$ MAR variations correlate well with the rad ratio, except between 370 to 340 ka, 290 and 270 ka, and 150 and 90 ka (see Figs 10 and 12). In Core MD 85668, carbonate MAR peak values mostly characterize glacial isotope stages. As previously stated, the sedimentation pattern in the Madingley Rise core (MD 90940) would suggest a regional control of oceanic processes whereas in the Somali Basin core (MD 85668), sedimentation would be more related to global climatic changes.

The use of carbonate MAR raises, however, the problem of the importance of carbonate dissolution. Marked variations in carbonate MAR can result from surface productivity, and/or dissolution variations. The depths of deposition (3,875 m for core MD 90940 and 4,020 m for

core MD 85668) are close to the present day CCD (around 3,800 m), making carbonate dissolution an important factor of sedimentation. According to Bassinot et al. (1994), the grain size of the sediment of the Northwestern Indian Ocean reflects the strength of the carbonate dissolution that is weakening the foraminiferal tests, and breaking them into smaller pieces. To test this possibility the sediment from Core MD 90940 was sieved into two fractions: < and >36 μm. Well preserved foraminiferal tests were observed in the coarser fraction despite some broken tests. The smaller fraction, that is prevalent in weight (from 55% to 75%) is mostly made of coccolithophorids. The presence of fragments and broken tests of foraminifers in the coarser fraction suggests that carbonate dissolution occurred, but no significant differences were observed between fractions accumulated in glacial and interglacial samples. Furthermore, the good correlation between the carbonate MAR and the rad ratio suggests that carbonate dissolution is not intense enough to strongly disturb the surface signal. The discrepancies observed between both records (Fig. 12) could, however, correspond to periods when the carbonate dissolution was stronger (e.g.: 150 to 105 ka, 310 to 290 ka). These data indicate that strong variations in the intensity of carbonate dissolution were relatively rare, and that the surface signal was not strongly disturbed. Vénec-Peyré et al. (1997) studied the effect of carbonate dissolution on the composition of the foraminiferal associations in Core MD 85668. Their results demonstrate that carbonate dissolution does not strongly disturb the composition of the species associations. They assumed that, even if not excluded, carbonate dissolution is not the main process controlling carbonate accumulation in this core.

Trace element (Ba, Mn, V, and P) contents and trace element MARs were analyzed because they can provide useful information on paleodepositional changes (Calvert and Pedersen, 1993; Lea and Spero, 1994; McManus et al., 1994; Paytan, 1995; Shimmield, 1992). Barite input being partly linked to surface productivity, barium record is frequently used to provide complementary information on paleoproductivity changes (Dymond et al., 1992; Francois et al., 1995; Gingele and Dahmke, 1994). In both cores, variations of bulk barium content correlate well with variations in terrigenous elements contents (Al, Fe, Mg, K, and Ti), and correlate negatively with carbonate contents variations. No correlation is observed between the bulk Ba content and the rad ratio in the Madingley Rise core. This may result from many factors. -1: barium is a minor component of feldspar (Shimmield et al., 1994 ; Shimmield and Jahnke, 1995) and is, thus, dependent on the terrigenous supply; -2: biogenic barium precipitates as barite, and is linked to surface productivity through siliceous

organisms, although small amounts of barium can be incorporated in foraminifer tests (Boyle, 1981; Lea and Boyle, 1989; Lea and Spero, 1994). The calcareous surface productivity may be not synchronous with the siliceous one, which can influence the Ba deposition in the sediment.

Results from sequential leaching of the sediment show that the barium sharing out is completely different between the sediment of Cores MD 90940 and MD 85668. In the "blue ocean" (Core MD 90940) barium is mainly present as barite, and can be related to the surface paleoproductivity, while in Core MD 85668, barium is mainly linked to the terrigenous input, with little or no barite (< 1%) found in the sediment. Despite the location of Core MD 85668 in the pelagic realm, its barium cannot be used as a paleoproductivity proxy. This lack of barite may result from various processes involving decreasing of barite precipitation, as well as barite dissolution within the water column and/or the sediment. Barite formation requires sulfate oversaturation in the surrounding microenvironment. Above the site of Core MD 85668, sedimentary particles settle across an intermediate layer of the Arabian Sea Water mass, which is oxygen-depleted (Swallow, 1984). The resulting strong discrepancies in the chemical parameters of the whole water column may have induced contrasted preservation/dissolution patterns regarding barite at both sites. For a similar surface productivity, a lesser amount of barite would, thus, reach the sediment in Core MD 85668 than in Core MD 90940. The lack of barite in Core MD 85668 can also be linked to barite dissolution. A significant amount (20%) of barium in the oxyhydroxides fraction was recorded in Core MD 85668. According to some authors (Thomson et al. 1995, Van Santvoort et al. 1996) this oxyhydroxides-bound barium is a residue of barite dissolution. Thus, our results would suggest that barite dissolution was more pronounced in Core MD 85668 than in Core MD 90940, where 10% only of the barium is oxyhydroxides-bound.

Intensity of barite dissolution being also related to the redox conditions in the sediment (Thomson et al., 1993, 1995; Van Santvoort et al. 1996), redox conditions can be estimated using both Mn and V contents records (Pruysers et al., 1993; Van Os et al., 1991). These two elements are known to have antinomic accumulation patterns: grossly, Mn precipitates mostly under oxic/suboxic (oxidizing) conditions, and V precipitates under reducing conditions (Calvert and Pedersen, 1993). The comparison between the Mn/Al and V/Al ratios in both cores exhibits a negative correlation (Fig. 10). High Mn content and low V content values were recorded in Core MD 90940. Mn content shows variations in this core, suggesting

changes in the redox conditions. Vanadium content is low, and its variations correlate well with variations in the terrigenous element contents, suggesting that the terrigenous input is the only V source at this site, and that no enrichment from the water column could occur. In Core MD 85668, Mn content is low, while V content values are higher than in Core MD 90940. These data suggest that redox conditions in Core MD 85668 were slightly more reducing than in Core MD 90940. Suboxic conditions within the sediment of Core MD 85668 would have, thus, hampered barite accumulation at this site.

In the Madingley Rise core (MD 90940), as stated above, barium appears to be linked to surface paleoproductivity. Insignificant terrigenous input, and good preservation of barite in the sediment results in a high barium content, mainly as barite. Under such conditions, barium can be considered as a paleoproductivity proxy.

5. Paleoproductivity and paleoceanographical interpretations

Comparison of the geochemical and biological data shows that paleoproductivity patterns were different at both sites. No marine organic matter being preserved in the sediment at both locations, no direct geochemical marker of paleoproductivity was available at these sites. The comparison between the other geochemical proxies and the rad ratio on the Madingley Rise permits to use the bulk MAR, the $CaCO_3$ MAR, and the barium MAR, as reliable paleoproductivity proxies. In the Somali Basin, variations of the foraminiferal and radiolarian assemblages compared to the bulk MAR indicate that the bulk MAR can be, there, used as a reliable paleoproductivity proxy. Due to the relatively low and uniform carbonate dissolution (Vénec-Peyré et al., 1997), the $CaCO_3$ MAR can also be used as a paleoproductivity proxy.

Low bulk MAR induced by very low terrigenous inputs, and high contents of pelagic carbonaceous debris are characteristic of pelagic sedimentation on the Madingley Rise. Peak values of the bulk MAR indicate that maximum paleoproductivity intervals are characteristic of glacial stages 2, 4, 6 and 8. The highest values of the bulk MAR are, however, recorded from the early part of isotope stage 9 (340 to 330 ka B.P.), reflecting an unique interglacial episode of intense surface productivity. In the Somali Basin, the downcore variations of bulk MAR and $CaCO_3$ MAR indicate that the episodes of maximum paleoproductivity occurred

also during glacial intervals (isotope stages 10, 6, 4, and 2). However, the paleoproductivity event at isotope stage 9 is not recorded.

High paleoproductivity periods are mainly recorded at both sites during glacial isotope stages, but some differences appear between both records. During glacial isotope stages 2 and 6, bulk MAR peak values are recorded in both cores, but acmes of productivity periods are, however, diachronous (Fig. 4). In the Madingley Rise area, these acme periods are located within the lower part of both these isotope stages, while in the Somali Basin, they occurred within the upper parts. Regarding isotope stage 4, this pattern is reversed with a high productivity period north of the Seychelles recorded at the end of the isotope stage, while the high productivity event of the same glacial interval recorded in the Somali Basin is placed at the beginning of the glaciation (Fig. 4).

Much different paleoproductivity events appear also between both sites during glacial isotope stages 10 and 8. Glacial isotope stage 10 is characterized by very high bulk MAR values in the Somali Basin, when the synchronous bulk MAR records of the Madingley Rise exhibit very low values (Fig. 4). Glacial isotope stage 8, and the 8/7 transition interval, show a different pattern at both locations. During this time interval, two paleoproductivity events are recorded on the Madingley Rise: the first one occurs in the upper part of isotope stage 8 (258 to 250 ka), and the second one at the 8/7 transition (245 to 220 ka). Data from the Somali Basin show relatively constant low productivity for the same period. Constant values calculated for this low paleoproductivity interval characterize, however, both isotope stages 8 and 7, suggesting that surface productivity was not enhanced during glacial isotope stage 8. Statistical analyses of foraminiferal and radiolarian populations deposited at this site during the same time interval demonstrated that glacial to deglacial transition between stages 8 and 7 did not follow the paleoceanographic patterns recorded into other glacial/interglacial cycles, i.e., a high paleoproductivity episode during the glacial isotope stage, followed by a sharp decrease at the transition (Vénec-Peyré et al., 1997). At the 8/7 transition, such an oceanographic pattern was not recorded.

Maximum bulk MAR values indicate, moreover, a very strong paleoproductivity event recorded on the Madingley Rise during interglacial isotope stage 9 (from 340 to 330 ka). Such a strong event was unexpected in an interglacial stage, because maximum productivity events are classically recorded during glacial isotope stages (Berger et al., 1989, Berger and Herguera, 1992). However, peak values are recorded for the bulk MAR and the Si/Al ratio in

the NW Arabian Sea (ODP sites 722 and 724) during this interglacial interval (Shimmield and Mowbray, 1991; Weedon and Shimmield, 1991). The good correlation between the bulk MAR and the rad ratio records, as well as the absence of reworked fauna in the samples of this fertile interval, clearly indicates that a strong productivity characterized this interglacial interval. This high productivity event is not recorded in the Somali Basin, where the same interval corresponds to the lowest bulk MAR values recorded.

The lack of synchronicity of the high productivity periods recorded at both sites cannot be interpreted as a time lag. For example, during isotope stage 6, the high productivity period takes place on the Madingley Rise before the Somali Basin, while during isotope stage 4, the high paleoproductivity period is recorded first in the Somali Basin, and next, on the Madingley Rise. Consequently, the depositional pattern being almost similar in sediments of both locations, the discrepancies occurring between the surface paleoproductivity records at both sites may be interpreted as indicative of two different paleoceanographic processes. Peak productivity events were, thus, controlled more by local/regional variations of paleoceanographic patterns than by global climatic changes.

The main process controlling surface productivity is the amount of nutrients available in the surface waters. This content is related to the mixing of the surface water with the nutrient-richer subsurface water, or with the renewal of the surface water. Both processes are linked to a reinforced circulation of the surface and subsurface waters. The difference between the paleoproductivity pattern at both sites suggests that origin and circulation of the surface waters were different at both sites during the time interval considered.

Today, the Madingley Rise is located under the South Equatorial Current (SEC) in summer and the Equatorial Counter Current (ECC) in winter (Fig. 2). Assuming that, during glacial intervals, surface circulation was more or less analogous to the present winter surface circulation, the relatively short high productivity periods recorded in glacial stages on the Madingley Rise may be interpreted as a result of the weakening, or a northward shift, of the ECC. During interglacial intervals, the circulation of the surface waters can be compared to the present summer circulation. ECC disappears and SEC is located at 10°S, limiting the renewal of the surface waters on the Madingley Rise. In that case, the productivity event in isotope stage 9 could testify to a shift of this surface current system, or a local change of the circulation of the surface waters in this area.

In the Somali Basin, the surface waters are formed by the Somali Current (SC) that flows NE-SW during winter and SW-NE during summer (Fig. 2). During glacial intervals, the southwest monsoon was weakened and a reversed winter-type NE-SW circulation of the SC was probably dominant (Anderson and Prell, 1993; Duplessy, 1982; Prell et al., 1980). The longer intervals of high productivity recorded during glacial periods testify, thus, to a good renewal of nutrients by a sustained activity of the SC that was not, however, related to any increased upwelling activity.

6. Conclusions

Major and trace element measurements, combined with analyses of radiolarian and foraminifers assemblages, were applied to two piston cores located in the pelagic equatorial belt of the Northwestern Indian Ocean. One core is located on the Madingley Rise, far from any terrestrial influence. The other core was collected in the Somali Basin, in an area submitted to a moderate terrestrial supply.

Our data show that no marine organic matter was preserved at both locations. The comparison of the normalized contents of major and trace elements (Fe/Al, Mg/Al, Ba/Al, Cu/Al, and Ni/Al) with a biological marker, such as the rad ratio (Madingley Rise), or with the variations of the foraminiferal and radiolarian assemblages (Somali Basin) prevents us from using these normalized contents as direct paleoproductivity proxies. Calculated bulk MAR and element MARs show, however, downcore changes similar to the biological markers variations, suggesting that they can be used as paleoproductivity proxies.

A combined use of geochemical and biological markers provides more accurate information on the paleoproductivity events recorded in these apparently homogeneous pelagic sediments that are very poor in organic matter.

Our main results point out that, in both cases, geochemical proxies, and especially the barium, present contrasted distribution patterns, although the petrographic differences between the two pelagic sites are minor. The sequential leaching procedure shows that the barium is mainly biogenic on the Madingley Rise, and almost exclusively lithogenic in the Somali Basin. Barium data must be, thus, carefully interpreted whenever used as paleoproductivity proxies.

Enhanced paleoproductivity periods are mainly recorded during glacial isotope stages at both locations. Random distribution of peak productivity events in both sedimentological records can only be explained by local variations of paleoceanographic patterns. The maximum paleoproductivity event recorded during interglacial isotope stage 9 on the Madingley Rise was not observed in the Somali Basin and must be also related to local variations of oceanographic patterns. Some regional factors intervene and disturb the global climatic signal. A weakening of the northward shift of the Equatorial Counter Current (ECC) could offer an interpretation of this maximum paleoproductivity period during interglacial stage 9 on the Madingley Rise.

Studies in progress on other piston cores from the Amirante Passage area will provide supplementary data to better interpret this unique paleoproductivity event.

Acknowledgments

We thank Nicole MOUREAU (Université Paris-Sud Orsay) and Maurice TAMBY (Muséum National d'Histoire Naturelle) for their technical cooperation during this study, Catherine PIERRE and Jean-François SALIEGES from the Laboratoire d'Océanographie Dynamique et Climatologie provided a much needed help in the oxygen isotope analyses, and François BAUDIN, from Université Pierre et Marie Curie (Jussieu), for his help in the measurement of the organic carbon. Thanks are due to Cathy NIGRINI, who kindly revised our first draft. Margaret DELANEY provided a very constructive review, and two anonymous reviewers were of great help to improve the quality of this paper.

References

Anderson, D.M. and Prell, W.L., 1993. A 300 kyr record of upwelling off Oman during the late Quaternary: evidence of the Asian Southwest monsoon. *Paleoceanography*, 8: 193-208.

Arrhenius, G.O.S., 1952. Sediment cores from the east Pacific. *Sweedish Deep Sea Expeditions Records*, 5: 1-227.

Bassinot, F.C., Beaufort, L., Vincent, E., Labeyrie, L.D., Rostek, F., Müller, P.J., Quidelleur, X. and Lancelot, Y., 1994. Coarse fraction fluctuations in pelagic carbonate sediments

from the tropical Indian Ocean: A 1500-kyr record of carbonate dissolution. *Paleoceanography*, 9: 579-600.

Berger, W.H., 1968. Radiolarian skeletons: solution at depth. *Science*, 159: 1237-1238.

Berger, W.H., Smetacek, V.S. and Wefer, G., 1989. Ocean productivity and paleoproductivity. An overview. In: W.H. Berger et al. (Editors), Production of the ocean: Present and past, Life Science Research Report 44, Wiley and Sons: 1-34.

Berger, W.H. and Herguera, J.C., 1992. Reading the sedimentary record of the ocean's productivity. In: P.G. Falkowski and A.D. Woodhead (Editors), Primary productivity and biochemical cycles in the sea, Plenum Press, New York: 455-486.

Bishop, J.K.B., 1988. The barite-opal-organic carbon association in oceanic particulate matter. *Nature*, 332: 341-343.

Boyle, E.A., 1981. Cadmium, zinc, copper and barium in foraminifera tests. *Earth Planet. Sci. Lett.*, 53: 11-35.

Brongersma-Sanders, M., Stephan, K.M., Kwee, T.G. and De Bruin, M., 1980. Distribution of minor elements in cores from the South West Africa shelf with notes on plankton and fish mortality. *Mar. Geol.*, 37: 91-131.

Bruce, J.G. and Beatty, W.H., 1985. Some observations of the coalescing of Somali eddies and description of the Socotra eddy. *Oceanol. Acta*, 8: 207-209.

Calvert, S.E. and Pedersen, T.F., 1993. Geochemistry of recent oxic and anoxic sediments: Implications for the geological record. *Mar. Geol.*, 113: 67-88.

Caulet, J.P., Debrabant, P. and Fieux, M., 1988. Dynamique des masses d'eaux océaniques et sédiment quaternaire sur la marge d'Afrique de l'est et dans le bassin de Somalie. Résultats préliminaires de la mission MD 44-INDUSOM du Marion-Dufresne. *C.R. Acad. Sci., Paris*, 307 (2): 281-288

Collier, R. and Edmond, J., 1984. The trace element geochemistry of marine biogenic particulate matter. *Prog. Oceanogr.*, 13: 113-199.

Currie, R.J., 1992. Circulation and upwelling off the coast of south-east Arabia. *Oceanol. Acta*, 15: 43-60.

Dehairs, F., Chesselet, R. and Jedwab, J., 1980. Discrete suspended particles of barite and barium cycle in the open ocean. *Earth Planet. Sci. Lett.*, 49: 528-550.

Dehairs, F., Lambert, C.E., Chesselet, R. and Risler, N., 1987. The biological production of marine suspended barite and the baryum cycle in the Western Mediterranean Sea. *Biogeochemistry*, 4: 119-139.

Dehairs, F., Stroobants, N. and Goeyens, L., 1991. Suspended barite as tracer of biological activity in the Southern Ocean. *Mar. Chem.*, 35: 399-410.

Düing W., Molinari R.L. and Swallow J.C., 1980: Somali Current. *Science*, 209: 588-590.

Duplessy, J.C., 1982. Glacial to interglacial contrasts in the northern Indian Ocean. *Nature*, 295: 494-498.

Dymond, J., Suess, E. and Lyle, M., 1992. Barium in deep-sea sediment: A geochemical proxy for paleoproductivity. *Paleoceanography*, 7: 163-181.

El Foukali, H., 1995. Le contrôle paléoclimatique de la sédimentation quaternaire dans le bassin de Somalie (Océan Indien du nord-ouest).Thesis. *Museum Natl. Hist. Nat.*, Paris, 214 p.

Espitalié, J., Deroo, G. and Marquis, F., 1985. La pyrolise Rock-Eval et ses applications (1). *Rev. Inst. Fr. Petrol.*, 40 (5): 563-579.

Francois, R., Honjo, S., Manganini, S.J. and Ravizza, G.E., 1995. Biogenic barium fluxes to the deep sea: Implications for paleoproductivity reconstruction. *Global Biogeochem.* Cycles, 9: 289-303.

Gingele, F. and Dahmke, A., 1994. Discrete barite particles and barium as tracers of paleoproductivity in south Atlantic sediments. *Paleoceanography*, 9: 151-168.

Goldberg, E.D. and Arrhenius, G.O.S., 1958. Chemistry of Pacific pelagic sediments. Geochim. *Cosmochim. Acta*, 13: 1523-212.

Johnson, D.A., Schneider, D.A., Nigrini, C.A., Caulet, J.P. and Kent, D.V., 1989. Pliocene-Pleistocene radiolarians events and magnetostratigraphic calibrations for the tropical Indian Ocean. *Mar. Micropal.*, 14: 33-66.

Johnson, T.C., 1974. The dissolution of siliceous microfossils in surface sediments of the eastern tropical Pacific. *Deep Sea Res.*, 21: 851-864.

Johnson, T.C., 1976. Biogenic opal preservation in pelagic sediments of a small area in the eastern tropical Pacific. *Geol. Soc. Amer. Bull.*, 87: 1273-1282.

Kling, S.A. and Boltovskoy, D., 1995. Radiolarian vertical distribution patterns across the southern California Current. *Deep Sea Res.*, 42: 191-231.

Lea, D.W. and Spero, H.J., 1994. Assessing the reliability of paleochemical tracers: Barium uptake in the shells of planktonic foraminifera. *Paleoceanography*, 9: 445-452.

Lea, D.W and Boyle, E.A., 1989. Barium content of benthic foraminifera controlled by bottom water composition. *Nature*, 338: 751-753.

Lyle, M., Heath, G.R. and Robbins, J.M., 1984. Transport and release of transition elements during early diagenesis: Sequential leaching from MANOP sites M and H. Part I: pH 5 acetic acid leach. Geochim. *Cosmochim. Acta*, 48: 1705-1715.

McManus, J., Berelson, W.M., Klinkhammer, G.P., Kilgore, T.E. and Hammond, D.E., 1994. Remobilisation of barium in continental margin sediments. *Geochim. et Cosmochim. Acta*, 58: 4899-4907.

Murray, D.W. and Prell, W.L., 1992. Pliocene and Pleistocene climatic oscillation and monsoon upwelling recorded in sediments from the Owen Ridge, Northwestern Arabian sea. In: C.P. Summerhayes et al. (Editors), Upwelling systems: Evolution since the Early Miocene, Geol. Soc. Spec. Publ., 64: 301-321.

Ouahdi, R., 1997. Variations de la productivité au nord-ouest de l'Océan Indien lors des derniers 70 000 ans dans l'upwelling de Socotra et de Somalie: Enregistrements géochimiques. *Bull. Soc. Géol. Fr.*, 168: 93-107.

Paytan, A., 1995. Marine barite, a recorder of ocean chemistry, productivity and circulation. Thesis. San Diego Univ. 111 pp.

Philander, S.G.H. and Delecluse, P., 1983. Coastal current in low latitudes (with application to the Somali and El Ni" o currents). *Deep-Sea Res.*, 30: 887-902.

Prell, W.L., Hutson, W.H., Williams, D.F., B..., W.H., Geitzenauer, K. and Molfino, B., 1980. Surface circulation of the Indian Ocean during the Last Glacial Maximum, approximately 18,000 yr BP. *Quatern. Res.*, 14: 309-336.

Pruysers, P.A., DeLange, G.J. Middelburg, J.J. and Hydes, D.J., 1993. The diagenetic formation of metal-rich layers in sapropel-containing sediments in the eastern Mediterranean. *Geochim. et Cosmochim. Acta*, 57: 527-536.

Robbins, J.M., Lyle, M. and Heath, G.R., 1984. A sequential extraction procedure for partitioning elements among co-existing phases in marine sediments. *Rep. College Oceanography, Oregon State Univ.* 45p.

Shackleton, N.J., Hall, M.A., Pate, D., Meynadier, L. and Valet, J.-P., 1993. High resolution stable isotope stratigraphy from bulk sediment. *Paleoceanography*, 8: 141-148.

Shimmield, G.B., 1992. Can sediment geochemistry record changes in coastal upwelling paleoproductivity ? Evidence from Northwest Africa and the Arabian Sea. In: C.P. Summerhayes et al. (Editors), Upwelling systems: Evolution since the Early Miocene, *Geol. Soc. Spec. Publ.*, 64: 9-46.

Shimmield, G.B. and Mowbrays, R., 1991. The inorganic geochemical record of Northwestern Arabian Sea: A history of productivity variation over the last 4,000 ky from sites 722A and 724. In: Prell W.L. et al. (Editors), *Proc. ODP, Sci. Res.*, 117: 409-429.

Shimmield, G.B., Derrick, S., Mackensen, A., Grobe, H. and Pudsey, C., 1994. The history of barium, biogenic silica and organic carbon accumulation in the Weddel Sea and the Antarctic Ocean during the last 150,000 years. In: R. Iahn et al. (Editors), Carbon cycling in the glacial ocean: constraints on the ocean role in global change. Quantitative approaches in paleoceanography. *NATO ASI Series* (1): Global environmental changes, 17: 555-574.

Shimmield, G.B. and Jahnke, R.A., 1995. Particle flux and its conversion to the sediment record: Open ocean upwelling systems. In: C.P. Summerhayes et al. (Editors), Upwelling in the ocean: modern processes and ancient records: 172-191.

Stroobants, N., Dehairs, F., Goeyens, L., Vanderheidjen, N. and Van Grieken, R., 1991. Barite formation in the Southern Ocean water column. *Mar. Chem.*, 35: 411-421.

Swallow, J.C., 1980. The Indian Ocean Experiment: Introduction. *Science*, 209: 588-589.

Swallow, J.C., 1984. Some aspects of the physical oceanography of the Indian Ocean. In M.V. Angel (Editors), Marine sciences of the northwest Indian Ocean and adjacent waters, Proceedings of the Mahabiss John Murray International Symposium, Egypt, 3-6 September 1983, *Deep Sea Reserch* part A, Oceanographic Research papers, 31: 639-650.

Swallow, J.C. and Bruce, J.G., 1966. Current measurements off the Somali coast during the southwest monsoon of 1964. *Deep-Sea Res.*, 13: 861-888.

Tchernia, P., 1978. Océanographie Régionale: Description physique des océans et des mers. *ENSTA*. 19 pl, 275 pp.

Thomson, J., Higgs, N.C., Croudace, I.W., Colley, S. and Hydes, D.J., 1993. Redox zonation of elements at an oxic/post-oxic boundary in deep-sea sediments. *Geochim. et Cosmochim. Acta*, 57: 579-595.

Thomson, J., Higgs, N.C., Wilson, T.R.S., Croudace, I.W., De Lange, G.J. and Van Santvoort, P.J.M. , 1995. Redistribution and geochemical behaviour of redox sensitive elements around S1, the most recent eastern Mediterranean sapropel. *Geochim. et Cosmochim. Acta*, 59: 3487-3501.

Torres, M.E., Brumsack, H.J., Bohrman, G. and Emeis, K.C., 1996. Barite fronts in continental margin sediments: a new look at Ba remobilization in the zone of sulfate reduction and formation of heavy barite in diagenetic fronts. *Chem. Geol.*, 127: 125-139.

Tribovillard, N.P., Caulet, J.P., Vergnaud-Grazzini, C., Moureau, N. and Tremblay, P., 1996. Lack of organic matter accumulation on the upwelling-influenced Somalia margin in a glacial-interglacial transition. *Mar. Geol.*, 133: 157-182.

Turekian, K.K. and Wedepohl, K.H., 1961. Distribution of the elements in some major units of the Earth's crust. *Geol. Soc. Am. Bull.*, 72: 175-191.

Van Capellen, P. and Ingall. E. D., 1994. Benthic phosphorus regeneration, net primary production, and ocean anoxia: A model of the coupled marine geochemical cycles of carbon and phosphorus. *Paleoceanography*, 9: 677-692.

Van Os, B.J.H., Middelburg, J.J. and De Lange, G.J., 1991. Possible diagenetic mobilization of barium in sapropelic sediment from the eastern Mediterranean. *Mar. Geol.*, 100: 125-136.

Van Santvoort, P.J.M., De Lange, G.J., Thomson, J., Cussen, H., Wilson, T.R.S., Krom, M.D. and Strähle, K., 1996. Active post-depositional oxidation of the most recent sapropel (S1) in sediments of the eastern Mediterranean sea. *Geochim. et Cosmochim. Acta*, 60: 4007-4024.

Vénec-Peyré, M.T., Caulet, J.P. and Vergnaud-Grazzini, C., 1995. Paleohydrographic changes in the Somali Basin (58N upwelling and equatorial areas) during the last 160 kyr, based on correspondence analysis of foraminiferal and radiolarians assemblages. *Paleoceanography*, 10: 473-491.

Vénec-Peyré, M.T., Caulet, J.P. and Vergnaud-Grazzini, C., 1997. Glacial-interglacial changes in the equatorial part of the Somali Basin (NW Indian Ocean) during the last 355 ky. *Paleoceanography*, 12: 640-649.

Von Breymann, M.T., Emeis, K.C. and Suess, E., 1992. Water depth and diagenetic constraints on the use of barium as a paleoproductivity indicator. In: C.P. Summerhayes

et al. (Editors), Upwelling systems: Evolution since the Early Miocene, *Geol. Soc. Spec. Publ.*, 64: 273-284.

Warren, B.A., 1974. Deep flow in the Madagascar and Mascarene basins. *Deep-Sea Res.*, 21: 1-21.

Warren, B.A., 1981. Transindian hydrographic section at 188S: Property distributions and circulation in the South Indian Ocean. *Deep-Sea Res.*, 13: 759-788.

Warren, B.A., Stommel, H. and Swallow, J.C., 1966. Water masses and patterns of flow in the Somali Basin during the southwest monsoon of 1964. *Deep-Sea Res.*, 28: 825-860.

Weedon, G.P. and Shimmield, G.B., 1991. Late pleistocene upwelling and productivity variations in the Northwestern Indian Ocean deduced from spectral analyses of geochemical data from sites 722 and 724. In W.L. Prell et al. (Editors), *Proc. ODP, Sci. Res.*, 117: 431-440.

Yasuda, Y., Amano, K. and Yamanoi, T., 1990. Pleistocene climatic changes as deduced from a pollen analysis of site 717 cores. In : J.R. Cochran et al. (Editors), *Proc. ODP., Sci., Res.*, 116:249-261.

Paleoproductivity and paleoceanographic changes in the Amirante Passage area (Equatorial Indian Ocean): 200 kyr of lower pelagic productivity

Hélène Jacot Des Combes[a,b], Nicolas P. Tribovillard[a] and Jean-Pierre Caulet[b].

a Laboratoire de Sédimentologie et Géodynamique, URA CNRS 719, Université de Lille I, 59655 VILLENEUVE D'ASCQ (FRANCE).

b ESA 7073, Laboratoire de Géologie, MNHN, 43 rue Buffon 75005 PARIS (FRANCE).

Keywords: NW Indian Ocean, pelagic sedimentation, paleoproductivity, geochemical proxies, barium, sequential leaching, radiolarian index.
Océan indien du NW, sédimentation pélagique, paléoproductivité, marqueurs géochimiques, baryum, attaques ménagées, index de radiolaires.

Accepté pour publication à la Société Géologique de France

Abstract

Major and selected trace element (Al, Fe, Mg, K, Ba, Mn, V, Cu, Ni, and Ti) records were analyzed in a core recovered in the Amirante Passage (Equatorial Indian Ocean) in order to monitor the sedimentary response to pelagic productivity in this area during the last 500 kyr. Geochemical proxies such as bulk Mass Accumulation Rate (MAR), Al-normalized major and trace element contents, and MARs were compared to a radiolarian index, used as a biological marker of paleoproductivity. A special attention is paid to the barium record, and a sequential leaching procedure determined the main Ba-carrier fraction in the sediment, and, thus, the amount of biogenic barium. The sedimentation in the Amirante Passage is characterized by a low bulk MAR and low terrigenous inputs. Distribution of Ba within the different fractions of the sediment indicates that both terrigenous inputs and biologic activity are the main processes carrying Ba to the sediment. Barium cannot, thus, be used as a single paleoproductivity proxy. The bulk MAR variations are directly related to the variations of the rad ratio, reflecting a direct link between surface productivity and pelagic sedimentation at this site. The bulk MAR record exhibits peak values during glacial and interglacial intervals from 500 ka to 238 ka, and constant low values from 238 ka to 38 ka, suggesting a period of low surface productivity from the 8/7 to the 3/2 isotope stages transition. This pattern does not correspond with a marked change in the wind strength, and a shift in the circulation of the surface currents system is hypothesized to explain such a long low productivity interval.

Version française abrégée

Paléoproductivité et variations paléocéanographiques dans le Passage des Amirantes (Océan Indien équatorial) : 200 ka de faible productivité

La sédimentation pélagique dans le Passage des Amirantes est étudiée pour les derniers 500 ka à partir de la carotte MD 90929 (6.59°S, 52.03°E, 3 071 m de fond, fig. 1). Le sédiment est composé d'une boue gris-jaune clair à coccolithes et foraminifères, la teneur en carbonate étant dosée par calcimétrie Bernard. La composition chimique du sédiment est déterminée par des attaques chimiques ($HClO_4$, HNO_3, et HF) sur le sédiment total, et grâce à des attaques chimiques séquentielles [Lyle et al., 1984] sur des échantillons sélectionnés le long de la carotte. La teneur en matière organique (TOC) est dosée par Leco. Le taux d'accumulation total (bulk MAR en g/cm^2/ka), ainsi que les taux d'accumulation des éléments (Si, Al, Fe, Mg, K, Ba, Mn, V, Cu, Ni, et Zn) qui en découlent sont calculés par le produit du taux de sédimentation linéaire (cm/ka) et de la densité humide (g sédiment sec/cm^3 sédiment humide). Les différents marqueurs géochimiques sont ensuite comparés à un marqueur biologique de la paléoproductivité, ici un index de radiolaires (TSRI) déjà utilisé comme marqueur de la paléoproductivité dans cette région [Jacot Des Combes et al, in press].

Le sédiment est daté par comparaison pic à pic entre la courbe de $\delta^{18}O$ obtenue sur le sédiment total et la courbe de référence SPECMAP [Imbrie & Imbrie, 1980] (fig. 2). On compare également la courbe de la carotte MD 90929 avec la courbe isotopique obtenue sur le sédiment total de la carotte MD 85668, considérée comme une courbe de référence pour les sédiments de l'Océan Indien du NW [Shackleton et al., 1993]. Compte tenu de la différence dans les taux d'accumulation entre les carottes, l'âge isotopique obtenu pour la carotte MD 90929 (479 ka à 524 cm) est contrôlé et confirmé par des marqueurs biostratigraphiques comme l'apparition de *Buccinosphaera invaginata* et la disparition de *Stylatractus universus* (radiolaires).

D'une façon générale, les variations du taux de sédimentation présentent deux parties bien distinctes (fig. 3). Entre 500 ka et 238 ka, on observe des variations marquées avec de fortes valeurs (3.5 g/cm^2/kyr) localisées aux périodes de transition entre les stades isotopiques (12-11, 9-8 et 8-7). Entre 238 et 38 ka, les valeurs du bulk MAR restent constantes et faibles (0.5 g/cm^2/kyr). Ses variations sont cependant synchrones avec celles du TSRI et peuvent être

directement utilisées comme indicateurs des variations de la productivité de surface. On peut donc utiliser le bulk MAR comme un marqueur des changements de productivité.

Le sédiment ne comporte pas de matière organique en quantité significative, mais est très riche en calcite (de 54.2 à 84.7 %). Les teneurs en baryum sont relativement élevées dans toute la carotte (de 670 à 1765 ppm), mais comme pour les teneurs en $CaCO_3$, ces variations de teneurs ne se corrèlent pas avec celles du TSRI (fig. 4). Par contre, les variations des taux d'accumulation des éléments sont bien corrélées avec celles du TSRI (figs. 5 et 6). De plus, l'enrichissement du sédiment en baryum, indiqué par le rapport Ba/Al, montre un lien plus fort avec les variations des rapports Mg/Ca et Ti/Al, indicateurs des apports détritiques (dolomite et argiles et minéraux lourds), qu'avec celles du TSRI, c'est à dire de la productivité (figs. 4 et 6). Enfin, les résultats des attaques séquentielles montrent que le baryum se situe à 36 % dans la phase terrigène et à 40 % dans la phase résiduelle sous forme de barytine, le reste du baryum se répartissant entre la phase carbonatée et la fraction des oxy-hydroxydes (fig. 7). Le baryum a donc, sur ce site, des origines terrigènes autant que biogènes, et ne peut pas être utilisé globalement comme un marqueur de paléoproductivité. Les autres éléments en traces étudiés (Cu, Mn, Ni, V, et Zn) sont généralement considérés comme des indicateurs de conditions d'oxydo-réduction des sédiments [Calvert and Pedersen, 1993]. Sur ce site, on constate que les teneurs de Cu, Ni, V, et Zn sont relativement faibles et fortement corrélées aux variations des éléments terrigènes (Al, Ti) et que l'enrichissement du sédiment en ces éléments comparés à l'Al est donc en fait lié aux variations de la force du vent (fig. 8). Le manganèse montre des teneurs relativement élevées, et le rapport Mn/Al présente des variations qui lui sont propres (fig. 8).

L'ensemble de ces résultats suggère que des conditions oxiques ont prévalu dans cette zone pendant les derniers 500 ka. Les taux de sédimentation des différents éléments chimiques sont fortement influencés par le bulk MAR et reprennent la distribution en deux principales parties : variations entre 500 et 238 ka, valeurs faibles et constantes entre 238 et 38 ka (figs. 5 et 6). Les différents indicateurs permettent de suggérer sur ce site une forte variation de la paléoproductivité de surface au cours de l'intervalle de temps considéré. En effet, compte tenu de la variété des marqueurs utilisés, les résultats observés privilégient l'hypothèse des variation de production plutôt que des variations des conditions de préservation de cette production.

La comparaison entre les marqueurs de productivité (TSRI et bulk MAR) et l'index de la force des vents (Ti/Al) ne montre aucune corrélation. Ceci suggère que les variations de la productivité enregistrées dans le Passage des Amirantes n'ont pas été induites par un champ de

vent, local ou régional, mais plutôt par une modification de la circulation des courants de surface. En effet, la productivité de surface dépend de la teneur des eaux de surface en nutriments. Le renouvellement de ces nutriments dans les eaux de surface est lié à l'intensité du mélange entre les eaux de surface, pauvres, et les eaux de subsurface, plus riches en nutriments. Ce mélange, directement contrôlé par la circulation des eaux de surface, peut également avoir lieu entre deux masses d'eaux de surface d'origine différente. Actuellement, le site de la carotte MD 90929 est localisé sous le courant sud équatorial (SEC) durant toute l'année, à l'exception de trois mois pendant l'hiver (de janvier à mars) où il reste situé sous un des tourbillons qui relient le SEC au contre courant équatorial (ECC) (fig. 9). Au bout d'un certain temps, les eaux de surface de ces tourbillons deviennent de plus en plus oligotrophiques, en raison de leur isolement progressif de la circulation générale. Si on considère que la circulation des courants de surface pendant l'hiver et l'été peut donner une idée de la circulation des courants de surface pendant les stades glaciaires et interglaciaires, réciproquement, on peut expliquer la période de faible productivité de surface observée entre 238 et 38 ka par le maintien du site étudié sous un tourbillon oligotrophique entre le SEC et l'ECC. Cette situation résulterait d'un ralentissement du déplacement vers le nord du système actuel des courants de surface dans cette région. Une telle modification de l'alternance entre les positions d'hiver et d'été de ce système a déjà été envisagée pour expliquer les modifications de la paléoproductivité dans un autre site de l'océan Indien équatorial [Jacot Des Combes et al., in press].

Introduction

Paleoproductivity reconstructions using all available proxies, such as geochemical and biological markers, are generally confined to specific areas. Continental margins and upwelling systems are preferentially studied because of their high surface productivity related to a restricted area [Martin et al., 1987; Berger et al., 1989; Berger and Herguera, 1992]. Reconstruction of paleoproductivity in these areas raises, however, some problems such as the multiple sources of material (terrigenous and biogenic) and the rapid changes in redox conditions [McManus et al, 1994; Tribovillard et al., 1996; Martinez, 1997; Ouahdi, 1997]. Due to stable redox conditions, the pelagic domain is a promising area for recognizing the relationship between export productivity and geochemical proxies, mostly because some of them (Ba, Cu, Ni, Zn) are also sensible to changes in redox conditions [Van Os et al., 1991; Calvert and Pedersen, 1993; Pruysers et al., 1993; Thomson et al., 1993, 1995; Paytan, 1995. Paytan and

Kastner, 1996; Tribovillard et al., 1996; Van Santvoort et al., 1996]. In the pelagic domain, it is, however, difficult to establish a direct relationship between variations in geochemical proxies and export productivity using the total organic carbon (TOC) content, because of its limited preservation in pelagic sediments [Tribovillard et al., 1996; Jacot Des Combes et al., in press]. Since variations in carbonate content are controlled either by surface paleoproductivity or by carbonate dissolution [Bassinot et al., 1994], comparison of the $CaCO_3$ accumulation rate, as well as other proxies (Ba, Cu, and Ni records) with paleoproductivity markers that are independent of the geochemical record, such as the biological markers, may be useful to establish the reliability of the geochemical record of export productivity.

Current studies in the NW Indian Ocean show that the pelagic realm is less homogeneous than expected. A previous study highlighted the occurrence of different accumulation patterns between two pelagic subdomains of the Somali Basin [Jacot Des Combes et al., in press]. These differences were related to the presence of two surface water circulation systems rather than to an input of terrigenous material in the Somali Basin interfering with the biogenic record.

The goal of this paper is to confirm previous results in the equatorial Indian Ocean and determine the inorganic geochemical signal of the paleoproductivity recorded in pelagic sediments from another area of the equatorial Indian Ocean. A core from the Amirante Passage area at the southern edge of the Somali Basin (fig. 1) was selected for the present study in order to check the reliability of paleoproductivity reconstructions using geochemical proxies, with a special focus on barium.

Major and trace elements such as Al, Fe, Mg, K, Ba, Mn, V, Ni, Cu, Ti, and Zn are commonly used as markers of both the input of material and the sedimentary conditions. Aluminum, Fe, K, Mg, and Ti, mostly linked with terrigenous debris such as quartz, feldspars and clay minerals, can be used to characterize the terrigenous input. Manganese, V, Cu, Ni, and Zn are strongly dependent on changes in redox conditions within the sediment. These trace metals are divided between those (Mn and V) whose valency varies as a function of the redox potential, and those (Cu, Ni, and Zn) whose valency does not change, but which precipitate as highly insoluble sulfides [Calvert and Pedersen, 1993]. Manganese is known to precipitate under oxic conditions as insoluble poorly crystallized oxyhydroxides [Calvert and Pedersen, 1993]. An enrichment in the other elements (Cu, Ni, V and Zn) indicates suboxic to anoxic conditions in the bottom waters, or within the sediment. Barium, and, to a lesser degree Cu, Ni, and Zn, are related to biogenic activity, but they can also depend on diagenesis through changes in redox

conditions [Calvert and Pedersen, 1993]. Copper, Ni and Zn are also known to be easily linked with organic matter through metal-organic complexes [Tribovillard et al., 1996; and references therein]. Barium is generally considered as a reliable paleo-productivity proxy, when present as barite, due to its resistance to diagenetic processes [Shimmield and Mowbray, 1991; Dymond et al., 1992; Shimmield, 1992; Calvert and Pedersen, 1993; Gingele and Dahmke, 1994; Lea and Spero, 1994; Shimmield et al., 1994; Francois et al., 1995]. Formation of barite in living organisms, or in microenvironments of decaying organic matter through sulphate oversaturation, suggests that biogenetic barium content can be used as an indicator of surface biologic productivity [Goldberg and Arrhenius, 1958; Dehairs et al., 1980, 1987, 1991; Stroobants et al., 1991; Dymond et al., 1992; Gingele and Dahmke, 1994]. Such a process is supposed to occur preferentially within biosiliceous debris, such as diatoms and, possibly, radiolarians [Dehairs et al., 1980, 1987, 1991; Bishop, 1988]. Barium can also be remobilized, due to barite dissolution during sulfate reduction [Thomson et al., 1993, 1995; De Lange et al., 1994; Van Santvoort et al. 1996]. Sediments located under areas of high surface water productivity usually undergo reducing conditions and are not favorable to barite preservation [Von Breymann et al., 1992]. The protocole proposed by Lyle et al. [1984] is used to perform a sequential leaching on this sediment to determine the main barium carrier-phase, and, thus, the origin of the barium. Surface productivity is, at this site, monitored through variations in the radiolarian index (TSRI) previously used in this area of the Equatorial NW Indian Ocean [Jacot Des Combes et al., in press].

2. Oceanographic setting and material

The Indian Ocean has no northern source of deep water, and the waters constituting the deep and bottom waters of the NW Indian Ocean enter the Somali Basin through the Amirante Passage. They are represented by a water mass having a southern origin, mostly originating in the Crozet Basin [Barton et Hill, 1989; Johnson et al., 1991]. In this area, the surface flow is mainly west- to northwestward but is subjected to monsoonal variations (fig. 1a). At depths between 500 m and 1500 m, transport is mainly southward due to the outflow of water masses from the Arabian Sea [Warren, 1974]. Below 3500 m, the Lower Circumpolar Water (LCPW) enters the Somali Basin over the Amirante Passage sill. Nephelometer data indicate that between 3500 m and the bottom of the sill there is a relatively high content of suspended sediment in the

water column that can be related to a strong northward transport [Johnson and Damuth, 1979] (fig. 1b).

Core MD 90929, recovered in the Amirante Passage (6.590°S, 52.030°E) (fig. 1a) during the MD 64 SOMIRMAS cruise of the R/V "*Marion-Dufresne*" in 1990, is located within the equatorial productivity belt that extends from 5° N to 10° S. This core was recovered at a water depth of 3072 m, where the settling of planktonic and aeolian particles from the surface layer is not disturbed by the strong northward flow near the bottom of the passage [Warren, 1974; Johnson and Damuth, 1979; Fieux and Swallow, 1988; Barton and Hill, 1989; Johnson et al., 1991]. The sediment is a light yellow-gray coccolithophorid calcareous ooze (47.5 to 90 % of $CaCO_3$) with some planktic foraminifera and radiolarians, and terrigenous debris such as quartz (< 2 %), feldspar (<1 %), and clay minerals (1 to 15 %). No turbidites, or reworked levels, were recognized.

3. Analytical methods

The age model constructed for this core is based on an oxygen-isotope analysis of the bulk carbonate analyzed every 10 cm using a mass spectrometer (OPTIMA). The age and depth of control points are given in Table I.

Isotopic event	Age of control point (ka)	Depth in core (cmbsf)
2.2	19	39
3.3	53	57
5.5	122	99
7.1	194	139
7.5	238	154
8.2	249	174
8.3	257	204
8.4	269	214
8.6	299	224
9.1	310	274
9.2	320	284
9.3	331	314
11.3	405	376
12.2	434	474
12.33	461	514
13.13	502	537
14.3	552	554
15.1	574	604
15.2	585	624
15.3	596	634

Table I: Age and depth of the control points used to establish the age of Core MD 90929.
Age et profondeur des points de contrôle utilisés pour établir l'âge de la carotte MD 90929.

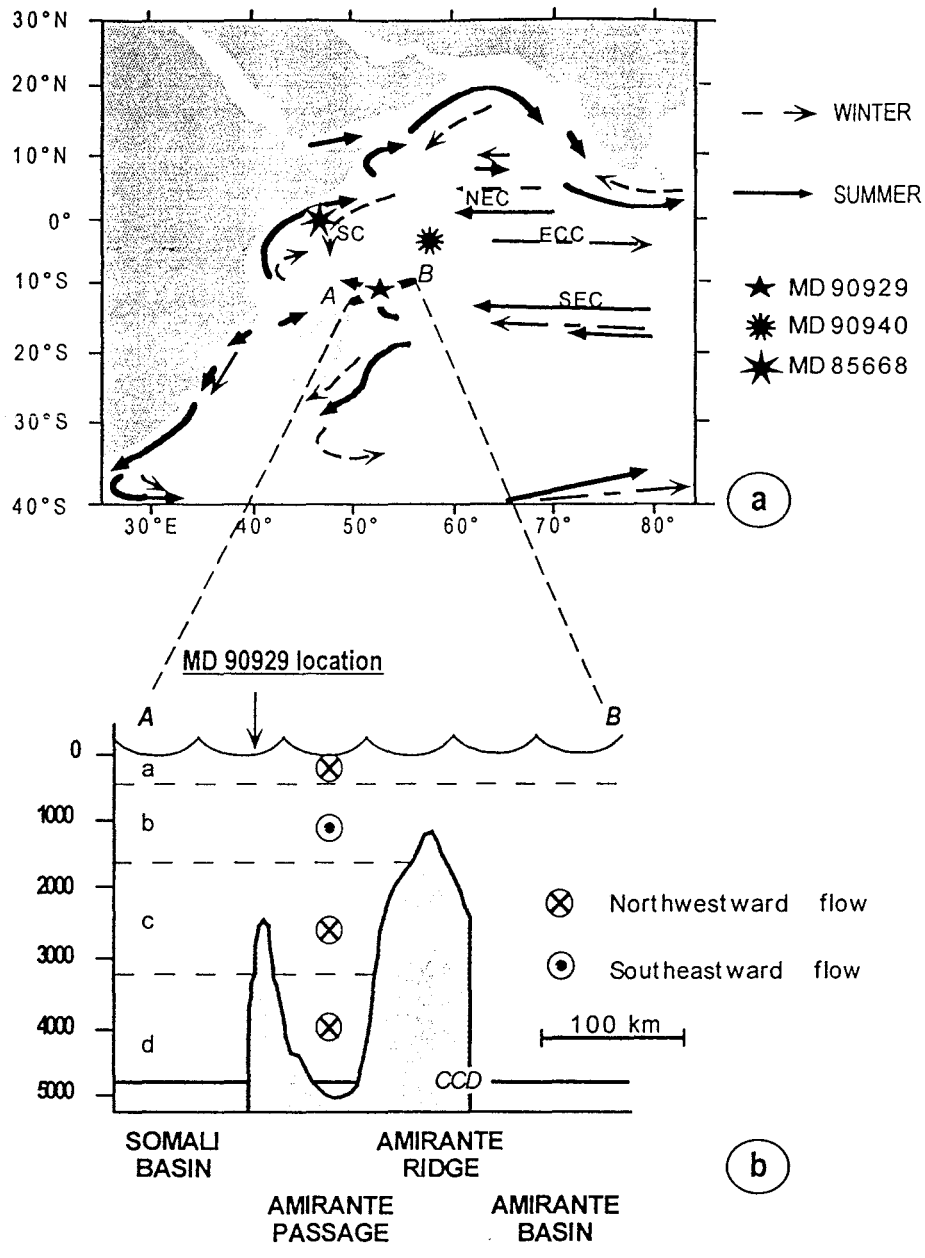

Figure 1: Present oceanographic patterns and location map of Cores MD 90929, MD 90940 and MD 85668.

a: map of the surface currents in the NW Indian Ocean. NEC: North Equatorial Current. SEC: South Equatorial Current. ECC: Equatorial Counter Current. SC: Somali Current.

b: profile of oceanic circulation in the Amirante Passage. a: surface water. b: intermediate depth water flowing from the Arabian Sea. c: deep water. d: bottom water. The direction of flow is indicated by the symbols on the right side of the drawing.

Schema océanographique actuel et carte de localisation des carottes MD 90929, MD 90940 et MD 85668.

a: *Carte des courants de surface dans l'Océan Indien du NW. NEC: courant nord équatorial. SEC: courant sud équatorial. ECC: contre courant équatorial. SC: courant de Somalie.* **b:** *Profil de la circulation dans le Passage des Amirantes. a: eaux de surface. b: eau intermédiaire venant de la mer d'Arabie. c: eaux profondes. d: eaux de fond. La direction des courants est indiquée par les symboles définis à droite de la figure*

Total organic content (TOC) measurements were performed on 47 samples of the bulk sediment using Leco analysis. Carbonate content was measured every 10 cm with a Bernard calcimeter. The amount of major and significant trace elements (Ba, Ti, Mn, V, Cu, Ni, Cr, and U) was measured in the following way: 100 mg of bulk sediment were dried at 105°C for 24 hours and thoroughly ground in an agate mortar mill prior to $HClO_4$, HNO_3 and HF acid digestion. The trace elements were measured with a ICP-spectrometer (ICP-MS and ICP-AES). The analytical precision and accuracy of the results were both found to be equal to, or better than, 5 % for all elements. Data were checked by comparison with international standards (BR Basalt, GH Granite, DR-N Diorite and other standards) and with the help of replicate samples. These results are summarized in table II. The enrichment in the studied elements compared to the terrigenous fraction is estimated through the respective ratios of the elements with Al (table. III).

In order to determine the main carrier-phase of barium, a sequential leaching procedure was performed on eight samples taken at irregular intevals along the core. The protocol used in this study is derived from that described by Robbins et al. [1984] and Lyle [1984] and was used in a previous study on pelagic sediments from Madingley Rise and the Somali Basin (NW Indian Ocean) [Jacot Des Combes et al., in press]. The dried and ground samples were subjected to a pH 5 acetic acid extraction to remove adsorbed and calcite-bound elements, and then to treatment with a pH 5 hydroxyl amine hydrochloride solution to remove elements adsorbed on poorly crystalline ferromanganese oxyhydroxides. The pH 9 sodium sulphate extraction of the organic matter was not carried out, as organic matter content in Core MD 90929 is insignificant. An extra treatment with HF was added to dissolve the silicate-bound barium (HF alone does not dissolve barite). Residual elements were determined from the difference between the total content (from the bulk analysis) and the sum of the three partial extractions. After each step, element concentrations were measured by ICP spectrometry. The results are summarized in table V.

Depth (cmbsf)	Age (ka)	TSRI	CaCO3 (%)	Si (%)	Al (%)	Fe (%)	Mg (%)	K (%)	Ti (ppm)	Ba (ppm)	Cu (ppm)	Ni (ppm)	Zn (ppm)	Mn (ppm)	Mo (ppm)	U (ppm)	V (ppm)
8	4	0.26	72.1	6.3	1.6	0.9	0.5	0.3	899	1124	71	49	30	465	0.75	0.50	25
18	9	0.51	78.9	4.5	1.3	0.7	0.4	0.2	719	796	55	43	26	387	0.56	0.43	20
29	14	0.85	80.9	4.0	1.3	1.7	0.5	0.3	719	825	60	75	34	1007	1.62	0.39	23
39	19	0.11	78.0	4.8	1.4	0.9	0.5	0.2	839	971	38	54	31	697	1.06	0.51	26
49	38	0.28	76.5	5.3	1.5	0.9	0.5	0.3	899	1045	49	48	32	232	0.59	0.40	25
57	53	0.28	78.9	4.7	1.4	0.8	0.5	0.2	779	840	45	41	28	232	0.33	0.43	23
69	73	0.34	84.7	3.3	0.9	0.5	0.4	0.2	480	670	28	36	20		0.43	0.29	14
80	91	0.32	81.9	4.0	1.1	0.6	0.4	0.2	540	703	32	43	26	542	0.88	0.42	19
89	106	0.22	80.3	4.5	1.1	0.6	0.4	0.2	600	826	42	42	28	465	0.77	0.34	17
99	122	0.43	81.8	4.0	1.1	0.7	0.4	0.2	600	746	34	36	22		0.31	0.43	19
107	136	0.58	82.7	3.8	1.0	0.6	0.4	0.2	540	740	37	40	22	232	0.46	0.34	15
119	158	0.17	77.8	5.0	1.4	0.8	0.5	0.2	779	794	43	38	25	542	0.51	0.38	21
129	176	0.36	65.6	7.7	2.3	1.4	0.7	0.4	1319	1027	66	43	35	620	0.55	0.52	32
139	194	0.34	66.9	8.0	2.1	1.3	0.6	0.4	1199	1098	63	42	38		0.24	0.53	31
147	217	0.43	72.8	6.0	1.8	1.0	0.5	0.3	959	969	63	38	26		0.23	0.39	21
154	238	0.22	73.5	5.9	1.8	1.1	0.5	0.3	1019	1094	53	36	31		0.17	0.39	24
164	244	0.41	74.7	5.7	1.8	1.0	0.5	0.3	959	1049	62	37	30		0.21	0.38	23
174	249	0.56	69.1	7.0	2.2	1.4	0.6	0.4	1259	1402	72	40	35	232	0.23	0.45	30
184	252	0.75	67.8	7.5	2.3	1.3	0.6	0.4	1259	1299	84	42	37	155	0.32	0.52	30
194	254	3.59	76.4	5.2	1.5	0.9	0.5	0.3	839	1014	54	41	29	387	0.26	0.38	24
204	257	1.15	74.0	5.9	1.6	1.0	0.6	0.3	899	1177	50	44	28	232	0.19	0.48	24
214	269	0.77	76.5	5.0	1.5	0.9	0.5	0.3	839	942	49	43	31	155	0.24	0.38	26
224	299	0.48	75.3	5.4	1.7	1.1	0.6	0.3	899	998	58	41	32	155	0.26	0.41	28
237	302	0.67	73.2	5.8	1.5	1.0	0.6	0.3	899	1049	57	52	33	929	0.33	0.40	28
244	303	1.45	76.6	4.7	1.4	0.9	0.5	0.3	779	871	50	39	29	232	0.10	0.37	21
254	306	1.45	78.1	4.3	1.4	0.8	0.5	0.2	779	829	49	42	28	155	0.18	0.31	22
264	308	1.50	74.4	5.1	1.6	1.0	0.5	0.3	899	1031	58	37	30	155	0.14	0.37	23
274	310	0.71	61.5	9.4	2.4	1.6	0.7	0.4	1439	1664	88	53	52	155	0.22	0.52	38
284	320	0.40	69.7	6.5	1.8	1.1	0.5	0.3	1019	1317	72	36	34	155	0.13	0.44	26
294	324	0.67	74.0	5.2	1.5	0.9	0.5	0.3	839	918	61	44	31	310	0.17	0.33	25
304	327	0.60	71.8	6.1	1.9	1.2	0.6	0.3	1139	1173	73	41	36	465	0.20	0.45	29
314	331	0.29	76.2	5.4	1.5	0.9	0.5	0.2	779	960	52	41	27	310	0.23	0.34	22
324	343	0.19	82.9	3.6	1.0	0.6	0.4	0.2	540	697	47	32	22	542	0.19	0.31	16
334	355	1.09	79.7	4.7	1.1	0.7	0.4	0.2	540	902	45	42	24	465	0.22	0.27	18
344	367	0.37	80.3	4.8	0.9	0.5	0.4	0.2	480	864	39	36	23	155	0.08	0.25	15
354	379	0.41	79.6	4.8	1.2	0.7	0.4	0.2	600	852	41	45	24	232	0.22	0.35	21
364	391	0.24	66.0	7.7	2.3	1.5	0.7	0.5	1379	1333	83	51	45	232	0.25	0.55	36
376	405	0.34	72.8	6.3	1.9	1.2	0.5	0.3	1139	1026	64	46	38	155	0.23	0.42	28
386	408	0.22	72.1	6.3	1.9	1.2	0.5	0.4	1139	1207	71	40	37	232	0.17	0.49	27
394	410	0.36	67.5	7.6	2.3	1.4	0.6	0.4	1319	1257	75	49	43	232	0.24	0.46	34
407	414	0.86	64.6	7.8	2.4	1.5	0.6	0.5	1319	1484	88	43	45	232	0.19	0.58	35
414	416	1.29	78.6	4.7	1.4	0.8	0.5	0.2	779	683	45	42	26	387	0.17	0.34	23
426	420	1.34	74.4	6.3	1.4	0.9	0.5	0.3	779	1065	49	48	38	232	0.11	0.35	25
434	422	1.10	69.5	7.1	1.8	1.2	0.6	0.3	1079	1157	57	51	36	232	0.25	0.50	30
447	426	0.82	64.4	7.7	2.3	1.5	0.7	0.4	1319	1306	86	49	49	155	0.25	0.59	36
454	428	0.85	66.5	7.6	2.3	1.5	0.6	0.3	1379	1271	76	51	43	155	0.28	0.62	36
464	431	0.43	58.2	9.6	2.9	1.7	0.7	0.5	1679	1765	104	50	57	232	0.33	0.73	44
474	434	0.38	49.0														
484	441	0.48	49.3	4.8	1.3	0.8	0.5	0.3	719	1015	46	36	28	310	0.15	0.34	20
495	448	0.55	46.9														
504	454	0.35	49.1	5.8	1.6	1.0	0.5	0.3	959	1011	60	41	33	155	0.19	0.45	25
514	461	0.23	48.3														
524	479		48.5	5.8	1.7	1.0	0.5	0.3	899	1149	60	41	32	155	0.20	0.40	24

Table II: TSRI and major and trace elements contents in Core MD 90929. Element concentrations are given in % or in ppm (μg/g). The TSRI corresponds to the ratio of the number of individuals of radiolarian species characteristic of the thermocline depth to the number of individuals of radiolarian species characteristic of the surface layer (see text for more details).

TSRI et teneurs en éléments majeurs et en traces. Les teneurs en éléments sont exprimées en % ou en ppm (μg/g). Le TSRI correspond au rapport du nombre d'individus d'espèces de radiolaires caractéristiques de la profondeur de la thermocline sur le nombre d'individus d'espèces de radiolaires caractéristiques de la surface (voir le texte pour plus de détails).

Depth (cmbsf)	Age (ka)	Mg/Ca ($x10^4$)	Si/Al	Fe/Al	Mg/Al	K/Al	Ti/Al ($x10^4$)	Ba/Al ($x10^4$)	Cu/Al ($x10^4$)	Ni/Al ($x10^4$)	Zn/Al ($x10^4$)	Mn/Al ($x10^4$)	Mo/Al ($x10^4$)	U/Al ($x10^4$)	V/Al ($x10^4$)
8	4	184.2	3.8	0.5	0.3	0.2	1480.1	1850.0	117.0	80.5	49.2	764.8	0.5	0.30	40.3
18	9	141.0	3.5	0.6	0.3	0.1	917.6	1015.3	69.5	54.6	32.9	493.9	0.4	0.34	25.8
29	14	163.4	3.1	1.3	0.4	0.2	921.4	1056.6	76.3	95.8	42.9	1289.5	1.3	0.30	29.7
39	19	164.2	3.4	0.6	0.4	0.2	1181.5	1367.0	52.9	75.3	43.5	981.2	0.8	0.36	37.2
49	38	186.8	3.5	0.6	0.4	0.2	1365.9	1587.3	74.7	73.4	49.2	352.9	0.4	0.26	37.8
57	53	160.7	3.4	0.6	0.4	0.2	1072.4	1155.9	61.8	56.1	38.5	319.7	0.2	0.31	31.9
69	73	124.8	3.9	0.6	0.5	0.2	416.3	581.5	24.3	31.5	16.9		0.5	0.33	12.3
80	91	131.4	3.8	0.6	0.4	0.2	568.2	740.4	33.7	44.9	27.1	570.9	0.8	0.40	19.6
89	106	144.8	4.1	0.6	0.4	0.2	659.9	909.3	46.7	46.6	30.6	511.5	0.7	0.31	18.2
99	122	134.3	3.7	0.6	0.4	0.2	659.9	821.2	37.1	40.0	24.5		0.3	0.39	20.4
107	136	131.2	3.8	0.6	0.4	0.2	536.8	736.3	36.5	39.7	22.2	231.2	0.5	0.34	15.0
119	158	164.3	3.7	0.6	0.4	0.2	1068.3	1088.4	58.4	51.7	33.7	743.1	0.4	0.28	28.8
129	176	253.7	3.3	0.6	0.3	0.2	3064.3	2386.1	152.9	100.6	80.9	1439.5	0.2	0.22	73.9
139	194	235.6	3.8	0.6	0.3	0.2	2544.6	2330.2	132.9	88.7	80.4		0.1	0.25	64.9
147	217	187.0	3.4	0.6	0.3	0.2	1700.6	1718.0	111.7	67.5	46.8		0.1	0.22	37.8
154	238	181.0	3.3	0.6	0.3	0.2	1850.1	1985.9	96.2	65.4	56.5		0.1	0.21	43.7
164	244	184.0	3.2	0.6	0.3	0.2	1705.7	1865.4	109.9	66.3	53.7		0.1	0.21	40.4
174	249	227.9	3.1	0.6	0.3	0.2	2825.1	3146.1	162.0	88.6	79.2	521.4	0.1	0.20	67.3
184	252	244.9	3.3	0.6	0.3	0.2	2871.7	2963.1	192.3	96.7	83.3	353.3	0.1	0.23	69.1
194	254	179.0	3.5	0.6	0.4	0.2	1257.1	1518.7	81.5	61.7	43.4	580.0	0.2	0.25	36.1
204	257	195.3	3.7	0.6	0.4	0.2	1413.5	1850.1	77.8	69.8	44.5	365.2	0.1	0.31	37.4
214	269	184.9	3.4	0.6	0.4	0.2	1252.6	1405.9	73.6	64.6	46.0	231.2	0.2	0.25	38.2
224	299	206.1	3.2	0.6	0.3	0.2	1527.7	1695.5	98.2	69.5	54.9	263.1	0.2	0.24	46.9
237	302	195.9	3.8	0.6	0.4	0.2	1389.7	1621.1	87.5	80.4	50.8	1436.2	0.2	0.26	43.6
244	303	164.7	3.3	0.6	0.3	0.2	1117.8	1249.2	71.1	55.9	41.2	333.2	0.1	0.26	30.7
254	306	157.7	3.2	0.6	0.4	0.2	1060.0	1127.6	66.5	56.4	38.1	210.7	0.1	0.23	29.2
264	308	179.2	3.3	0.6	0.3	0.2	1413.5	1620.6	91.2	58.6	47.5	243.5	0.1	0.24	36.0
274	310	309.7	3.9	0.6	0.3	0.2	3479.9	4024.6	213.6	127.5	125.8	374.6	0.1	0.21	91.7
284	320	199.9	3.5	0.6	0.3	0.2	1866.2	2411.7	132.0	65.7	62.6	283.6	0.1	0.24	47.6
294	324	183.1	3.4	0.6	0.3	0.2	1297.0	1418.7	94.9	68.6	47.8	478.7	0.1	0.21	38.9
304	327	212.8	3.2	0.6	0.3	0.2	2188.3	2253.5	139.3	78.8	69.4	892.7	0.1	0.23	55.5
314	331	159.4	3.7	0.6	0.3	0.2	1142.5	1407.4	75.8	60.3	39.3	454.1	0.2	0.23	32.7
324	343	129.5	3.4	0.6	0.4	0.2	562.5	726.7	48.6	33.7	22.4	565.2	0.2	0.30	16.8
334	355	133.0	4.3	0.6	0.4	0.2	591.1	988.2	49.2	46.0	25.9	509.1	0.2	0.25	20.2
344	367	124.8	5.3	0.6	0.4	0.2	434.0	781.9	34.9	32.5	20.8	140.2	0.1	0.28	13.7
354	379	144.1	4.0	0.6	0.4	0.2	710.7	1010.0	49.0	53.7	28.2	275.4	0.2	0.30	24.7
364	391	274.3	3.3	0.6	0.3	0.2	3196.3	3090.0	191.2	117.8	104.8	538.6	0.1	0.24	84.4
376	405	187.9	3.3	0.6	0.3	0.2	2158.1	1943.9	121.1	86.6	71.2	293.5	0.1	0.22	53.6
386	408	191.6	3.3	0.6	0.3	0.2	2188.3	2318.8	137.2	76.1	70.1	446.3	0.1	0.26	52.3
394	410	240.0	3.3	0.6	0.3	0.2	3050.3	2907.2	174.4	113.1	99.9	537.3	0.1	0.20	78.4
407	414	257.2	3.3	0.6	0.3	0.2	3148.0	3542.1	210.0	102.2	106.5	554.6	0.1	0.24	82.6
414	416	158.9	3.4	0.6	0.3	0.2	1084.8	950.7	62.9	58.6	35.9	539.0	0.1	0.24	31.3
426	420	184.6	4.6	0.6	0.4	0.2	1064.2	1454.2	67.0	65.3	52.4	317.2	0.1	0.26	33.7
434	422	221.0	3.9	0.6	0.3	0.2	1964.6	2106.4	103.6	93.0	64.6	423.0	0.1	0.27	54.4
447	426	282.4	3.4	0.6	0.3	0.2	3001.5	2972.1	195.5	110.4	111.1	352.5	0.1	0.26	81.7
454	428	256.3	3.2	0.6	0.3	0.1	3210.9	2959.7	176.5	118.3	99.7	360.7	0.1	0.27	83.8
464	431	332.9	3.3	0.6	0.3	0.2	4832.8	5081.6	299.4	142.8	164.1	668.9	0.1	0.25	126.7
474	434	0.0													
484	441	155.7	3.7	0.6	0.4	0.2	921.4	1300.0	58.8	46.6	36.1	396.8	0.1	0.27	26.0
495	448	0.0													
504	454	183.5	3.6	0.6	0.3	0.2	1558.5	1642.6	97.0	66.0	53.6	251.7	0.1	0.28	40.0
514	461	0.0													
524	479	180.8	3.5	0.6	0.3	0.2	1484.9	1897.3	99.6	66.9	52.3	255.8	0.1	0.24	39.0

Table III: Mg/Ca ratio and major and trace element contents normalized to the Al content, expressed as wt %/wt %, or as ppm/wt %.

Rapport Mg/Ca et teneurs en principaux éléments normalisées à l'Al, exprimées en wt %/wt % ou en ppm/wt %.

Depth (cmbsf)	Age (ka)	bulk MAR	CaCO3 MAR	Si MAR	Al MAR	Fe MAR	Mg MAR	K MAR	Ti MAR	Ba MAR	Cu MAR	Ni MAR	Zn MAR	Mn MAR	Mo MAR	U MAR	V MAR
8	4	1.3	1.0	84.3	22.0	11.8	6.8	4.1	1199.4	1499.1	94.8	65.2	39.9	619.7	1.00	0.67	32.7
18	9	1.4	1.1	64.5	18.3	10.4	6.1	2.7	1031.6	1141.4	78.2	61.4	37.0	555.3	0.80	0.62	29.0
29	14	1.5	1.2	61.4	19.7	26.0	7.8	4.0	1106.1	1268.4	91.6	115.0	51.5	1547.9	2.49	0.60	35.7
39	19	0.6	0.5	29.0	8.5	5.3	3.0	1.5	507.7	587.3	22.7	32.4	18.7	421.6	0.64	0.31	16.0
49	38	0.4	0.3	19.5	5.6	3.3	2.0	1.2	329.6	383.0	18.0	17.7	11.9	85.1	0.22	0.15	9.1
57	53	0.4	0.3	19.8	5.8	3.6	2.1	1.0	327.7	353.2	18.9	17.2	11.8	97.7	0.14	0.18	9.8
69	73	0.4	0.4	15.0	3.9	2.3	1.8	0.9	215.2	300.6	12.6	16.3	8.7		0.19	0.13	6.4
80	91	0.4	0.4	17.2	4.5	2.7	1.8	0.8	231.0	301.0	13.7	18.2	11.0	232.1	0.38	0.18	8.0
89	106	0.4	0.3	19.0	4.7	2.7	1.9	0.8	254.0	350.0	18.0	17.9	11.8	196.9	0.33	0.14	7.0
99	122	0.4	0.3	17.0	4.6	2.8	1.8	0.9	252.6	314.3	14.2	15.3	9.4		0.13	0.18	7.8
107	136	0.4	0.3	15.5	4.1	2.4	1.7	0.8	223.3	306.3	15.2	16.5	9.2	96.2	0.19	0.14	6.2
119	158	0.4	0.3	18.8	5.1	3.2	1.8	0.9	292.4	297.9	16.0	14.1	9.2	203.4	0.19	0.14	7.9
129	176	0.4	0.2	27.4	8.3	4.8	2.4	1.5	470.1	366.0	23.5	15.4	12.4	220.8	0.20	0.19	11.3
139	194	0.3	0.2	23.3	6.2	3.9	1.7	1.1	347.5	318.2	18.1	12.1	11.0		0.07	0.15	8.9
147	217	0.2	0.2	13.5	4.0	2.3	1.2	0.8	215.8	218.0	14.2	8.6	5.9		0.05	0.09	4.8
154	238	0.5	0.3	27.6	8.5	5.3	2.4	1.4	475.6	510.6	24.7	16.8	14.5		0.08	0.18	11.2
164	244	1.3	1.0	73.5	23.1	13.0	6.7	4.1	1245.9	1362.6	80.3	48.5	39.2		0.27	0.49	29.5
174	249	1.6	1.1	114.5	37.0	22.7	9.8	6.2	2073.3	2308.9	118.9	65.1	58.1	382.6	0.38	0.74	49.4
184	252	2.3	1.6	171.7	52.5	29.8	14.3	9.9	2899.1	2991.3	194.1	97.6	84.1	356.7	0.74	1.20	69.8
194	254	2.5	1.9	130.0	37.5	23.3	13.1	6.9	2101.2	2538.6	136.2	103.1	72.6	969.4	0.65	0.95	60.3
204	257	0.9	0.7	52.0	13.9	8.4	4.9	2.7	792.8	1037.7	43.6	39.1	24.9	204.8	0.17	0.42	21.0
214	269	0.3	0.2	16.0	4.7	3.0	1.7	0.9	266.8	299.5	15.7	13.8	9.8	49.2	0.08	0.12	8.1
224	299	0.5	0.4	26.2	8.2	5.1	2.8	1.6	432.7	480.3	27.8	19.7	15.5	74.5	0.13	0.20	13.3
237	302	3.1	2.3	179.2	47.6	30.6	17.3	9.0	2771.4	3232.9	174.4	160.3	101.4	2864.1	1.02	1.23	86.9
244	303	3.4	2.6	160.2	48.6	30.3	17.0	9.0	2641.6	2952.3	168.1	132.2	97.3	787.5	0.34	1.25	72.5
254	306	3.4	2.6	146.7	46.0	28.4	16.3	8.4	2636.4	2804.4	165.4	140.4	94.7	524.0	0.61	1.05	72.7
264	308	3.3	2.4	166.1	51.1	31.6	17.1	9.4	2923.0	3351.2	188.5	121.2	98.2	503.5	0.46	1.20	74.4
274	310	1.0	0.6	92.3	23.9	15.5	7.1	3.9	1419.1	1641.2	87.1	52.0	51.3	152.8	0.22	0.51	37.4
284	320	1.0	0.7	67.1	19.0	11.8	5.6	3.6	1056.5	1365.3	74.7	37.2	35.5	160.6	0.13	0.46	27.0
294	324	2.0	1.5	103.0	30.5	18.6	10.4	5.4	1657.2	1812.6	121.2	87.7	61.0	611.7	0.34	0.65	49.8
304	327	1.9	1.4	115.8	36.2	22.7	10.9	6.6	2145.5	2209.5	136.6	77.2	68.0	875.3	0.38	0.85	54.4
314	331	0.9	0.7	47.1	12.8	7.8	4.1	2.1	682.9	841.2	45.3	36.0	23.5	271.5	0.20	0.30	19.5
324	343	0.6	0.5	22.3	6.5	3.9	2.6	1.2	336.4	434.6	29.1	20.1	13.4	338.0	0.12	0.19	10.0
334	355	0.9	0.7	43.7	10.2	6.1	3.8	1.9	501.4	838.3	41.7	39.0	21.9	431.8	0.20	0.25	17.1
344	367	0.6	0.5	28.6	5.4	3.3	2.3	1.0	286.7	516.4	23.1	21.5	13.7	92.6	0.05	0.15	9.0
354	379	0.6	0.5	28.3	7.0	4.1	2.6	1.2	356.4	506.5	24.6	26.9	14.1	138.1	0.13	0.21	12.4
364	391	0.5	0.3	40.1	12.0	7.6	3.6	2.4	714.9	691.1	42.8	26.3	23.4	120.5	0.13	0.29	18.9
376	405	0.9	0.7	56.7	17.2	10.7	4.8	2.9	1032.2	929.7	57.9	41.4	34.1	140.4	0.21	0.38	25.6
386	408	2.3	1.7	147.0	45.0	27.9	12.4	8.4	2669.6	2828.8	167.3	92.8	85.5	544.5	0.40	1.15	63.7
394	410	2.2	1.5	167.2	51.1	31.7	13.7	8.1	2914.0	2777.2	166.6	108.0	95.4	513.3	0.53	1.02	74.9
407	414	2.2	1.4	169.9	52.0	32.0	13.8	10.1	2871.4	3230.8	191.6	93.2	97.1	505.8	0.41	1.26	75.3
414	416	2.4	1.9	113.0	33.3	20.2	11.5	5.8	1864.3	1633.8	108.1	100.7	61.7	926.3	0.41	0.81	53.8
426	420	2.4	1.8	147.8	32.2	20.1	12.2	6.7	1837.8	2511.5	115.8	112.7	90.6	547.9	0.26	0.83	58.2
434	422	2.2	1.6	159.3	40.7	25.8	13.1	6.5	2410.8	2584.9	127.1	114.2	79.3	519.1	0.56	1.12	66.8
447	426	2.2	1.4	172.3	50.7	32.5	15.4	9.1	2935.5	2906.8	191.2	107.9	108.6	344.7	0.56	1.31	79.9
454	428	2.4	1.6	179.2	55.2	34.7	15.3	8.3	3271.4	3015.5	179.8	120.5	101.5	367.5	0.66	1.47	85.4
464	431	2.1	1.2	196.0	59.1	35.9	15.2	10.6	3443.3	3620.5	213.3	101.7	116.9	476.6	0.68	1.50	90.3
474	434	1.5	1.2														
484	441	1.1	0.8	50.9	13.7	8.3	5.0	2.9	769.6	1085.9	49.1	38.9	30.2	331.4	0.16	0.36	21.7
495	448	1.2	0.9														
504	454	1.1	0.8	63.6	17.7	11.0	5.7	3.6	1045.7	1102.2	65.1	44.3	36.0	168.9	0.21	0.49	26.8
514	461	0.6	0.4														
524	479	0.4	0.3	24.0	6.9	4.2	2.2	1.4	375.3	479.5	25.2	16.9	13.2	64.6	0.08	0.17	9.8

Table IV: Bulk MAR and significant elements MARs. Bulk MAR is given in g/cm^2/kyr, major element MARs are given in mg/cm^2/kyr, and trace element MARs are given in µg/cm^2/kyr. *Taux de sédimentation global et des différents éléments chimiques. Le taux de sédimentation du bulk est exprimé en g/cm^2/kyr, le taux de sédimentation des éléments majeurs en mg/cm^2/kyr, et le taux de sédimentation des éléments en trace en µg/cm^2/kyr.*

Samples	dbsf (cm)	69	129	174	274	324	364	414	464
	age (ka)	73	176	249	310	343	391	416	431
Carbonate-	ppm Ba	90	96	58	134	172	92	104	91
linked fraction	% Ba	13.4	9.4	4.1	8.1	24.7	6.9	15.2	5.2
Oxyhydroxide-	ppm Ba	72	130	142	197	90	154	97	194
bound fraction	% Ba	10.8	12.7	10.1	11.8	12.9	11.6	14.2	11.0
Terrigenous	ppm Ba	217	380	490	860	84	840	265	700
fraction	% Ba	32.4	37.0	35.0	51.7	12.1	63.0	38.8	39.7
Residual (barite)	ppm Ba	291	421	712	473	351	247	217	780
fraction	% Ba	43.4	41.0	50.8	28.4	50.4	18.5	31.8	44.2

Table V: Distribution of barium within the different sediment fractions: carbonate, oxyhydroxides, aluminosilicates and residual (barite) fractions.
Répartition du baryum entre les différentes fractions du sédiment: carbonates, oxihydroxides, aluminosilicates et résidu (barytine).

A radiolarian index was used as an independant proxy to monitor variations in surface paleoproductivity. Based upon the observations of Kling and Boltovskoy [1995] on the vertical distribution of plankton in the eastern Pacific, the abundance of some radiolarian species characteristic of the surface layer (*Heliodiscus asteriscus*, *Lithopera bacca*, and *Siphonosphaera polysiphonia*), and of the thermocline layer (*Cycladophora d. davisiana*, *Cycladophora d. cornutoïdes*, *Cyrtolagena laguncula*, *Eucyrtidium calvertense*, *Larcopyle butchlii* and *Spongopyle osculosa*) were counted at each level. The ratio of the total number of specimens characteristic of the thermocline layer versus the total number of specimens characteristic of the surface layer was calculated. This radiolarian index (called TSRI) was used as an indicator of the fertility of the upper layers of the ocean: when the food supply in the surface layer increases, the surficial planktic populations, including the radiolarians, thrive. The resulting increase in fecal pellets and food transport towards the deeper water masses allows the thermocline populations to grow. As a result, the thermocline/surface ratio calculated for the exported populations of radiolarians increases.

Radiolarians are sensible to opal dissolution during settling of their skeletons through the water column and within the sediment. Opal dissolution modifies the composition of fossil radiolarian assemblages. Since sea water is always silica-undersaturated in the water column, temporal variations in radiolarian populations at the water/sediment interface can be considered as being linked mostly to variations in surface productivity rather than to variations in dissolution strength [Berger, 1968]. Within the sediment, it is known that opal dissolution occurs within the first 20 centimeters beneath the water/sediment interface, but in areas subjected to a

significant export of siliceous debris, this dissolution leads to silica saturation of the interstitial water and dissolution stops at nearly 20/30 cm beneath the interface [Johnson, 1974, 1976]. Under fertile water masses, variations in the content and composition of the radiolarian population in the sediments can, thus, be considered as representative of surface productivity changes.

Radiolarian slides were prepared following the classical procedure of Sanfilippo et al., [1985]. Occurrences of all representatives of the selected species found on a single microscope slide (24 x 32 mm) were counted in samples taken at 10 cm intervals. Variations of the TSRI are presented in table II.

Bulk sediment mass accumulation rates (MAR) were calculated by multiplying the linear sedimentation rate (LSR) derived from the age model by the dry bulk density (DBD) (table IV). The DBD was obtained from the ratio: g dry weight/cm^3 wet volume. Element fluxes were calculated by multiplying the element content and the bulk MAR.

4. Results and interpretation

4.1. Chronological framework

The age model for Core MD 90929 is based on an oxygen-isotope analysis of 65 bulk sediment samples taken at 10 cm intervals. Previous work has shown that oxygen-isotope analysis of bulk sediment provides globally correct ages in this area [Shackleton et al., 1993]. The $\delta^{18}O$ was calculated relative to the PDB and a graphic correlation was done by close peak to peak adjustment to the SPECMAP stack record (fig. 2).

The $\delta^{18}O$ record in Core MD 90929 was measured on the bulk sediment, and compared with the $\delta^{18}O$ record for Core MD 85668 [Shackleton et al., 1993], that is considered as a reference stack for oxygen isotope analysis of bulk sediment in this area. Due to differences in sampling and sedimentation rates in the two cores (fig. 2), a peak to peak correlation for the last 100 kyr is not significant. It is, however, possible to see that the global trend of the $\delta^{18}O$ record of the bulk sediment in Core MD 90929 is similar to the one observed for Core MD 85668. The $\delta^{18}O$ values are, however, more negative in Core MD 85668 than in Core MD 90929.

A biostratigraphic control was used to test the reliability of the isotope age model established for Core MD 90929. The evolutionnary transition leading to the first appearance of the radiolarian species *Buccinosphaera invaginata* Haeckel was observed at a sediment level dated at 176 ka by the isotope curve, and the last appearance of *Stylatractus universus* Hays was

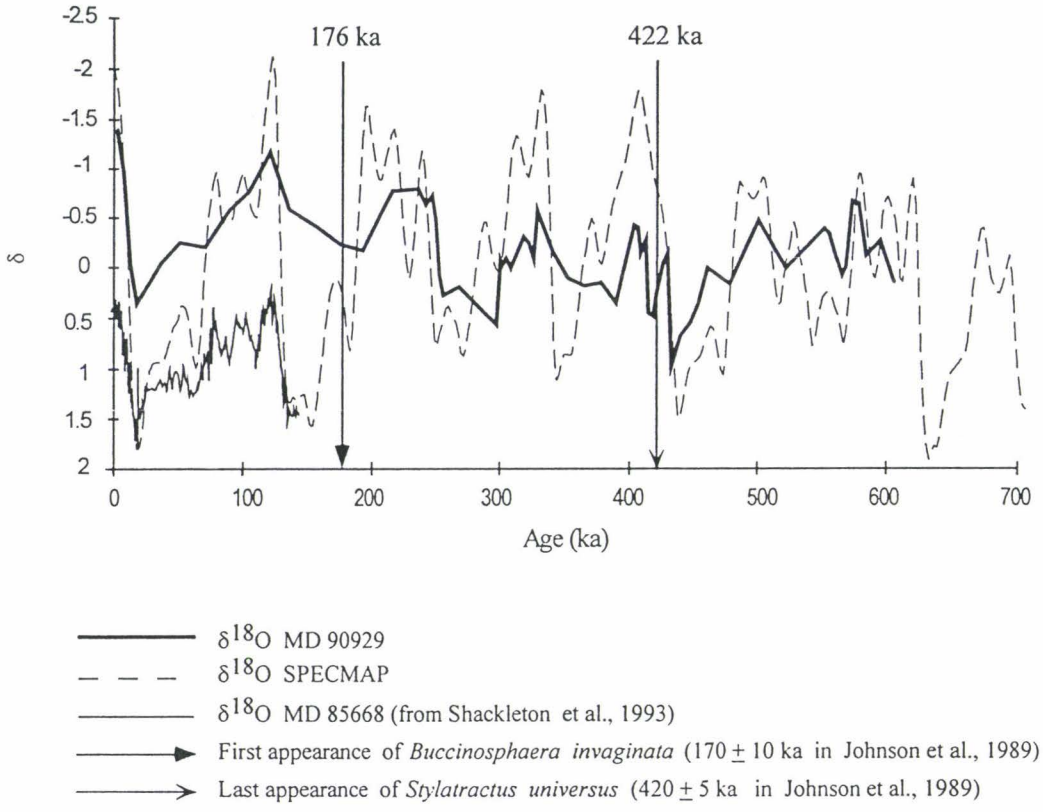

Figure 2: Oxygen isotope record for the bulk carbonate in Core MD 90929 (bold solid line) compared to the SPECMAP $\delta^{18}O$ stack (dashed line) and to the $\delta^{18}O$ of the bulk sediment of Core MD 85668 (Shackleton et al., 1994) (thin solid line). The first appearance of *Buccinosphaera invaginata*, and the last appearance of *Stylatractus universus* are indicated.
Courbe du $\delta^{18}O$ mesuré sur le sédiment total de la carotte MD 90929 (ligne pleine épaisse) comparée à la courbe de référence SPECMAP (courbe en pointillés) et à la courbe du $\delta^{18}O$ obtenue sur le sédiment total de la carotte MD 85668 (Shackleton et al., 1994)(ligne pleine fine). Les dates de première apparition de Buccinosphaera invaginata et d'extinction de Stylatractus universus sont indiquées.

observed at 422 ka. These ages are consistent with estimated absolute ages for these events, i.e. 170 ± 10 ka and 420 ± 5 ka, respectively, in the Central Indian Basin [Johnson et al., 1989]. Twenty major isotopic events recognized in this core are summarized in table I. The oldest sample (6.46 mbsf) is dated at 607 ky.

4.2. The Bulk Mass Accumulation Rate (MAR)

Bulk MAR values calculated for Core MD 90929 during the last 500 ky fall between 0.2 g/cm^2/kyr and 3.4 g/cm^2/kyr (fig. 3), and are comparable to the bulk MAR record in Core MD 90940 located on Madingley Rise [Jacot Des Combes et al., in press]. High bulk MAR values characterize both glacial/interglacial and interglacial/glacial transitions, except between isotope stages 7 and 2 (fig. 3), when consistently low values are recorded (0.5 g/cm^2/kyr). Significant

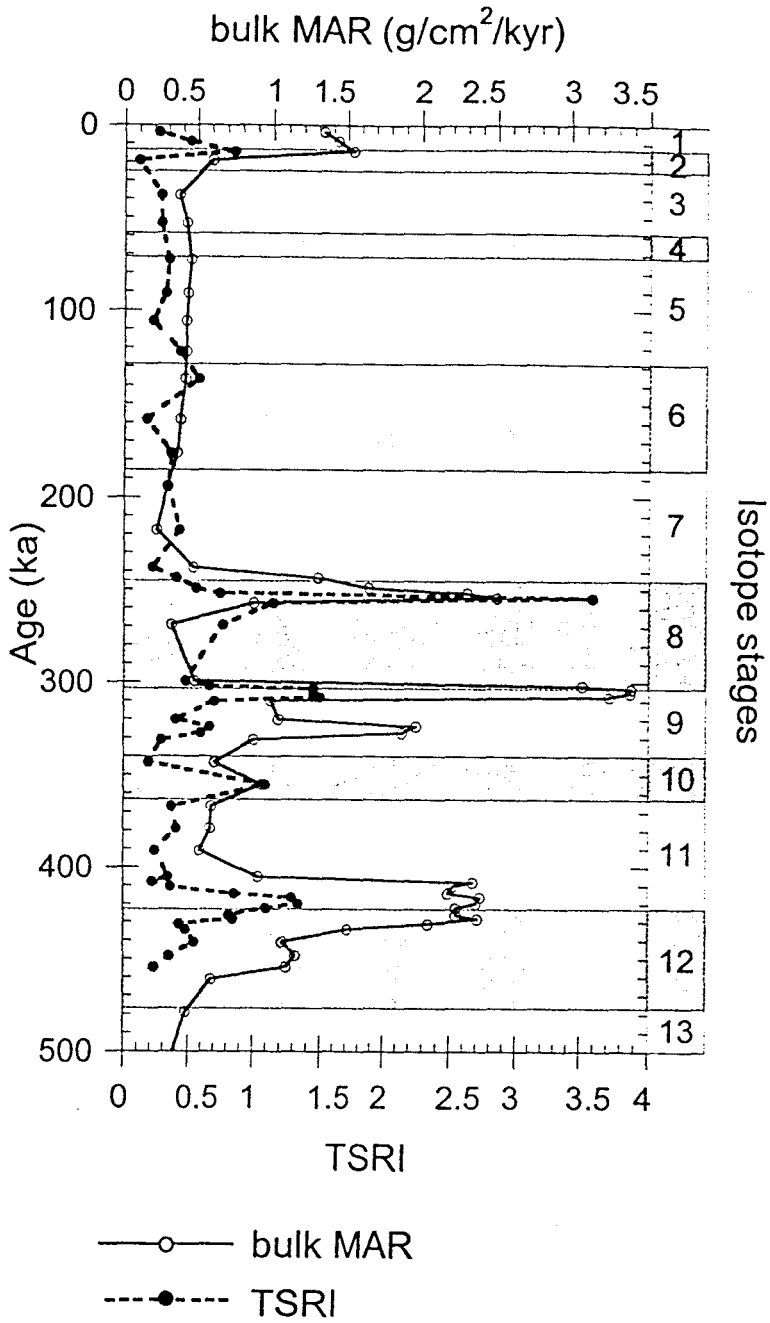

Figure 3: Variations of bulk MAR (thin solid line) and of TSRI (thick dashed line) versus age in Core MD 90929. The TSRI corresponds to the ratio of the number of individuals of radiolarian species characteristic of the thermocline depth to the number of individuals of radiolarian species characteristic of the surface layer (see text for more details). Isotope stages are identified on the right.
Variations du taux de sédimentation du sédiment total et du TSRI en fonction du temps. Le TSRI correspond au rapport du nombre d'individus d'espèces de radiolaires caractéristiques de la profondeur de la thermocline sur le nombre d'individus d'espèces de radiolaires caractéristiques de la surface (voir le texte pour plus de détails).

increases in MAR values are recorded at 15, 250, 305 ka, in the interval between 323 and 327 ka, and between 410 and 430 ka. In this last interval, three equal peak MAR values are observed: at 422, 420-416, and 408 ka (fig. 3).

As well as the bulk MAR, all element MARs exhibit very low values from 238 ka to 38 ka, i.e. from 8-7 to 3-2 isotope stage transitions.

4.3 The Radiolarian Index

The TSRI shows a strong variation from 0.11 to 3.59 (fig. 3). The maximum value (3.59) is recorded at 254 ka (end of isotope stage 8). Other peak values (>1) are observed at 257 ka, from 308 to 303 ka, at 355 ka, and from 422 to 416 ka. These peak values are located within both glacial and interglacial intervals. As well as bulk MAR and element MARs, the TSRI record exhibits continuously low values during the interval across the 8-7 isotope stage transition and during the last glacial maximum.

4.4. Geochemical proxies

4.4.1. Element contents and accumulation rates

Organic content ranks in abundances below the detection threshold for the Leco analyser (0.2 %) for all the samples studied.

Carbonate content varies beween 54.2 % and 84.7 %. The carbonate fraction is composed of planktic foraminifera and coccolithophorids. During the last 500 kyr, changes in carbonate content exhibit marked alternations. High values (>75 %) occur between 73 and 136 ka, and between 343 and 379 ka, while lower values of $CaCO_3$ are recorded between 176 and 194 ka, at 310 ka, 414 ka, and between 426 and 431 ka, i.e. during glacial as well as interglacial intervals (fig. 4).

$CaCO_3$ MAR varies from 0.2 g/cm^2/kyr to 2.6 g/cm^2/kyr with high values characterizing the intervals between 244 and 254 ka, 302 and 308 ka, 323 and 327 ka, and 408 and 431 ka, where the second peak value is stronger compared to the others. The maximum carbonate MAR values occurred at the 9-8 transition (fig. 5).

Amounts of non carbonate components are relatively low. Silica content varies from 3.3 to 9.5 % (most of this fraction is made of opal), Al content from 0.8 to 2.9 %, and Ti content from 480 to 1679 ppm (e.g. Al: fig. 4). Terrigenous elements also show a homogeneous distribution throughout the core, with higher values recorded from 176 to 194 ka, 249 to 252 ka,

at 310 ka, from 390 to 414 ka and from 426 to 431 ka, i.e. during glacial as well as interglacial intervals.

Barium content is relatively high throughout the core (from 670 ppm to 1765 ppm). Peak values are recorded from 249 to 252 ka, at 310 ka, from 390 to 414 ka and from 426 to 431 ka, i.e. during glacial as well as interglacial intervals (fig. 4).

The barium MAR record is similar to that of the terrigenous elements with peak values located from 4 to 14 ka, at 250 ka, 299 and 310 ka, 327 ka, 410-414 ka, and 426-431 ka (fig. 6). Barium MAR varies from 0.2 mg/cm^2/kyr at 218 ka to 3.2 mg/cm^2/kyr at 302 ka). As with the terrigenous element MARs, the Ba MAR values record a double-spike between 4 and 14 ka, 302 and 308 ka, and 408 and 431 ka (i.e. 2-1, 9-8 and 12-11 isotope stage transitions) where the maximum values are observed.

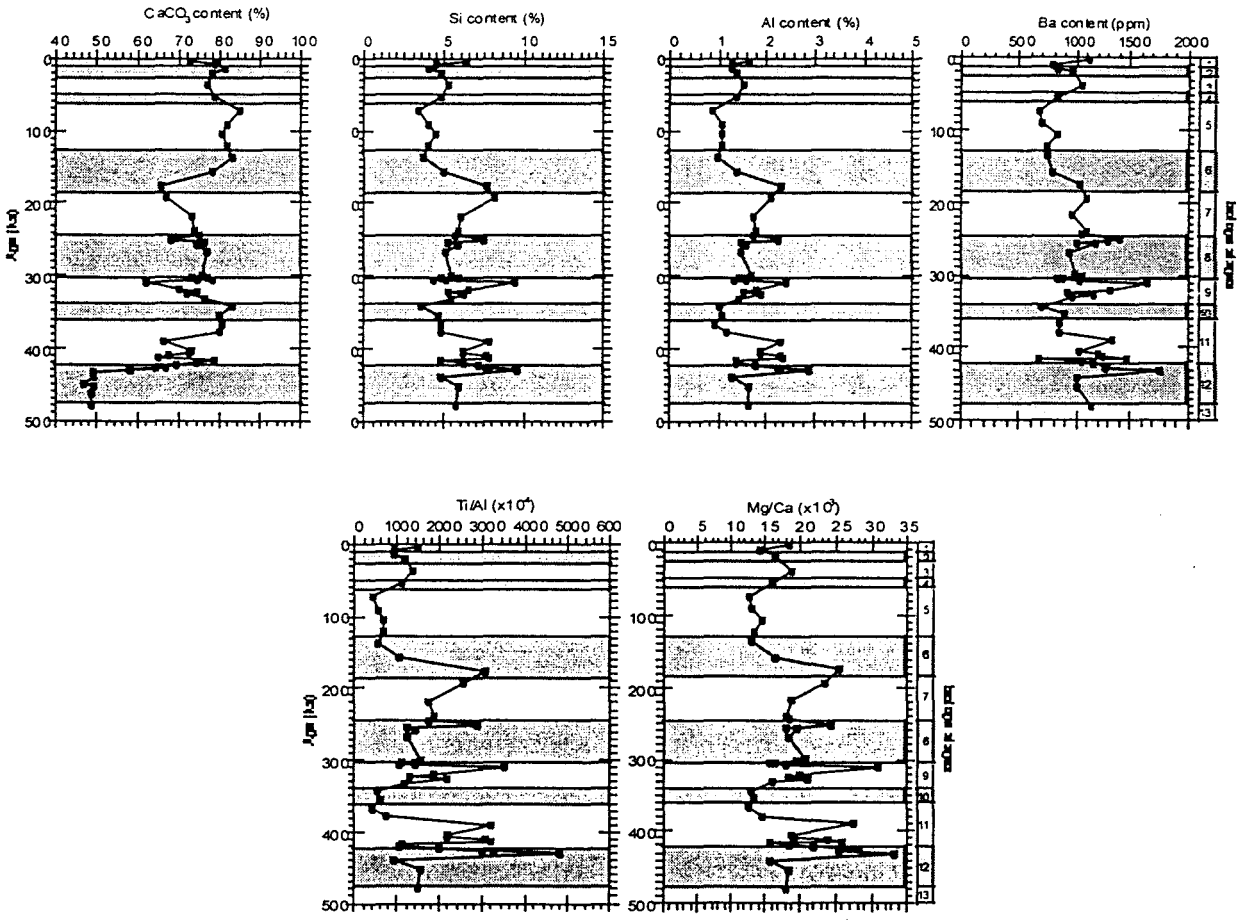

Figure 4: Variations of $CaCO_3$, Si, Al, and Ba contents, and of Ti/Al and Mg/Ca ratios versus age. Isotope stages are identified on the right.
Variations des teneurs en $CaCO_3$, Si, Al, et Ba, et des rapports Ti/Al et Mg/Ca, et en fonction du temps. Les stades isotopiques sont identifiés à droite.

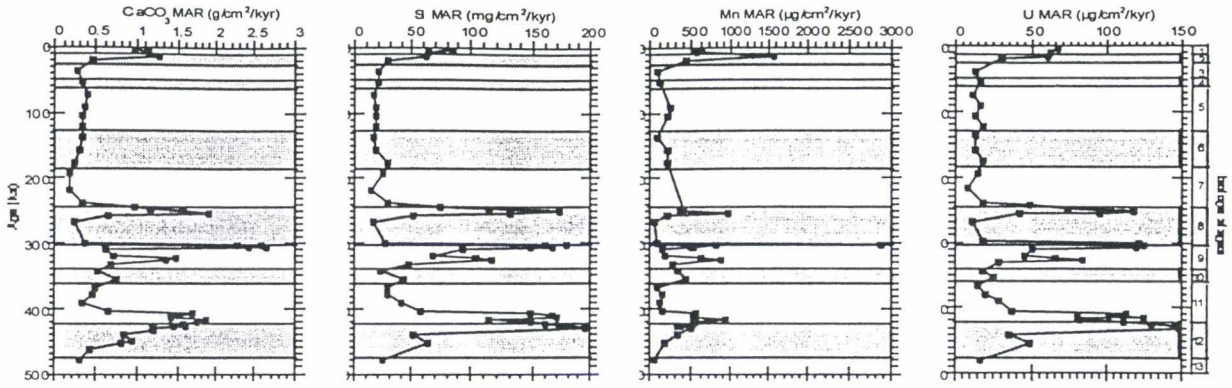

Figure 5: Variations of the $CaCO_3$, Si, Mn and U MARs versus age. Isotope stages are identified on the right.

Variations des taux de sédimentation de $CaCO_3$, Si, Mn et U en fonction du temps. Les stades isotopiques sont identifiés à droite.

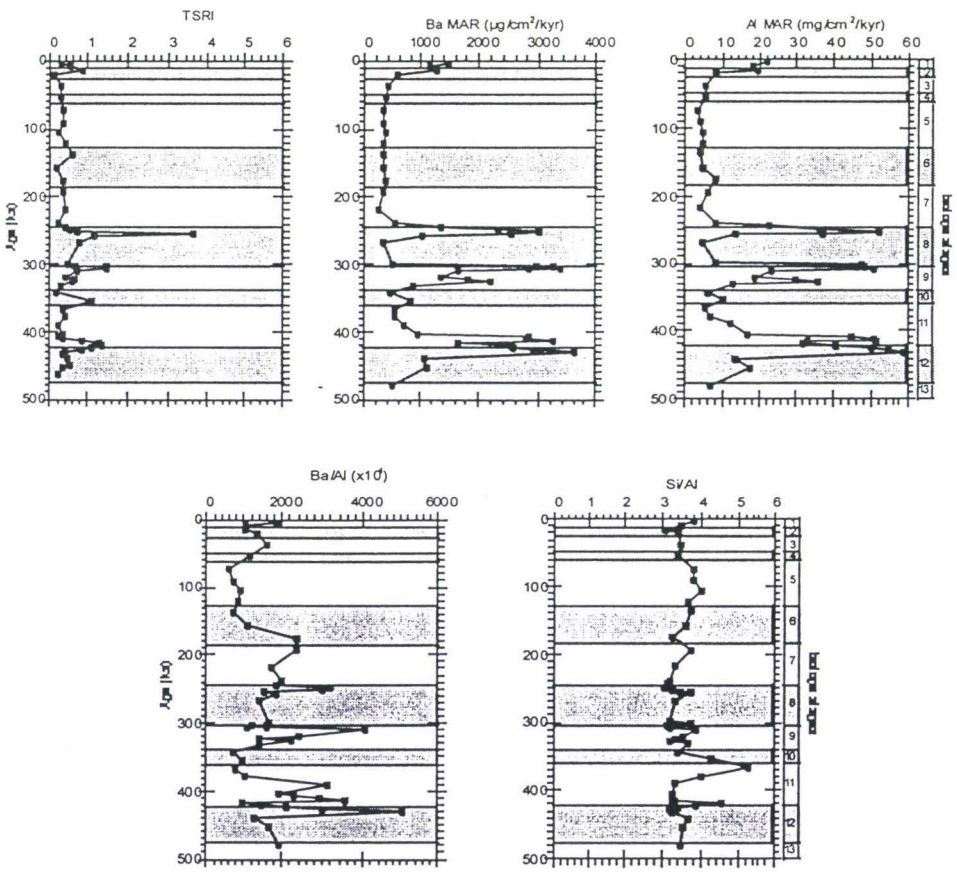

Figure 6: Variations of the TSRI, the Ba and Al MARs, and the Ba/Al and Si/Al ratios, expressed as wt %/wt % for Si/Al, and as 10^4 ppm /wt % for Ba/Al, versus age. Isotope stages are identified on the right.

Variations du TSRI, des taux d'accumulation de Ba et Al,et des rapports Ba/Al et Si/Al, exprimés en wt %/wt % pour Si/Al, et en 10^4 ppm /wt % pour Ba/Al, en fonction du temps. Les stades isotopiques sont identifiés à droite.

Copper, V, and Zn contents correlate well with the previously mentioned elements. These good correlations indicate that these trace metals were supplied with the terrigenous particles. Nickel content is low (32 ppm to 75 ppm) and shows maximum values at 14 ka, 302 ka, 310 ka, 391 ka, and from 422 to 431 ka.

Terrigenous elements MAR, i.e. Si, Al, Fe, Mg, K, Ti, Cu, V and Zn exhibit peak values that characterize glacial as well as interglacial intervals: from 4 to 14 ka, at 250 ka, 299 and 310 ka (double-
spike at the 9-8 transition), 327 ka, 410-414 ka, and 426-431 ka (e.g. Al and Si: figs. 5 and 6). The oldest peaks are located within the 12-11 transition interval.

Manganese content varies from 155 to 1007 ppm. High values occur at 14 ka, from 91 to 106 ka, from 158 to 176 ka, at 301 ka, and from 343 to 355 ka, and correspond to glacial and interglacial intervals. Manganese content values are below the detection range at 73 ka, 122 ka, and from 194 to 244 ka. Molybdenum and uranium contents vary from 0.08 to 1.62 ppm and from 0.25 to 0.73 ppm, respectively. Two Mo peak values are recorded: at 10 and 100 ka. No enrichment, compared to the average deep sea carbonate value [Turekian and Wedepohl, 1961], is recorded along the core.

Manganese MAR values are relatively low (from 0.1 to 2.9 $mg/cm^2/kyr$). The maximum value is recorded at the 9-8 transition (302 to 308 ka) where a single-spike occurs. Another peak value (1.6 $mg/cm^2/kyr$) is recorded at 14 ka. Other peak values (from 0.9 to 1 $mg/cm^2/kyr$) are found at at 254, 327, and 416 ka. Molybdenum MAR is also relatively low (from 4 to 249 $\mu g/cm^2/kyr$) and presents variations similar to the bulk MAR ones, except at 100 ka, when a local peak value (50 $\mu g/cm^2/kyr$) can be observed. The uranium MAR presents a variation similar to the bulk MAR, except between the present and 10 ka, when a decrease is observed instead of a peak value.

4.4.2. Results of sequential leaching

Data show that barium distribution within the different fractions of the sediment is variable (fig. 7). Mean distribution shows that 11 % of the Ba is linked to the carbonate fraction, 13 % is oxyhydroxide bound, 36 % is of terrigenous origin and 40 % is accumulated as barite. However, apart from the barium content of the oxyhydroxides fraction that remains almost constant (from 10.1 to 14.2 %), the barium content of the three other phases varies widely, especially in the terrigenous (from 12.1 to 63 %) and barite (from 18.5 to 50.8 %) phases. The

fact that the barite part of the Ba content is variable and rather low precludes consideration of Ba abundance as a reliable paleoproductivity proxy.

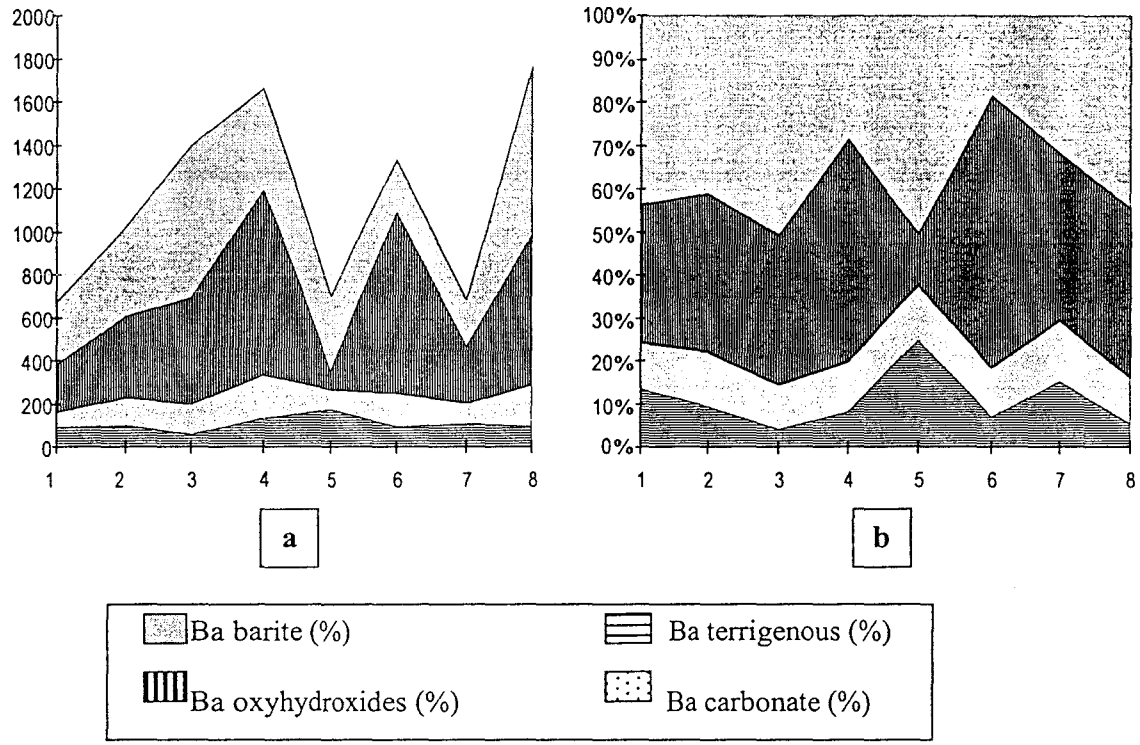

Figure 7: Distribution of barium bound to the different sediment fractions: carbonate, oxyhydroxides, aluminosilicates and residual (barite) fractions.
a: variations in ppm. **b:** % of each fraction relative to the bulk barium content.
Répartition du baryum entre les différentes fractions du sédiment: carbonates, oxyhydroxydes, aluminosilicates et résidu (barytine).
a: *Variations en ppm.* **b:** *% de chaque fraction rapporté au sédiment total.*

4.4.3. Normalized contents

The Mg/Ca and Ti/Al ratios are considered as indicators of wind strength because they express the enrichment of the sediment in detrital material of continental origin (dolomite from the Arabian sabkhas, and heavy and clay minerals) [Weedon and Shimmield, 1991; Shimmield, 1992; Tribovillard et al., 1996; Martinez, 1997; and references therein]. Variations in both these proxies are synchronous throughout the core (fig. 4) and suggest periods of enhanced winds occuring at 431 ka, from 414 to 416 ka, at 391 ka, 310 ka, 252 ka, and 176 ka; and lower wind strength from 343 to 379 ka, and from 73 to 136 ka, i.e. during glacial as well as interglacial intervals.

The Si/Al ratio does not correlate with wind strength proxies; maximum Si/Al values are recorded at 420 ka, and 367 ka, intervals and correspond to low Ti/Al values. Both Si/Al and

Ti/Al ratios show opposite variations, except from 324 ka to 299 ka, and from 244 ka to 194 ka, i.e. during interglacial stages 9 and 7 (figs. 4 and 6). This may be related to the presence of Si in some sediment fraction where the Ti content is negligible (opal, quartz...). Fe/Al ratio values remain constant around 0.6 except near 14 ka, where a maximum value of 1.32 is observed.

Relatively high values of the Ba/Al ratio point to the levels where some Ba enrichment occurs. Variations in this ratio are synchronous with those of the Ti/Al ratios, indicating that barium enrichment is synchronous with the increase in terrigenous input, mainly due to the wind (figs. 4 and 6). Such a concordance is also observed for the V/Al, Cu/Al, Ni/Al, and Zn/Al ratios (e.g. Cu: fig. 8).

The Mn/Al ratio exhibits differences with the wind strength proxies, especially from 9 to 91 ka, from 252 to 257 ka, from 303 to 324 ka, and from 331 to 367 ka, i.e. during isotope stages 9 to 7, and 5 to 1 (fig. 8). The Mo/Al ratio presents two peak values at 10 ka and 100 ka, that correspond to levels with a high Mo content. The U/Al ratio shows limited variations and remains between 200 and 400 x10 $^{-4}$ along the length of the core (fig. 8).

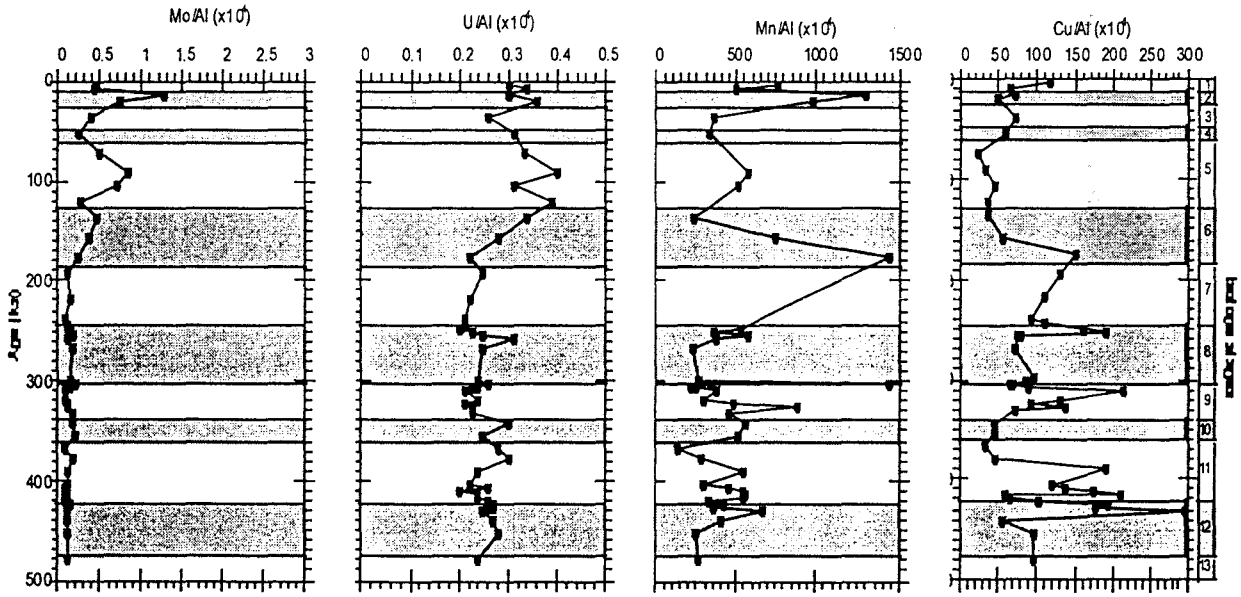

Figure 8: Variations of the Mo/Al, U/Al, Mn/Al and Cu/Al ratios, expressed as 10^4 ppm /wt %, versus age. Isotope stages are identified on the right.

Variations des rapports Mo/Al, U/Al, Mn/Al et Cu/Al, exprimés en 10^4 ppm /wt %, en fonction du temps. Les stades isotopiques sont identifiés à droite.

5. Discussion of the geochemical proxies

The sediment in Core MD 90929 contains no organic carbon. Furthermore, due to a water depth (3072 m) close to the actual CCD (between 4,500 and 5,000 m deep), bulk MAR variations can be linked to variations in either surface productivity or carbonate dissolution. In such an environment, the TSRI index measured in Core MD 90929 is a direct proxy for export productivity, and a comparison of the variations in the geochemical proxies to the variations in this index permits testing of their reliability as paleoproductivity indicators. In the same way, since the radiolarian index is completely independent of the age model established in Core MD 90929, a comparison of the bulk MAR with the TSRI will resolve the question raised about the process (surface productivity or carbonate dissolution) that controls the sedimentation rate at this site.

The bulk MAR profile shows a particular pattern in its upper part with a constant lack of variations from isotope stage 7 to isotope stage 2, i.e. from 38 to 238 ka (fig. 3). This long interval of constant low MAR values was unexpected. First, the sediment from this core seems to be homogenous and no visible lithologic or color limits can be observed. Second, such a pattern has never been observed in cores recovered in the NW Indian Ocean [Shimmield and Mowbrays; 1991; Weedon and Shimmield, 1991; Caulet et al., 1992; El Foukali, 1995; Vénec-Peyré et al., 1995; 1997; Tribovillard et al., 1996; Ouahdi, 1997; Jacot Des Combes et al., in press]. Furthermore, studies realized in this area have shown that the 6-5 transition (130 ka) is generally strongly recorded in the sediment, especially by bulk MAR variations [Vénec-Peyré et al., 1995, 1997; Tribovillard et al., 1996]. For all these reasons, the reliability of the bulk MAR record in this interval is questionable. Three hypotheses are discussed below to explain such a pattern.

The first hypothesis addresses the reliability of the age model. As stated above, the difference in the sampling intervals and sedimentation rates within Core MD 90929 and reference Core MD 85668, limits the possibility of establishing a peak to peak correlation between both $\delta^{18}O$ records, and the biostratigraphic markers provide only two control points. One of these control points is, however, located within the interval of low bulk MAR values. We can, thus, suppose that this part of the age model is correct.

The second hypothesis presumes a period of strong carbonate dissolution, leading to a diminution of the carbonate flux towards the sea floor, and thus, to a decrease in the bulk MAR, and the third hypothesis is linked to a decrease in surface productivity during this period. However, the good correlation between the bulk MAR and the radiolarian index favors the third

hypothesis. The "dissolution hypothesis" would result in a lack of correlation between the TSRI and the bulk MAR during the period of low bulk MAR values, and that is not observed. At 140 ka, however, a short period of dissimilarity between the bulk MAR and TSRI record can be recognized. This may indicate that, at this time, carbonate dissolution may have occurred (fig. 3). Since the radiolarian index is completely independent of the age model, the good correlation between the TSRI and the bulk MAR reinforces the reliability of the bulk MAR record as a paleoproductivity proxy, and consequently, of the age model. Furthermore, the positive correlation between the bulk MAR and the TSRI (fig. 3) demonstrates that sedimentation is, at this site, primarily linked to paleoproductivity even if terrigenous influences become significant, e.g. the 410-428 ka bulk MAR peak value.

This radiolarian index can, thus, be used to check the importance of carbonate dissolution on the sedimentary record. In previous studies of the NW Indian Ocean [Bassinot et al., 1994] carbonate dissolution has been considered as the main sedimentary process. Discrepancies between the radiolarian index and the carbonate MAR records indicate the part of the carbonate content (or MAR) variation induced by dissolution. Comparing the carbonate MAR with the radiolarian index shows two major differences (figs. 5 and 6). First, an increase in the TSRI is recorded in the upper part of isotope stage 6 (136 ka), while no increase is observed in the $CaCO_3$ MAR (fig. 5). This suggests an episode of enhanced carbonate dissolution. Then, at the 12-11 transition, a high $CaCO_3$ MAR period is marked by three successive peaks, the second (416 ka) being the strongest. During the same interval, the TSRI records a single peak corresponding to this strongest peak. The first peak of carbonate MAR at 428 ka is also recorded in the TSRI, but as a shoulder on the strongest spike's slope rather than as a definite spike. On the other hand, the carbonate MAR peak value recorded at 408 ka corresponds to a very low value of the TSRI, possibly indicating very high carbonate productivity at this period. These results indicate that the record of paleoproductivity variations derived from the carbonate record during the last 460 ka is not significantly disturbed by carbonate dissolution at depths between 3,000 and 4,000 m. Such an assumption was already made in a study of other cores from the NW Indian Ocean [Vénec-Peyré et al., 1997].

Since the non-carbonate part of the sediment (15.3 to 45.8 %) is composed of terrigenous elements and an insignificant biogenic silica fraction, the bulk MAR peak values that do not correspond to the radiolarian index peaks correlate with high values of the terrigenous elements MAR. The transition interval between isotope stages 12 and 11 (408 to 431 ka), where three bulk

MAR spikes are recorded, is representative of the complementary nature of biogenic and terrigenous sediment sources and the comparison between the bulk MAR and the element MARs highlights the wide range of accumulation processes occurring in this region (figs. 3, 5 and 6).

* The first spike (408 ka) corresponds to enhanced carbonate production, siliceous production and terrigenous input.

* The second spike (418 ka) correspond to enhanced carbonate productivity only.

* The third spike (428 ka) corresponds to enhanced carbonate production and terrigenous input.

Within the group of terrigenous elements, Si may exhibit a particular behavior because it also reflects siliceous plankton production. Silica content and MAR records are, thus, more ambiguous to interpret because both terrigenous and biogenic inputs are difficult to identify. Silica content and MAR variations exhibit a strong correlation with Al content and Al MAR, respectively. Most of the high values of the Si/Al ratio are characterized by correspondingly high values of the TSRI, indicating high productivity intervals. The peaks of the the Si/Al ratio located at 320 ka and 106 ka correspond, however, to high values of the Ti/Al ratio, indicating an aeolian origin. The Si content, and Si MAR records are, thus, unreliable for use as paleoproductivity proxies despite the occurrence of some siliceous productivity, and the presence of opal in the sediment.

Since barium is usually considered a potentially useful paleoproductivity proxy, and is preferentially linked to siliceous plankton [Dehairs et al., 1980, 1987, 1991; Bishop, 1988], the comparison between the Ba MAR, the Ba content, and the Ba/Al ratio, and the TSRI will determine the reliability of this metal as a paleoproductivity proxy in pelagic sediments. The comparison of these proxies (fig. 6) shows that there is no correlation between variations in the Ba content and the TSRI. Except for a few isochronous high values, higher TSRI values generally correspond to lower Ba contents (figs. 4 and 6). The intensity of the variations in the Ba content being lower than those of the bulk MAR, the variations in the Ba MAR can, thus, be considered as mainly due to bulk MAR changes. The Ba MAR record exhibits, however, specific variations, especially at 9 ka, between 300 and 308 ka, and between 410 and 426 ka. During these intervals, the Ba MAR is in phase with the terrigenous elements MAR. Moreover, Ba enrichment of the sediment (Ba/Al), represented by the barite content, correlates more closely with the Ti/Al ratio than with the TSRI (figs. 4 and 6) and it is, therefore, probably linked to

increases in wind strength. Finally, no correlation is observed between the TSRI and the barite content determined by sequential leaching in the sediment. According to some authors [Thomson et al. 1995; Van Santvoort et al. 1996] the oxyhydroxides-bound barium is a residue of barite dissolution. The lack of correlation between the TSRI and the barite content could be related to a stronger barite dissolution, but no correlation is observed between the TSRI and the sum of the Ba content in the barite and oxyhydroxides fractions. According to these results, it is difficult to use either the Ba content, or the Ba MAR, as a paleoproductivity proxy.

In Core MD 90929, the good correlation between Cu, Ni, V, and Zn contents from one part of the core and Al and Ti contents from another part of the core indicates that the trace element abundances are not influenced by the redox conditions of the depositionnal environments. This fact, together with the lack of Mo and U enrichment throughout the core (fig. 8) demonstrates that the environmental conditions were fully oxygenated.

On the other hand, Cu, Ni, and Zn are known to be linked to the organic matter through metal-organic complexes [Calvert and Pedersen, 1993; Tribovillard et al., 1996; and references therein]. The Cu, Ni, and Zn records exhibit a better correlation with the wind strength proxies than with the TSRI, indicating a terrigenous origin rather than a biogenic enrichment. In such a sediment, neither Cu, Ni, nor Zn can be considered, even indirectly, as paleoproductivity proxies.

6. Paleoproductivity and paleoceanographical interpretations

High paleoproductivity periods in oceanic areas are classically recorded during glacial stages [Berger et al., 1989; Berger and Herguera, 1992]. In Core MD 90929, this model is more or less recognized during the time interval extending from 500 to 238 ka, as testified by the relatively high values of the paleoproductivity markers from glacial and transitional sediments, i.e. the radiolarian index as well as the bulk MAR. The time interval from 38 to 238 ka differs markedly from the older interval (from 238 to 500 ka). The low values of both bulk MAR and TSRI indicate that this difference is related to changes in biogenic input from the surface layer rather than to a change in the strength of the carbonate dissolution. No drastic changes are, however, observed in the trace element contents, indicating that the diagenetic conditions at this site remained nearly constant or had insignificant changes. Such a change in surface productivity was totally unexpected because such a lack of variability has never been recorded during this time interval in the equatorial belt of the NW Indian Ocean, and especially at the 6-5 transition

(130 ka) which exhibits marked changes at other Indian sites [Shimmield and Mowbray, 1991; Weedon and Shimmield, 1991; Caulet et al., 1992; El Foukali, 1995; Vénec-Peyré et al., 1995, 1997; Tribovillard et al., 1996; Ouahdi, 1997; Jacot Des Combes et al., in press].

A hypothesis is proposed herein to explain the reduced paleoproductivity recorded during the 238-38 ka interval. In present-day oceans, the main process controlling surface productivity is the amount of nutrients available in the surface waters. A high nutrient content is maintained either through the mixing of the surface water with the nutrient-richer subsurface water, or through a lateral renewal of the surface water. Both processes are induced by reinforced circulation of the surface and subsurface waters resulting from changes in the local wind field, or from global oceanic circulation changes. The variations in the wind strength index (Ti/Al) recorded at this site do not correlate with the paleoproductivity proxies, and no major change in the Ti/Al ratio is observed at the 8-7 transition. Hence, variations in paleoproductivity may be related to changes in the general oceanic circulation of the surface water masses. Such an interpretation was already offered for another pelagic site, located in the equatorial Indian Ocean close to the studied area [Jacot des Combes et al., in press]. In that case, the variations in the paleoproductivity proxies on Madingley Rise during the last 400 kyr were explained by a sporadic shift of the surface currents system of the equatorial NW Indian Ocean between its actual winter and summer positions (fig. 9). The minimum and maximum bulk MAR values being similar at both sites, and some high productivity periods being synchronous (despite a small time lag) in both cores (e.g. during isotope stage 9, and upper part of isotope stage 8), a similar mechanism can be proposed to explain paleoproductivity changes in the Amirante Passage. Assuming that circulation of surface waters during glacial episodes was more or less the same as present winter circulation of surface waters, and that the summer pattern roughly represents the interglacial stages, the variations in surface paleoproductivity in the Amirante Passage can be explained by a shifting of the surface currents system between present winter and summer positions. Today, the Core MD 90929 location is subjected

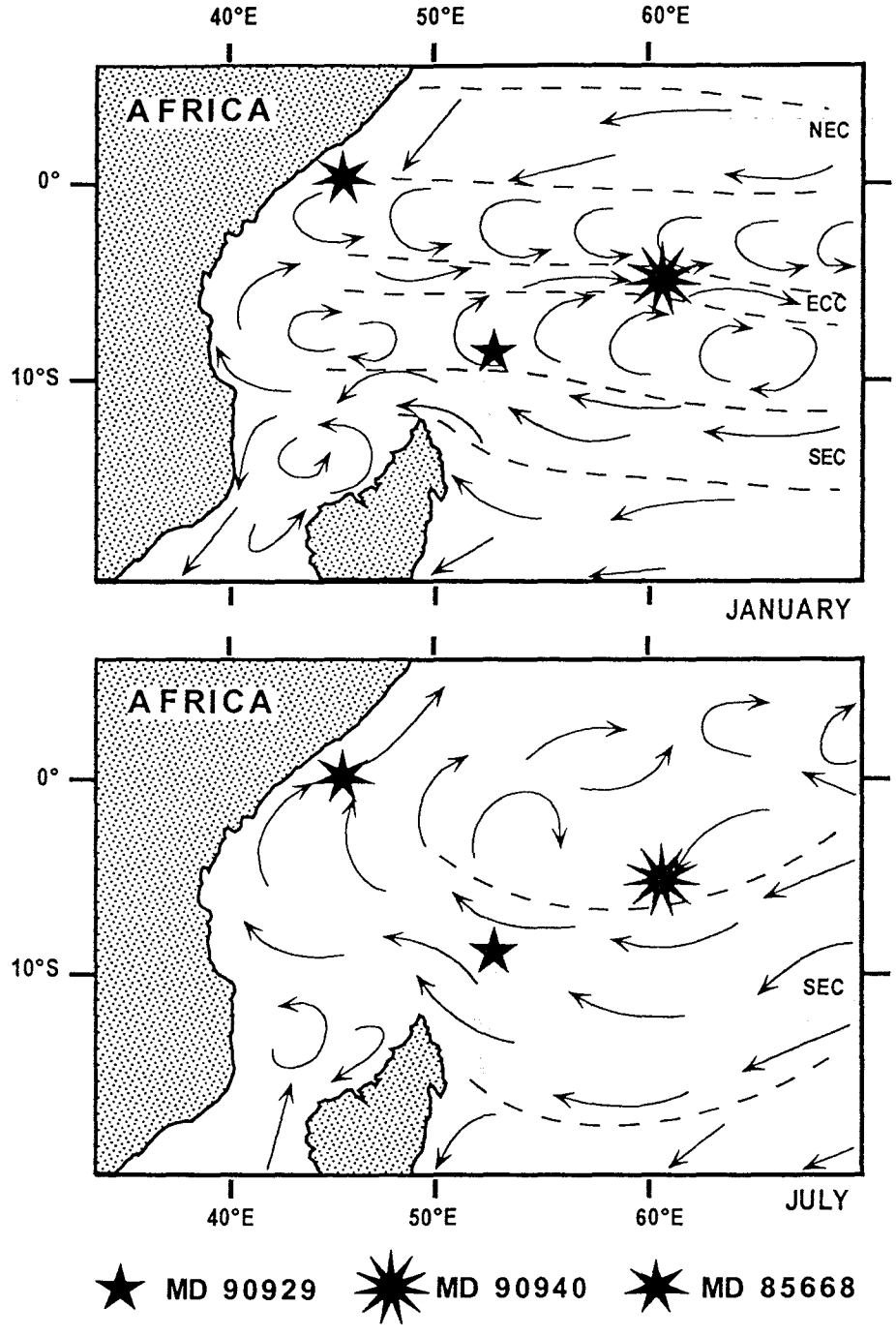

Figure 9: Seasonnal maps of present-day surface oceanic circulation in the Northwestern Indian Ocean. NEC: North Equatorial Current. SEC: South Equatorial Current. ECC: Equatorial Counter Current. The shaded area represents the SEC.

Cartes de la circulation de surface actuelle dans l'Océan Indien du NW. NEC: courant nord équatorial. SEC: courant sud équatorial. ECC: contre courant équatorial. La région grisée correspond au SEC.

to the influence of the South Equatorial Current (SEC) throughout the year except during three months in winter (January-March) when the site is under one of the gyres extending between the SEC and the Equatorial Counter Current (ECC) (fig. 9) [Atlas of the Pilot Charts, Indian Ocean,

1991]. The surface waters located in the center of this gyre are isolated from the general circulation and become progressively oligotrophic. Because of the impoverishment of the surface layer in nutrients, productivity decreases to a minimum that roughly corresponds to a recycled production, with little or no material exported towards the sea floor. The northward shift of the surface circulation system at the end of the winter induces a renewal in the water masses of the Amirante Passage, leading to a greater input of nutrients, enhancing surface productivity, and, thus, export productivity. A persistent weakening of this northward shift could induce the gyre to remain at its winter position. Such a situation would lead to a recycled production in the surface layer, limiting, or even stopping, the export of organic matter to the deeper layers. The constant low values recorded by the bulk MAR and the TSRI during the 38-238 ka interval may be the result of such a paleoceanographic pattern.

A similar process may explain the high productivity period recorded during isotope stage 9 (320-350 ka), both in the Amirante Passage and on Madingley Rise. This enhanced surface paleoproductivity may correspond to a consistent northward shift of the oceanic circulation.

Conclusions

The study of the sediments recovered in Core MD 90929 from the Amirante Passage provides complementary information on the paleoproductivity and paleoceanographic changes in the southern part of the equatorial belt of the NW Indian Ocean.

The comparison between the TSRI and the bulk MAR index indicates that the latter is a reliable paleoproductivity proxy. A similar good correlation has already been observed on Madingley Rise (North of the Seychelles). Moreover, the minimum and maximum values of the bulk MAR are of the same order of magnitude at both locations. The terrigenous content is low, and export productivity is the main process responsible for sediment accumulation at the Amirante Passage site. Trace element records, and especially the one for barium, are related to changes in wind strength rather than to surface productivity changes. Barium is almost equally distributed between the terrigenous (36 %) and the barite (40 %) fractions. On Madingley Rise, the barium is mainly present as barite and can be used as a reliable paleoproductivity proxy. At both sites, no significant amount of TOC is detected, and according to trace metal records, the depositional environment remained fully oxygenated during the time interval considered.

The surface paleoproductivity record in the Amirante Passage can be divided into three intervals. From 500 to 238 ka when all proxies record strong variations of exported productivity

with peak values observed during transition intervals between isotope stages 12-11 (408-431 ka), 9-8 (302-308 ka), and 8-7 (244-254 ka). A peak value that is synchronous with the maximum bulk MAR values observed on Madingley Rise is also recorded during interglacial isotope stage 9. From 238 to 38 ka, a particularly low paleoproductivity pattern is observed in the Amirante Passage with consistently low values of both the bulk MAR and the TSRI. Such an oligotrophic episode was not observed on Madingley Rise and has never been reported from this region of the Indian Ocean. From 38 ka to the present variations in surface productivity are recorded with a peak value at the last deglaciation. At this last site, the variations in surface productivity were mostly related to the general circulation of surface water masses rather than to local wind effects. A weakening in the seasonal oscillation of the surface currents system between its northern and southern limits is hypothesized to explain these variations in surface productivity.

Surface productivity is not homogeneous within the equatorial belt of the NW Indian Ocean. The discrepancies observed between the northern and southern part of the belt may be linked more to regional than to global paleoceanographic changes. Relationships between changes in the regional factors, such as the oscillation of the southern belt oligotrophic gyres, and global climatic changes (mostly glacial/interglacial alternations) are still unknown and will need further investigation.

Aknowledgements

We thank Seng PHETMANH (Université Paris-Sud Orsay), Pierre CLEMENT and Maurice TAMBY (MNHN) for their technical cooperation during this study. Catherine PIERRE and Jean-François SALIEGES from LODYC provided much needed help in the oxygen isotope analyses, and François BAUDIN, from the Université Pierre et Marie Curie (Jussieu) was helpful for the measurement of the organic carbon. Catherine NIGRINI elegantly reshaped our sometimes poor English.

References

Atlas of the Pilot charts, Indian Ocean (1991). - Third Edition - Defense Mapping Agency Hydrographic/Topographic Center, Washington D.C., 12 p.

Barton E.D. & Hill A.E. (1989). - Abyssal flow through the Amirante Trench (Western Indian Ocean). - *Deep Sea Res.*, **36**: 1121-1126.

Bassinot F.C., Beaufort L., Vincent E., Labeyrie L.D., Rostek F., Müller P.J., Quidelleur X. & Lancelot Y. (1994). - Coarse fraction fluctuations in pelagic carbonate sediments from the tropical Indian Ocean: A 1500-kyr record of carbonate dissolution. - *Paleoceanography*, **8**: 579-600.

Berger W.H. (1968). - Radiolarian skeletons: solution at depth. - *Science*, **159**: 1237-1238.

Berger W.H. & Herguera J.C. (1992). - Reading the sedimentary record of the ocean's productivity. *In*: Falkowski P.G. & Woodhead A.D. Eds., Primary productivity and biochemical cycles in the sea, Plenum Press, New York: 455-486.

Berger W.H., Smetacek V.S. & Wefer G. (1989). - Ocean productivity and paleoproductivity-An overview. *In*: Berger W.H. et al., Eds, Production of the ocean: Present and past, *Life Science Research Report 44,* Wiley and Sons: 1-34.

Bishop J.K.B. (1988). - The barite-opal-organic carbon association in oceanic particulate matter. - *Nature*, **332**: 341-343.

Calvert S.E. & Pedersen T.F. (1993). - Geochemistry of recent oxic and anoxic sediments: Implications for the geological record. - *Mar. Geol.*, **113**: 67-88.

Caulet J.P., Vénec-Peyré M.T., Vergnaud-Grazzini C. & Nigrini C. (1992). - Variations of South Somalia upwelling during the last 160 kyr: radiolarian and foraminiferal record in Core MD 85674. *In*: Summerhayes C.P. et al. Eds., Upwelling systems: Evolution since the early Miocene, *Geol. Soc.Spec. Publ.*, **64**: 379-389.

De Lange G.J., Van Os B., Pruysers P.A., Middleburg J.J., Castradori D., Van santvoort P., Müller P.J., Eggenkamp H. & Prahl F.G. (1994). - Possible early diagenetic alteration of palaeo proxies. *In*: Iahn R. et al. Eds., carbon cycling in the Glacial Ocean: constraints on the ocean role in global change. Quantitative approaches in the paleoceanography, *NATO ASI Series, Serie I Global environmental changes*, **17**: 225-258.

Dehairs F., Chesselet R. & Jedwab J. (1980). - Discrete suspended particles of barite and barium cycle in the open ocean. - *Earth Planet. Sci. Lett.*, **49**: 528-550.

Dehairs F., Lambert C.E. Chesselet R. & Risler N. (1987). - The biological production of marine suspended barite and the barium cycle in the Western Mediterranean Sea. - *Biogeochemistry*, **4**: 119-139.

Dehairs F., Stroobants N. & Goeyens L. (1991). - Suspended barite as tracer of biological activity in the Southern Ocean. - *Mar. Chem.*, **35**: 399-410.

Dymond J., Suess E. & Lyle M. (1992). - Barium in deep-sea sediment: A geochemical proxy for paleoproductivity. - *Paleoceanography*, 7: 163-181.

El Foukali H. (1995). - Le contrôle paléoclimatique de la sédimentation quaternaire dans le bassin de Somalie (Océan Indien du Nord-Ouest). – PhD thesis. Museum Natl. Hist. Nat., Paris, 214 p.

Fieux M. & Swallow J.C. (1988). - Flow of deep water in the Somali Basin. - *Deep Sea Res.*, **35**: 303-309.

Francois R., Honjo S., Manganini S.J. & Ravizza G.E. (1995). - Biogenic barium fluxes to the deep sea: Implications for paleoproductivity reconstruction. - *Global Biogeochem. Cycles*, **9**: 289-303.

Gingele F. & Dahmke A. (1994). - Discrete barite particles and barium as tracers of paleoproductivity in south Atlantic sediments. - *Paleoceanography*, **9**: 151-168.

Goldberg E.D. & Arrhenius G.O.S. (1958). - Chemistry of Pacific pelagic sediments. - *Geochim. Cosmochim. Acta*, **13**: 153-212.

Imbrie J.& Imbrie J.Z. (1980). – Modeling the climatic response to orbital variations. *Science*, **207**: 943-953.

Jacot des Combes H., Caulet J.P. & Tribovillard N.P. (1998). - Pelagic productivity changes in the equatorial area of the NW Indian Ocean during the last 400 kyr. - *Mar. Geol.*, (in press).

Johnson D.A., Schneider D.A., Nigrini C.A., Caulet J.P. & Kent, D.V. (1989). - Pliocene-Pleistocene radiolarian events and magnetostratigraphic calibrations for the tropical Indian Ocean. - *Mar. Micropal.*, **14**: 33-66.

Johnson G.C. & Damuth J.E. (1979). - Deep thermohaline flow and current-controlled sedimentation in the Amirante Passage: Western Indian Ocean. - *Mar. Geol.*, **33**: 1-44.

Johnson G.C., Warren B.A. & Olson D.B. (1991). - Flow of bottom water in the Somali Basin. - *Deep Sea Res.*, **38**: 637-652.

Johnson T.C. (1974). - The dissolution of siliceous microfossils in surface sediments of the eastern tropical Pacific. - *Deep Sea Res.*, **21**: 851-864.

Johnson T.C. (1976). - Biogenic opal preservation in pelagic sediments of a small area in the eastern tropical Pacific. - *Geol. Soc. Amer. Bull.*, **87**: 1273-1282.

Kling S.A. & Boltovskoy D. (1995). - Radiolarian vertical distribution patterns across the southern California Current. - *Deep Sea Res.*, **42**: 191-231.

Lea D.W. & Spero H.J. (1994). - Assessing the reliability of paleochemical tracers: Barium uptake in the shells of planktonic foraminifera. - *Paleoceanography*, **9**: 445-452.

Lyle M., Heath G.R. & Robbins J.M. (1984). - Transport and release of transition elements during early diagenesis: Sequential leaching from MANOP sites M and H. Part I pH 5 acetic acid leach. - *Geochim. Cosmochim. Acta*, **48**: 1705-1715.

McManus J., Berelson W.M., Klinkhammer G.P., Kilgore T.E. & Hammond D.E. (1994). - Remobilisation of barium in continental margin sediments. - *Geochim. et Cosmochim. Acta*, **58**: 4899-4907.

Martin J.H., Knauer G.A., Karl M.D. & Broenkow W.W. (1987). - VERTEX: carbon cycling in the northeast Pacific. - *Deep Sea Res.*, **34**: 267-285.

Martinez P. (1997). - Paléoproductivités du système d'upwellings nord-ouest africain et variations climatiques au cours du Quaternaire terminal. - PhD thesis, University Bordeaux I, 298 pp.

Ouahdi R. (1997). - Variations de la productivité au nord-ouest de l'Océan Indien lors des derniers 70000 ans dans l'upwelling de Socotra et de Somalie: Enregistrements géochimiques. - *Bull. Soc. Géol. Fr.*, **168**: 93-107.

Paytan A. (1995). – Marine barite, a recorder of ocean chemistry, productivity and circulation. – PhD dissertation, University of California, San Diego, 111 pp.

Paytan A. and Kastner M. (1996). – Benthic Ba fluxes in the central Equatorial Pacific, implications for the oceanic Ba cycle. *Earth Planet. Sci. Lett.*, **142**: 439-450.

Pruysers P.A., DeLange G.J. Middelburg J.J. & Hydes D.J. (1993). - The diagenetic formation of metal-rich layers in sapropel-containing sediments in the eastern Mediterranean. - *Geochim. et Cosmochim. Acta*, **57**: 527-536.

Robbins J.M., Lyle M. & Heath G.R. (1984). - A sequential extraction procedure for partitioning elements among co-existing phases in marine sediments. - Rep. College Oceanography, Oregon State Univ. 45p.

Sanfilippo A., Westberg-Smith M.J. & Riedel W.R. (1985). - Cenozoic Radiolaria. *In*. Bolli H.M. et al., Eds., Plankton stratigraphy, Cambridge Univ. Press, 631-712.

Shackleton N.J., Hall M.A., Pate D., Meynadier L. & Valet J.-P. (1993). - High resolution stable isotope stratigraphy from bulk sediment. - *Paleoceanography*, **8**: 141-148.

Shimmield G.B. (1992). - Can sediment geochemistry record changes in coastal upwelling paleoproductivity? Evidence from Northwest Africa and the Arabian Sea. *In*:

Summerhayes C.P. et al. Eds., Upwelling systems: Evolution since the early Miocene, *Geol. Soc.Spec. Publ.*, **64**: 9-46.

Shimmield G.B. & Mowbrays R. (1991). - The inorganic geochemical record of Northwestern Arabian Sea: A history of productivity variation over the last 4000 ky from Sites 722A and 724. *In*: Prell W.L. et al. Eds., *Proc. ODP, Sci. Res.*, **117**: 409-429.

Shimmield G.B., Derrick S., Mackensen A., Grobe H. & Pudsey C. (1994). - The history of barium, biogenic silica and organic carbon accumulation in the Weddel Sea and the Antarctic Ocean during the last 150,000 years. *In*: Iahn R. et al. Eds., Carbon cycling in the glacial ocean: constraints on the ocean role in global change. Quantitative approaches in paleoceanography, *NATO ASI Series (1): Global environmental changes*, **17**: 555-574.

Stroobants N., Dehairs F., Goeyens L., Vanderheidjen N. & Van Grieken R. (1991). - Barite formation in the Southern Ocean water column. - *Mar. Chem.*, **35**: 411-421.

Thomson J., Higgs N.C., Croudace I.W., Colley S. & Hydes D.J. (1993). - Redox zonation of elements at an oxic/post-oxic boundary in deep-sea sediments. - *Geochim. et Cosmochim. Acta*, **57**: 579-595.

Thomson J., Higgs N.C., Wilson T.R.S., Croudace I.W., De Lange G.J. & Van Santvoort P.J.M. (1995). - Redistribution and geochemical behaviour of redox sensitive elements around S1, the most recent eastern Mediterranean sapropel. - *Geochim. et Cosmochim. Acta*, **59**: 3487-3501.

Tribovillard N.P., Caulet J.P., Vergnaud-Grazzini C., Moureau N. & Tremblay P. (1996). - Lack of organic matter accumulation on the upwelling-influenced Somalia margin in a glacial-interglacial transition. - *Mar. Geol.*, **133**: 157-182.

Turekian K.K. and Wedepohl K.H. (1961). - Distribution of the elements in some major units of the Earth's crust. - *Geol. Soc. Am. Bull.*, **72**: 175-191.

Van Os B.J.H., Middelburg J.J. & De Lange G.J. (1991). - Possible diagenetic mobilization of barium in sapropelic sediment from the eastern Mediterranean. - *Mar. Geol.*, **100**: 125-136.

Van Santvoort P.J.M., De Lange G.J., Thomson J., Cussen H., Wilson T.R.S., Krom M.D. & Ströhle K. (1996). - Active post-depositional oxidation of the most recent sapropel (S1) in sediments of the eastern Mediterranean sea. - *Geochim. et Cosmochim. Acta*, **60**: 4007-4024.

Vénec-Peyré M.T., Caulet J.P. & Vergnaud-Grazzini C. (1995). - Paleohydrographic changes in the Somali Basin (5°N upwelling and equatorial areas) during the last 160 kyr, based on

correspondence analysis of foraminiferal and radiolarians assemblages. - *Paleoceanography*, **10**: 473-491.

Vénec-Peyré M.T., Caulet J.P. & Vergnaud-Grazzini C. (1997). - Glacial-interglacial changes in the equatorial part of the Somali Basin (NW Indian Ocean) during the last 355 ky. - *Paleoceanography*, **12**: 640-649.

Von Breymann M.T., Emeis K.C. & Suess E. (1992). - Water depth and diagenetic constraints on the use of barium as a paleoproductivity indicator. *In*: Summerhayes C.P. et al. Eds., Upwelling systems: Evolution since the early Miocene, *Geol. Soc. Spec. Publ.*, **64**: 273-284.

Warren B.A. (1974). - Deep flow in the Madagascar and Mascarene basins. - *Deep-Sea Res.*, **21**: 1-21.

Weedon G.P. & Shimmield G.B. (1991). - Late Pleistocene upwelling and productivity variations in the Northwestern Indian Ocean deduced from spectral analyses of geochemical data from Sites 722 and 724. *In*: Prell W.L et al. Eds., *Proc. ODP, Sci. Res.*, **117**: 431-440.

2° PARTIE
PALÉOCÉANOGRAPHIE ET PALÉOPRODUCTIVITÉ DANS L'UPWELLING DE SOCOTRA (OCÉAN INDIEN DU NORD OUEST)

Les upwellings ont un rôle important dans les cycles chimiques et biologiques des océans en remplaçant les eaux de surface que l'activité biologique a rendu stériles par des eaux froides de subsurface riches en nutriments. Ces nutriments soutiennent alors l'activité biologique en induisant une nouvelle production. Les upwellings peuvent être de nature saisonnière (océan Indien du nord-ouest) ou constante (côtes du Pérou par exemple). On a longtemps considéré comme seuls upwellings les grandes résurgences costales telles que celles du Pérou ou du courant de Californie. Aujourd'hui, on englobe sous le terme d'upwelling toutes les remontées d'eaux de semi-profondeur, que ce soit au niveau de la ceinture équatoriale pélagique ou le long des continents. Partout où ils sont actifs, les phénomènes d'upwelling jouent un rôle important dans le contrôle de la distribution des nutriments et les sédiments qui se déposent à leur aplomb sont considérés comme des pièges à carbone, silice et phosphore dont l'existence et la variabilité permet de retracer l'évolution de la productivité au cours du temps.

La reconstruction de la variabilité temporelle des systèmes à upwelling à partir des archives sédimentaires est fondée sur une série d'estimations à la fois sur le fonctionnement des upwellings actuels et sur la représentativité des marqueurs géochimiques ou biologiques de cette activité. La variabilité et la complexité des systèmes à upwelling sont immenses du fait que les processus physiques qui s'y déroulent et la réponse biologique qui en résulte ne sont pas linéairement couplés. Les modèles actuels sont donc très imparfaits. Les marqueurs sédimentés de cette activité sont conditionnés par de si nombreux processus (productivité, dissolution, diagenèse, oxydation/réduction du milieu...) qu'à l'heure actuelle, on n'a pas encore trouvé de traceur uniquement représentatif de l'intensité des remontées d'eaux de subsurface. Le mieux que l'on puisse faire est donc d'établir les reconstructions sur l'utilisation conjointe de plusieurs marqueurs, géochimiques et biologiques, à partir de séries sédimentaires bien datées et observées à haute résolution. La comparaison des indications fournies par ces différents marqueurs va permettre de minimiser les ambiguïtés d'interprétation et reconnaître la nature et le rôle de chacune des variables intervenues dans l'archivage de la mémoire des upwellings.

C'est dans cet esprit qu'est conçu le travail sur la reconstruction des modifications paléocéanographiques et des paléoproductivités récentes dans la zone de l'upwelling de Socotra (nord du bassin de Somalie), présenté dans cette troisième partie de thèse.

Une série d'études sur les variations dans le temps des tourbillons de Somalie et Socotra a montré que, d'une façon générale, l'activité des upwellings liés au courant de Somalie et engendrés par la mousson indienne, n'était pas en phase avec les grands cycles climatiques au cours des derniers 160 000 ans (Caulet, et al., 1992; Vénec-Peyré et al., 1995; Ouahdi, 1997). Dans tous les cas, l'advection continue d'eaux semi-profondes a surimposé l'effet des conditions locales masquant la composante glaciaire/interglaciaire, notamment en uniformisant les conditions hydrologiques aux transitions climatiques. Toutes les données étudiées suggèrent que les structures des masses d'eaux de surface ont été différentes de celles qui ont caractérisé aux mêmes périodes l'océan pélagique. Les intervalles à haute productivité ne caractérisent pas ainsi les périodes glaciaires, suivant le schéma classique. Leur périodicité varie d'une zone d'upwelling à l'autre, sur des distances très courtes, reflétant l'extrême variabilité géographique et temporelle du phénomène. D'une façon générale, ces travaux, basés soit sur des analyses géochimiques, soit sur des études micropaléontologiques, ont montré la difficulté d'utiliser des marqueurs de nature différente pour reconstruire des processus sporadiques très localisés.

Ce travail est donc une nouvelle tentative pour reconstruire la paléohydrologie et la paléoproductivité de l'upwelling de Somalie en combinant des marqueurs géochimiques et biologiques, tout en profitant de l'expérience déjà acquise. Pour étendre dans le temps les résultats déjà obtenus, une nouvelle carotte (MD 962073) réalisée en 1996 au cours de la Mission MD 104-PEGASOM, et englobant les derniers 250 000 ans, a fait l'objet d'analyses géochimiques qui ont été comparées avec des données micropaléontologiques. L'ensemble des résultats sur le dernier cycle climatique est rediscuté en comparaison avec les données publiées par R. Ouahdi (1997) qui sont basées sur la carotte MD 85682, localisée à peu près à 60 km de la précédente, mais avec un intervalle de temps plus réduit (72 000 ans).

En résumé, il apparaît que les maximums d'intensité dans la remontée des masses d'eau de subsurface ont surtout pris place pendant les stades interglaciaires, plus particulièrement entre 230 et 200 000 ans, 100 et 80 000 ans et vers 40 000 ans. La matière organique déposée durant ces épisodes est en majorité d'origine planctonique, quoique des débris continentaux y figurent également. Une bonne corrélation entre l'enrichissement en matière organique du sédiment et la teneur en silice biogène indique que l'apport organique marin résulte d'une fertilité accrue en

diatomées (blooms sporadiques mais fréquents). Les teneurs en baryum sont ici un bon marqueur de la productivité bien qu'une partie du baryum présent soit d'origine terrigène. L'abondance des radiolaires caractéristiques de remontées d'eaux semi-profonde n'est pas corrélée pendant la période considérée avec les variations des marqueurs géochimiques de la fertilité, en raison probablement de l'existence de structures hydrologiques particulières. D'une façon générale, les conditions locales ont plus influé sur la paléoproductivité que les modifications climatiques à grande échelle.

Monitoring the variations of the Socotra upwelling system during the last 250 ka: a geochemical approach

Hélène Jacot Des Combes[1], Jean Pierre Caulet[2], and Nicolas Tribovillard[1].

1: Sédimentologie et Géodynamique, URA CNRS 719, UFR des Sciences de la Terre, Université Lille I, 59655 VILLENEUVE D'ASCQ, FRANCE.

2: Laboratoire de Géologie, ESA 7073, Muséum National d'Histoire Naturelle, 43 rue Buffon, 75005 PARIS, FRANCE.

Keywords: NW Indian Ocean, upwelling, geochemistry, barium, sequential leaching, radiolarians.

Soumis à Paleoceanography

Abstract

A new giant piston core (MD 962073) recovered from the Socotra gyre area (Somali-Socotra upwelling system, NW Indian Ocean) provides both biological and geochemical records that permit to reconstruct the variations of the paleoproductivity and the paleoceanic changes that occurred during the last 250 kyr in this region.

The main geochemical markers that were used are the contents and MARs in carbonate, organic carbon, and major and trace elements (Si, Al, Fe, Mg, K, Ti, Ba, P, Mn, Mo, U, V, Cu, Ni, and Zn). Distribution of barium within the different fractions of the sediment was quantitatively estimated through leaching procedure. Biological markers were mostly quantitative data on the abundance of radiolarian species characteristic of upwelling areas (URI) and the ratio of the number of radiolarian species living at the depth of the thermocline to the number of radiolarian species living at the surface (TSRI).

At this site, the variations of the geochemical record, and especially the enrichment of sediments in organic carbon, silica, and trace element (P, Cu, Ni, and Zn) compared to Al monitor the variations of the surface paleoproductivity. However, the variations of the Ba/Al ratio as well as the balanced distribution of Ba within the different fractions of the sediment show that the barium cannot be considered at this site as a reliable paleoproductivity proxy. The comparison of geochemical and biological data indicates that, at this site, URI (radiolarian index) is not a reliable proxy for reconstruction of strong vertical advection of subsurface water. Variations of the redox conditions, monitored by the variations of the Mo/Al and U/Al ratios, suggests that suboxic conditions have prevailed during the last 250 kyr at this site, with short time intervals characterized by more anoxic conditions. All data show that the advection of subsurface waters in the Socotra gyre was intensified at 235, 170, 140, 95 and 85 ka, i.e. during both glacial and interglacial isotope stages.

Comparing our data from the Socotra gyre area (10°N) with published observations from the Somali gyre area (5°N), controlled by the onset of the Southwest Indian monsoon, shows that periods of intensified paleoproductivity were not synchronous at both sites. Two explanations can be offered. Different origin of subsurface waters that are recognized in both gyres may have resulted in different control of nutrient regeneration and terrigenous input. Subsurface waters at Socotra are less controlled by the deep oxygenated water masses that are recognized in the central part of the Somali Basin and at the Somali gyre. Continental influence is less marked at 10°N than at 5°N. On the other hand, the location of the sites relative to the geographic

distribution of the upwelling systems is different. The Socotra site is located under the present central position of the upwelled waters while the Somali site is located at the fringe of the 5°N gyre. Our data confirm the important geographic and temporal variability of the Quaternary upwelling systems, sporadically induced by the Indian monsoon.

Introduction

The northwestern Indian Ocean is characterized by the Indian monsoon, induced by a strong seasonally reversal of winds. This atmospheric process deeply influences the circulation of the surface water masses in this region, and leads to the occurrence of upwelling systems, along the western coast of the northwestern Indian Ocean, from the Arabian Sea to the Somali coast (Bruce and Beatty, 1985; Anderson and Prell, 1991; 1993; Clemens et al., 1991; Caulet et al., 1992). Several paleoceanographic reconstructions have already been realized upon these upwelling systems, using both biogenic and geochemical markers (Clemens and Prell, 1991; Murray and Prell, 1991; Shimmield and Mowbray, 1991; Zahn and Pedersen, 1991; Caulet et al., 1992; Murray and Prell, 1992; Anderson and Prell, 1993; Hermelin and Shimmield, 1995; Vénec-Peyré et al., 1995; Vergnaud-Grazzini et al., 1995; Tribovillard et al., 1996; Ouahdi, 1997a; Vénec-Peyré et al., 1997; Vénec-Peyré and Caulet, submitted). The upwelling systems of the Somali Basin include two major distinct gyres: the Somali gyre, located at 5°N, and the Socotra gyre, centered at 10°N (Düing et al., 1980; Swallow, 1980; Quadfasel and Schott, 1982; Schott and Quadfasel, 1982; Fieux, 1987). Sediments from many piston cores recovered in both these areas show that the sedimentary record is significantly different between the Somali gyre and the Socotra gyre. According to Ouahdi (1997a), the sediments recovered under the Somali gyre are characterized by a significant terrigenous input, whereas the sediments recovered under the Socotra gyre are mostly composed of biogenic material with a lower terrigenous input. In both areas, the content in siliceous plankton of the sediment is significant (5 to 10 % of diatoms and radiolarians). This siliceous plankton is considered as the main planktonic group inducing an enhanced export of surface productivity (Caulet et al., 1992; Vénec-Peyré et al., 1995; Vergnaud-Grazzini et al., 1995; Vénec-Peyré et al., 1997; Vénec-Peyré and Caulet, submitted). Till today, the reconstruction of paleoproductivity changes in these areas, and especially under the Socotra gyre, was, however, restrained to relatively short periods. Due to the high sediment mass accumulation rate recorded in such environments, the length of the piston cores recovered in

these area is the main factor limiting paleoclimatic reconstructions to short time intervals: 168 kyr for the Somali gyre, and 72 kyr for the Socotra gyre (Tribovillard et al., 1996; Ouahdi,1997a; Vénec-Peyré and Caulet, submitted). Recent progress in piston coring allows to recover longer cores, and thus, to span a longer time interval. Core MD 962073 had been recovered in order to provide a longer record of the variations of the intensity of the Socotra upwelling system (Giannesinni et al., in prep). This core is analyzed following the protocol already used in previous analyses of the geochemical record of the sediments recovered under both the Somali and the Socotra gyres, including an isotope build age model, a bulk sediment chemical analysis, and a sequential leaching procedure to determine the main Ba-carrier fractions of the sediment (Tribovillard et al., 1996; Ouahdi,1997a). The biological record of the variations of the upwelling intensity through time is obtained through the variations of the radiolarian index characteristic of the upwelling areas: upwelling radiolarian index, called URI (Caulet et al., 1992) as well as through the variations of another radiolarian index, that was already used to monitor the variations of surface productivity in the pelagic domain of the northwestern Indian Ocean (Jacot Des Combes et al., in press; Jacot Des Combes et al., submitted). Combination of both these radiolarian indexes will allow us to determine the time intervals when surface productivity was related to the upwelling activity periods, non-upwelling periods, and episodes with a pelagic-type surface productivity. These new data will be compared to the data previously published to complement the reconstruction of the variations of the Socotra and Somali upwelling systems and their possible relationship.

Oceanographic settings

In the NW Indian Ocean, and more particularly along the Somali coast, the hydrological conditions are subjected to the climatic variations induced by the summer Indian monsoon. The monsoon winds, blowing from the southwest generate the Somali current along the eastern African coast. This northeastward current is made of relatively cold and salt-poor water masses (Swallow and Bruce, 1966, Warren et al., 1966). The Somali Current induces two gyres along the coast: the southern gyre, called the Somali gyre, located at 5°N, and the northern gyre, called the Socotra gyre, located at 10°N. Both these gyres are dependent from the intensity of the monsoon (Düing et al., 1980; Swallow, 1980, Quadfasel and Schott, 1982; Schott and Quadfasel, 1982; Fieux, 1987).

In both the upwelling areas linked to these gyres, surface waters are nutrient-rich (Smith and Codispoti, 1980) and cold: 18°C in the Somali gyre, and 17.7°C in the Socotra gyre (Brown et al., 1980). The intermediate water masses that flow up to the surface originate from a depth of 200 m in the Socotra gyre, and 100 m in the Somali gyre (Smith and Codispoti, 1980). Previous studies have shown that the Socotra gyre is more productive than the Somali gyre because the upwelled waters are nutrient-richer (Smith and Codispoti, 1980). Sediments from cores recovered under the Somali gyre (MD 85674) contain a more important terrigenous fraction than the sediment from cores recovered under the Socotra gyre (MD 85682) (Ouahdi, 1997a).

In the Somali Basin, at depths comprised between 500 and 2,500 m, a salty, oxygen-poor water mass, originating from the Red Sea and the Arabian Sea flows southeastward. Below a depth of 2,500 m, a cold, oxygen-rich water mass flows northward from the Southern Ocean (Fieux et al., 1986).

Material and methods

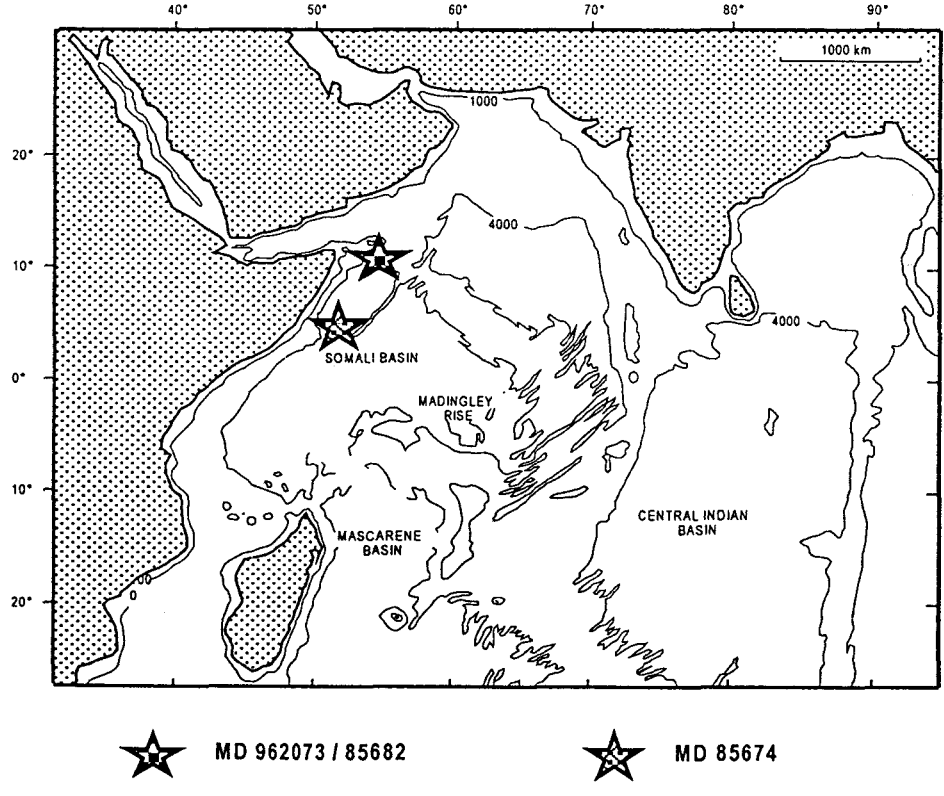

Figure 1: Location map of piston cores in both the Socotra gyre (MD 85682 and 962073) and in the Somali gyre (MD 85674)

Core MD 962073 (10.936°N, 52.616°E, 3,142 m depth) was recovered in 1996, during the MD 104-Pegasom cruise of the "*R/V Marion-Dufresne*", under the Socotra gyre and in the vicinity (60 km) of Core MD 85682 (Fig. 1).

The sediment is a light gray carbonate ooze, with 5 to 10 % of siliceous plankton debris and 5 % of detrital components (mostly quartz, feldspars; ...). A total of 85 samples was analyzed, from a depth of 4 mbsf to the bottom of the core (32.96 mbsf), with a 30 cm sampling step. The depth of 4 mbsf was chosen to provide an interval of comparison with Core MD 85682.

The age model for Core MD 962073 is based on an oxygen-isotope analysis of 98 bulk sediment samples retrieved every 30 cm using a mass spectrometer (OPTIMA). Based on assumptions made after the sedimentation rate recorded in Core MD 85682, the sampling step of 30 cm was chosen to provide a time interval between the samples shorter than the precession period (20 ka). Oxygen-isotope analyses of bulk sediments were already used to date sediments from the Indian Ocean and provided reliable ages in this area (Shackleton et al., 1993; Jacot Des Combes et al, in press; Jacot Des Combes et al, accepted).

TOC contents were measured on the bulk sediment through LECO analysis, and palynofacies samples were prepared according to classical procedures (Combaz, 1980). Carbonate content was measured with a Bernard calcimeter. The amount of major and significant trace elements (Ba, Cu, Cr, Mn, Mo, Ni, P, Ti, U, V, and Zn) was measured in the following way: 100 mg of bulk sediment were dried at 105°C for 24 hours and thoroughly ground in an agate mortar mill prior to a $HClO_4$, HNO_3 and HF acid digestion. The final residue was taken up in 1M HCl. The trace elements were measured with a ICP-spectrometer (ICP-MS). The analytical precision and accuracy of the results were both found to be equal to, or better than, 5 % for all elements. Data were checked by comparison with international standards and with the help of replicate samples. These results are summarized in Table 1

Enrichment of the sediment in the elements compared to the terrigenous fraction was estimated through the respective ratios of these elements with Al (Table 3)

Age (ka)	$CaCO_3$ (%)	TOC (%)	Si (%)	Al (%)	Fe (%)	Mg (%)	K (%)	Ba (ppm)	P (ppm)	Cu (ppm)	Ni (ppm)	Zn (ppm)	Mn (ppm)	Mo (ppm)	U (ppm)	V (ppm)	Ti (ppm)
31*	68.67	0.97	7.06	1.17	0.71	0.87	0.32	653	654.62	33.1	44.3	43.5		1.61	4.48	39.9	659
36	71.13	1.01	6.20	1.16	0.71	0.87	0.33	577	785.54	31.7	48.8	36.4	200	1.67	4.32	33.2	719
38	70.76	1.10	6.55	1.12	0.76	0.84	0.31	608	741.90	30.3	50.8	38.1	200	2.06	4.02	33.5	659
44	73.37	0.39		1.16				380					190			50.0	
48	74.82	0.35		1.10				450					195			41.0	
52	64.58	0.89		1.72				310					205			58.0	
56	70.72	0.79	6.05	1.50	0.89	0.96	0.40	419	785.54	36.1	57.5	41.2		1.39	4.46	43.4	899
59	69.53	0.80		1.40				370					190			46.0	
64	75.64	0.50	5.44	1.32	0.80	0.89	0.37	442	610.97	34.3	49.9	36.4		1.34	3.73	43.2	719
69	72.71	0.78		1.25				470					180			49.0	
72*	68.65	1.05	6.42	1.32	0.85	0.95	0.33	651	785.54	36	54.8	40.5		1.38	4.39	42.9	779
73	69.1	0.84		1.40				505					180			48.0	
75	70.59	0.77	6.50	1.25	0.74	0.88	0.32	520	698.26	40.7	42.3	41.9		1.10	3.26	39.8	719
77	74.62	0.75		0.84				500					160			28.0	
78	72.98	0.85	5.47	1.08	0.67	0.68	0.26	565	785.54	36.2	48.1	39.1		1.68	3.83	37.5	600
80	73.48	0.75		1.00				570					170			40.0	
82*	70.71	0.98	5.57	1.37	0.78	0.83	0.35	368	785.54	35.3	48.1	42		0.78	3.5	45.3	839
83	70.97	0.64		1.34				365					170			55.0	
85	73.66	0.91	5.56	0.79	0.48	0.65	0.23	577	785.54	33.5	37.2	32.9		1.02	3.85	29.6	540
87	72.99	0.73		0.73				585					150			27.0	
89	73.23	0.47	7.12	0.87	0.55	0.70	0.23	594	785.54	32.1	42.4	33		2.84	3.06	25.9	480
90	74.16	0.63		0.85				540					155			29.0	
92	77.42	0.19	5.42	0.99	0.63	0.68	0.26	533	785.54	32.4	46.9	36.9		1.65	3.73	33.0	540
94	76.57	0.50		0.96				560					170			40.0	
95	72.07	0.73	5.85	1.39	0.92	0.77	0.35	548	741.90	38.7	58.9	41.2	200	1.69	4.21	41.8	779
97	70.81	0.91		1.15				565					160			47.0	
102	67.79	0.83	7.11	1.43	0.85	0.89	0.36	485	829.18	41.5	53.2	37.5		1.54	3.48	45.2	839
106	69.67	0.90		0.97				670					150			56.0	
111	65.44	0.92	8.74	1.31	0.81	0.92	0.33	782	829.18	40.7	51	44.4		3.99	4.83	44.2	779
115	61.93	0.96		1.33				840					150			54.0	
120	72.71	0.85	6.61	1.15	0.65	0.99	0.31	516	872.82	33.3	40.7	38.3		1.76	5.11	34.0	779
122	65.32	0.61		1.35				770					190			57.0	
124*	70.43	0.56	7.21	1.29	0.78	0.78	0.31	850	785.54	41.8	44.7	52.7		1.38	3.52	42.1	899
126	71.57	0.51		1.36				400					170			38.0	
129	73.81	0.72	5.52	1.46	0.83	1.00	0.37	330	829.18	29.2	51.1	39.7		0.87	3.46	47.8	839
133	67.02	1.09		1.17				585					175			48.0	
137	68.96	0.89	7.06	1.40	0.83	1.12	0.37	480	872.82	27.4	50	39.8		1.28	4.37	39.4	839
140	68.89	0.98		1.40				580					220			56.0	
144	70.03	0.85	6.32	1.59	0.99	1.10	0.42	543	872.82	31.6	58.2	41.5	200	1.42	4.27	45.6	1019
147	70.75	0.56		1.43				340					200			56.0	
151*	63.7	0.81	8.15	1.89	1.13	1.22	0.50	320	698.26	28.5	66.9	46.2	200	1.45	3.56	61.4	1019
155	63.05	0.82		1.84				400					250			67.0	
158	67.16	0.89	7.41	1.75	1.01	1.17	0.46	493	741.90	27.7	61.1	42	200	1.40	4.25	51.5	1019
162	63.1	1.02		1.77				415					240			59.0	
165	59.8	1.21	8.42	2.16	1.18	1.33	0.57	447	741.90	30.8	65.1	51.9	200	1.20	3.86	61.1	1199
169	71.26	1.79		1.29				510					220			47.0	
172	67.16	0.78	7.06	1.87	1.06	1.04	0.49	472	698.26	35	59.9	44.7	200	0.76	3.7	53.3	1079
176	68.9	0.55		1.67				420					220			65.0	
180	70.41	0.97	5.91	1.46	0.87	0.95	0.40	550	1003.74	34	43.5	36.9	200	1.11	4.42	44.0	959
183	67.05	0.88		1.55				725					230			57.0	
187*	60.72	0.94	9.89	1.58	1.01	0.99	0.42	728	916.46	37.2	48	50.7		1.78	3.72	45.0	1019
189	66.06	0.47		1.79				480					190			66.0	
194	73.29	0.71	6.22	1.07	0.67	0.63	0.27	711	829.18	37.9	30.4	39		1.70	3.81	32.7	719
199	76.99	0.71		0.99				440					150			36.0	
204	68.58	1.14	7.32	0.89	0.62	0.69	0.24	583	698.26	35.5	32.4	33.2		2.18	4.04	34.2	480
208	68.98	1.01		1.01				600					130			38.0	
213	74.85	0.78	5.38	0.99	0.60	0.69	0.28	595	872.82	33.8	28.5	42.6		1.61	5	36.1	659
216	77.89	0.42		0.85				450					140			26.0	
220	82.59		3.27	0.74	0.48	0.53	0.22	272	741.90	30.6	25	25.6		2.13	3.22	22.2	480
223	90.25			0.70				420					110			19.0	
226	73.92	0.51	6.49	0.94	0.57	0.68	0.25	479	698.26	27.7	25.1	28.8		1.81	2.65	23.2	659
229	78.41	0.63		0.90				460					120			29.0	
233	75.75	0.68	5.46	1.17	0.69	0.68	0.31	453	741.90	27.1	24.5	34.1		1.82	2.78	31.5	779
236	75.36	0.76		0.66				540					87			29.0	
239	74.8	0.42	5.45	0.98	0.55	0.60	0.26	665	654.62	31.4	29.5	38.4		1.54	4.36	34.5	659
242	82.05	0.49		0.78				150					130			28.0	
248	76.56	0.48	4.34	1.13	0.74	0.78	0.33	292	741.90	24.8	36.6	29.8		2.12	3.22	34.4	659

Table 1: Carbonates, TOC, Major and Trace elements contents.
Samples identified with a * were submitted to the sequential leaching procedure

Age (ka)	TOC/Al	Si/Al	Fe/Al	Mg/Al	Mg/Ca	K/Al	Ba/Al (x10⁴)	P/Al (x10⁴)	Cu/Al (x10⁴)	Ni/Al (x10⁴)	Zn/Al (x10⁴)	Mo/Al (x10⁴)	Mn/Al (x10⁴)	U/Al (x10⁴)	V/Al (x10⁴)	Ti/Al (x10⁴)
31*	0.83	6.03	0.61	0.75	318.64	0.27	558.30	559.68	28.30	37.88	37.19	1.38		3.83	34.11	563.82
36	0.87	5.35	0.62	0.75	306.24	0.29	497.83	677.75	27.35	42.10	31.41	1.44	172.56	3.73	28.64	620.69
38	0.98	5.84	0.68	0.75	300.3	0.27	541.89	661.23	27.01	45.28	33.96	1.84	178.25	3.58	29.86	587.75
44	0.34						327.59						163.79		43.10	
48	0.32						409.09						177.27		37.27	
52	0.52						180.23						119.19		33.72	
56	0.53	4.04	0.59	0.64	339.68	0.27	279.75	524.48	24.10	38.39	27.51	0.93		2.98	28.98	600.40
59	0.57						264.29						135.71		32.86	
64	0.38	4.13	0.61	0.67	302.26	0.28	335.41	463.63	26.03	37.87	27.62	1.02		2.83	32.78	545.91
69	0.62						376.00						144.00		39.20	
72*	0.79	4.85	0.64	0.72	339.36	0.25	492.03	593.71	27.21	41.42	30.61	1.04		3.32	32.42	589.03
73	0.6						360.71						128.57		34.29	
75	0.62	5.21	0.59	0.7	310.33	0.26	416.33	559.05	32.59	33.87	33.55	0.88		2.61	31.87	575.98
77	0.89						595.24						190.48		33.33	
78	0.79	5.07	0.62	0.63	229.4	0.24	523.32	727.59	33.53	44.55	36.22	1.56		3.55	34.73	555.27
80	0.75						570.00						170.00		40.00	
82*	0.72	4.06	0.57	0.61	281.83	0.25	268.47	573.08	25.75	35.09	30.64	0.57		2.55	33.05	612.30
83	0.47						272.39						126.87		41.04	
85	1.14	7.01	0.6	0.81	215.24	0.29	726.83	989.52	42.20	46.86	41.44	1.28		4.85	37.29	679.65
87	1						801.37						205.48		36.99	
89	0.54	8.21	0.64	0.81	248.51	0.27	684.37	905.05	36.98	48.85	38.02	3.27		3.53	29.84	552.56
90	0.74						635.29						182.35		34.12	
92	0.2	5.47	0.64	0.69	226.77	0.26	538.56	793.73	32.74	47.39	37.28	1.67		3.77	33.34	545.18
94	0.52						583.33						177.08		41.67	
95	0.52	4.22	0.66	0.55	264.35	0.25	395.21	535.04	27.91	42.48	29.71	1.22	144.24	3.04	30.15	562.05
97	0.8						491.30						139.13		40.87	
102	0.58	4.96	0.59	0.62	328.4	0.25	338.16	578.13	28.94	37.09	26.15	1.07		2.43	31.51	585.19
106	0.93						690.72						154.64		57.73	
111	0.7	6.68	0.62	0.71	357.94	0.25	598.21	634.31	31.13	39.01	33.97	3.05		3.69	33.81	596.19
115	0.72						631.58						112.78		40.60	
120	0.74	5.73	0.56	0.86	351.6	0.27	447.24	756.51	28.86	35.28	33.20	1.53		4.43	29.47	675.50
122	0.45						570.37						140.74		42.22	
124*	0.44	5.6	0.61	0.6	279.69	0.24	660.94	610.81	32.50	34.76	40.98	1.07		2.74	32.74	699.23
126	0.37						294.12						125.00		27.94	
129	0.49	3.78	0.57	0.69	340.91	0.26	225.92	567.66	19.99	34.98	27.18	0.6		2.37	32.72	574.59
133	0.93						500.00						149.57		41.03	
137	0.64	5.06	0.6	0.8	410.71	0.27	343.55	624.70	19.61	35.79	28.49	0.92		3.13	28.20	600.70
140	0.7						414.29						157.14		40.00	
144	0.53	3.97	0.62	0.69	394.34	0.26	340.86	547.91	19.84	36.53	26.05	0.89	125.55	2.68	28.63	639.76
147	0.39						237.76						139.86		39.16	
151*	0.43	4.3	0.6	0.64	471.92	0.26	168.89	368.54	15.04	35.31	24.38	0.77	105.56	1.88	32.41	537.90
155	0.44						217.39						135.87		36.41	
158	0.51	4.24	0.58	0.67	441.97	0.27	282.28	424.79	15.86	34.98	24.05	0.8	114.52	2.43	29.49	583.54
162	0.58						234.46						135.59		33.33	
165	0.56	3.89	0.54	0.62	532.98	0.26	206.51	342.74	14.23	30.07	23.98	0.55	92.40	1.78	28.23	553.92
169	1.38						395.35						170.54		36.43	
172	0.42	3.77	0.56	0.56	385.7	0.26	251.93	372.70	18.68	31.97	23.86	0.41	106.75	1.97	28.45	575.98
176	0.33						251.50						131.74		38.92	
180	0.66	4.05	0.6	0.65	327.61	0.27	376.53	687.16	23.28	29.78	25.26	0.76	136.92	3.03	30.12	656.67
183	0.57						467.74						148.39		36.77	
187*	0.6	6.27	0.64	0.63	396.99	0.27	461.60	581.09	23.59	30.43	32.15	1.13		2.36	28.53	646.20
189	0.26						268.16						106.15		36.87	
194	0.66	5.79	0.62	0.58	216.21	0.25	661.79	771.79	35.28	28.30	36.30	1.58		3.55	30.44	669.61
199	0.71						444.44						151.52		36.36	
204	1.28	8.24	0.7	0.77	244.47	0.27	655.70	785.33	39.93	36.44	37.34	2.45		4.54	38.46	539.41
208	1						594.06						128.71		37.62	
213	0.79	5.43	0.61	0.7	231.27	0.29	601.21	881.92	34.15	28.80	43.04	1.63		5.05	36.48	666.33
216	0.5						529.41						164.71		30.59	
220		4.41	0.64	0.72	160.32	0.29	367.10	1001.30	41.30	33.74	34.55	2.87		4.35	29.96	647.29
223							600.00						157.14		27.14	
226	0.54	6.93	0.6	0.72	231.3	0.27	511.34	745.40	29.57	26.79	30.74	1.93		2.83	24.77	703.97
229	0.7						511.11						133.33		32.22	
233	0.58	4.65	0.59	0.57	224.23	0.26	385.56	631.45	23.07	20.85	29.02	1.55		2.37	26.81	663.33
236	1.15						818.18						131.82		43.94	
239	0.43	5.57	0.56	0.62	199.21	0.26	679.20	668.59	32.07	30.13	39.22	1.57		4.45	35.24	673.53
242	0.63						192.31						166.67		35.90	
248	0.42	3.83	0.65	0.69	250.51	0.29	257.82	655.05	21.90	32.32	26.31	1.87		2.84	30.37	582.26

Table 2: Al normalized contents of TOC, Major and Trace elements.
Samples identified with a * were submitted to the sequential leaching procedure

In order to determine the main carrier-phase of the barium, a sequential leaching procedure was performed on eight samples scattered along the core. These samples were chosen to provide a wide range of barium contents. The protocol used in this study is derived from that described by Robbins et al. (1984) and Lyle (1984) and was already adapted to a previous study on pelagic sediments from the Madingley Rise, the Somali Basin (NW Indian Ocean; Jacot Des Combes et al., in press) and the Amirante Passage (Jacot Des Combes et al., submitted). Briefly, the dried and ground samples were subjected to a pH 5 acetic acid extraction to remove adsorbed and calcite-bound elements, and then to a treatment with a pH 5 hydroxyl amine hydrochloride solution to remove elements adsorbed on poorly crystalline ferromanganese oxy-hydroxides. The pH 9 sodium sulfate extraction of the organic matter was not carried out in Core MD 962073 because of too low TOC values. An extra treatment with HF was added to dissolve the silicate-bound barium (HF alone does not dissolve barite). Residual elements were determined from the difference between the total content (from the bulk analysis) and the sum of the three partial extractions. After each step, element concentrations were measured by ICP spectrometry. The results are summarized in Table 3.

Sample depth (cmbsf)		500	980	1160	1626	1866	2166	2706	3186
Sample age (ka)		31	72	82	124	151	187	-	-
Carbonate-linked fraction	ppm Ba	73	73	57	83	57	77	68	133
	% Ba	11.2	11.2	15.5	9.8	17.8	10.6	24.1	22.1
Oxyhydroxide-bound fraction	ppm Ba	97	103	49	113	50	108	49	90
	% Ba	14.9	15.8	13.3	13.3	15.6	14.8	17.4	14.9
Terrigenous fraction	ppm Ba	280	260	170	240	130	400	70	170
	% Ba	42.9	39.9	46.2	28.2	40.6	54.9	24.8	28.2
Residual = barite fraction	ppm Ba	203	215	92	414	83	143	95	210
	% Ba	31.1	33.0	25.0	48.7	25.9	19.6	33.7	34.8

Table 3: Data of the sequential leaching.
-: no data available

Bulk sediment mass accumulation rates (MAR) were calculated by multiplying the linear sedimentation rate (LSR) derived from the age model and the dry bulk density (DBD). The DBD was obtained by calculating the ratio: g dry weight / cm^3 wet volume.

Elements fluxes were calculated from the formula:

$$\text{Flux} = \text{element concentration (ppm)} \times \text{MAR} \times 10^{-6}.$$

Age (ka)	Bulk MA	$CaCO_3$ MAR	COT MAR	Si MAR	Al MAR	Fe MAR	Mg MAR	K MAR	Ba MAR	P MAR	Cu MAR	Ni MAR	Zn MAR	Mn MAR	Mo MAR	U MAR	V MAR	Ti MAR
31*	8.2	6.0	79.8	581.5	96.4	58.8	72.0	26.0	5379.5	5392.8	272.7	364.9	358.4		13.3	36.9	328.7	5432.6
36	9.9	6.2	100.3	614.3	114.9	70.7	86.1	32.9	5718.7	7785.6	314.2	483.7	360.8	1982.2	16.6	42.8	329.0	7130.1
38	8.4	7.5	92.4	549.5	94.1	64.0	70.8	25.8	5101.9	6225.4	254.3	426.3	319.7	1678.3	17.3	33.7	281.1	5533.6
44	14.0	7.4	54.5		161.9				5304.6					2652.3			698.0	
48	10.6	8.0	37.6		117.1				4790.3					2075.8			436.4	
52	10.4	7.5	92.2		178.2				3212.4					2124.3			601.0	
56	8.9	7.6	70.1	539.1	133.4	79.1	85.4	35.5	3732.0	6996.6	321.5	512.1	367.0		12.4	39.7	386.6	8009.5
59	5.4	7.2	43.0		74.9				1980.6					1017.1			246.2	
64	4.6	7.6	22.8	249.9	60.6	37.0	40.8	16.8	2031.8	2808.5	157.7	229.4	167.3		6.2	17.1	198.6	3306.9
69	5.4	7.5	42.1		67.9				2551.7					977.2			266.0	
72*	8.8	7.2	91.8	562.0	115.8	74.1	82.9	29.1	5696.4	6873.6	315.0	479.5	354.4		12.1	38.4	375.4	6819.5
73	12.4	7.4	103.9		173.3				6251.5					2228.2			594.2	
75	12.9	8.6	99.9	841.8	161.7	96.0	114.0	41.9	6732.2	9039.9	526.9	547.6	542.5		14.2	42.2	515.3	9313.7
77	12.3	6.1	91.9		103.2				6144.9					1966.4			344.1	
78	12.7	6.9	107.5	693.7	136.8	85.1	85.6	32.6	7160.4	9955.3	458.8	609.6	495.5		21.3	48.5	475.2	7597.6
80	12.8	7.3	95.8		128.5				7324.5					2184.5			514.0	
82*	13.7	5.9	134.5	760.4	187.2	106.0	113.7	47.6	5026.2	10729.	482.1	657.0	573.6		10.7	47.8	618.7	11463.3
83	12.8	7.1	81.6		171.8				4680.1					2179.8			705.2	
85	12.0	10.3	109.1	668.2	95.4	57.1	77.5	27.9	6931.8	9437.1	402.5	446.9	395.2		12.3	46.3	355.6	6481.9
87	11.3	7.8	82.6		82.5				6610.2					1694.9			305.1	
89	11.5	7.6	54.1	820.7	100.0	63.7	80.6	26.8	6843.6	9050.4	369.8	488.5	380.2		32.7	35.3	298.4	5525.6
90	12.0	6.6	75.7		102.2				6493.2					1863.8			348.7	
92	12.9	4.1	24.9	696.7	127.3	81.0	87.6	33.1	6854.2	10101.	416.7	603.1	474.5		21.2	48.0	424.4	6938.4
94	12.8	3.5	64.1		123.0				7177.1					2178.8			512.7	
95	12.7	3.9	92.0	741.2	175.6	116.0	97.0	44.2	6940.8	9396.6	490.2	746.0	521.8	2533.1	21.4	53.3	529.4	9871.0
97	6.3	6.2	57.5		72.3				3553.8					1006.4			295.6	
102	4.3	8.4	35.4	303.4	61.2	36.1	38.1	15.2	2068.1	3535.8	177.0	226.9	159.9		6.6	14.8	192.7	3578.9
106	4.8	9.0	43.8		47.0				3246.5					726.8			271.4	
111	4.3	8.0	39.4	375.9	56.2	34.9	39.7	14.3	3364.6	3567.6	175.1	219.4	191.0		17.2	20.8	190.2	3353.2
115	4.2	7.8	40.6		56.3				3554.5					634.7			228.5	
120	4.4	9.3	37.5	291.3	50.9	28.7	43.6	13.5	2274.4	3847.2	146.8	179.4	168.8		7.8	22.5	149.9	3435.2
122	7.2	8.9	44.4		97.8				5578.8					1376.6			413.0	
124*	10.3	9.0	57.8	743.4	132.6	80.8	80.2	31.7	8766.4	8101.6	431.1	461.0	543.5		14.2	36.3	434.2	9274.3
126	9.4	8.6	47.7		128.0				3765.7					1600.4			357.7	
129	6.9	8.3	49.7	380.2	100.6	57.3	69.0	25.7	2273.1	5711.5	201.1	352.0	273.5		6.0	23.8	329.3	5781.2
133	4.9	7.7	53.6		57.5				2877.0					860.6			236.1	
137	5.8	8.3	51.6	410.6	81.2	48.4	64.9	21.7	2790.8	5074.7	159.3	290.7	231.4		7.4	25.4	229.1	4879.8
140	7.5	8.9	73.5		105.1				4354.4					1651.7			420.4	
144	6.3	9.0	52.9	395.5	99.6	61.7	69.0	26.0	3395.8	5458.5	197.6	364.0	259.5	1250.8	8.9	26.7	285.2	6373.6
147	6.5	9.0	35.9		92.5				2199.2					1293.7			362.2	
151*	5.9	4.0	47.7	477.8	111.1	66.5	71.4	29.2	1876.8	4095.2	167.2	392.4	271.0	1173.0	8.5	20.9	360.1	5977.3
155	6.2	2.7	50.5		113.7				2471.2					1544.5			413.9	
158	8.3	3.3	73.5	614.2	144.7	84.0	96.9	38.5	4084.7	6146.9	229.5	506.2	348.0	1657.1	11.6	35.2	426.7	8444.1
162	5.9	2.7	61.0		105.3				2467.8					1427.2			350.8	
165	6.3	2.5	76.3	531.8	136.7	74.2	84.2	36.2	2823.7	4686.5	194.6	411.2	327.8	1263.4	7.6	24.4	386.0	7574.0
169	6.4	3.1	113.9		82.3				3252.7					1403.1			299.8	
172	6.4	4.9	50.2	454.9	120.8	68.1	67.2	31.6	3042.3	4500.6	225.6	386.1	288.1	1289.1	4.9	23.8	343.5	6955.3
176	6.4	7.1	34.8		106.2				2671.1					1399.1			413.4	
180	6.3	6.6	61.0	372.2	91.9	55.0	59.6	25.1	3461.6	6317.3	214.0	273.8	232.2	1258.8	7.0	27.8	276.9	6037.0
183	5.9	4.6	52.2		92.0				4303.1					1365.1			338.3	
187*	5.6	3.0	53.2	556.4	88.8	56.7	55.7	23.8	4097.3	5158.0	209.4	270.2	285.3		10.0	20.9	253.3	5735.9
189	6.5	3.8	30.3		116.7				3128.3					1238.3			430.1	
194	5.4	5.5	37.9	333.7	57.7	36.0	33.7	14.7	3816.6	4451.0	203.4	163.2	209.4		9.1	20.5	175.5	3861.7
199	4.8	4.8	34.1		47.7				2119.8					722.7			173.4	
204	4.4	4.4	50.5	325.6	39.5	27.7	30.6	10.7	2592.0	3104.4	157.8	144.0	147.6		9.7	18.0	152.1	2132.3
208	4.6	4.0	47.0		46.9				2785.2					603.5			176.4	
213	5.9	4.6	45.6	315.0	58.0	35.2	40.6	16.5	3486.4	5114.3	198.1	167.0	249.6		9.4	29.3	211.5	3864.1
216	7.7	6.5	32.4		65.3				3459.3					1076.2			199.9	
220	7.5	4.9		246.1	55.8	35.8	40.0	16.3	2048.5	5587.4	230.5	188.3	192.8		16.0	24.3	167.2	3612.0
223	7.6	5.7			53.3				3200.3					838.2			144.8	
226	7.4	4.7	37.3	478.9	69.1	41.8	49.8	18.4	3533.0	5150.2	204.3	185.1	212.4		13.4	19.5	171.1	4864.0
229	7.6	5.1	47.4		68.1				3480.2					907.9			219.4	
233	7.6	4.8	51.4	412.7	88.8	52.3	51.1	23.2	3424.1	5607.7	204.8	185.2	257.7		13.8	21.0	238.1	5890.8
236	7.3	4.7	55.5		48.3				3953.9					637.0			212.3	
239	8.1	4.4	34.2	441.2	79.3	44.2	48.8	20.8	5383.1	5299.0	254.2	238.8	310.8		12.5	35.3	279.3	5338.2
242	6.1	4.6	29.8		47.4				911.1					789.6			170.1	
248	3.0	5.0	14.5	130.9	34.2	22.4	23.7	10.0	881.3	2239.1	74.8	110.5	89.9		6.4	9.7	103.8	1990.2

Table 4: Bulk, $CaCO_3$, TOC, Major, and Trace element MARs
Bulk and $CaCO_3$ MARs are in g/ cm^2/kyr, Major and trace elment MARs are in mg/ cm^2/kyr.
Samples identified with a * were submitted to the sequential leaching procedure

Radiolarian associations were used as an independent proxy to monitor the variations of the surface paleoproductivity. Two different indexes based on the variations of the specific composition of radiolarians assemblages were used. The upwelling radiolarian index (URI) corresponds to the ratio of the percent of species characteristic of fertile (upwelling) areas to the total number of specimens counted on a slide (3,000 to 8,000) multiplied by 1,000. Variations of this index are indicative of the variations of the intensity of the upwelling (Caulet et al., 1992). The thermocline/surface radiolarian index (TSRI) corresponds to the ratio of the abundance of six radiolarian species living in or below the thermocline layer (below 200 m deep: *Cycladophora d. davisiana*, *Cycladophora d. cornutoïdes*, *Cyrtolagena laguncula*, *Eucyrtidium calvertense*, *Larcopyle bütschli*, and *Spongopyle osculosa*) to the abundance of three radiolarian species restricted to the surface layer (less than 50 m deep: *Heliodiscus asteriscus*, *Lithopera bacca*, and *Siphonosphaera polysiphonia*). TSRI is considered as an indicator of the level of fertility of the surface layer of the ocean: higher surface fertility results in an increased export of fecal pellets and food towards deeper oceanic levels allowing the thermocline populations to thrive, and increasing the proportion of thermocline species in the radiolarian populations accumulated in sediments (Jacot Des Combes et al., in press; Jacot Des Combes et al., accepted).

Radiolarians being sensible to opal dissolution during the settling of their skeletons through the water column and within the sediment, opal dissolution impact may modify the composition of fossil radiolarian assemblages. Sea water being always silica-undersaturated from the surface to the bottom of the ocean, temporal variations in radiolarian populations at the water/sediment interface are, however, considered as mostly linked to variations in the surface productivity rather than to variations of the dissolution strength (Berger, 1968). After deposition, previous studies have shown that opal dissolution occurs within the first centimeters below the water/sediment interface, but in areas submitted to significant export of siliceous debris, this dissolution leads to a Silica saturation of the interstitial water and the dissolution stops at nearly 20/30 cm below the interface (Johnson, 1974; 1976). Under fertile water masses, the variations of radiolarian content and composition in sediments can, thus, be considered as representative of the surface productivity changes.

Radiolarian slides were prepared following a classical procedure (Sanfilippo et al, 1985). Occurrences of representatives of selected radiolarian species were counted in 145 samples. Sampling step was every 10 cm in the upper part of Core MD 962073 (0 to 710 cm) to establish

a comparison with Core MD 85682. Below this level, radiolarian species were counted at the same levels as the geochemical analyses. Variations of the URI and TSRI are presented in Table 5.

Depth (cmbsf)	Age (ka)	URI	TSRI	Depth (cmbsf)	Age (ka)	URI	TSRI
0	0.0	0.56	0.55	890	59.3	0.87	0.40
10	0.6	1.45	0.60	910	62.4	0.80	0.48
20	1.3	1.58	0.53	930	65.5	0.49	0.27
30	1.9	0.75	0.62	950	68.7	1.63	0.95
40	2.5	1.05	0.40	970	70.1	1.36	0.58
50	3.2	1.06	0.24	990	71.5	1.01	0.78
70	4.4	1.39	0.30	1020	73.6	1.58	0.94
90	5.7	0.64	0.36	1040	75.1	1.51	0.25
110	6.9	0.83	0.41	1070	76.7	1.25	0.56
130	8.2	1.01	0.36	1100	78.4	1.14	0.57
150	9.5	0.77	0.26	1130	80.0	0.92	0.26
170	10.7	0.66	0.33	1160	81.7	0.60	0.37
190	12.0	0.80	0.62	1190	83.4	0.64	0.44
210	13.3	1.20	0.22	1220	85.1	0.56	0.31
230	14.5	1.15	0.46	1250	86.8	1.65	0.00
250	15.8	0.79	0.57	1280	88.5	1.32	0.25
270	17.1	1.84	0.35	1310	90.2	1.57	0.89
290	18.3	1.68	0.61	1340	91.9	1.33	0.83
300	18.9	0.74	0.32	1370	93.6	0.59	0.40
310	19.6	1.34	0.66	1400	95.3	1.32	0.19
320	20.2	1.23	0.62	1430	97.0	0.85	0.40
330	20.8	1.31	0.62	1460	102.0	0.79	0.71
340	21.5	0.89	0.89	1490	106.0	1.04	1.38
350	22.1	1.79	0.61	1520	110.6	0.84	3.00
360	22.7	1.07	0.50	1550	115.1	0.62	0.85
370	23.4	1.07	1.12	1580	119.6	1.02	1.07
380	24.0	1.59	0.54	1596	122.0	0.36	0.46
390	24.6	1.04	0.55	1626	124.0	0.19	0.24
400	25.3	0.87	0.66	1656	126.0	0.22	0.32
410	25.9	3.89	1.00	1686	129.0	0.31	0.81
420	26.5	2.94	1.05	1716	133.0	1.75	1.10
430	27.2	1.61	0.52	1746	136.6	0.59	1.10
450	28.4	1.39	1.38	1776	140.2	0.49	1.29
470	29.7	1.45	3.11	1806	143.8	0.74	1.22
480	30.3	1.28	1.03	1836	147.4	0.94	0.53
490	30.9	2.12	1.37	1866	150.9	0.36	0.37
510	32.2	1.57	1.16	1896	154.5	0.70	0.50
530	33.5	0.99	1.00	1926	158.1	0.78	0.89
550	34.7	1.35	0.36	1956	162.0	0.39	1.27
560	35.4	1.69	0.64	1986	165.3	0.42	0.89
570	36.0	1.28	0.64	2016	168.9	0.34	1.40
590	38.0	1.25	0.35	2046	172.5	0.38	0.43
600	38.7	1.25	0.35	2076	176.1	0.32	0.97
610	39.3	1.25	0.43	2106	179.6	0.30	0.87
620	40.0	0.80	0.43	2136	183.2	0.52	0.38
630	40.7	0.78	0.89	2166	186.8	1.19	0.91
650	42.0	1.18	0.62	2186	189.2	0.56	0.26
660	42.7	0.95	0.33	2226	194.0	0.48	0.26
670	43.3	1.13	0.38	2256	198.8	0.53	0.50
680	44.0	1.63	0.86	2286	203.5	0.41	0.27
690	44.7	1.33	0.33	2316	208.3	0.31	0.41
700	45.3	1.48	0.19	2346	213.0	0.18	0.38
710	46.0	1.16	0.36	2376	216.3	0.35	0.30
720	46.7	1.47	0.32	2406	219.6	0.19	0.47
740	48.0	1.76	0.51	2436	223.0	0.21	0.37
750	48.8	1.09	0.33	2466	226.1		
770	50.3	0.63	0.50	2496	229.4	0.39	0.20
790	51.8	0.54	0.67	2526	232.7	0.35	0.59
810	53.3	0.60	0.18	2556	236.0	0.49	0.55
830	54.8	0.78	0.35	2586	239.0	0.65	0.57
850	56.3	1.22	0.40	2616	242.0	0.12	0.38
870	57.8	0.82	0.26	2646	248.0	0.94	1.18

Table 5: Variations of URI and TSRI

Results

a. The chronological framework

Isotope data obtained for Core MD 962073 are compared with the age model published for Core MD 85682 (Ouahdi, 1997a) as to control the coherence between both sets of data (Fig. 2). The isotope record of Core MD 85682 was measured on representatives of *G. bulloides* picked up every 10 cm along the 716 m long piston core. Due to the difference in the sampling step, the isotope curve obtained for Core MD 85682 has been smoothed. Comparison between the isotope curves of Core MD 962073 and the smoothed isotope curve from Core MD 85682 (Fig. 2) shows that the records obtained for levels located above the 490 cmbsf sample (30.9 ka) present the same trend, despite significant alternations between low and high oxygen isotope values in the isotope record of Core MD 962073. Differences occur, however, in the sedimentation rate, especially from 716 to 490 cmbsf samples (from 46.3 to 30.9 ka).

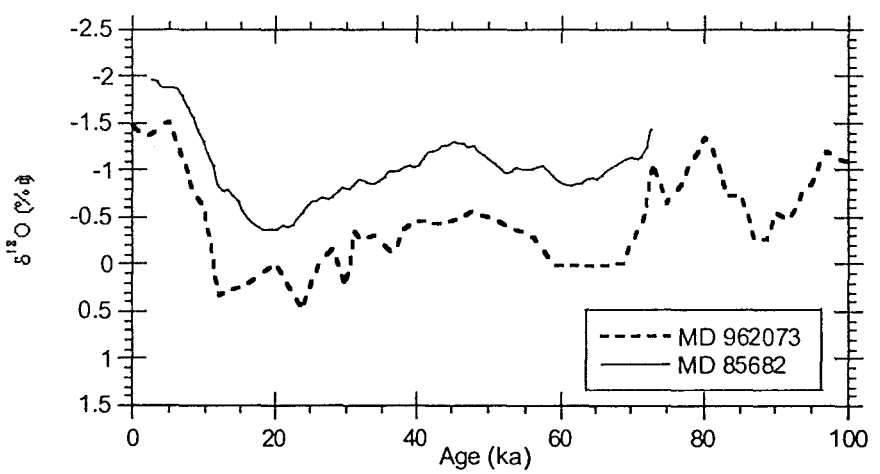

Figure 2: Comparison of the $\delta^{18}O$ curve from Core MD 962073 (this study) with the smoothed $\delta^{18}O$ curve from core MD 85682 (from Ouahdi, 1997)

To check the consistency between both isotope records, abundance of the radiolarian species *Cycladophora davisiana* was measured at each site, and the variations of abundances along each core were compared (Fig. 3). As for the isotope record, the difference in the sampling step leads to some gaps in the interpretation of this marker, but both records can be considered as synchronous from 415 cmbsf level (26.2 ka) to the top of the cores (Fig. 3). From 716 to 410

cmbsf, significant discrepancies can be observed. These data suggest that the sedimentation patterns were different at both sites below a depth of 410 cmbsf (25.9 ka).

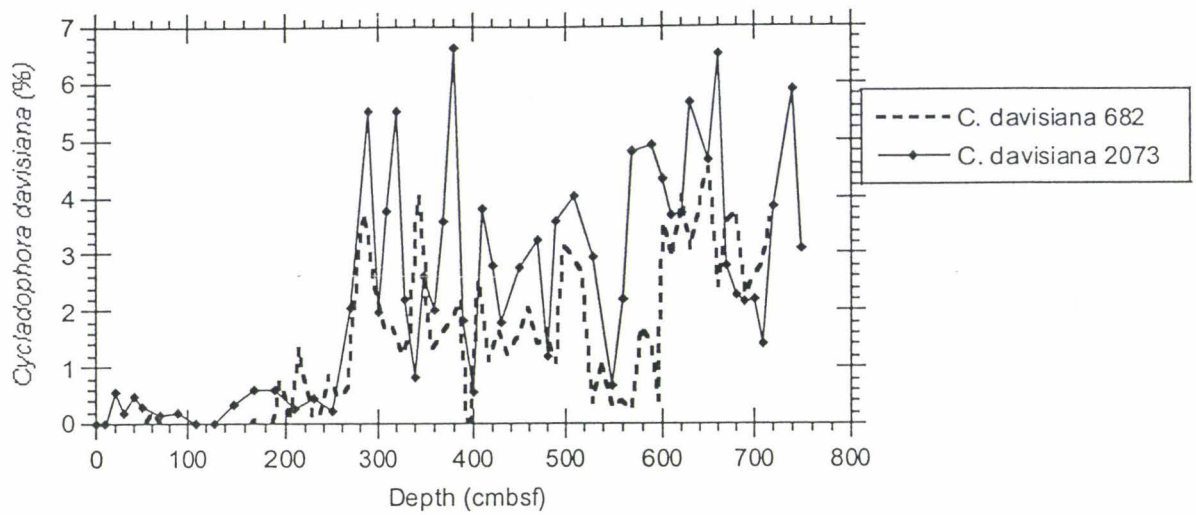

Figure 3: Variation of *Cycladophora davisiana* content in Cores MD 962073 and 85682

The discrepancies observed between the age models and *C. davisiana* records of Cores MD 85682 and 962073 prompted us to use stratigraphic markers to control the reliability of the isotope age model of Core MD 962073. The first occurrence of the radiolarian species *Buccinosphaera invaginata* was observed in Core MD 962073 at a sediment level dated 170 ka by the isotopic age model. This age is fairly consistent with the absolute age estimated for this event at 170 ±10 ka in the Central Indian Basin (Johnson et al., 1989). Micropaleontological and lithological examinations of samples indicate, however, that the sediments from the bottom of the core are strongly disturbed, especially below 2,646 cmbsf (occurrence of reworked radiolarian species indicative of a Mio-Pliocene age). The last occurrence of the radiolarian species *Stylatractus universus*, that occurred at 425 ka (Hayes and Shackleton, 1976), is observed in the 2,886 cmbsf sample of Core MD 962073, that is dated 381 ka by the isotope bulk curve. Due to the co-occurrence of reworked specimens, this discrepancy can be related to reworking processes, and may correspond either to a hiatus in the sedimentary column or to a very condensed MAR. No significant differences were, however, recorded in the mineralogical or chemical composition of the sediment. As a result, the mass accumulation rates (bulk MAR) tentatively calculated after the isotopic age model for isotope stages 10, 9, and 8, are, thus, significantly different from the bulk MAR values calculated above this time interval and exhibit low and constant values. Discrepancies between both isotope and biostratigraphic age models, as

well as occurrence of reworked deposits in sediments observed below 2,646 cmbsf, suggest that the chronology available below this level is not precise. This study is, thus, restricted to the time interval from 248 ka to Present.

b. Variations of the biogenic markers

The URI (upwelling radiolarian index) record presents high values at 135 and 35 ka, with a maximum value at 26 ka. Low values are recorded from 250 to 150 ka, and an increasing trend is observed from 250 ka to the isotope transition 3/2 (24 ka; Fig. 4).

The TSRI (thermocline/surface radiolarian index) presents a different record, with high values recorded at 110 and 30 ka. Low values are recorded during isotope stage 7 (245-185 ka), from 100 to 45 ka, and from 20 ka to Present (Fig. 4)

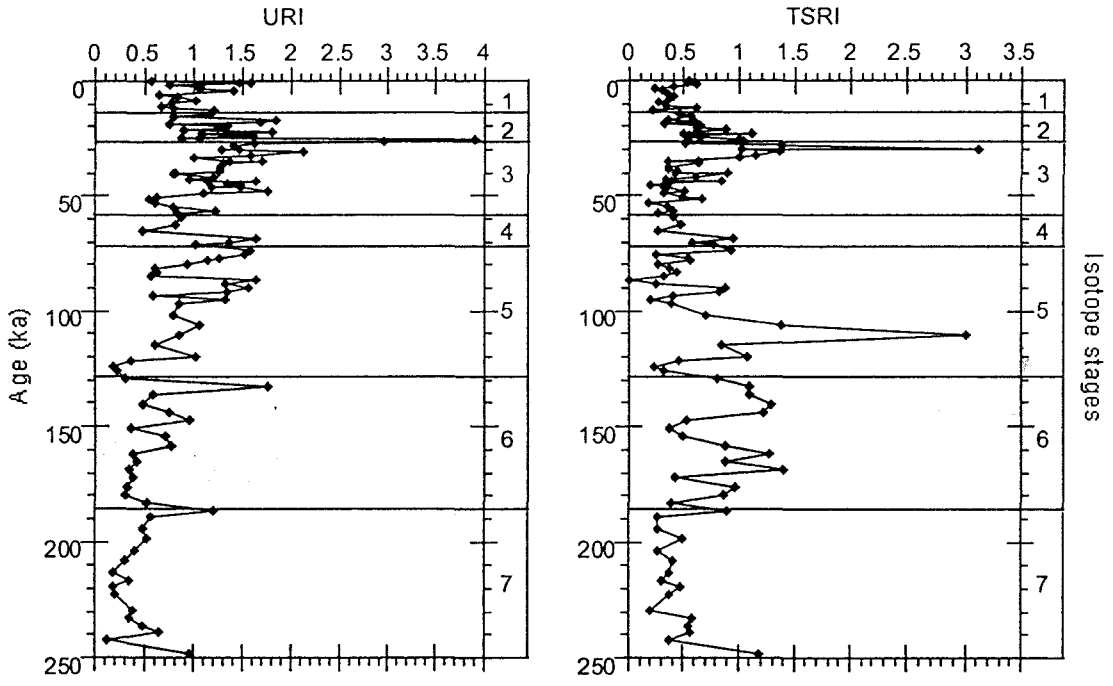

Figure 4: Variations of URI and TSRI.
Glacial isotope stages figured as shaded areas

c. Variations of the geochemical markers

The carbonate content varies from 60 to 90 %, with significant fluctuations (~ 20 %) extending from the isotopic transition 8/7 (248 ka) to the end of isotope stage 3 (25 ka; Fig. 5). Lower values of $CaCO_3$ contents are recorded during isotope stages 6 and 5 (from 125 to 72 ka), and higher values characterize the lower part of isotope stage 7 (from 250 to 220 ka). No

correlation is observed between the variations of the $CaCO_3$ content and the radiolarian proxies (URI and TSRI; Figs. 4 and 5).

The TOC content is comparatively small for sediments deposited under an upwelling area. It varies from 0.1 to 1.8 % with strong changes of its values along the sedimentary sequence (fig. 5). Peak values rate usually around 1 % with a maximum of 1.8 % at 170 ka (isotope stage 7). These contents are of the same order as those measured under the Somali gyre (Caulet et al., 1987). A negative correlation is observed between the TOC and $CaCO_3$ content, and TOC and URI variations are not correlated (Figs. 4 and 5).

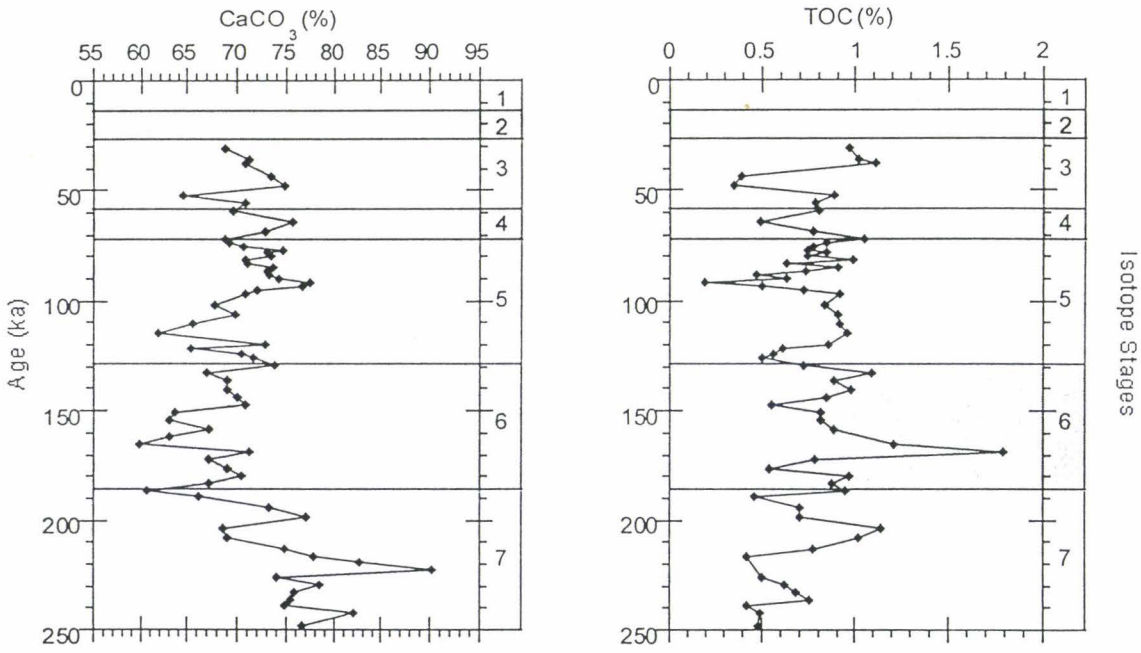

Figure 5: Variations of the CaCO3 and TOC contents
Glacial isotope stages figured as shaded areas

Palynofacies analyses were performed on selected samples and show that the organic matter is, at this site, made of both marine (amorphous organic matter, scolecodonts, and foraminifer linings) and terrigenous (high plants debris, pollen and spores) material.

The Si content varies from 3 to 11 % but its peak values are opposed to those of the $CaCO_3$ content: i.e. high values of Si content are recorded during isotope stages 6 (165-155 ka), and 5 (110-100 ka; Table 1).

The Al content varies from 0.3 to 2.3 % with low values observed during isotope stage 7 (245 to 190 ka) and high values located from the 7/6 transition to the lower part of isotope stage 3 (190 to 50 ka; Table 1). The variations of the Fe, Mg, K, and Ti contents are similar to the Al content changes along the core, and no Al-enrichment compared to Ti is observed.

The Ba content varies from 100 to 900 ppm with strong variations. These values are lower than those observed in the Somali gyre and in the pelagic domain (Ouahdi, 1997; Jacot Des Combes et al., in press; Jacot Des Combes et al., accepted). High values mostly characterize interglacial intervals, especially isotope stages 7 (245-185 ka) and 5 (128-72 ka). The variations of the Ba content along the core (Table 1) are opposed to the variations of the elements of the terrigenous group (Al, Fe, Mg, and K; Table 1). No correlation is, however, recorded between the Ba content and the $CaCO_3$, COT, or Si contents. The P content varies from 600 to 1,100 ppm (Table 1). Variations of the P content along the core follow the changes in the TOC content, despite the difference in the sampling step.

The Cu content varies from 20 to 45 ppm with higher values recorded during interglacial isotope stages 7 (245-185 ka) and 5 (128-72 ka). During the glacial isotope stage 6, a significant decrease in the Cu content is recorded. Nickel and Zn contents present variations different from the Cu ones, but similar to those recorded for the elements of the terrigenous group (Al, Fe, Mg, and K), with lower values occurring during isotope stage 7 (245-185 ka), maximum values during isotope stage 6 (185-128 ka), and high values from the upper part of isotope stage 6 to isotope stage 3 (185-30 ka; Table 1).

The Mn content varies from 70 to 250 ppm and shows increasing values from isotope stage 7 to isotope stage 6 (245-128 ka), when the maximum values are observed (Table 1). These values are higher than those observed in the Somali gyre, but are lower than those observed in the pelagic domain (Ouahdi, 1997; Jacot Des Combes et al., in press; Jacot Des Combes et al., accepted). These variations are similar to those recorded for the elements of the terrigenous group (Al, Fe, Mg, and K). The Mo content varies from 0.5 to 4 ppm, with higher values located during interglacial stages (Table 1). The U content varies from 2.5 to 5.5 ppm with variations similar to those recorded for the Mo content: higher values recorded during isotope stage 6 (185-128 ka), while lower values are observed during isotope stage 7, especially between 240 and 220 ka (Table 1). The V content varies from 16 to 68 ppm in the same way as elements of the terrigenous groups: low values during isotope stage 7 (245-185 ka), and high values from the 7/6 transition to the upper part of isotope stage 3 (185-30 ka; Table 1).

d. Variations of the normalized contents

The element/Al ratios are used to estimate the enrichment of the sediment in these elements compared to the terrigenous supply.

The TOC/Al ratio varies from 0.2 to 1.4 with well-marked variations all along the sedimentological record. High values characterize the interglacial isotope stages 7, 5, and 3, but also the glacial isotope stage 6 (169 ka; Fig. 6). These values are significantly higher than those observed in the Somali gyre (Ouahdi, 1997).

The Si/Al ratio varies from 3.5 to 12. The silica-enrichment is higher than in the Somali gyre (Ouahdi, 1997). High values are recorded during the interglacial isotopes stages 7, 5, and 3. These peaks are synchronous with the high values of the TOC/Al ratio, despite the difference in the sampling step of both markers (Fig. 6).

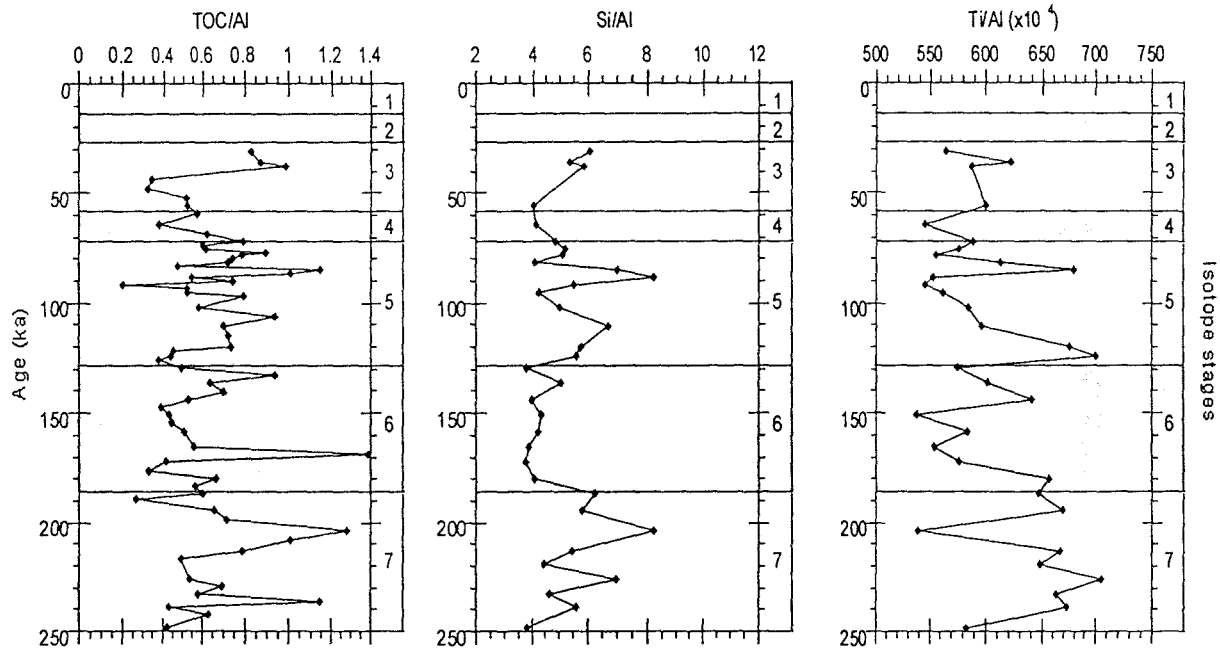

Figure 6: Variations of the TOC/Al, Si/Al, and Ti/Al ratios
Glacial isotope stages figured as shaded areas

The Fe/Al ratio varies from 0.53 to 0.71 with higher values observed in both glacial and interglacial stages. No correlation is observed between the Fe/Al ratio and the TOC/Al ratio. The Mg/Al ratio shows strong variations (from 0.54 to 0.86) all along the sedimentological record, with peak values located in both glacial and interglacial stages. A similar record is observed for the K/Al ratio (from 0.238 to 0.293), but peak values are not synchronous with higher values of the Fe/Al, nor the Mg/Al ratios. The Ti/Al ratio varies from 520 to 710×10^{-4}. Higher values are recorded during isotope stages 7 and 5, while lower values are observed during isotope stages 7,

6, 5, and 4 (Fig. 6). The values of the Ti/Al ratio are lower at this site than in the other sites, but the Madingley Rise. On the contrary, the values of the Si/Al ratio are higher than in any other site (Ouahdi, 1997; Jacot Des Combes et al., in press; Jacot Des Combes et al., accepted). The discrepancies observed between the variations of the Ti/Al and Si/Al ratios suggest that these elements have different sources. The common peak value observed at 85 ka may result from a terrigenous supply, or an increased wind field, whereas the TOC/Al and Si/Al peak values recorded at 205 ka, that correspond to a low Ti/Al value, may be related to enhanced siliceous productivity.

The Ba/Al ratio varies from $160x10^{-4}$ to $840x10^{-4}$ with strong variations along the sedimentological record, especially from isotope stage 7 to isotope stage 3 (245-30 ka). Ba/Al peak values characterize both interglacial stages 7 (245-185 ka) and 5 (128-72 ka). Variations of this ratio are more or less synchronous to those observed for the Si/Al ratio (Figs. 6 and 7). The P/Al ratio varies from 350 to $1,000x10^{-4}$, and presents variations similar to the barium ones, but with very low values within isotope stage 6 (175-150 ka; Fig. 7).

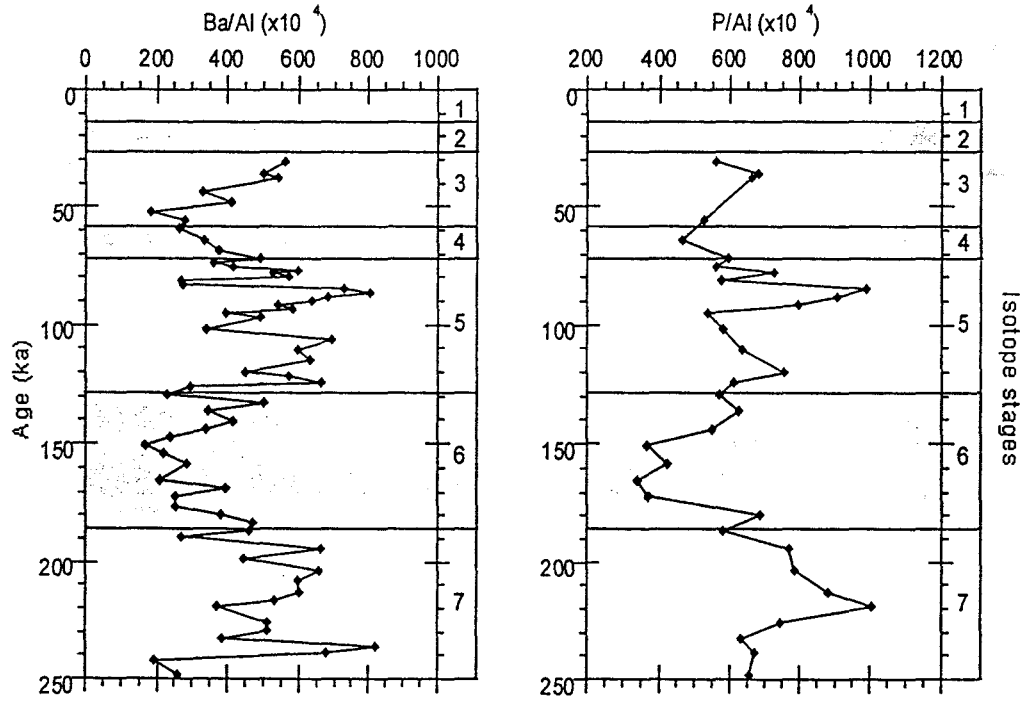

Figure 7: Variations of the Ba/Al and P/Al ratio
Glacial isotope stages figured as shaded areas

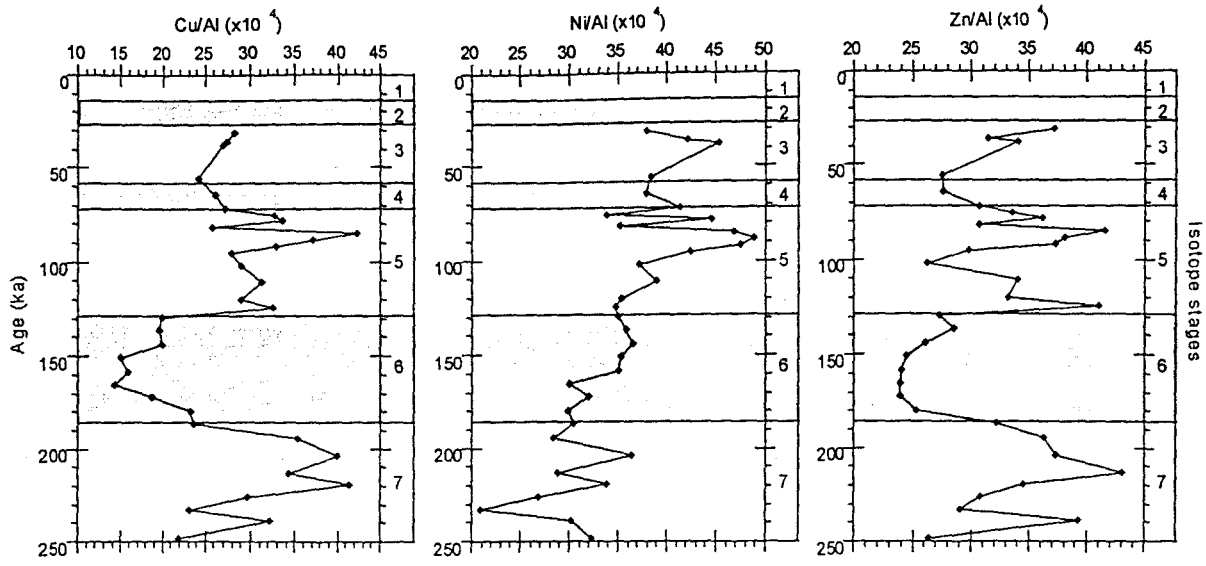

Figure 8: Variations of the Cu/Al, Ni/Al, and Zn/Al ratios
Glacial isotope stages figured as shaded areas

The Cu/Al ratio varies from $10x10^{-4}$ to $45x10^{-4}$, with high values located within interglacial stages 7 (245-185 ka) and 5 (128-72 ka). Its variations are similar to the variations of the P/Al ratio, with minimum values during isotope stage 6 (170 to 150 ka). The variations of the Cu/Al ratio along the core are also similar to those recorded for the Si/Al ratio (Figs. 6 and 8). The Ni/Al ratio varies from $20x10^{-4}$ to $50x10^{-4}$. A marked increase of this ratio is recorded in the time interval between isotope stages 7 and 5 (245-72 ka). The variations of the Zn/Al ratio are synchronous with those recorded for the Cu/Al ratio, but minimum values remains above $20x10^{-4}$ (Fig. 8).

The Mn/Al ratio varies from $90x10^{-4}$ to $210x10^{-4}$, with maximum values in interglacial intervals, especially during isotope stages 5 (128-72 ka) and 3 (49-30 ka). The high values observed during isotope stage 6 correspond to the maximum values of the TOC content. No correlation is, however, recorded between the TOC content and the Mn/Al ratio. The Mo/Al ratio varies from $0.4x10^{-4}$ to $3.4x10^{-4}$, with high values characterizing interglacial stages. The variations of the Mo/Al ratio are similar to those of the Si/Al ratio (Figs. 6 and 9). The U/Al ratio, which varies from $1.8x10^{-4}$ to $5.1x10^{-4}$, also presents higher values during interglacial intervals, but they are not synchronous with the high values of the Si/Al ratio, especially during isotope stage 7 (Fig. 9).

The Mg/Ca ratio varies from $150x10^{-4}$ to $550x10^{-4}$. Maximum values are recorded during isotope stage 6 (170-140 ka), whereas minimum values are observed during isotope stage 7 (240-190 ka). Higher values are also observed from the isotope transition 6/5 to the isotope stage 3

(128-30 ka). The variations of the Mg/Ca ratio along the core are synchronous with those of the Fe/Al, Mg/Al, K/Al, and Ti/Al ratios.

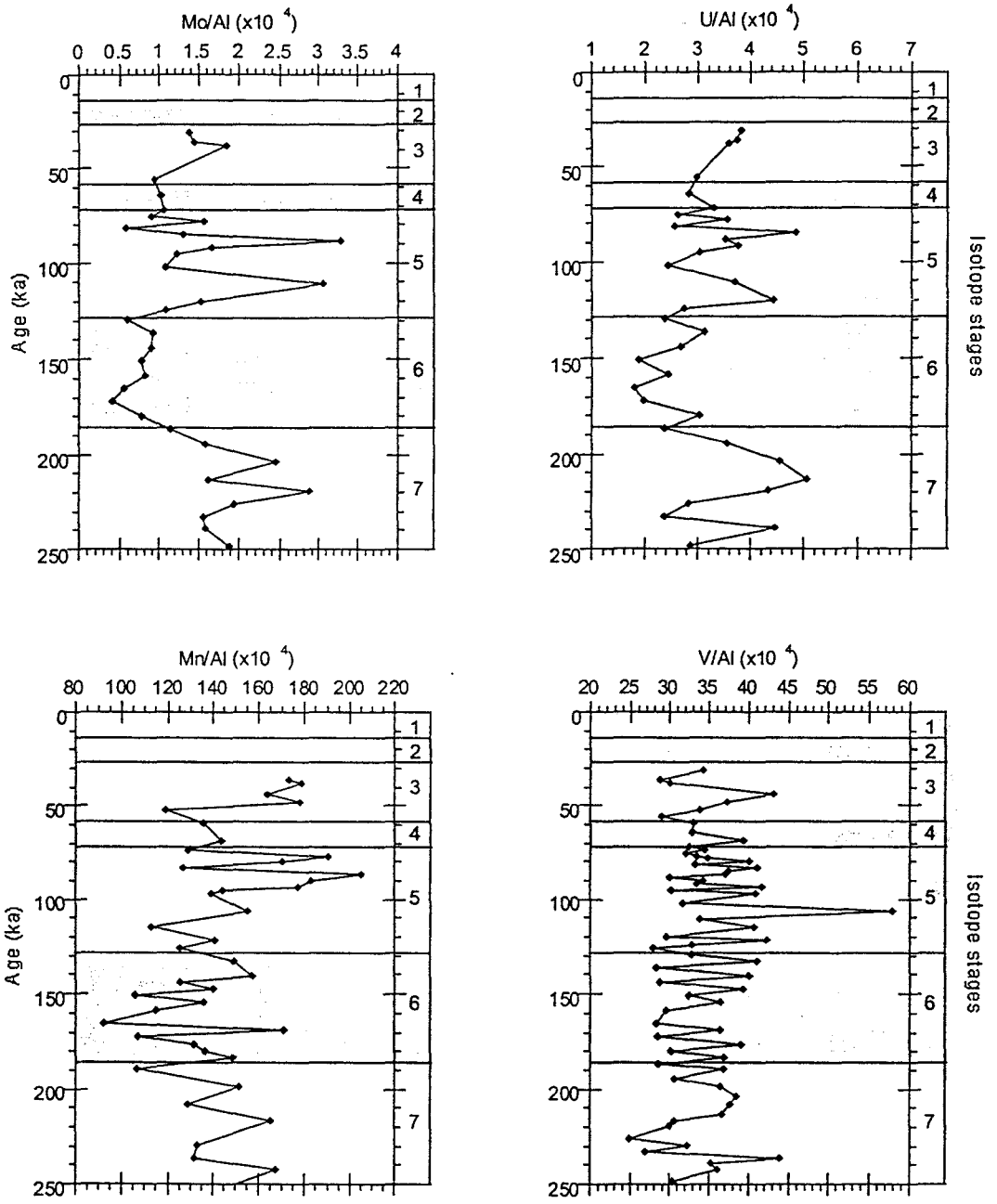

Figure 9: Variations of the Mn/Al, Mo/Al, U/Al, and V/Al ratios
Glacial isotope stages figured as shaded areas

e. Results of the sequential leaching

Eight samples (identified by a * in the tables giving the results of the bulk analyses) analyzed through the sequential leaching procedure give the mean distribution of the barium in the sediment:

15 % of the bulk Ba is located in the carbonate fraction

15 % of the bulk Ba is located in the oxy-hydroxides fraction

39 % of the bulk Ba is located in the aluminosilicates fraction

31 % of the bulk Ba is located in the residual fraction, and is assumed to be deposited as barite.

The distribution of Ba within the different fractions shows, however, some marked differences between the samples, especially in the extent of the barite fraction (19.6 to 48.7 %), and of the aluminosilicates fraction (24.8 to 54.9 %; Fig. 10). The sample located at 1,626 cmbsf, that is dated 124 ka, exhibits a significantly higher barite content than the other samples, whereas samples located at 1,160 and 2,166 cmbsf, i.e. 82 and 187 ka, present a large amount of terrigenous-Ba. Both barite and the terrigenous-linked Ba appear to be the main barium sources at this site. Except for the Ba-carbonates, whose part seems to increase with depth, no trend is observed in the barium distribution. Moreover, the variations observed between the samples do not seem to be influenced by the depositional time, or the glacial-interglacial cycles.

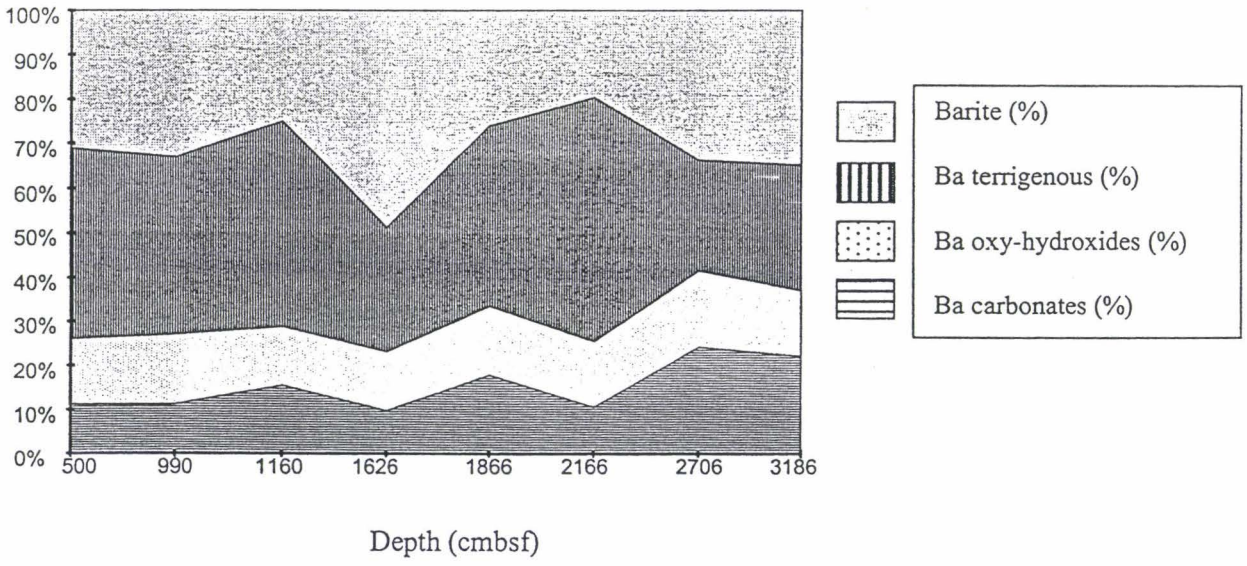

Figure 10: Distribution of barium within the different fractions of eight sediment samples

f. Variations of Mass Accumulation Rates (MAR)

The bulk MAR varies from 4 to 14 g/cm^2/kyr, with maximum values recording during isotope stage 5 (128-72 ka) and 3 (49-24 ka). These interglacial intervals are also characterized by strong variations between high and low bulk MAR values (Fig. 11). These values are significantly higher than those recorded in the pelagic domain, but are similar to those observed

in the Somali gyre (Ouahdi, 1997, Jacot Des Combes et al., in press; Jacot Des Combes et al., accepted).

The $CaCO_3$ MAR varies from 2.3 to 10.3 g/cm^2/kyr, with high values observed from 150 to 40 ka, i.e. from mid-stage 6 to mid-stage 3, whereas minimum values are recorded during the lower part of isotope stage 6 (170-150 ka; Fig. 11). An abrupt change in the $CaCO_3$ MAR is observed at 150 ka. This may be related to a difference in the carbonates deposition/preservation pattern. Due to the differences in the bulk MAR values between the pelagic domain and the upwelling system, the element MAR values will be significantly higher in the upwelling system than in the pelagic domain. The $CaCO_3$ MAR values in the Socotra gyre are, however, similar to those observed in the Somali gyre (Tribovillard et al., 1996).

The TOC MAR varies from 15 to 135 mg/cm^2/kyr, with maximum values in the lower part of isotope stage 6 (170-160 ka) and the upper part of isotope stage 5 (85-70 ka). Minimum values are recorded during isotope stage 7 (230-190 ka; Fig. 11). These values are higher than those observed in the Somali gyre (Ouahdi, 1997).

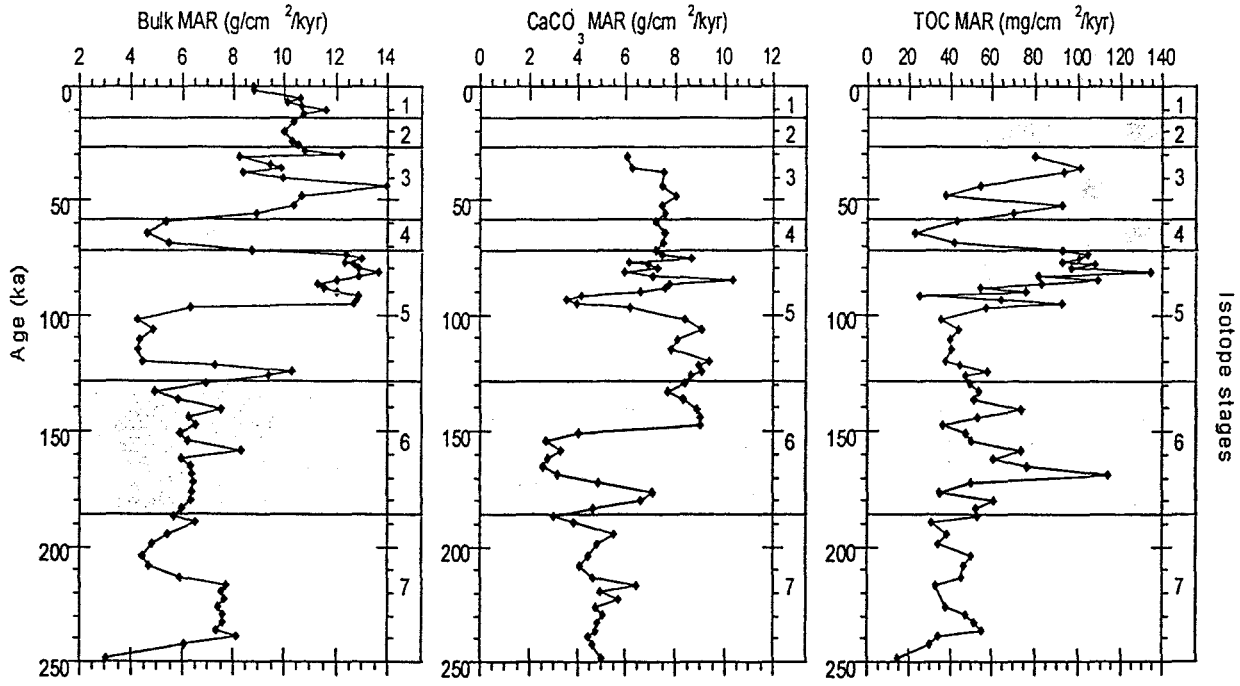

Figure 11: Variations of the bulk, $CaCO_3$, and TOC MARs
Glacial isotope stages figured as shaded areas

The Si MAR varies from 100 to 900 mg/cm^2/kyr, with maximum values during the second half of isotope stage 5 (100 to 70 ka). High values are also recorded during isotope stages

7, 6, and 3. The minimum values are observed during isotope stages 7 and 4 (Fig. 12). These values are lower than those observed in the Somali gyre (Tribovillard et al., 1996).

The Al MAR varies from 34.2 to 187.2 mg/cm^2/kyr, with variations similar to the bulk MAR variations, except during isotope stage 6 (170-155 ka), when high Al MAR values are observed. Marked variations are also observed from the 7/6 transition to the upper part of isotope stage 3 (190-30 ka). The records of Fe, Mg, K, and Ti MAR are similar to the Al MAR record, despite the difference in the sampling step of these markers (Fig. 12). The terrigenous element MARs are lower in the Socotra gyre than in the Somali gyre (Tribovillard et al., 1996).

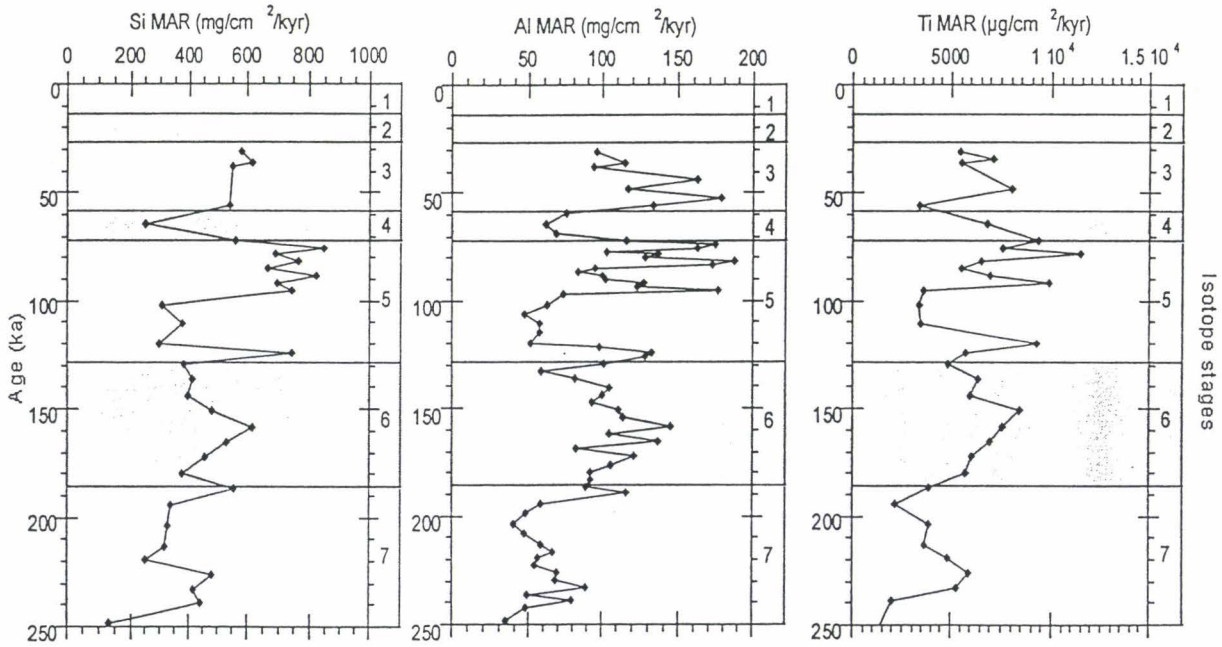

Figure 12: Variations of the Si, Al, and Ti MARs
Glacial isotope stages figured as shaded areas

The Ba MAR varies from 881 to 8,766 µg/cm^2/kyr, with high values observed within isotope stage 5 (125 and 100-70 ka). During isotope stages 7, and 6, the Ba MAR remains constant between 2,000 and 4,000 µg/cm^2/kyr. Minimum Ba MAR values are observed at the 8/7 transition (245 ka). The P MAR varies from 223.9 to 1,072.9 µg/cm^2/kyr. The P MAR variations are synchronous with the Ba MAR changes (Fig. 13). These values are of the same order as those observed in the Somali gyre (Tribovillard et al., 1996; Ouahdi, 1997).

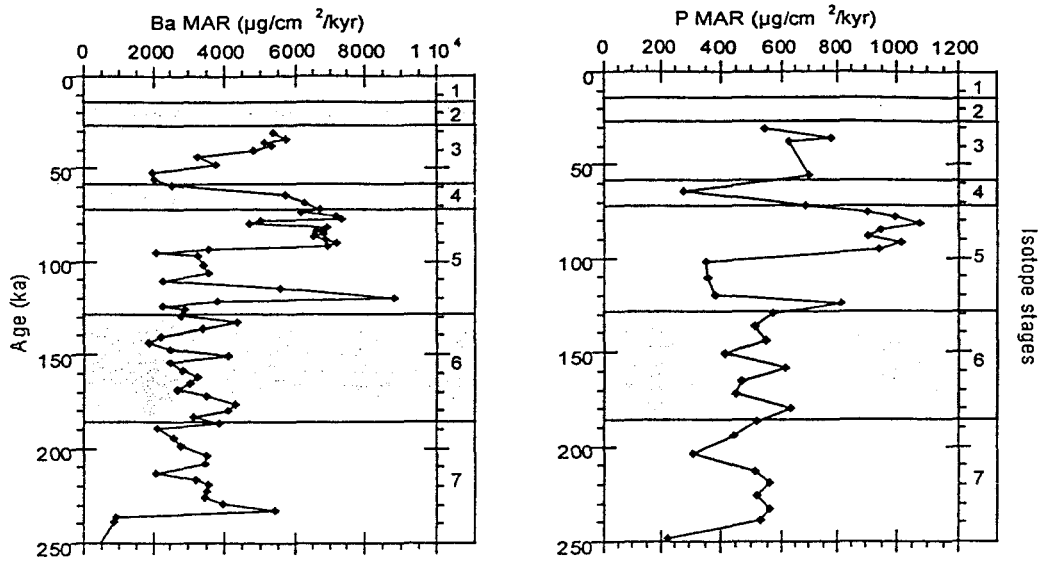

Figure 13: Variations of the Ba and P MARs
Glacial isotope stages figured as shaded areas

The Cu MAR varies from 75 to 527 µg/cm²/kyr, with high values observed in the upper part of isotope stage 5 (100 to 75 ka), and low values recorded at the 8/7 transition (245 ka). Isotope stages 7, and 6 are characterized by constant Cu MAR values (between 200 and 280 µg/cm²/kyr). The Ni MAR varies from 111 to 746 µg/cm²/kyr, and presents variations synchronous with the Al MAR changes, despite the difference in the sampling step of both markers. The Zn MAR values varies from 90 to 574 µg/cm²/kyr, with variations synchronous with the Cu MAR changes (Fig. 14).

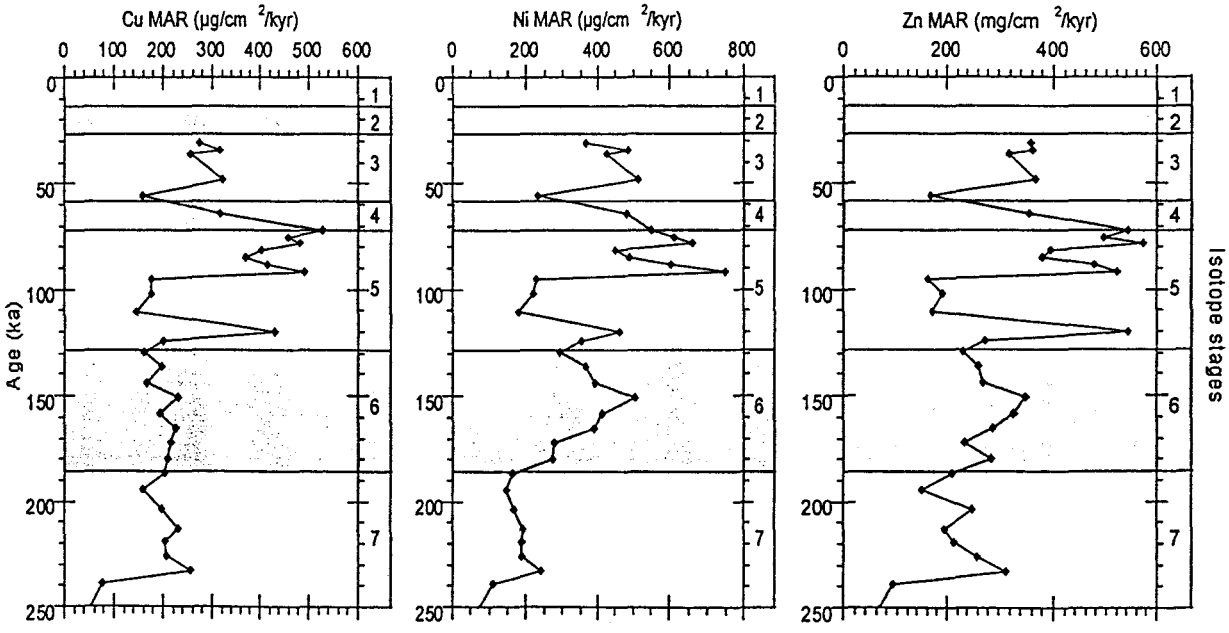

Figure 14: Variations of the Cu, Ni, and Zn MARs
Glacial isotope stages figured as shaded areas

The Mn MAR varies from 635 to 2,652 μg/cm^2/kyr, with high values observed during the upper part of isotope stage 5 (100 to 75 ka), and isotope stage 3 (59-30 ka), whereas minimum values are observed during isotope stage 7 (245-200 ka). The Mo MAR varies from 4.9 to 32.7 μg/cm^2/kyr, with maximum values observed during isotope stage 5 (95-85 ka). Local peak values are also observed during isotope stages 7 (220 ka) and 3 (40 ka). Minimum values are observed during isotope stage 6 (180-165 ka). The U MAR varies from 9.7 to 53.3 μg/cm^2/kyr, with maximum values recorded during the upper part of isotope stage 5 (100 to 75 ka). The U MAR variations are synchronous with the Cu MAR changes. The V MAR varies from 103.8 to 705.2 μg/cm^2/kyr and shows variations synchronous with the Al MAR changes (Fig. 15).

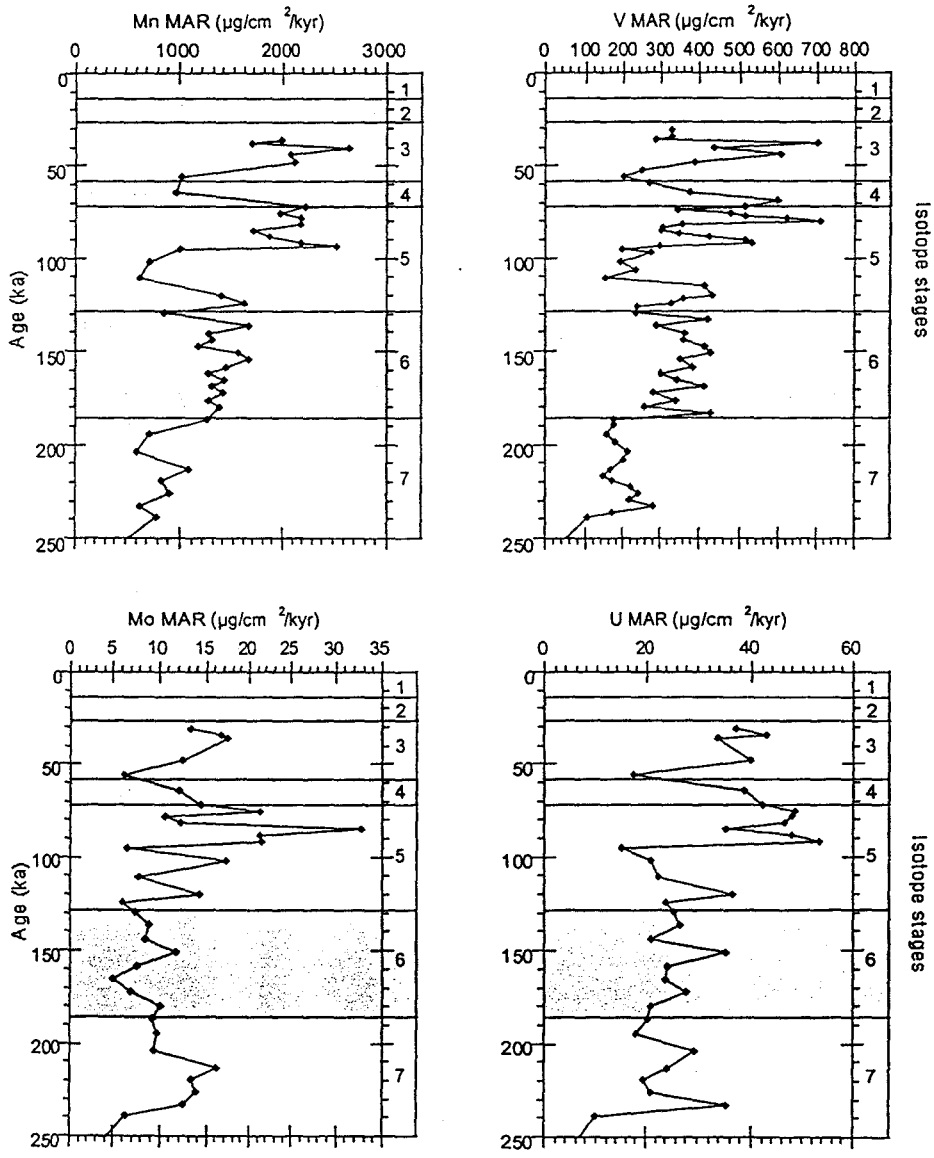

Figure 15: Variations of the Mn, Mo, U, and V MARs
Glacial isotope stages figured as shaded areas

Discussion

A. Variations of the upwelling system of Socotra from 248 ka to 72 ka (Core MD 962073)

The time interval from 72 ka to Present having already been studied (Ouahdi, 1997), this section will discuss the new results obtained from Core MD 962073.

High accumulation rates characterize all interglacial stages as shown by the variations of the bulk MAR in Core MD 962073. In coastal upwelling areas, the bulk MAR may result from both terrigenous input and enhanced surface productivity.

A.1. The organic content

The sediment from Core MD 962073 containing from 0.1 to 1.8 % of organic matter, variations of the TOC content, or the TOC MAR, could be used to monitor the variations of the upwelling intensity through time. However, composition of the organic matter shows that, at this site, the organic matter fraction may have both terrestrial and marine origins. Palynofacies analyses realized upon selected samples show that organic content is mainly made of amorphous organic matter, with relatively abundant zooplankton fragments and scolecodonts, foraminifer linings, dinoflagellate cysts, but also with a non neglectible fraction of terrestrial organic matter, composed of spores, pollen, and higher plant debris (ligneous fragments and cuticles). Additionally, mycelia were observed.

The analyses performed on the sediment do not allow to measure the part of the marine organic matter in the sediment. The comparison of the TOC content and the TOC/Al ratio shows, however, that the variations of both proxies are synchronous, and no common peak values can be recorded between TOC and Al contents, e.g. during isotope stage 6, characterized by a maximum terrigenous input, mean values of both TOC and TOC/Al are recorded (Figs. 5 and 10). On the other hand, high TOC/Al episodes correspond to both interglacial isotope stage 5 (120 ka, 110 ka, 105 ka, 90 to 80 ka, 75 ka) and glacial isotope stage 6 (165 ka, 160 ka, 140 ka, 135 ka). All these data suggest that, despite a non neglectible part of terrestrial input, the organic matter is mainly made of marine debris, and that the variations of the enrichment of the sediment in organic matter were controlled mainly by the surface productivity, without marked effects of

dilution by terrigenous supply. The TOC/Al ratio is, thus, considered in this core as a reliable proxy to monitor the variations of the surface productivity and the upwelling intensity.

According to the sediment examination, the marine organic matter may derive from both siliceous and calcareous planktonic populations. The TOC/Al ratio does not, however, present a correlation with the $CaCO_3$ content, and TOC MAR changes follow the Si MAR rather than the $CaCO_3$ MAR variations, despite a lack of synchronicity during isotope stage 6 (Figs. 11 and 12). On the other hand, the silica enrichment of the sediment seems to have a marked biogenic origin rather than a purely terrigenous one: no correlation is observed between the Si and Al contents, whereas a positive correlation is observed between TOC/Al and Si/Al, except during isotope stage 6 (Fig. 6). A positive correlation is also observed between the TOC/Al ratio and the Si_{excess} content, that is calculated following the formula: $Si_{excess} = Si_{tot} - (Al \times 3.8)$, where 3.8 is the correcting coefficient calculated for this site. As already observed, this isotope stage is characterized by maximum values of the terrigenous input, and the relation between TOC/Al and Si/Al may be disturbed by these detrital inputs. The disturbance induced by the terrigenous inputs may also explain the lack of strong correlation between the Si content and both the TOC content and TOC/Al ratio (Figs. 5 and 6). These data indicate that a significant fraction of the marine organic matter is produced by the siliceous plankton (diatoms and radiolarians) rather than by the calcareous plankton. Such an interpretation confirms observations previously made on intensity changes of the Socotra gyre indicating that, at this site, productivity is mainly of siliceous origin (Ouahdi, 1997a; Vénec-Peyré and Caulet., submitted). Different hypotheses may explain such an importance of the siliceous production. First, upwelling systems being very fertile areas, the enhanced input of nutrients creates suitable environments for diatom blooms. In the California Basin, and on the Peru and Angola Margins, these siliceous plankton blooms lead to the accumulation of diatomites at the bottom of the ocean (Aplin et al., 1992; Diester-Haas et al., 1992; Meyers, 1992; White et al., 1992). Diatomites are not recorded in the sediments of the east-African Margin, but the predominance of siliceous plankton may explain that the variations of the organic matter and the silica content are correlated.

The main organic component of the pelagic sediments in the northwestern Indian Ocean is represented by the amorphous organic matter, very likely originating from the phytoplankton (Tyson, 1995). Due to its composition, and especially to its low lipid content, the organic matter produced by coccolithophorids, or more generally by the mineral-walled plankton, is known to have a low potential of preservation in the sediment (Noël et al., 1993; Tribovillard et al., 1994a;

1996). This lability may explain that the organic matter produced at Socotra by the coccolithophorids of the plankton would not be preserved in the sediment.

These interpretations on the origin of the organic matter are based on biological processes, but chemical processes, such as carbonate dissolution may also disturb the biogenic signal originating from the surface. The intensity of carbonate dissolution is mainly related to the depth of the lysocline/CCD couple, but may also depends on the intensity of the decay of the organic matter, that releases dissolved CO_2 in the water column, and renders marine water more aggressive toward carbonates. Previous studies performed upon assemblages of foraminifer species in the Socotra upwelling system at equivalent depths (Vénec-Peyré and Caulet., submitted; and personal communication) indicate that carbonate dissolution had no significant impact on the species assemblages. The abrupt change in the carbonate accumulation during isotope stage 6 may be related to a marked variation in the carbonate productivity. It can be, thus, considered that, at this site, carbonate dissolution is not the main process controlling the variations of the carbonate content of the sediment.

A.2. The radiolarian indexes

Significant differences are observed between variations of URI (Upwelling Radiolarian Index) and TSRI (Thermocline/Surface Radiolarian Index) records. The URI record presents an increasing trend from the lower part of isotope stage 7 (240 ka) to the 3/2 transition (24 ka), whereas TSRI shows low values during isotope stage 7 (245-185 ka) and from 90 to 40 ka (Fig. 4). Such diachroneity was, however, expected, due to the nature of both these proxies. TSRI is a reliable paleoproductivity proxy in the pelagic domain, where a neat stratification separates the surface water masses from the deeper water masses located below the thermocline. Under upwelling conditions, such a stratification no longer exists, and the TSRI is less reliable. On the other hand, URI is specifically used in upwelling areas. A combined use of both radiolarian indexes may help distinguish periods when the upwelling is the main factor of surface productivity, and periods when advection of subsurface water is less intense and an improved stratification may occur.

Our data show a lack of correlation between both URI and TSRI on one hand, and the bulk MAR on the other hand. This may be related to the input of terrigenous material at this site. The variations of the terrigenous input cannot disturb the composition of the radiolarian assemblages, but may have a significant influence on the variations of the bulk MAR. A similar

lack of correlation is observed between the radiolarian indexes and both the TOC/Al and Si/Al ratios, that can be related to variations in the diatom population at this site. The lack of correlation between URI and the TOC MAR is, however, more puzzling, suggesting that one group of proxies (radiolarian or geochemical) does not monitor the variations of the surface paleoproductivity. The organic matter is known to be sensitive to decaying both in the water column and within the sediment, but, as said before, the positive correlations between the TOC/Al and Si/Al ratios, and between the TOC and Si MARs, suggest that, at this site, the TOC-enrichment is controled by surface productivity rather than by preservation processes. The trace element variations may, thus, be considered as a reliable proxy for the paleoproductivity changes at this site. The variations of the TOC/Al ratio indicates that high productivity periods occurred mainly within interglacial stages 7 (240 and 210-200 ka), 5 (110, 85, and 80 ka) and 3 (40 ka), and during glacial stage 6 (165 and 135 ka), when the absence of a Si/Al peak value suggests a different source of organic matter, e.g. organic-walled plankton.

The absence of correlation between the changes in the surface productivity and the variations of URI may be interpreted in three main ways. First, due to the seasonal characteristic of the northwestern Indian Ocean upwelling system, the proportion of the radiolarian species characteristic of upwelling environments is less important than in populations accumulated under upwelling systems where seasonal changes are weaker (e.g. the Peru Margin and the California Current system). The "radiolarian upwelling signal" may, thus, be disturbed by the "non-upwelling radiolarian" input. Second, the siliceous plankton is not made only by radiolarians. Diatoms are also abundant in sediments from upwelling areas and are of significant importance in the plankton blooms responsible for the enhanced surface productivity recorded in the upwelling systems (Schuette and Schrader, 1979; 1981a; Schrader and Sorknes, 1991; Schrader, 1992). The variations of the diatom population having no influence on the URI variations, changes in the surface paleoproductivity related to this plankton group may explain the diachroneity between the URI and the geochemical records. Finally, the carbonate plankton, especially the coccolithophorids, is a main component of the sediment recovered under the Socotra gyre, and may be originating a fraction of the organic matter produced in the surface layer. According to these assumptions, we consider that, at this site, the variations of the trace element records will be considered as a more reliable proxy than the URI fluctuations for the reconstruction of paleoproductivity changes.

A.3. The terrigenous input

Variations of the terrigenous input can be monitored through the variations of some chemical elements. Data from Core MD 962073, and especially the positive correlation between the Al content on one side, and the Fe, Mg, K, Ti, Mn, Ni, and V contents on the other side, indicate that these chemical elements are associated. According to the origin of Al, and to the correlation between the Al and Ti contents, this group of elements can be considered as a "terrigenous group". The variations of the terrigenous input along the sedimentary sequence are different within the following three time intervals:

★ In isotope stage 7 (245-185 ka) relatively low values of the terrigenous element contents are observed.

★ In isotope stage 6 (185-128 ka) maximum terrigenous input is recorded.

★ From the 6/5 transition (128 ka) to the isotope stage 3 (30 ka), lower values are recorded. These values are, however, higher than those recorded during isotope stage 7, except for the upper part of isotope stage 5 (100 to 80 ka).

Similar variations are also shown by the values of the Mg/Ca ratio, but not by the values of the Ti/Al ratio. Both these ratios are considered in this area as wind strength proxies (Weedon and Shimmield, 1991; Shimmield, 1992; and references therein). Such a difference between the variations of the Mg/Ca and Ti/Al ratios indicates that two sources of detrital material are available. According to the location of this site close to the east-African coast, these sources are probably the western-northwestern winds and the direct input from the African continent, through continental weathering and/or river outflows. Regional distribution of these elements in the western Indian Ocean confirms such a difference between the Mg/Ca and Ti/Al ratios, that is also observed on a regional scale. The Mg/Ca ratio presents increasing values in sediments closer to the coast than the Ti/Al ratio (Jacot Des Combes et al, submitted), and is, thus, considered as a marker mainly related to direct continental input (continental weathering or river outflows), whereas the Ti/Al ratio is considered more as a wind strength proxy (Weedon and Shimmield, 1991; Shimmield, 1992). The sediments deposited under the Socotra gyre exhibits contents in terrigenous elements that vary synchronously with the Mg/Ca ratio. This correlation indicates that the terrigenous input mostly originates from the near African coast, rather than being carried by the winds from more distant areas.

A.4. The trace element record of paleoproductivity

Variations of surface productivity may also be monitored at this site through the variations of trace elements, such as Ba, P, Cu, and Zn. In Core MD 962073, the Al-normalized contents of these trace elements grossly correlate with the Ti/Al ratio, indicating that the main factor controlling the accumulation is the wind strength. The higher values of these ratios may correspond either to a terrigenous input, or to an enhanced upwelling system. The close examination of the curves indicates that the Al-normalized trace element records correlate better with both Si/Al and TOC/Al ratios and show relatively high values during interglacial stages (Fig. 10). Such data indicate a correlation between the enrichment of the sediment in these elements and the surface productivity. In such an environment with both biological and terrigenous inputs, the use of barium as paleoproductivity proxy may, however, be questionable. Due to both its biogenic and terrigenous origins, the record of the barium in the sediment may not correspond to the barium content resulting from the surface productivity. The positive correlation observed at this site between Ba/Al and both Si/Al and TOC/Al (Figs. 6 and 7) indicates, however, a strong link between the Ba-enrichment and the surface productivity. Such a correlation is coherent with the observation of barite formation in particular microenvironments, especially debris of siliceous plankton where the decay of organic matter induces sulfate saturation that leads to barite formation (Bishop, 1988; Dehairs et al., 1980; 1987; 1991). Results of the sequential leaching procedure show, however, that the barium is not uniquely deposited as barite. Barite represents on average 31 % of the bulk Ba, whereas the terrigenous barium represents on average 38 % of the bulk Ba. In spite of significant variations in the Ba distribution in the different analyzed samples, both terrigenous and biogenic inputs appear to be the main Ba carrier to the sediment in Core MD 962073. The balanced distribution of barium between the terrigenous and the biogenic fraction may have implied barium variations that are not correlated with both the biogenic and the terrigenous changes, because of the combined influence of both terrigenous and biogenic inputs. In this region, the variations of the intensity of the upwelling being monitored by the seasonal reversions in the wind field, the sedimentation conditions are submitted to drastic changes between periods when the upwelling system is active, characterized by rapid inputs of organic matter after planktonic blooms, and periods when the upwelling is not established. The range of variations of the proxies related to surface productivity, including Ba, may, thus, be wide between these two sorts of intervals. If we consider that the terrigenous input is more permanent than the biogenic accumulation under the upwelling gyre, the large variations

of the biogenic input may have a stronger influence on the bulk barium than the terrigenous input that remains present and relatively low all along the core (Al < 2.5 %). This could explain that the barium record is more influenced by the changes in the surface productivity. Barite may also be dissolved under reducing conditions and, according to some authors (Thomson et al., 1993; 1995; Van Santvoort et al., 1996), a fraction of the barium thus released may be fixed on Mn oxy-hydroxides lying above or under the layer where reducing conditions occur. If such a process occurs at this site, the relatively low and constant fraction of Ba measured in the oxy-hydroxide fraction suggests that the intensity of barite dissolution did not undergo marked variations at this site for the last 400 kyr. The variations in redox conditions will be more precisely reconstructed through the variations of the Mo and U record (see below).

A.5. The redox conditions

As observed before, the palynofacies analyses, especially the composition of the marine fraction of the organic facies (significant abundance of amorphous organic matter and the presence of well represented animal debris) testify to a rather diversified food chain. The primary production must have fed a zooplankton population, which contributed to lower the organic export to the sediment. This is echoed in the trace elements distribution. The sediment of Core MD 962073 shows small V-, Cu-, Zn-, P-, and Ba-enrichment and some Mn depletion, relative to average deep sea carbonates (Turekian and Wedepohl, 1961). Moreover, contents in these elements do not present any relationship with the total organic content. This lack of correlation may indicate that the organic input to the sediment sustained at best moderate sulfate reduction recorded by the slight V, Cu, and Zn enrichment and Mn depletion (Calvert and Pedersen, 1993; Jones and Manning, 1994; Dean et al., 1997). According to these observations, the sediment was not strongly reducing, if any.

In order to precise the variations of the redox conditions at this site, U and Mo records are compared. According to Crusius et al. (1996), the sediment is U-enriched under suboxic conditions and Mo-enriched under anoxic conditions. The comparison of the U and Mo records, as well as the comparison of the Mo/Al and U/Al records, permits to recognize the transitions between suboxic and anoxic sediments (Martinez, 1996; and references therein). According to Turekian and Wedepohl (1961) deep sea carbonates contain on average 1 to 2 ppm of U and 3 ppm of Mo. In Core MD 962073, U content varies from 2.5 to 5.5 ppm and the Mo content varies from 0.5 to 4 ppm. These data show that the sediment of Core MD 962073 is slightly

enriched in U but not in Mo. The U/Al and Mo/Al records present slightly different variations. As for the U content, the U/Al ratio records a U-enrichment along the core. The Mo/Al ratio indicates that Mo-enrichment has occurred from 250 to 205 ka, and at 110 and 90 ka, i.e. during isotope stages 7 and 5. The enrichment of the sediment in U suggests that suboxic conditions prevailed at this site for the last 250 kyr. The few levels of Mo-enrichment indicates, however, that these suboxic conditions have evolved towards more anoxic environments. Time intervals when these anoxic conditions are observed correspond to isotope stages characterized by high productivity periods (isotope stages 7 and 5). High surface productivity leading to a higher export of organic matter towards the bottom, the decay of this enhanced input of organic matter may increase the oxygen consumption at the water-sediment interface and, thus, be responsible for the short shifting from suboxic to more anoxic conditions. As said before, these slightly suboxic conditions did not seem, however, to influence the Ba, P, Cu, Ni, and Zn record of the surface paleoproductivity.

B. Variations of the Socotra upwelling intensity from 72 ka to Present (Cores MD 962073 and 85682)

Changes in the productivity of the Socotra gyre during this time interval have already been studied through geochemical and biogenic proxies after Core MD 85682, recovered 60 km southwest from the Core MD 962073 site, and 50 m shallower (Ouahdi, 1997a; Vénec-Peyré and Caulet, submitted). Core MD 85682 is 7.16 m long and corresponds to the sediment record of the last 72 kyr. No geochemical data from Core MD 962073 were available for this time interval because this site was studied to provide complementary information on the variations of the upwelling intensity before isotope stage 4. Bulk MAR values are, however, calculated for both sites and will be compared. Micropaleontological data are provided for reconstruction of the variations of the Socotra upwelling.

According to Ouahdi (1997a) high productivity periods were recognized in the Socotra upwelling system (Core MD 85682) from 50 to 40 ka, and during the Holocene, whereas low productivity was recorded during isotope stages 4 (72-59 ka) and 2 (24-12 ka). The high surface productivity intervals were characterized by high TOC, P, bio-Ba, Zn, and V MARs, the last two proxies being related to more reducing conditions, and by a slight increase of the $\delta^{13}C$ in *G.*

sacculifer, indicating that the water column was slightly reducing. The variations of the surface productivity recorded in core MD 85682 correlate with the variations of the bulk MAR recorded in Core MD 962073. In this latter core, the TOC/Al, Si/Al, and Ba/Al ratios present, however, slightly different variations, especially with no high productivity recorded from 50 to 40 ka. Such a difference may be related to the high geographical variability of upwelling systems, where the high productivity areas are constrained to narrow plumes (Abrantes, 1992; Anderson et al., 1992; Smith, 1992).

In Core MD 85682, high productivity periods do not correspond to high URI values, that may be related, at this site, to deep water fertility (Caulet et al., in prep). This assumption would also explain the general lack of correlation between the variations of URI and the geochemical proxies in core MD 962073.

At both sites, the geochemical record seems to be considered as a reliable proxy to reconstruct paleoproductivity changes, whereas URI seems to be related more to deep water fertility than to surface water production. Complementary data are, however, needed before a full explanation can be proposed.

Conclusions

The variations in the intensity of the Socotra upwelling system (NW Indian Ocean) for the last 250 kyr are monitored through both geochemical analyses and associations of radiolarian species. The combination of the independent data sets obtained from both these groups of proxies testifies to an increased activity of the upwelling system during interglacial intervals, especially during the time intervals (240 ka, 210-200 ka, 165, 135, 110, 85, 80 and 40 ka.

Organic matter is, at this site, of two different origins. A non neglectible part is made of terrestrial plant debris, but the other part is of marine origin. The positive correlation between the TOC-enrichment and the Si-enrichment suggests that the marine organic matter accumulated at this site is mostly produced by the siliceous plankton.

The variations of the surface productivity can be monitored a this site through the variations of trace elements: Ba, P, Cu, and Zn. Nevertheless, the results of the sequential leaching procedure indicate that barite represents on average only 31 % of the bulk barium, whereas terrigenous-Ba represents 38 % of the bulk barium. The barium distribution in the

different fractions of the sediment varies, however, from one sample to the other. Such variations may be related to the temporal cycle of the upwelling activity, that leads to an alternation between sediments deposited during active upwelling and sediments deposited while the upwelling is inactive. Consequently, even in a setting dominated by upwelling-induced productivity, barium appears to be a proxy delicate to handle, being still strongly influenced by terrigenous supply. This element cannot, thus, be used alone to monitor the variations of paleoproductivity and must be combined to independent markers.

A comparison of the results from Core MD 962073 with those from Core MD 85682, located less than 60 km southwest from Core MD 962073, shows that, at both sites, the geochemical record may be used to reconstruct the variations of surface paleoproductivity, whereas the upwelling radiolarian index (URI) seems to be related to deep water fertility.

The east-African upwelling system does not function as other upwelling systems, such as offshore Peru, or western Africa. Contrarily to less seasonally constrained upwelling systems, this summer restricted upwelling system induces neither marked organic matter accumulation, nor dysaerobic/anaerobic conditions within the sediment. It induces a slight marine organic matter enrichment (TOC content < 1.79 %, most frequently < 1 %). Redox sensitive trace metals do not explicitly record strongly anaerobic conditions. Data suggests that the organic matter produced in the surface water is almost entirely recycled within the water column. The export production reaching the sea floor is very low and of limited influence upon redox conditions. The system is so "efficient" as to recycle most of the production within the water column.

Acknowledgements

We thank Maurice TAMBY (MNHN) for his technical cooperation during this study. Catherine PIERRE and Jean-François SALIEGES from LODYC provided a much needed help in the oxygen isotope analyses, and François BAUDIN, from Université Pierre et Marie Curie (Jussieu) was helpful for the measurement of the organic carbon.

References

Abrantes, F., 1992. Paleoproductivity oscillations during the last 130 ka along the Portuguese and NW African margins. In: Summerhayes C.P. et al. (Editors), Upwelling systems: Evolution since the early Miocene, Geol. Soc.Spec. Publ., 64: 499-511.

Anderson, D.M., and Prell, W.L., 1991. The coastal upwelling gradient off Oman during the Late Pleistocene. In: Prell W.L. et al. (Editors), Proc. ODP, Sci. Res., 117: 265-276.

Anderson, D.M. and Prell, W.L., 1993. A 300 kyr record of upwelling off Oman during the late Quaternary: evidence of the Asian southwest monsoon. *Paleoceanography*, 8: 193-208.

Anderson, D.M., Brock, J.C., and Prell, W.L., 1992. Physical upwelling processes, upper ocean environment and the sediment record of the southwest monsoon. In: Summerhayes C.P. et al. (Editors), Upwelling systems: Evolution since the early Miocene, Geol. Soc.Spec. Publ., 64: 121-131.

Aplin, A.C., Bishop, A.N., Clayton, C.J., Kearsley, A.T., Mossman, J.R., Patience, R.L., Rees, A.W.G., and Rowland, S.J., 1992 A lamina-scale geochemical and sedimentological study of sediments from the Peru Margin (site 680, ODP Leg 112). In: Summerhayes C.P. et al. (Editors), Upwelling systems: Evolution since the early Miocene, Geol. Soc.Spec. Publ., 64: 131-151.

Berger, W.H., 1968. Radiolarian skeletons: solution at depth. *Science*, 159: 1237-1238.

Bishop, J.K.B., 1988. The barite-opal-organic carbon association in oceanic particulate matter. *Nature*, 332: 341-343.

Brown, O.B., Bruce, J.G., and Evans, R.H., 1980. Evolution of sea surface temperatures in the Somali Basin during the southwest monsoon of 1979. *Science*, 209: 595-597.

Bruce, J.G. and Beatty, W.H., 1985. Some observations of the coalescing of Somali eddies and description of the Socotra eddy. *Oceanol. Acta*, 8: 207-209.

Calvert, S.E. and Pedersen, T.F., 1993. Geochemistry of recent oxic and anoxic sediments: Implications for the geological record. *Mar. Geol.*, 113: 67-88.

Caulet J.P., Vénec-Peyré M.T., Vergnaud-Grazzini C. & Nigrini C. (1992). Variations of South Somalia upwelling during the last 160 kyr: radiolarian and foraminiferal record in core MD 85674. In: Summerhayes C.P. et al. (Editors), Upwelling systems: Evolution since the early Miocene, Geol. Soc.Spec. Publ., 64: 379-389.

Clemens, S.C. and Prell, W.L., 1991. One million year record of summer monsoon winds and continental aridity from the Owen Ridge (site 722) Northwest Arabian Sea. In: Prell W.L. et al. (Editors), Proc. ODP, Sci. Res., 117: 365-368.

Clemens, S., Prell, W.L., Murray, D., Shimmield, G.B., and Weedon, G., 1991. Forcing mechanisms of the Indian Ocean monsoon. *Nature*, 353: 720-725.

Combaz, A., 1980. Les kérogènes vus au microscope. In: B. Durand (Editor), Kerogen. Technip, Paris. 55-111.

Crusius, J., Pedersen, T.F., Calvert, S.E., and Sage, D., 1996. Sedimentary Re and Mo enrichment as tracers of low-oxygen conditions: observations and modeling. EOS 77, AGU Fall Meeting, p. F299.

Dean, W.E., Gardner, J.V. and Piper, D.Z., 1997. Inorganic geochemical indicators of glacial-interglacial changes in productivity and anoxia on the California continental margin. *Geochim. Cosmochim. Acta*, 61 (21): 4507-4518.

Dehairs, F., Chesselet, R. and Jedwab, J., 1980. Discrete suspended particles of barite and barium cycle in the open ocean. *Earth Planet. Sci. Lett.*, 49: 528-550.

Dehairs, F., Lambert, C.E., Chesselet, R. and Risler, N., 1987. The biological production of marine suspended barite and the baryum cycle in the Western Mediterranean Sea. *Biogeochemistry*, 4: 119-139.

Dehairs, F., Stroobants, N. and Goeyens, L., 1991. Suspended barite as tracer of biological activity in the Southern Ocean. *Mar. Chem.*, 35: 399-410.

Diester-Haas, L., Meyer, P.A., and Rothe, P., 1992. The Benguela Current and associated upwelling on the southwest African Margin: a synthesis of the Neogene-Quaternary sedimentary record at DSDP sites 362 and 532. In: Summerhayes C.P. et al. (Editors),

Upwelling systems: Evolution since the early Miocene, Geol. Soc.Spec. Publ., 64: 331-343.

Düing W., Molinari R.L. and Swallow J.C., 1980: Somali Current. *Science*, 209: 588-590.

Fieux, M., 1987. Océan Indien et mousson. ICO 14th session, UNESCO, PARIS, 11 pp.

Fieux, M., Schott, F., and Swallow, J.C., 1986. Deep boundary current in the Western Indian Ocean revisited. *Deep Sea Res.*, 33: 415-426.

Hays, J.D., and Scakleton, N.J., 1976. Globally synchronous extinction of the radiolarian *Stylatractus universus*. *Geology*, 4: 649-652.

Hermelin, J.O.R., and Shimmield, G.B., 1995. Impact of productivity events on benthic foraminiferal fauna in the Arabian Sea over the last150,000 years. *Paleoceanography*, 10: 85-116.

Jacot Des Combes, H., Caulet, J.P., and Tribovillard N.P. Pelagic productivity changes in the equatorial area of the NW Indian Ocean during the last 400 kyr. *Mar. Geol.*, in press.

Jacot Des Combes, H., Tribovillard N.P., and Caulet, J.P. Paleoproductivity and paleoceanography changes in the Amirante Passage area (Equatorial Indian Ocean): 200 kyr of lower pelagic productivity. *Bull Soc. Geol. Fr.*, accepted.

Jacot Des Combes, H., Caulet, J.P., and Tribovillard N.P. Geochemical approach of the regional diversity of the sedimentary processes in the NW Indian Ocean since the Middle Pleistocene: A synthesis. Submitted to Mar. Chem.

Johnson, D.A., Schneider, D.A., Nigrini, C.A., Caulet, J.P. and Kent, D.V., 1989. Pliocene-Pleistocene radiolarians events and magnetostratigraphic calibrations for the tropical Indian Ocean. *Mar. Micropal.*, 14: 33-66.

Johnson, T.C., 1974. The dissolution of siliceous microfossils in surface sediments of the eastern tropical Pacific. *Deep Sea Res.*, 21: 851-864.

Johnson, T.C., 1976. Biogenic opal preservation in pelagic sediments of a small area in the eastern tropical Pacific. *Geol. Soc. Amer. Bull.*, 87: 1273-1282.

Jones, B., and Manning, D.A.C., 1994. Comparison of geochemical indices used for the interpretation of paleoredox conditions in ancient mudstones. *Chem. Geol.*, 114: 111-129.

Lyle, M., Heath, G.R. and Robbins, J.M., 1984. Transport and release of transition elements during early diagenesis: Sequential leaching from MANOP sites M and H. Part I: pH 5 acetic acid leach. *Geochim. Cosmochim. Acta*, 48: 1705-1715.

Martinez, P. 1997. Paléoproductivités du système d'upwellings nord-ouest africain et variations climatiques au cours du Quaternaire terminal. Ph.D thesis, Université de Bordeaux I, 298 pp.

Meyers, P.A., 1992. Organic matter variations in sediments from DSDP sites 362 and 532: evidence of upwelling changes in the Benguela Current upwelling system. In: Summerhayes C.P. et al. (Editors), Upwelling systems: Evolution since the early Miocene, Geol. Soc.Spec. Publ., 64: 323-331.

Murray, D.W. and Prell, W.L., 1991. Pliocene to Pleistocene variations in calcium carbonate, organic carbon, and opal on the Owen Ridge, Northern Arabian Sea. In: Prell W.L. et al. (Editors), Proc. ODP, Sci. Res., 117: 343-365.

Murray, D.W. and Prell, W.L., 1992. Pliocene and Pleistocene climatic oscillation and monsoon upwelling recorded in sediments from the Owen Ridge, Northwestern Arabian sea. In: C.P. Summerhayes et al. (Editors), Upwelling systems: Evolution since the Early Miocene, Geol. Soc. Spec. Publ., 64: 301-321.

Noël, D.,Busson, G., Cornée, A., and Mangin, A.-M., 1993. Les coccolithophoridées fossiles ne peuvent plus être considérés comme caractéristiques du seul environnement pélagique. *Bull. Soc. Géol. Fr.*, 164: 493-502.

Ouahdi, R., 1997a. Variations de la productivité au nord-ouest de l'océan Indien lors des derniers 70 000 ans dans l'upwelling de Socotra et de Somalie: Enregistrements géochimiques. *Bull. Soc. Géol. Fr.*, 168: 93-107.

Ouahdi, R., 1997b. Paléocéanographie et paléoproductivité liées à la mousson indienne dans le bassin de Somalie, le golfe d'Aden et la mer Rouge durant les derniers 460 000 ans. PhD Thesis, Mus. Ntal. Hist. Nat. 165 pp.

Quadfasel, D.R., and Schott, F., 1982. Water-mass distribution at intermediate layers off the Somali coast during the onset of the southwest monsoon 1979. *J. Phys. Ocean.*, 7: 1358-1372.

Robbins, J.M., Lyle, M. and Heath, G.R., 1984. A sequential extraction procedure for partitioning elements among co-existing phases in marine sediments. Rep. College Oceanography, Oregon State Univ. 45p.

Sanfilippo A., Westberg-Smith M.J. & Riedel W.R., 1985. Cenozoic Radiolaria. *In.* Bolli H.M. et al., Eds., Plankton stratigraphy, Cambridge Univ. Press, 631-712.

Schott, F., and Quadfasel, D.R., 1982. Variability of the Somali current system during the onset of the southwest monsoon 1979. *J. Phys. Ocean.*, 12: 1940-1943.

Schrader, H. 1992. Peruvian coastal primary paleo-productivity during the last 200 000 years. In: Summerhayes C.P. et al. (Editors), Upwelling systems: Evolution since the early Miocene, Geol. Soc. Spec. Publ., 64: 391-411.

Schrader, H., and Sorknes, R., 1991. Peruvian coastal upwelling: Late Quaternary productivity changes revealed by diatoms. *Mar. Geol.*, 97: 233-249.

Schuette, G., and Schrader, H., 1979. Diatom taphocoenoses in the coastal upwelling area off Western South America. *Nova Hedwigia, Beihefte*, 64: 359-378

Schuette, G., and Schrader, H., 1981a. Diatoms in surface sediments: A reflection of coastal upwelling. American Geophysical Union. Washington: 372-380.

Shackleton, N.J., Hall, M.A., Pate, D., Meynadier, L. and Valet, J.-P., 1993. High resolution stable isotope stratigraphy from bulk sediment. *Paleoceanography*, 8: 141-148.

Shimmield, G.B., 1992. Can sediment geochemistry record changes in coastal upwelling paleoproductivity? Evidence from Northwest Africa and the Arabian Sea. In: C.P. Summerhayes et al. (Editors), Upwelling systems: Evolution since the Early Miocene, Geol. Soc. Spec. Publ., 64: 9-46.

Shimmield, G.B. and Mowbrays, R., 1991. The inorganic geochemical record of Northwestern Arabian Sea: A history of productivity variation over the last 4,000 ky from sites 722A and 724. In: Prell W.L. et al. (Editors), Proc. ODP, Sci. Res., 117: 409-429.

Smith, R.L., 1992. Coastal upwelling in the modern ocean. In: Summerhayes C.P. et al. (Editors), Upwelling systems: Evolution since the early Miocene, Geol. Soc.Spec. Publ., 64: 9-29.

Smith, S.L., and Codispoti, L.A., 1980. Southwest monsoon of 1979: chemical and biological response of Somali coastal waters. *Science*, 209: 597-599.

Swallow, J.C., 1980. The Indian Ocean Experiment: Introduction. *Science*, 209: 588-589.

Swallow, J.C. and Bruce, J.G., 1966. Current measurements off the Somali coast during the southwest monsoon of 1964. *Deep-Sea Res.*, 13: 861-888.

Tribovillard, N.P., Rivière, M., Ouahdi, R., Lallier-vergès, E., and Caulet, J.P., 1994a. L'absence d'un enrichissement marqué en matière organique dans des sédiments déposés en contexte d'upwelling: le courant de somalie. *Bull. Soc. Geol. Fr.*, 165: 65-75.

Tribovillard, N.P., Caulet, J.P., Vergnaud-Grazzini, C., Moureau, N. and Tremblay, P., 1996. Lack of organic matter accumulation on the upwelling-influenced Somalia margin in a glacial-interglacial transition. *Mar. Geol.*, 133: 157-182.

Turekian, K.K. and Wedepohl, K.H., 1961. Distribution of the elements in some major units of the Earth's crust. *Geol. Soc. Am. Bull.*, 72: 175-191.

Tyson, R.V., 1995. Sedimentary organic matter, organic facies and palynofacies. Chapman and Hall, London. 615 pp.

Vénec-Peyré, M.T., Caulet, J.P. and Vergnaud-Grazzini, C., 1995. Paleohydrographic changes in the Somali Basin (5°N upwelling and equatorial areas) during the last 160 kyr, based on correspondence analysis of foraminiferal and radiolarians assemblages. *Paleoceanography*, 10: 473-491.

Vénec-Peyré, M.T., Caulet, J.P. and Vergnaud-Grazzini, C., 1997. Glacial-interglacial changes in the equatorial part of the Somali Basin (NW Indian Ocean) during the last 355 ky. *Paleoceanography*, 12: 640-649.

Vénec-Peyré, M.T., and Caulet, J.P. Paleoproductivity changes during the last 72,000 years in the upwelling system of Socotra (Somali Basin, N.W. Indian Ocean): Biological signatures. Submitted to Mar. Micropal.

Vergnaud-Grazzini, C., Caulet, J.P., and Vénec-Peyré, M.T., 1995. Late Quaternary evolution of fertility indicators and monsoon in the Somalian Basin, Northwestern Indian Ocean. *Bull. Soc. Geol. Fr.*, 166: 259-270.

Warren, B.A., Stommel, H. and Swallow, J.C., 1966. Water masses and patterns of flow in the Somali Basin during the southwest monsoon of 1964. *Deep-Sea Res.*, 28: 825-860.

Weedon, G.P. and Shimmield, G.B., 1991. Late pleistocene upwelling and productivity variations in the Northwestern Indian Ocean deduced from spectral analyses of geochemical data from sites 722 and 724. In W.L. Prell et al. (Editors), Proc. ODP, Sci. Res., 117: 431-440.

White, L.D., Garrison, R.E., and Barron, J.A., 1992. Miocene intensification of upwelling along the California margin as recorded in siliceous facies of the Monterey Formation and

offshore DSDP sites. In: Summerhayes C.P. et al. (Editors), Upwelling systems: Evolution since the early Miocene, Geol. Soc. Spec. Publ., 64: 429-443.

Zahn, R. and Pedersen, T.F., 1991. Late Pleistocene evolution of surface and mid-depth hydrography at the Oman Margin: planktonic and benthic isotope records. In: Prell W.L. et al. (Editors), Proc. ODP, Sci. Res., 117: 291-308.

3° PARTIE
SYNTHÈSE DE L'ENREGISTREMENT GÉOCHIMIQUE DANS DES SÉDIMENTS RÉCENTS DE L'OCÉAN INDIEN OCCIDENTAL

Les résultats présentés dans les chapitre précédents indiquent que l'enregistrement géochimique peut être un marqueur utisable lors des reconstructions des variations des conditions paléocéanographiques ou de la paléoproductivité dans un certain nombre de sites de l'Océan Indien du nord-ouest. Cet enregistrement varie cependant d'un site à l'autre et des différences importantes peuvent apparaître entre deux sites *a priori* similaires. La question qui se pose maintenant est de savoir si l'enregistrement géochimique stocké dans le sédiment peut permettre de séparer les sites en groupes et de vérifier si ces "groupes géochimiques" correspondent à des "groupes océanographiques" (domaine pélagique, systèmes d'upwelling, ou zones côtières). Afin de réaliser une synthèse à l'échelle régionale, les nouvelles données obtenues dans ce travail sont comparées à des résultats provenant d'autres sites et publiés dans des études antérieures.

Les marqueurs géochimiques (bulk MAR, teneurs en $CaCO_3$ et COT, rapports COT/Al, Si/Al, Fe/Al, K/Al, Mg/Al, Ba/Al, P/Al, Cu/Al, Ni/Al, Zn/Al, Mn/Al, V/Al, Ti/Al, et Mg/Ca) sont étudiés et comparés dans dix sites de l'océan Indien occidental, situés depuis la ceinture équatoriale jusqu'au golfe d'Aden et la mer d'Arabie. Une telle comparaison implique un grand nombre de données. Afin de faciliter la présentation de ces données, les marqueurs géochimiques ont été divisés en deux groupes. Les marqueurs dits "directs" (bulk MAR, teneurs en $CaCO_3$ et COT, rapports COT/Al, Si/Al, et Ti/Al) dont les variations traduisent directement celles des principaux facteurs intervenant dans la sédimentation : taux d'accumulation, source et nature du matériel sédimentaire (biogène, terrigène). Les marqueurs dits "indirects" sont ceux dont les variations peuvent être contrôlées par plusieurs facteurs. Les messages des marqueurs directs seront comparés entre eux, afin de préciser leur origine et leur signification, puis l'enregistrement des marqueurs indirects sera interprété en fonction du message des marqueurs directs. La séparation des sites en "familles" va s'effectuer selon deux méthodes. La première est la détermination pour les marqueurs géochimiques de valeurs seuil distinguant les différents groupes de sites. Cette méthode s'appuie sur la comparaison des valeurs minimales, moyennes et

maximales de chaque marqueur à chaque site, qui fournit une comparaison à l'échelle régionale. Le second moyen de séparer les sites est la détermination de comportements chimiques particuliers caractérisant chaque famille de sites, et notamment la détermination de relations existant éventuellement entre des marqueurs au sein de chaque site. A chaque site, les variations des marqueurs indirects seront comparées aux variations des marqueurs directs, on parlera alors d'échelle locale.

Les résultats obtenus lors de cette synthèse montrent que certains marqueurs géochimiques présentent, à l'échelle régionale et/ou locale des enregistrements particuliers, permettant de classer les sites dans des familles. Le rapport Mg/Al permet de séparer sans ambiguïté les sites en deux familles. L'étude des autres marqueurs géochimiques dans chacun de ces groupes permet de déterminer que la famille ayant le plus fort rapport Mg/Al est composé de sites où la production de surface est le principal facteur contrôlant la sédimentation alors que l'autre famille, avec un faible rapport Mg/Al, comprend les sites où les apports terrigènes perturbent le message venant de la surface. De même, l'enrichissement du sédiment en phosphore (rapport P/Al) est significativement plus élevé dans les sites où le message sédimentaire induit par la productivité de surface est dominant par rapport à celui lié aux apports terrigènes. Les rapports Si/Al et COT/Al permettent de séparer les sites localisés sous un upwelling, où la productivité de surface est élevée et majoritairement due au plancton siliceux, des autres où la productivité est plus faible et est surtout liée au plancton carbonaté. Le rapport Mg/Ca permet également de séparer les sites en deux familles, celle fortement influencée par les apports terrigènes, spécialement issus des rivières et du lessivage des continents, et celle plutôt influencée par la productivité de surface, où les apports terrigènes sont principalement éoliens. Les autre marqueurs géochimiques, qu'ils soient directs ou indirects, ne permettent pas de séparations aussi nettes entre les sites, que ce soit par l'intermédiaire des valeurs seuil ou des associations entre marqueurs. On observe généralement une transition entre les sites à l'échelle régionale. C'est, par exemple, le cas lorque l'on compare les teneurs en $CaCO_3$ et en COT.

Cette transition générale permet toutefois d'isoler certains sites dont la réponse géochimique s'écarte de la tendance générale. C'est le cas du site localisé dans le passage des Amirantes (entre Madagascar et les Seychelles), caractérisé par un matériel terrigène différent de celui des autres sites (associant Ti, Ba, Cu, Ni, Mn, et V), probablement issu des bassins situés au sud de Madagascar. De la même façon, le site du golfe d'Aden se caractérise par de fortes teneurs en Mn et en V, issus de l'activité hydrothermale de la mer Rouge alors que les deux sites

localisés en mer d'Arabie présentent une teneur en quartz plus élevée que les autres sites, probablement originaires de la péninsule Arabique. Le message géochimique permet donc, dans cette région de l'Océan Indien occidental, de préciser les sources du matériel sédimentaire et de mettre en évidence les particularités de chaque site.

Geochemical approach of the regional diversity of the sedimentary processes in the NW Indian Ocean since the Middle Pleistocene: A synthesis

Hélène Jacot Des Combes (1 & 2), Nicolas Tribovillard (1), and Jean Pierre Caulet (2)

(1): Laboratoire de Sédimentologie et Géodynamique, URA CNRS 719, Université de Lille I, 59655 VILLENEUVE D'ASCQ (FRANCE).

(2): ESA 7073, Laboratoire de Géologie, MNHN, 43 rue Buffon 75005 PARIS (FRANCE).

En préparation pour soumission à Marine Chemistry

Introduction

The inorganic geochemical record of the oceanic sediments is commonly used to reconstruct paleoceanographic and paleoclimatic variations. Major, minor, and trace elements such as Si, Al, Fe, Mg, K, Ba, Mn, V, Ni, Cu, Ti, and Zn, are considered as markers of both deposition and accumulation patterns (e.g. Brumsack, 1980; 1983; 1986; Collier and Edmond, 1984; Shimmield and Mowbray, 1991; Dymond et al., 1992; 1997; Calvert and Pedersen, 1993; Gingele and Dahmke, 1994; Paytan and Kastner, 1996; Dean et al., 1997; Jacot Des Combes et al., in press; accepted). Aluminum, Fe, K, Mg, and Ti, mostly linked with terrigenous debris such as quartz, feldspars and clay minerals, are useful for characterizing the lithogenic fraction in pelagic sediments. Manganese, V, Cu, Ni, and Zn are known to be strongly dependent on changes in redox conditions within the sediment. Barium, and, to a lesser degree Cu, Ni, and Zn, are related to biogenic activity, but they can also depend on diagenesis through changes in redox conditions (Calvert and Pedersen, 1993). Copper, Ni and Zn are also known to be easily linked with organic matter through metal-organic complexes (Jones and Manning, 1994; Dean et al., 1997). Analyses of changes in oceanic paleoproductivity are based on the good correlation observed between the contents in some trace metals, especially barium, and the total organic carbon (TOC) in the material recovered from some sediment traps and the sediments from piston cores (Goldberg and Arrhenius, 1958; Dymond et al., 1992; Shimmield, 1992; Von Breymann et al., 1992; De Lange et al., 1994). Due to its low solubility, barium is generally considered as a reliable paleoproductivity proxy when present as barite (Shimmield and Mowbray, 1991; Dymond et al., 1992; Shimmield, 1992; Gingele and Dahmke, 1994; Shimmield et al., 1994; Francois et al., 1995; Paytan and Kastner, 1996). Formation of barite in living organisms, or in microenvironments of decaying organic matter through local sulfate oversaturation, suggests that the biogenic barium content can be used as an indicator of surface biologic productivity (Goldberg and Arrhenius, 1958; Stroobants et al., 1991; Dymond et al., 1992; Von Breymann et al., 1992; Gingele and Dahmke, 1994). Such a process is supposed to occur preferentially within siliceous-organism debris, such as diatoms and, possibly, radiolarians (Dehairs et al., 1980; 1987; 1991; Bishop, 1988). Barium can also be remobilized under strongly reducing conditions, as sulfate reduction may dissolve barite (Thomson et al., 1993; 1995; De Lange et al., 1994; Van Santvoort et al. 1996), and be present in the lithogenic fraction, mostly within feldspar. The correct interpretation of the message carried by the barium implies the knowledge of the

distribution of Ba within the different fractions of the sediment. The sequential leaching protocol established by Lyle et al. (1984) permits to identify the various Ba-carrier phases of the sediment: bio-Ba (present as barite), lithogenic-Ba and the Ba more or less tightly linked with oxy-hydroxides and carbonates. Moreover, the complementary study of trace metals, that are sensitive to changes in redox conditions, helps to distinguish the diagenetic barite from the biogenic one. However, such a protocol is long and difficult to generalize to every sample at every site. Data obtained through this protocol from previous studies will, thus, be used as complementary information.

The method of reconstruction of the paleoproductivity changes through the geochemical record was applied to samples from ten cores recovered in the equatorial western Indian Ocean, particularly in the pelagic domain (Jacot Des Combes et al., in press; Jacot Des Combes et al., accepted). The results obtained for these three cores studied in this realm indicate that the geochemical record is not homogeneous through the equatorial belt. Two major differences are observed. First, the enrichment of the sediment in trace metals (such as Ba, Cu, and Ni), is related to different processes: on the Madingley Rise (Core MD 90940), this enrichment varies with the surface productivity, whereas in the Amirante Passage (Core MD 90929), high contents of these trace metals correlate with the enrichment of the sediment in Ti. Then, the barium distribution within the different fractions of the sediment strongly differs from one site to the other, and may be related to different processes and different sources. These unexpected results seem to indicate that the pelagic region of the western Indian Ocean cannot be considered as an homogenous domain. In order to precise the message carried by the geochemical proxies in this region of the Indian Ocean, our data from three sites in the pelagic realm of the equatorial western Indian Ocean are compared to published data of the same order from other sites located in the western Indian Ocean (Jacot Des Combes et al., in press; Jacot Des Combes et al., accepted).

The goal of this paper is to use geochemical proxies, and particularly the trace element record (Ba, Cu, Mn, Ni, Ti, V, and Zn) to determine the main processes controlling the sedimentation at different sites from the pelagic environments, and undergoing contrasted influences: true pelagic conditions, enhanced productivity conditions, lithogenic supply influence. Is the major and trace metal distribution consistent within each of the three studied environments, and does its record mark differences between the three environments? Two potential ways of classification will be used in this paper. First, a comparison of the mean,

minimum and maximum values of selected proxies at a regional scale will help to determine threshold values that separate groups of sites. Then, a comparison of the variations of the same proxies at the individual site scale will help to recognize a characteristic behavior of these proxies for each group of sites corresponding to the three types of oceanic environments of the western Indian Ocean. To achieve this goal, results from previous studies realized on sediments from ten cores recovered in the Gulf of Aden and the northwestern Indian Ocean, from its northern limit to its equatorial belt are compared to previously published data (Clemens and Prell, 1991; Murray and Prell, 1991; Shimmield and Mowbray, 1991; Zahn and Pedersen, 1991; Tribovillard et al., 1996; Ouahdi, 1997a, b). The inorganic geochemical records from each site are compared, with a special focus on barium, to establish a model of the inorganic geochemical response to Pleistocene changes in the paleoproductivity and paleoceanography patterns within this region.

Material and methods

The ten sites used in this comparison were recovered in the Gulf of Aden and the northwestern Indian Ocean, between 19°N and 6°S. The location of the sites is shown in Fig. 1 and the precise coordinates of each site are given in Table 1. The piston cores were recovered mostly during several oceanographic cruises of the R/V "*Marion Dufresne*" (Caulet et al., 1992), and sites 722 and 724 were drilled during ODP Leg 117 (Prell et al., 1989) (Table 1).

Piston Core and ODP Site	Abridged number (on figures)	Latitude (°N)	Longitude (°E)	Depth (m)	Age interval (ka)	Mission or leg
MD 85664	**664**	0.036	43.128	744		MD 44-INDUSOM
MD 85668	**668**	-0.010	46.023	4020	0 - 356	MD 44-INDUSOM
MD 85674	**674**	3.112	50.236	4875	109 - 161	MD 44-INDUSOM
MD 85682	**682**	10.535	52.235	3092	0 - 73	MD 44-INDUSOM
MD 90929	**929**	-6.590	52.030	3071	0 - 479	MD 64-SOMIRMAS
MD 90940	**940**	-5.335	61.401	3875	0 - 381	MD 65-SEYMAMA-SHIVA
MD 921002	**1002**	12.022	44.317	1327	0 - 17	MD 73-RED SED
MD 962073	**2073**	10.936	52.616	3142	31 - 248	MD 104-MOZAPHARE-PEGASOM
ODP site 722	**722**	16.626	59.760	2028	6 - 502	ODP Leg 117
ODP site 724	**724**	18.462	57.786	593	6 - 355	ODP Leg 117

Table 1: Location, recovering depth, time interval considered, and name of the recovering cruise of the ten studied sites.

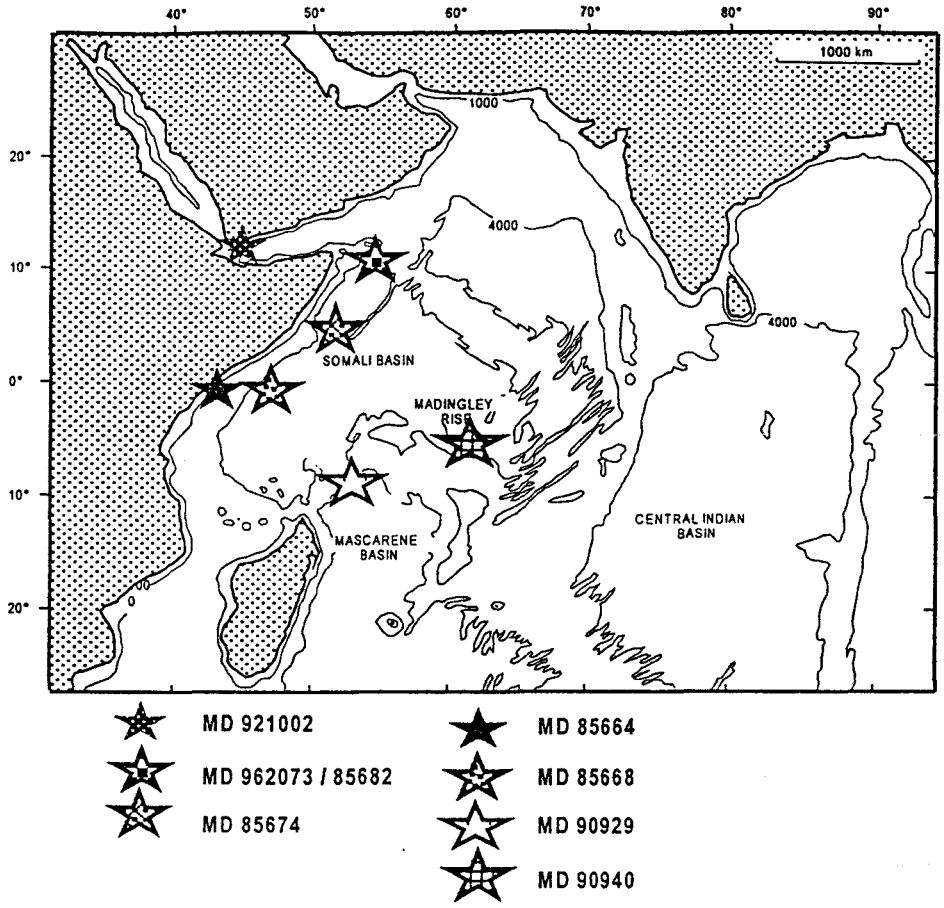

Figure 1: Location map indicating the location of the studied sites.

The sediment samples from cores MD 962073 (Jacot Des Combes et al., submitted), MD 90929 (Jacot Des Combes et al., accepted), MD 90940 (Jacot Des Combes et al., in press), MD 85664, MD 85668, and MD 85674 (Tribovillard et al., 1996), MD 85682 and MD 921002 (Ouahdi, 1997a, b), were analyzed following the same protocol.

The age model was established upon the $\delta^{18}O$ isotope record measured either on bulk sediment in Cores MD 90929 90940, and 962073 (Jacot Des Combes et al., in press; Jacot Des Combes et al., accepted; Jacot Des Combes et al., submitted), or on *G. ruber* and *G. sacculifer* in Cores MD 85668 and MD 85674 (Vénec-Peyré et al., 1995); and on *G. ruber* in Cores MD 85682 and MD 921002 (Ouahdi, 1997a and b).

Carbonate content was measured with a Bernard calcimeter. The amount of major and significant trace elements (Ba, Cu, Mn, Ni, Ti, V, and Zn) was analyzed in the following way: 100 mg of bulk sediment were dried at 105°C for 24 hours and thoroughly ground in an agate mortar mill prior to a $HClO_4$, HNO_3, and HF acid digestion. The final residue was taken up in 1M HCl. The trace elements were measured with an ICP-spectrometer (ICP-OES or ICP-MS).

The analytical precision and accuracy of the results were both found to be equal to, or better than, 5-10 % according to the abundance of the elements. Data were checked by comparison with international standards and with the help of replicate samples. The relative enrichment in the studied elements compared to the terrigenous fraction is estimated through Al-normalization (element/Al ratio).

Total Organic Carbon (TOC) content was measured on bulk sediment through LECO analyses for cores MD 85674, MD 85682, MD 921002 (Ouahdi, 1997a, b), MD 90929 (Jacot Des Combes et al., accepted), and MD 962073; and through Rock-Eval pyrolysis for cores MD 85664, MD 85668, MD 85674 (Tribovillard et al., 1996), and Core MD 90940 (Jacot Des Combes et al., in press). An intercalibration of both apparatus has been performed.

Bulk sediment mass accumulation rates (MAR) were calculated, for all piston cores with available data, by multiplying the linear sedimentation rate (LSR) derived from the isotopic age model by the dry bulk density (DBD). The DBD was obtained by the ratio: g dry weight / cm^3 wet volume. Element fluxes were next calculated from the formula:

$$\text{Flux} = \text{element concentration (ppm)} \times \text{MAR} \times 10^{-6}.$$

At ODP sites 722 and 724, major and trace element contents were measured through XRF analyses (Shimmield and Mowbray, 1991). The age model of Site 722 was established upon the *G. sacculifer* isotope record, and the bulk MAR is obtained following the same way as described above (Clemens and Prell, 1991). At site 724, the age model was obtained by multiplying the DBD with the LSR resulting from the isotope record of *Cibicidoides spp* (Zahn and Pedersen, 1991). In both cases, TOC was measured by a CNS analyzer (Murray and Prell, 1991; Zahn and Pedersen, 1991). In both sites, however, the bulk MAR and the TOC content were not determined at the same depth-levels than the geochemical proxies. A cross analysis of data from these sites with piston core data is, thus, impossible, and the values of drilling sites proxies are given for general comparison.

The comparison of the geochemical records from ten the sites provides an extended database. In order to make these data intelligible, the mean value of each geochemical proxies was classically calculated for each site, and minimum and maximum values of these proxies were retrieved from the published database. The comparison of the mean, minimum and maximum values of each proxy was preferred to a statistical calculation of the standard deviation, because of differences in the sampling step and number of studied samples, throughout the sites. Another difficulty raised by such a comparison is the fact that each site was

originally studied with a precise purpose. This leads to a difference between the proxies used at each site, and to the occurrence of "missing data" in the regional synthesis. The mean, minimum and maximum values of each proxy are given for each site in Tables 2 and 3, and are illustrated by figures 2 and 3.

Core number	CaCO3 (%)			COT (%)			COT/Al			Si/Al			Ti/Al (x10^4)			Bulk MAR (g/cm2/kyr)		
	min	mean	max	min	mean	max	min	mean	max	min	mean	max	min	mean	max	min	mean	max
ODP site 724 (1)	30.38	51.63	70.68	0.32	0.99	3.85	-	-	-	4.36	4.87	6.21	772.2	820.1	1060.2	3.66	12.79	22.93
MD 85664 (2)	21.83	54.43	79.94	0.80	1.01	1.30	0.11	0.16	0.21	2.33	2.62	2.99	600.0	951.0	1300.0	-	-	-
MD 921002 (3)	37.00	51.81	62.80	0.03	1.54	2.93	0.01	0.62	1.22	-	-	-	500.0	976.0	1600.0	-	-	-
ODP site 722 (4)	53.50	68.70	82.35	0.40	0.82	1.73	-	-	-	3.68	3.96	5.25	631.4	699.8	812.7	1.67	4.42	7.89
MD 90929 (5)	58.20	74.20	84.70	0.00	0.00	0.00	-	-	-	3.1	3.56	5.29	416.0	1660.0	4833.0	0.22	1.31	3.39
MD 85682 (6)	54.00	66.56	76.00	0.54	0.91	1.19	0.30	0.75	1.37	3.56	5.46	10.25	-	-	-	4.00	6.60	10.80
MD 962073	59.80	71.90	90.25	0.19	0.76	1.79	0.20	0.67	1.38	3.767	5.54	11.95	529.9	611.6	704.0	-	-	-
MD 90940 (7)	61.80	79.90	84.60	0.00	0.00	0.00	-	-	-	-	-	-	520.8	616.2	703.3	0.40	1.47	3.74
MD 85668 (8)	47.50	68.77	88.48	0.16	0.28	0.39	0.03	0.10	0.21	2.6	3.03	4.1	540.0	753.0	1200.0	2.23	3.62	6.31
MD 85674 (9)	3.81	37.15	70.03	0.10	0.65	1.21	0.04	0.11	0.21	2.89	3.25	4.06	-	796.0	1000.0	2.08	3.93	8.25

(1): calculated from data published by Zahn and Pedersen, 1991, (Appendix A and B); and Shimmield and Mowbray, 1991, (Appendix B).

(2): calculated from data published by Tribovillard et al., 1996, (Table 1).

(3): calculated from data published by Ouahdi, 1997b, (Annexes II).

(4): calculated from data published by Murray and Prell, 1991, (Appendix); Clemens and Prell, 1991, (Table 1, pp 368-369); and Shimmield and Mowbray, 1991, (Appendix A).

(5): calculated from data published by Jacot Des Combes et al., accepted, (Tables 2-4).

(6): calculated from data published by Ouahdi, 1997a, (tables1-2); and Ouahdi, 1997b, (Annexes II).

(7): calculated from data published by Jacot Des Combes et al., in press, (Tables 2-4).

(8): calculated from data published by Tribovillard et al., 1996, (Table 2).

(9): calculated from data published by Tribovillard et al., 1996, (Table 3).

Table 2: Minimum, mean, and maximum values of the "direct proxies": $CaCO_3$, TOC, TOC/Al, Si/Al, Ti/Al, and bulk MAR in the studied sites.
- : no data available.

The geochemical markers may be separated into two groups. The first group is made of six proxies ($CaCO_3$ and TOC contents, bulk MAR values, and TOC/Al, Ti/Al and Si/Al ratio values), whose variations may be directly related to variations of one of the major sedimentary processes. Carbonates being the main component of the sediments, the variations of the carbonate content can be linked either to surface productivity or to carbonate dissolution. Variations in the carbonate content will, thus, influence the sedimentation processes, either through the accumulation rate, or through the composition of the sediment. The TOC content should allow to separate the sites with significant organic matter production and/or preservation from the other sites, e.g. the pelagic sites where the TOC content may be neglectible. The accumulation of organic matter is also known to influence the redox conditions. Variations in

bulk MAR will be used to separate the sites, with low values that are characteristic of pelagic conditions. The sedimentation rate can also have an influence on the redox conditions. The Ti/Al ratio is known to be an indicator of wind strength in such pelagic environments (Weedon and Shimmield, 1991; Shimmield, 1992; Martinez, 1997; and references therein), and will, thus, be used as a terrigenous input proxy. The Si/Al ratio can also indicate the enrichment of the sediment in opal and/or in quartz, relative to alumino-silicates.

Core number	Fe/Al			K/Al			Mg/Al			Mg/Ca (x10^4)			Ba/Al (x10^4)			P/Al (x10^4)		
	min	mean	max	min	mean	max	min	mean	max	min	mean	max	min	mean	max	min	mean	max
ODP site 724 (1)	0.42	0.52	0.65	0.26	0.28	0.35	0.45	0.71	0.89	343.1	1011.8	2271.6	-	-	-	174.6	454.3	3484.1
MD 85664 (2)	0.68	0.81	0.98	0.19	0.26	0.39	0.27	0.31	0.37	600.0	1028.0	1700.0	28.0	42.8	55.0	87.7	106.4	133.2
MD 921002 (3)	0.51	0.75	0.88	-	-	-	-	-	-	670.0	923.4	1280.0	160.0	353.1	550.0	-	-	-
ODP site 722 (4)	0.56	0.63	1.64	-	-	-	-	-	-	-	-	-	64.2	204.3	719.2	150.8	237.3	402.6
MD 90929 (5)	0.54	0.62	1.32	0.15	0.18	0.22	0.23	0.33	0.47	124.8	190.2	332.9	582.0	1812.0	5082.0	-	-	-
MD 85682 (6)	0.33	0.54	1.06	0.25	0.35	0.56	0.46	0.63	1.07	167.9	301.6	513.9	163.3	429.8	769.9	214.5	385.9	715.1
MD 962073	0.54	0.61	0.70	0.24	0.26	0.29	0.53	0.68	0.88	160.6	295.0	557.2	138.9	447.8	818.2	342.7	661.4	1038.0
MD 90940 (7)	0.72	0.80	0.96	0.42	0.45	0.48	0.46	0.56	0.81	100.0	139.1	230.0	1230.0	1737.0	2266.0	277.8	429.8	1288.0
MD 85668 (8)	0.38	0.63	0.88	0.20	0.29	0.36	0.12	0.25	0.35	100.0	287.2	590.0	137.5	199.9	274.1	72.3	137.3	278.4
MD 85674 (9)	0.42	0.66	0.87	0.26	0.28	0.33	0.29	0.33	0.43	358.2	2800.0	16735.0	11.9	165.3	238.9	92.0	118.8	192.5

Core number	Mn/Al (x10^4)			V/Al (x10^4)			Cu/Al (x10^4)			Ni/Al (x10^4)			Zn/Al (x10^4)		
	min	mean	max	min	mean	max	min	mean	max	min	mean	max	min	mean	max
ODP site 724 (1)	94.8	124.2	218.6	-	-	-	-	-	-	-	-	-	-	-	-
MD 85664 (2)	33.6	56.4	74.8	11.13	14.84	19.58	2.58	3.84	4.94	-	-	-	6.20	10.47	14.11
MD 921002 (3)	600.0	1020.0	2900.0	110.00	230.00	360.00	-	-	-	-	-	-	-	-	-
ODP site 722 (4)	93.4	127.7	215.7	18.52	25.36	36.90	6.67	11.45	22.50	17.72	25.50	32.42	14.67	19.93	33.16
MD 90929 (5)	140.2	503.3	1439.0	12.32	44.44	126.70	24.30	102.50	299.40	31.50	72.22	142.80	16.93	56.46	125.80
MD 85682 (6)	-	-	-	26.09	32.60	44.23	5.59	18.22	30.00	-	-	-	18.84	30.21	43.27
MD 962073	92.4	145.5	210.5	24.69	33.96	57.73	20.73	34.00	48.85	14.23	28.19	42.20	23.86	32.04	43.74
MD 90940 (7)	138.3	687.0	2008.0	14.80	18.80	23.20	35.80	55.50	92.90	17.50	28.10	63.60	-	-	-
MD 85668 (8)	50.4	90.0	219.4	8.42	16.86	29.33	11.14	15.68	25.02	6.99	11.73	21.84	-	-	-
MD 85674 (9)	28.0	152.8	370.4	18.78	26.87	40.61	3.95	16.51	22.46	-	-	-	8.90	25.41	35.82

(1): calculated from data published by Zahn and Pedersen, 1991, (Appendix A and B); and Shimmield and Mowbray, 1991, (Appendix B).

(2): calculated from data published by Tribovillard et al., 1996, (Table 1).

(3): calculated from data published by Ouahdi, 1997b, (Annexes II).

(4): calculated from data published by Murray and Prell, 1991, (Appendix); Clemens and Prell, 1991, (Table 1, pp 368-369); and Shimmield and Mowbray, 1991, (Appendix A).

(5): calculated from data published by Jacot Des Combes et al., accepted, (Tables 2-4).

(6): calculated from data published by Ouahdi, 1997a, (tables1-2); and Ouahdi, 1997b, (Annexes II).

(7): calculated from data published by Jacot Des Combes et al., in press, (Tables 2-4).

(8): calculated from data published by Tribovillard et al., 1996, (Table 2).

(9): calculated from data published by Tribovillard et al., 1996, (Table 3).

Table 3: Minimum, mean, and maximum values of the "indirect proxies" in the studied sites.
- : no data available.

The "direct proxies", described above, may be influenced by different processes involved in both deposition and post-depositional transformations of the sediment. The values of selected geochemical proxies (Fe/Al, K/Al, Mg/Al, Ba/Al, P/Al, Mn/Al, V/Al, Cu/Al, Ni/Al, Zn/Al, and Mg/Ca), called "indirect proxies", will, then, be compared with values of the "direct proxies".

The presentation of the results will be divided into two parts. The first part will precise the source and the response of the "direct proxies" both at a regional and site scales. In the second part, the geochemical message carried by the "direct proxies" will be used as a reference to determine the nature and the information carried by the other geochemical markers, called "indirect proxies".

Results

graphs of successive plots of the mean, minimum, and maximum values of the geochemical proxies obtained at each site permits to recognize at a regional scale some geochemical trends that can be useful for paleoceanographic reconstructions. Such broad patterns cannot, however, be used for detailed paleoceanographic reconstructions at sample or specific time interval levels.

A comparison of the plotting of sites on these geochemical graphs will allow to determine the main depositional and paleoceanographic conditions characteristic of the global time interval considered at each site.

1. Variations of the "direct proxies"

Combined plots of "direct proxies" show a global positive correlation between the TOC content on one side and the Si/Al ratio (Fig. 2a) and the bulk MAR (Fig. 2b) on the other side. On this last plot, data from Cores MD 85664 is missing because no age model could be established for this sites (Tribovillard et al., 1996), and Core MD 921002 because no bulk MAR data are available (Ouahdi, 1997b), but the sites located under the upwelling areas of the Arabian sea and the Somali coast are characterized by higher values of TOC content, associated to higher sedimentation rates and significant biogenic silica inputs.

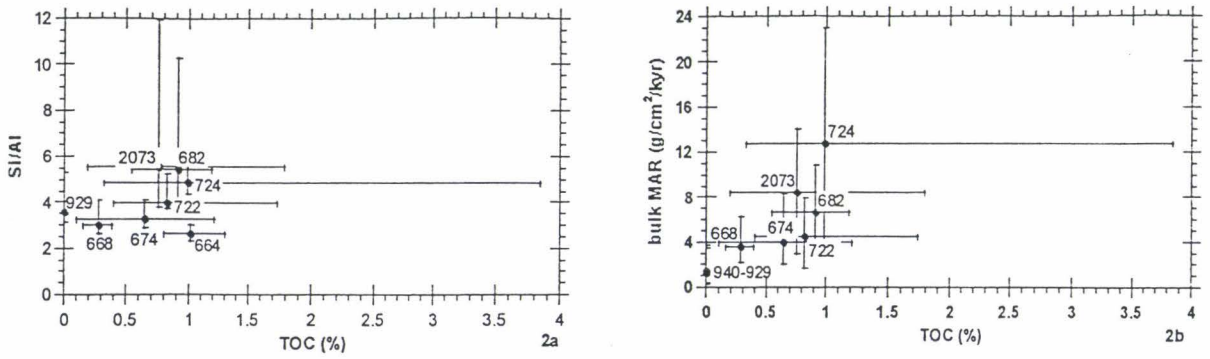

Figure 2a and b: Comparison of the "direct proxies" at a regional scale: TOC content with Si/Al ratio, and TOC content with bulk MAR

A global positive correlation is also recorded between the TOC content and the Ti/Al ratio (core MD 90929 excepted). A negative correlation is, however, observed (Core MD 85674 excepted) between the TOC content and the $CaCO_3$ content (Fig. 2c).

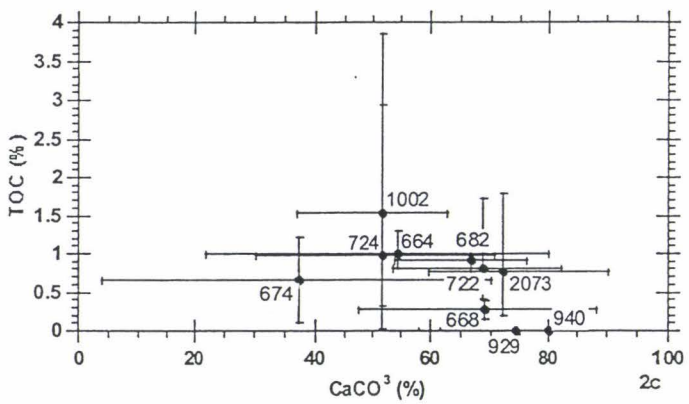

Figure 2c: Comparison of the "direct proxies" at a regional scale: $CaCO_3$ with TOC contents

A negative correlation is also observed between the $CaCO_3$ content from one part, and the Ti/Al ratio (Cores MD 85674 and 90929 excepted) and the bulk MAR (Core MD 85674 excepted) from the other part. According to these results, the site located in the Amirante Passage (Core MD 90929) is mainly characterized by the highest Ti/Al ratio, whereas the site located under the Somali upwelling gyre (Core MD 85674) presents the lowest carbonate content.

A global positive correlation can be remarked between the Si/Al ratio and the bulk MAR (Fig. 2d), and a negative one between the Ti/Al and Si/Al ratios (Fig. 2e).

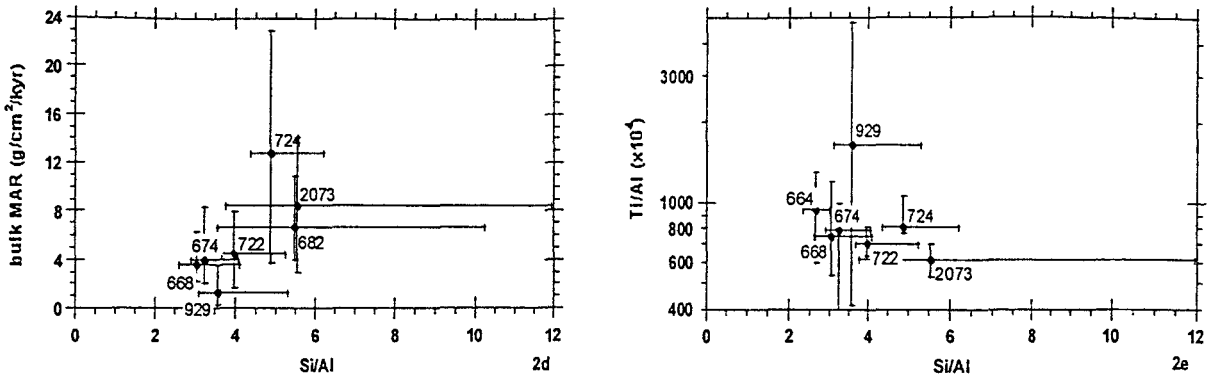

Figure 2d and e: Comparison of the "direct proxies" at a regional scale: Si/Al ratio with bulk MAR, and Si/Al with Ti/Al ratios

No correlations are observed between the TOC/Al ratio and the bulk MAR, and the Si/Al and Ti/Al ratios, but a separated plotting of the sites located under the Socotra gyre, that present relatively high TOC/Al mean values is observed on the graphs (Figs. 2f, 2g, 2h, 2i).

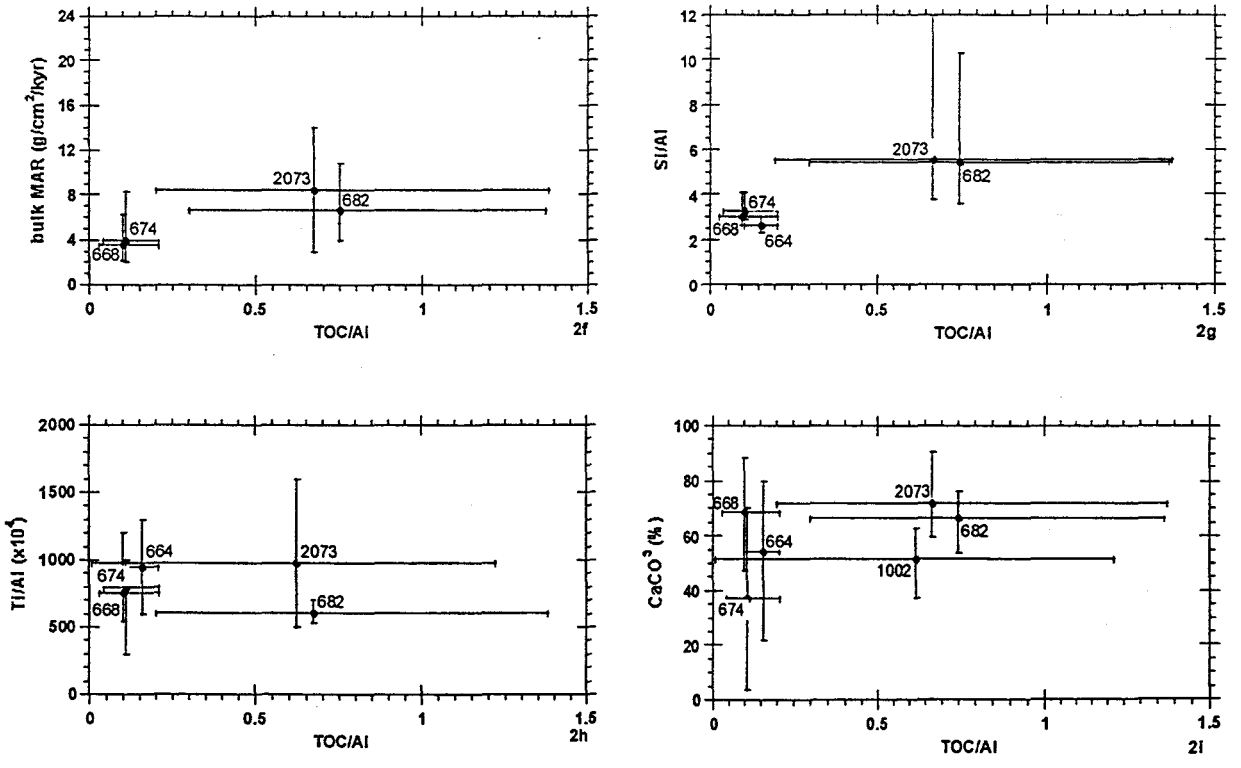

Figure 2f, g, h and i: Comparison of the "direct proxies" at a regional scale: TOC/Al ratio with bulk MAR, TOC/Al with Si/Al ratios, TOC/Al with Ti/Al ratios, and TOC/Al ratio with $CaCO_3$ content

2. Variations of the "indirect proxies"

a. Mg/Ca

At a regional scale, a positive correlation can be observed between the mean values of the Mg/Ca and the bulk MAR, despite the eccentric plotting of Core MD 85674. Such a correlation was not previously observed at any site scale.

On a regional scale, a negative correlation can be observed between mean values of Mg/Ca and $CaCO_3$ (Fig. 3a).

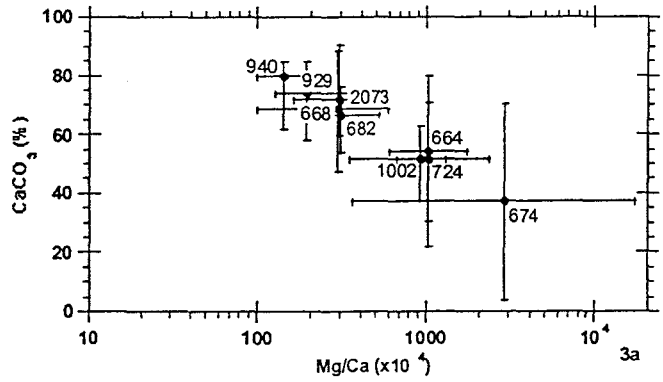

Figure 3a: Comparison of the "indirect proxies" with the "direct proxies" at a regional scale: Mg/Ca ratio with $CaCO_3$ contents

The Mg/Ca-$CaCO_3$ graph allows to separate the sites into three groups: in Core MD 85674 very high and variable Mg/Ca values correspond to relatively low, but variable $CaCO_3$ values. In the group of terrigenous-influenced sites (MD 85664, 921002, ODP site 724) mean Mg/Ca values are comparatively higher. In the group of less terrigenous-influenced cores (MD 85668, 85682, 90929, 90940, and 962073) lower Mg/Ca values correspond to high $CaCO_3$ values. Such a negative correlation was also recorded at individual site scale (see data in Shimmield and Mowbray, 1991; Tribovillard et al., 1996; Ouahdi, 1997a; b; Jacot Des Combes et al., in press; Jacot Des Combes et al., accepted; Jacot Des Combes et al., submitted).

Comparing the Mg/Ca ratio with the TOC content allows to separate the sites into two groups similar to those plotted in the Mg/Ca - $CaCO_3$ graph, except for Core MD 85674 that plots within the group presenting the lowest TOC content values (Fig. 3b). In this group, a negative correlation exists between the Mg/Ca ratio and the TOC content. In the other group, characterized by higher TOC values, no such correlation can be seen. At the individual site scale, there are no correlations between the Mg/Ca ratio and the TOC content, excepted in Core MD 85674 where a slightly positive correlation can be observed. The comparison of the Mg/Ca ratio

with the TOC/Al ratio shows a negative correlation within the time interval spanned by Cores MD 85668 and 85682 (Tribovillard et al., 1996; Ouahdi, 1997a). A less clear correlation is observed in Core MD 962073, that is, however, very close to Core MD 85682 (Jacot Des Combes et al., submitted).

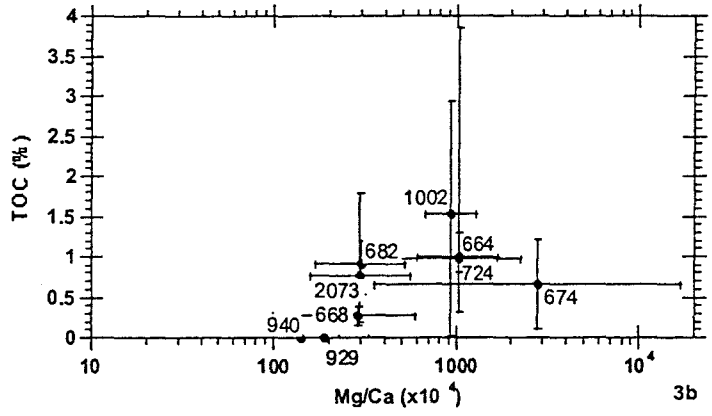

Figure 3b: Comparison of the "indirect proxies" with the "direct proxies" at a regional scale: Mg/Ca ratio with TOC contents

No correlation is observed, at a regional scale, between the Mg/Ca and Ti/Al ratios, (Cores MD 85674 and 90929 excepted), but a positive correlation is observed within piston cores MD 90940 and 90929 (Jacot Des Combes et al., in press; Jacot Des Combes et al., accepted).

No correlation is observed between the mean values of the Mg/Ca and Si/Al ratios, both at regional and site scales.

b. Mg/Al

A positive correlation exists at a regional scale between the Mg/Al ratio and the bulk MAR, but no such a correlation is recorded at the individual site scale.

All over the western Indian Ocean, a positive correlation is recorded between the Mg/Al and Ti/Al ratios (Fig. 3c).

Such a correlation allows to distinguish two groups of sites: a group, including Cores MD 85682, 962073, and ODP site 724, shows relatively high values of both the Mg/Al and Si/Al ratios. The second group, including Cores MD 85674, 85664, 85668, and 90929, exhibits relatively lower values of both the Mg/Al and Si/Al ratios. The same correlation was previously observed within Cores MD 85674, 85682, 90929, and 962073 (Tribovillard et al.; 1996, Ouahdi, 1997; Jacot Des Combes et al., accepted).

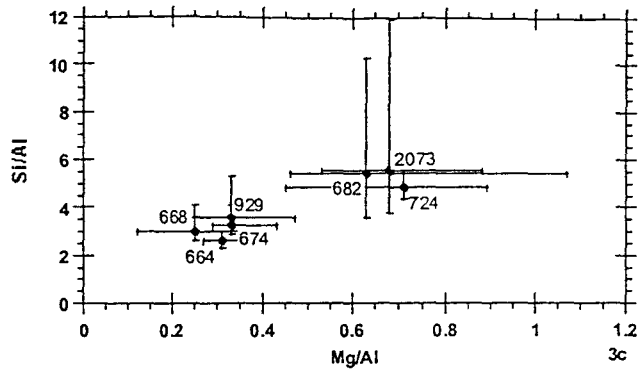

Figure 3c: Comparison of the "indirect proxies" with the "direct proxies" at a regional scale: Mg/Al with Ti/Al ratios

At a regional scale, no correlation is observed between mean values of the Mg/Al ratio and the $CaCO_3$ content. The Mg/Al-$CaCO_3$ graph emphasizes the separation of the sites within the groups already plotted on the Mg/Al-Si/Al graph, but allows to join Core MD 90940 to the first group described above. Such a lack of correlation between the Mg/Al ratio and the $CaCO_3$ content is also recorded at the individual site scale.

A comparison of the variations of Mg/Al ratio with the TOC content at a regional scale shows no correlation, but a clear distribution of the sites within the two groups described above can be observed on this plot (Fig. 3d).

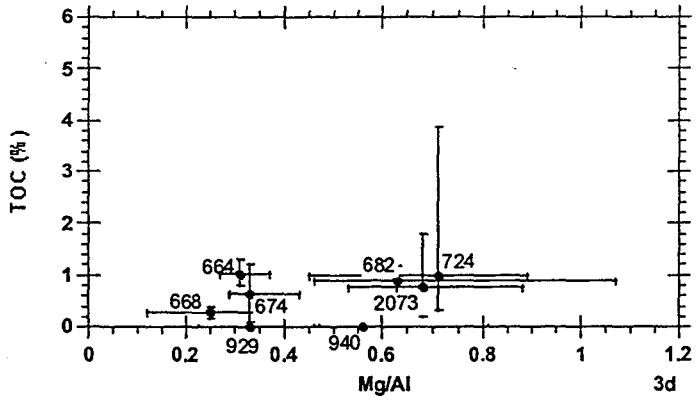

Figure 3d: Comparison of the "indirect proxies" with the "direct proxies" at a regional scale: Mg/Al ratio with TOC content

The same lack of correlation between the two proxies is recorded at each site. A positive correlation between Mg/Al and TOC/Al ratios is, however, observed in cores MD 85668, 85674, 85682, and 962073 whereas Core MD 85664 does not exhibit this correlation (Tribovillard et al., 1996, Ouahdi, 1997; Jacot Des Combes et al., accepted; submitted).

The distribution of the sites between the two groups already described is observed at a regional scale between Mg/Al and Ti/Al. This lack of correlation is also recorded within each core, excepted in cores MD 85674, and MD 90929, where a positive correlation is obvious (Ouahdi, 1997; Jacot Des Combes et al., accepted).

c. Fe/Al

At a regional scale, no correlation is observed between the Fe/Al ratio and any of the "direct proxies". This lack of correlation may result from very close mean values of the Fe/Al ratio, and from the wide range of variation of this ratio at each site. When comparing the mean values, a slight negative correlation can be observed between the Fe/Al and Si/Al ratios. Such a correlation is recorded at ODP site 724 only (Shimmield and Mowbray, 1991). Inversely, a positive correlation is recorded between both these proxies in Core MD 962073 (Jacot Des Combes et al., submitted). No correlations are observed between the Fe/Al ratio and the other markers, such as TOC, TOC/Al, $CaCO_3$, and Ti/Al at both regional and site scales.

d. K/Al

Comparing the K/Al ratio with the "direct proxies" gives results similar to those recorded for the Fe/Al ratio. A positive correlation is, however, observed between the K/Al and Si/Al ratios. Such a correlation is also recorded within Core MD 85664, and, less clearly, within Core MD 85668 (Tribovillard et al., 1996). As for the Fe/Al ratio, no correlation is observed between K/Al and TOC, TOC/Al, $CaCO_3$, and the bulk MAR, at both regional and site scales.

e. Ba/Al

At a regional scale, a positive correlation is observed between the Ba/Al and Si/Al ratios (Fig. 3e). This correlation was also recorded within Cores MD 85682, and 962073 (Ouahdi, 1997a; Jacot Des Combes et al., submitted). No correlation between the Ba/Al and Si/Al ratios was, however, observed within Cores MD 85674, 90929, and ODP site 722 (Shimmield and Mowbray, 1991; Tribovillard et al., 1996; Jacot Des Combes et al., accepted).

A positive correlation is also observed at a regional scale between the Ba/Al ratio and the $CaCO_3$ content. This correlation was observed within Core MD 85664, and at ODP site 722 (Shimmield and Mowbray, 1991; Tribovillard et al., 1996). In cores MD 90929, and 921002, a

negative correlation is, however, recorded (Ouahdi, 1997b; Jacot Des Combes et al., accepted). No correlation at all between these two proxies is observed in the other cores.

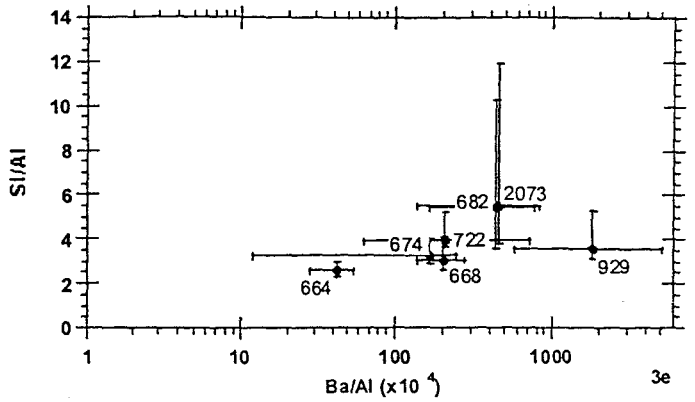

Figure 3e: Comparison of the "indirect proxies" with the "direct proxies" at a regional scale: Ba/Al with Si/Al ratios

At a regional scale, a negative correlation is observed between the Ba/Al and Ti/Al ratios, despite a high Ti/Al ratio in Core MD 90929 (Fig. 3f). This negative correlation is also recorded in Core MD 90940 (Jacot Des Combes et al., in press). In cores MD 90929 and 962073, a positive correlation can, however, be observed, but it is less obvious (Jacot Des Combes et al., accepted; submitted).

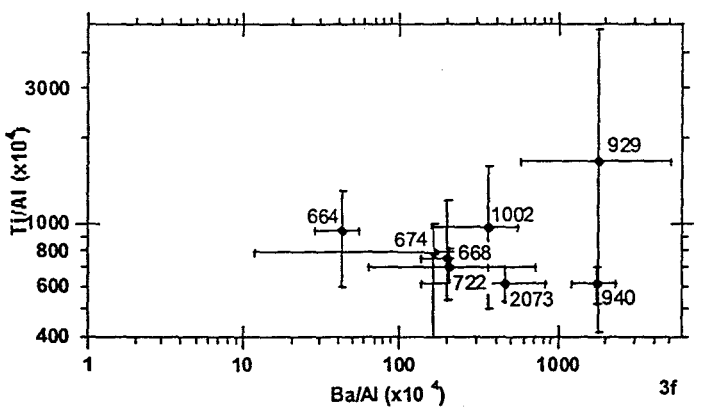

Figure 3f: Comparison of the "indirect proxies" with the "direct proxies" at a regional scale: Ba/Al with Ti/Al ratios

No correlation between the Ba/Al ratio and the TOC content is observed at the regional scale. This lack of correlation was also recorded within the sites. The comparison of the Ba/Al with the TOC/Al ratios shows, however, a positive correlation both at a regional scale (Fig. 3g) and within Cores MD 85664, 85674, 85682, and 962073 (Tribovillard et al., 1996; Ouahdi, 1997a; Jacot Des Combes et al., submitted).

The comparison of the Ba/Al ratio with the bulk MAR shows no correlation at a regional scale, but allows separating the cores into two groups (Fig. 3h). The first group is made of pelagic sites, with low bulk MAR and high Ba/Al values. The second group, made of the other sites, presents a positive correlation between both these proxies. No relation between these proxies was recorded within the sites.

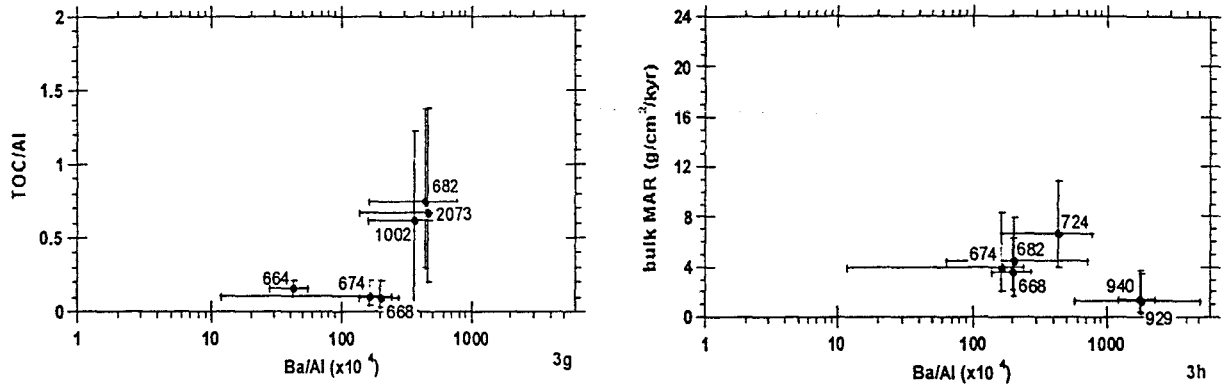

Figure 3g and h: Comparison of the "indirect proxies" with the "direct proxies" at a regional scale: Ba/Al with TOC/Al ratios, and Ba/Al ratio with bulk MAR

f. P/Al

At a regional scale, a positive correlation can be observed between the P/Al and Si/Al ratios (Fig. 3i). This correlation was also observed within Cores MD 85664, 85668, 85682, and 962073, but it is less cleat at this last (Tribovillard et al., 1996; Ouahdi, 1997a; Jacot Des Combes et al., submitted). No correlation is observed in Core MD 85674, and at ODP sites 722 and 724 (Shimmield and Mowbray, 1991; Tribovillard et al., 1996).

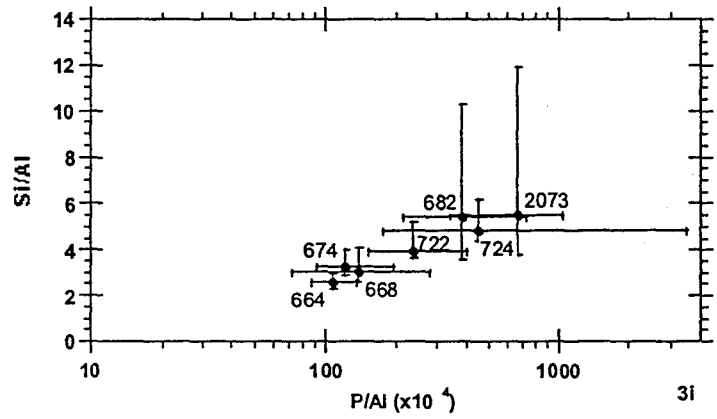

Figure 3i: Comparison of the "indirect proxies" with the "direct proxies" at a regional scale: P/Al with Si/Al ratios

A positive correlation can also be seen at a regional scale between the P/Al ratio and the $CaCO_3$ content, but the cores are more scattered. This relation was also observed in Core MD 85668, and at ODP site 722 (Shimmield and Mowbray, 1991; Tribovillard et al., 1996). The correlation is less clear in cores MD 85668, 85674, 90940, 962073, and at ODP site 724 (Shimmield and Mowbray, 1991; Tribovillard et al., 1996; Jacot Des Combes et al., in press; submitted); and no such relation is observed in Core MD 85682 (Ouahdi, 1997a).

A negative correlation between the P/Al and Ti/Al ratios is observed at a regional scale (Fig. 3j). Such a correlation was observed in Cores MD 85664 and 90929 (Tribovillard et al., 1996; Jacot Des Combes et al., accepted). Inversely, a positive correlation was observed between both these proxies in Cores MD 85668 and 962073 (Tribovillard et al., 1996; Jacot Des Combes et al., submitted).

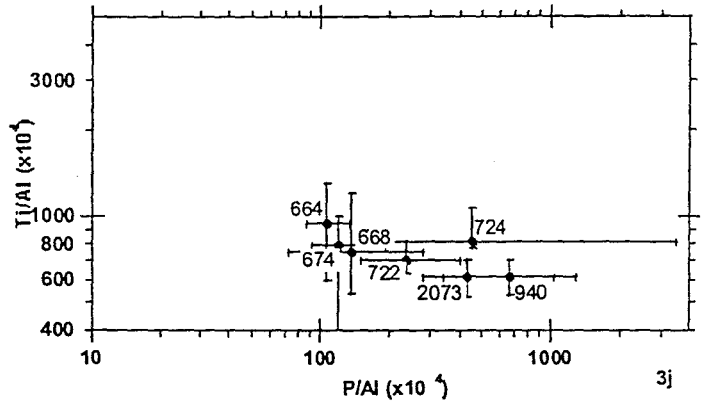

Figure 3j: Comparison of the "indirect proxies" with the "direct proxies" at a regional scale: P/Al with Ti/Al ratios

At a regional scale, no correlation is observed between the P/Al ratio and the TOC content. No correlation either is recorded within the cores between both these proxies. Comparing the P/Al and TOC/Al ratios shows no correlation either, but allos to separate the cores located under the Socotra gyre from the others (Fig. 3k). A positive correlation was observed within Cores MD 85668, 85682, and 962073, and at a lesser degree in Core MD 85674 (Tribovillard et al., 1996; Ouahdi, 1997a; Jacot Des Combes et al., submitted).

No correlation is observed between the P/Al ratio and the bulk MAR at both regional (Fig. 3l) and site scales.

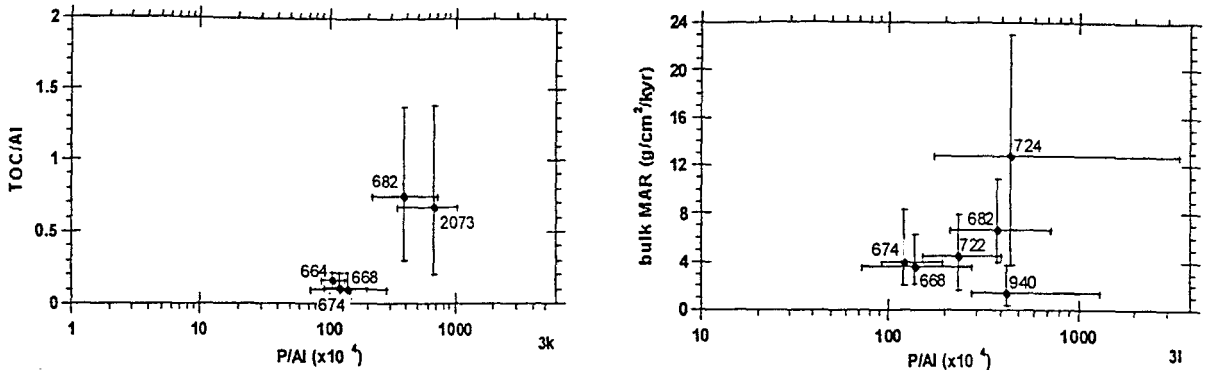

Figure 3k and l: Comparison of the "indirect proxies" with the "direct proxies" at a regional scale: P/Al with TOC/Al ratios, and P/Al ratio with bulk MAR

g. Mn/Al

A positive correlation can be observed between the Mn/Al and Si/Al ratios at a regional scale and within cores MD 85664, 962073, and, at a lesser degree in Core MD 85668 (Tribovillard et al., 1996; Jacot Des Combes et al., submitted).

On a regional scale, a negative correlation can be observed between the Mn/Al ratio and the TOC content (Fig. 3m). Such a correlation was also observed in Cores MD 85674 and 921002 (Tribovillard et al., 1996; Ouahdi, 1997b), but not in the other sites. No correlation is observed between the Mn/Al and TOC/Al ratios at a regional scale, but a positive one was recognized in Cores MD 85668, 85674, and 962073 (Tribovillard et al., 1996; Jacot Des Combes et al., submitted).

A negative correlation is observed at a regional scale between the Mn/Al ratio and the bulk MAR, despite the high bulk MAR values recorded at ODP site 724 (Fig. 3n). This correlation was not observed at the individual site scale.

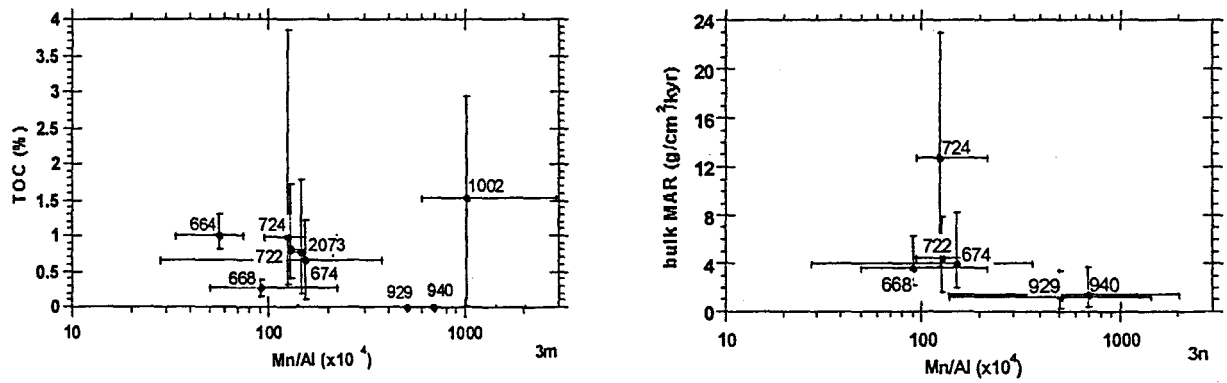

Figure 3m and n: Comparison of the "indirect proxies" with the "direct proxies" at a regional scale: Mn/Al ratio with TOC content, and Mn/Al ratio with bulk MAR

On a regional scale, no correlation, but a separation of the cores into two groups, can be seen at the Mn/Al-$CaCO_3$ plot. The first group, made of Cores MD 90929, 90940, and 921002, exhibits relatively high Mn/Al values, and the second one, made of Cores MD 85664, 85668, 85674, 962073, and ODP sites 722 and 724 with lower Mn/Al values. A positive correlation was, however, observed in Cores MD 85668, 85674, 90940, 921002, 962073, and in ODP site 722 (Shimmield and Mowbray, 1991; Tribovillard et al., 1996; Ouahdi, 1997b; Jacot Des Combes et al., submitted).

No correlation is observed between the Mn/Al and Ti/Al ratios, both at regional and individual site scales.

h. V/Al

A positive correlation can be observed at a regional scale between the V/Al ratio and the bulk MAR (Fig. 3o) but was not recorded within the sites.

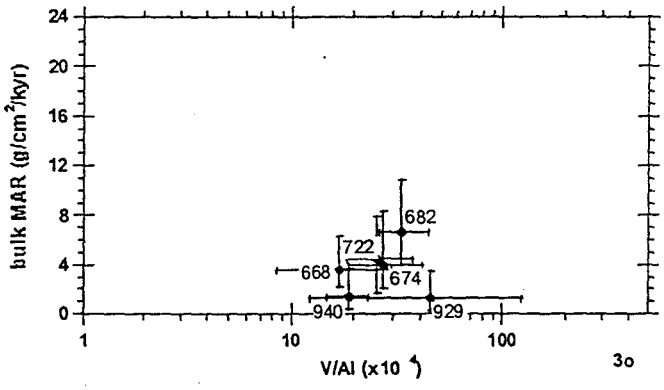

Figure 3o: Comparison of the "indirect proxies" with the "direct proxies" at a regional scale: V/Al ratio with bulk MAR

A positive correlation is also observed at a regional scale between the V/Al and Si/Al ratios. This correlation was also recorded in Core MD 85668 (Tribovillard et al., 1996).

On a regional scale, a negative correlation can be observed between the V/Al and Ti/Al ratios despite the eccentric plotting of Cores MD 90929 and 921002. This correlation was not observed within the cores. Inversely, in Cores MD 85668, 85674, 90929, and 90940 a positive correlation can be observed (Tribovillard et al., 1996; Jacot Des Combes et al., in press; accepted).

On a regional scale, no correlation is observed between the V/Al ratio and the $CaCO_3$ content, but Cores MD 85674 and 921002 are plotted apart from the others. Within cores MD

90929 and 921002, a negative correlation is observed (Ouahdi, 1997b; Jacot Des Combes et al., accepted), while in Core MD 85668 and ODP site 722, a positive one is observed (Shimmield and Mowbray, 1991; Tribovillard et al., 1996).

No correlation is observed between the V/Al ratio and the TOC content at both regional (Fig. 3p) and site scales. Comparing the V/Al ratio with the TOC/Al ratio shows no correlation at a regional scale, but a positive correlation between both these proxies in Cores MD 85674 and 85682 (Tribovillard et al., 1996; Ouahdi, 1997b).

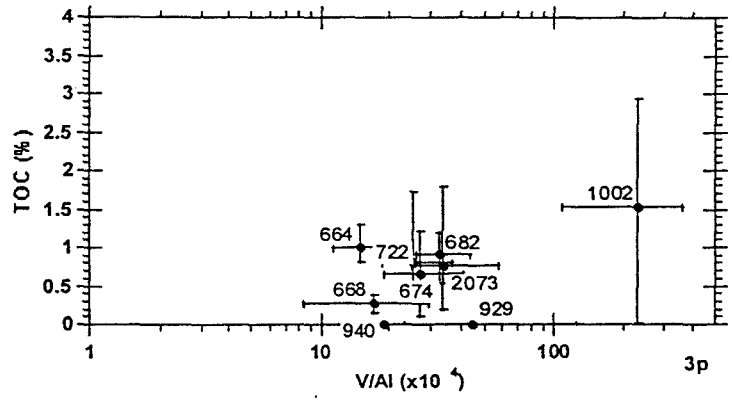

Figure 3p: Comparison of the "indirect proxies" with the "direct proxies" at a regional scale: V/Al ratio with TOC content

i. Cu/Al

A positive correlation can be observed between the Cu/Al ratio and the $CaCO_3$ content at a regional scale. This correlation was already recorded at ODP site 722 (Shimmield and Mowbray, 1991), while a negative correlation was observed in Core MD 90929, and less clearly, in Core MD 85664 (Tribovillard et al., 1996; Jacot Des Combes et al., accepted). No correlation was recorded at the other sites. The sediments from Cores MD 90929, 90940, and 962073 (Jacot Des Combes et al., in press; accepted; submitted) exhibit Cu/Al values above the deep sea carbonates average value (Turekian and Wedepohl, 1961), whereas the other sites are characterized by Cu/Al values located below this average value (Shimmield and Mowbray, 1991; Tribovillard et al., 1996; Ouahdi, 1997a; b).

On a regional scale, a positive correlation can be recognized between the Cu/Al and Si/Al ratios. This correlation was observed, but at a lesser degree, within each site located under the upwelling systems (Tribovillard et al., 1996; Ouahdi, 1997a; Jacot Des Combes et al., submitted).

On a regional scale, a negative correlation is observed between the Cu/Al ratio and the TOC content. This correlation is not recognized within the sites. No correlation at a regional scale is recorded between the Cu/Al and TOC/Al ratios, but a positive correlation was recorded within cores MD 85682 and 962073 (Ouahdi, 1997a; Jacot Des Combes et al., submitted).

The Cu/Al and Ti/Al ratios show a negative correlation, despite the high Ti/Al values measured in Core MD 90929. Within this core a positive correlation is recorded between both these proxies (Jacot Des Combes et al., accepted). Such a correlation was also observed in Core MD 85668, but less clearly (Tribovillard et al., 1996).

Comparing the Cu/Al ratio and the bulk MAR shows no correlation, but allows to separate the sites into two groups: the pelagic sites, with low bulk MAR (MD 90929 and 90940), and the other ones with higher bulk MAR. No correlation is observed at the individual site scale.

j. Ni/Al

A global positive correlation can be observed between the Ni/Al ratio and the $CaCO_3$ content, that was previously reported from Cores MD 85668 and 962073 (Tribovillard et al., 1996; Jacot Des Combes et al., submitted). Inversely, within Core MD 90929, a negative correlation is recorded between both these proxies (Jacot Des Combes et al., accepted).

A positive correlation can be observed at a regional scale between the Ni/Al and Si/Al ratios. This relation was also recognized within cores MD 85668, 962073, and at ODP site 722 (Shimmield and Mowbray, 1991; Tribovillard et al., 1996; Jacot Des Combes et al., submitted).

On a regional scale, a negative correlation can be observed between the Ni/Al ratio and the TOC content, despite the scattering of the plotting of sites. This correlation is not recognized at the site scale. No correlation is observed between the Ni/Al and TOC/Al ratios at a regional scale, but a positive correlation was, however, reported between the Ni/Al and the TOC/Al ratios in Core MD 962073 (Jacot Des Combes et al., submitted).

On a regional scale, a negative correlation is observed between the Ni/Al and the Ti/Al ratios, despite the "eccentric" plotting of Core MD 90929. This correlation is not recognized within the sites. Inversely, in Cores MD 85668 and 962073,and especially 90929, a positive correlation between both these proxies was observed (Tribovillard et al., 1996; Jacot Des Combes et al., accepted; submitted).

No correlation is recorded between the Ni/Al ratio and the bulk MAR both at regional and individual sites scales.

k. Zn/Al

A positive correlation is noted on a regional scale between the Zn/Al ratio and the $CaCO_3$ content. This correlation was previously recognized within Core MD 962073 and at ODP site 722 (Shimmield and Mowbray, 1991; Jacot Des Combes et al., submitted). Inversely, within Core MD 90929 and, at a lesser degree, within Core MD 85664, a negative correlation can be observed between both these proxies (Tribovillard et al., 1996; Jacot Des Combes et al., accepted).

A positive correlation can also be observed at a regional scale between the Zn/Al and the Si/Al ratio. This correlation was recognized within the sites located under the Socotra upwelling system (Ouahdi, 1997a; Jacot Des Combes et al., submitted) but not in the other sites.

On a regional scale, a negative correlation exists between the Zn/Al ratio and the TOC content. This correlation was not recorded at the individual site scale. Inversely, within the sites located under the upwelling systems (MD 85674, 85682, and 962073) a positive relation was observed (Tribovillard et al., 1996; Ouahdi, 1997a; Jacot Des Combes et al., submitted). Cores MD 85682 and 962073, but not 85674, exhibit high Zn/Al values compared to the deep sea carbonates average value (Turekian and Wedepohl, 1961).

A negative correlation is observed between the Zn/Al ratio and the bulk MAR, and between the Zn/Al and the Ti/Al ratios, at both regional and individual site scales.

<u>Discussion:</u> Is there a geochemical signature of the sedimentation in the western Indian Ocean ?

The wide range of data gathered for this paper helps to characterize each site by its geochemical record, i.e. the value of the geochemical proxies or the correlation between them, and to determine if the sediments from the western Indian Ocean present different specific geochemical signatures. Such a signature implies rather homogeneous records in the studied areas. However, some sites do not fit with the general pattern and present a particular record. Core MD 90929, for example, presents high values of the Ti/Al ratio, compared to the other sites, and a positive correlation between the Ti/Al ratio on one side, and the Ba/Al, Cu/Al, Ni/Al, V/Al, and Zn/Al ratios on the other side (Jacot Des Combes et al., accepted). Core MD 921002 presents high values of both the Mn/Al and V/Al ratios compared to the other sites (Ouahdi,

1997b). The interpretation of the variations of the geochemical proxies, and of their relation to deposition and accumulation processes, is the first step to establish a model of the geochemical response to paleoproductivity and paleoceanographic changes in the western Indian Ocean. The comparison of the "direct proxies" ($CaCO_3$ and TOC contents, Si/Al, Ti/Al, and TOC/Al ratios, and bulk MAR) will allow determining the main process controlling directly the sedimentation in each core. Furthermore, comparing the behavior of these proxies in the cores may help to establish the separation of these sites into groups that can be described as pelagic, terrigenous-, and upwelling-influenced environments. The "indirect proxies", that are more difficult to directly link with sedimentary processes give complementary information on the sediment sources and on depositional conditions.

Variations of the bulk MAR compared with variations of the other "direct proxies" help to recognize a classical accumulation pattern in this region of the Indian Ocean. The sediments accumulated with a lower sedimentation rate are mainly located in the pelagic domain and are made of biogenic carbonates. The input of other potential sources of sedimentary material (such as an enhanced surface productivity and/or the input of terrigenous debris) increases the sedimentation rate at the other locations. It is, thus, possible to observe in this region a gradual transition between the pelagic deposits, the sediments located closer to the coast, and the sediments recovered under the upwelling systems (Fig. 2). The separation between the pelagic sites and the others is especially obvious on the bulk MAR-Ba/Al graph, where Cores MD 90929 and 90940 are eccentrically plotted. Within the group made of the "non-pelagic" sites, the two sites located under the Socotra gyre present higher values of bulk MAR. The positive correlation that can be recognized within the "non–pelagic" sites group between the bulk MAR on one side, and the Ba/Al, P/Al, Si/Al, and TOC/Al ratios on the other side underlines the significant input of material from an enhanced surface productivity, and especially the organic matter produced by the siliceous plankton. It is, thus possible to use the bulk MAR mean values to separate the cores into well-defined groups, but the minimum and maximum values of the bulk MAR are not different enough to clearly separate the groups.

The variations of the bulk MAR are, however, related to the variations of the main components of the sediment: the biogenic carbonates, the terrigenous input, and the material resulting from surface productivity. At a regional scale, the usually negative correlation between the $CaCO_3$ content and the Ti/Al ratio reflects the opposition between the biogenic carbonate component, mainly made of coccolithophorids (Caulet et al., 1988; Shimmield and Mowbray,

1991; El Foukali, 1995; Jacot Des Combes et al., in press; accepted), and the terrigenous input, that increases at sites located near coastal areas. The plotting of Core MD 90929 apart from the other sites indicates that the conditions are different at this site, with both a high carbonate content and a high terrigenous input. This duality is less obvious at the individual site scale, especially at sites located close to the coastal area, where the terrigenous input also includes detrital carbonates (calcite or dolomite) mostly represented by turbidite levels rich in foraminiferal debris (Leclaire, 1974). A transition can be observed between "pelagic" sites, where carbonates are mainly of biogenic origin, and "terrigenous" sites, where the terrigenous input is made of both aluminosilicates and detrital carbonates.

The total bulk and composition of the terrigenous input may also influence the accumulation processes. The Mg/Ca ratio, as well as the Ti/Al ratio, were considered in this region as two proxies characteristic of detrital inputs, and, thus, indicative of the wind strength (Weedon and Shimmield, 1991; Shimmield, 1992; Tribovillard et al., 1996; and references therein). As a result, a positive correlation was expected between the Mg/Ca and the Ti/Al ratios, and a negative one between the Mg/Ca ratio and the $CaCO_3$ content. All data obviously exhibit a general negative correlation between the Mg/Ca ratio and the $CaCO_3$ content, both at the regional scale (Fig. 3a) and at the individual core scale. The process leading to the enrichment in Mg compared to Ca is, thus, occurring both at regional and local scales. In the western Indian Ocean, the negative correlation between the Mg/Ca ratio and the $CaCO_3$ content underlines the opposition between the carbonates of marine origin and the detrital carbonates, including the dolomite transported from the continent. The relation between the Mg/Ca and the Ti/Al ratios is not clear at the regional scale: first, because no correlation is observed between the Mg/Ca and Ti/Al ratios, and then, because of the eccentric plotting of Core MD 90929. The mean values of both these ratios allow to separate the cores into two clusters: the first one with relatively low values of both the Mg/Ca and Ti/Al ratios contains the sites located under the Socotra gyre and in the pelagic domain (Cores MD 85668 and 90940), whereas the second cluster, with higher values of both the ratios, is composed of sites located closer to the coast. No correlation is observed between both these proxies at the individual site scale, excepted in cores MD 90940 and especially 90929, that are located far from any coast. Such a behavior may indicate two sources for the Mg-enrichment. In the pelagic domain, far from any coast, winds are the major carrier of detrital material, transporting both Ti and Mg. Closer to the coast, where winds, continental weathering, and river outflow may be responsible for the terrigenous inputs, Mg and

Ti are not carried by the same vehicle. As the Mg-enrichment is stronger than the Ti-enrichment, the Mg may be mostly carried by river outflow or continental weathering, while Ti may remain carried mainly by winds. The Mg/Ca ratio may, thus, be considered in this region of the western Indian Ocean as a detrital input proxy, and more precisely as a wind strength index in the pelagic domain, and as a proxy for continental weathering and/or river inputs in the coastal domain. This process is observed in the northwestern Indian Ocean, but the Mg/Ca record in Core MD 90929 indicates that the source of the terrigenous input in the southern part of the western Indian ocean may be different. Moreover, the strong positive correlation observed at this site between the Ti/Al ratio on one side and the Mg/Al, Ba/Al, Cu/Al, Ni/Al, V/Al, and Zn/Al ratios on the other side (Jacot Des Combes et al., accepted) is not recognized at other sites. This indicates that the composition of the terrigenous material in the Amirante Passage is very different from the composition of the terrigenous material in the northwestern Indian Ocean, and may be related to a distinct source. The location of this site in the Amirante Passage (southern part of the equatorial belt of the western Indian Ocean) suggests that this material may have a southern origin, and that it could be carried by the bottom currents flowing from the Madagascar Basin into the Somali Basin through this strait. Today, the depth where the core was recovered is apparently above the bottom currents, but material transported may be deposited by the top of the nepheloid layer (Johnson and Damuth, 1979; Barton et Hill, 1989; Johnson et al., 1991). We can, thus, infer from these data that the terrigenous input is rather homogeneous in the considered area of the northwestern Indian Ocean, with wind transport as a single source of both Ti and Mg in the pelagic domain, and a differentiation of these sources in the coastal area, with Ti mainly carried by winds, and Mg mainly transported through continental weathering and/or river input. Moreover, another source of terrigenous material is recognized south of this area; this source is significant in the Amirante Passage, but neglectible further north.

The sites located under the upwelling systems present a more complicated sedimentation pattern. The sediment is mainly made of carbonate plankton, and especially coccolithophorids, indicating that these sites are subjected to the carbonaceous sedimentation. Due to their location, close to the coast, a significant fraction of the sediment is of terrestrial origin. The enhanced surface productivity implies input of specific material resulting from the enhanced surface productivity, especially debris of biosiliceous plankton. The correlations observed between the bio-influenced chemical parameters of the sediment ($CaCO_3$ and TOC contents, Si/Al and TOC/Al ratios) help to determine the main source of the organic matter in this region of the

Indian Ocean. Three sources, at least, are available: detrital organic carbon exported from the coastal area, organic carbon linked to the carbonate plankton, and organic carbon linked to the siliceous plankton. Comparing the relations of the TOC content and the TOC/Al ratio with the other proxies shows that, at all sites where the organic matter content is measurable (more than 0.01 %), both marine and detrital organic matter are found (Fig. 2). Such a result is confirmed by palynofacies analyses realized upon some cores (Tribovillard et al., 1996; Ouahdi, 1997a; Jacot Des Combes et al, submitted). The part of the organic matter that has a terrigenous origin is, however, difficult to estimate, and cannot be used to identify the sites strongly influenced by a terrigenous input. On the other hand, the nature of the marine organic matter may help differentiate the upwelling-induced sediments from the oligotrophic deposits. The sediments deposited under the upwelling area of the Somali Basin (MD 85674, 85682, and 962073) exhibit a strong correlation between the Si/Al and TOC/Al ratios, and no correlation between the $CaCO_3$ content and the TOC/Al ratio, suggesting that the relative enrichment of the sediment in organic matter is related to the production of biogenic silica, i.e. that the organic matter is produced mainly by the siliceous plankton (Vénec-Peyré et al., 1995; Ouahdi, 1997a). In sediments deposited in oligotrophic areas, such an enrichment in organic carbon is mainly related to an increase of the carbonate content, indicating that the calcareous plankton may be responsible for the primary production. The relation between the surface productivity and the sedimentary response is more difficult to monitor in the pelagic domain because of the absence of organic matter preserved in the sediment. Recent studies show, however, that, in cores from the pelagic domain, the variations of the bulk MAR, strongly correlate with the variations of the composition of the siliceous plankton, and especially radiolarians. Increases of the radiolarian population living at an intermediate depth correspond to high bulk MAR values, and thus to high paleoproductivity periods. This suggests that in such a pelagic environment, a non neglectible part of productivity may be related to biosiliceous plankton (Jacot Des Combes et al., in press, accepted). On the other hand, at both ODP sites 722 and 724, that are located in the Arabian Sea, the enrichment of the sediment in silica seems to be related to the increase of the Ti/Al ratio, and, thus, to the increase of the detrital input (Shimmield and Mowbray, 1991).

The comparison of the variations of the indirect proxies with those of the direct proxies provides complementary information on the origin of the biogenic-related fraction of the sediment. Comparison between the Mg/Al and the Si/Al ratios allows separating the sites into two clusters (Fig. 3c): the first group includes sites where both Mg/Al and Si/Al ratios are

relatively low due to a non-neglectible terrigenous input (Cores MD 85664, 85668, and 85674) and, more surprisingly, Core MD 90929; the other group is constituted by sites located under an upwelling areas, such as Cores MD 85682, 962073, and ODP site 724. As no silica data are available for Core MD 90940, the belonging of this last site to one of the groups must be determined by another proxy than the Si/Al ratio. The comparison of the Mg/Al ratio with the $CaCO_3$ content confirms this distribution into two groups and indicates that Core MD 90940 is linked to the second group. The distribution of the pelagic sites between the two groups permits to precise the sedimentation patterns associated with each group. In the first group, the sedimentation is mainly controlled by the terrigenous inputs. Among the sites associated to this group, three are located along the African coast (Cores MD 85664, 85668, and 85674), and are subjected to significant terrigenous inputs. The presence of Core MD 90929 in this group is, thus, surprising, and may result from the different source of terrigenous material discussed above. The second cluster is made of sites located under upwelling systems, both in the Arabian Sea and the Somali Basin. Core MD 90940 is not located under a coastal upwelling gyre, but under the equatorial productivity belt, where terrigenous influences are insignificant. At this site, the composition of the sediment, mainly made of carbonates, as well as the strong correlation between the bulk MAR and a radiolarian index that monitor the variations in the surface productivity indicates that the sedimentation is controlled by surface productivity (Jacot Des Combes et al., in press). The positive correlation observed at the regional scale between the Mg/Al and the Si/Al ratios is not recorded at the individual site scale, excepted in core MD 90929, where a marked negative relation between the Mg/Al ratio and the $CaCO_3$ content and a positive relation between the Mg/Al ratio and the Ti/Al ratio are recognized.

The positive correlation between the P/Al ratio and both the Si/Al and TOC/Al ratios, observed both at regional and individual site scales, suggests that the origin of the phosphorus is clearly related to biogenic processes, and especially to a production by the siliceous plankton (Fig. 3i-l). The P/Al ratio allows to separate the different sites into two clusters: the first group (Cores MD 85682, 90940, 962073, and ODP sites 722 and 724) includes sites where the P/Al ratio rates above the mean deep sea carbonates value determined from Turekian and Wedepohl (1961), and the second group (Cores MD 85664, 85668, and 85674) is constituted of sites with a P/Al ratio below the mean value. The first cluster is made of sites located under the Socotra gyre, under the Arabian Sea upwelling system, and under the equatorial belt of the Indian Ocean. The sedimentation at all these sites is, thus, strongly influenced by the enhanced surface productivity,

and especially by the siliceous plankton. The second cluster is composed of sites where the sedimentation is influenced by the terrrigenous input. The presence in this group of core MD 856874 indicates that under the Somali gyre, where both biogenic and detrital sources occur, the terrigenous influence monitor the geochemical response. As well as the Mg/Al ratio, the P/Al ratio permits to distinguish the sediments controlled by the biogenic processes (mostly the siliceous plankton productivity) from the sediments controlled by the input of terrigenous debris. A combined enrichment of the sediment in silica, TOC, and phosphorus is mainly recorded under the upwelling gyres, but also at sites where the variations of the siliceous significantly influence the variations of the surface productivity (Jacot Des Combes et al., in press). This enrichment can, thus, be considered as characteristic of environments where the siliceous plankton is the main producer. The enrichment of the sediment in phosphorus can, thus, be used as a reliable paleoproductivity proxy in this region of the Indian Ocean.

Many studies focused on barium, due to its potential relation with surface productivity especially when deposited as barite (Dehairs et al., 1980; 1987; 1991; Shimmield and Mowbray, 1991; Stroobants et al., 1991; Dymond et al., 1992; Shimmield, 1992; Calvert and Pedersen, 1993; Gingele and Dahmke, 1994; Lea and Spero, 1994; Shimmield et al., 1994; Francois et al., 1995; Torres et al., 1996). In sediments from the western Indian Ocean, a positive correlation can be observed at a regional scale between the Ba/Al ratio and both the Si/Al ratio and the $CaCO_3$ content, indicating a relation between the barium enrichment of the sediment and the surface productivity (Fig. 3e-h). The correlation with the organic matter content (TOC) is less clear, but this may be related to the occurrence of different sources of organic matter (marine and detrital) as well as to the lability of the marine organic matter. At the individual site scale, some different patterns can be recognized. The positive correlation observed between Ba/Al and TOC/Al in the cores located under the Somalian upwelling system (Tribovillard et al., 1996; Ouahdi, 1997; Jacot Des Combes et al., submitted), particularly under the Socotra gyre, as well as the positive correlation between Ba/Al and Si/Al recorded at the same sites, suggest that the barium enrichment is related to an enhanced production of organic matter by the siliceous plankton. At the sites located outside of the Somalian upwelling system, the origin of the Ba-enrichment of the sediment is less clear. In the Somali Basin, the pelagic site (Core MD 85668) also exhibits a positive correlation between the Ba/Al and Si/Al ratios, whereas the terrigenous site (Core MD 85664) exhibits correlations between the Ba/Al ratio on one side and both the Si/Al ratio and the $CaCO_3$ content on the other side, indicating two sources of barium (Tribovillard et al., 1996).

Due to the lack of data, it is not possible to compare the variations of th Ba/Al ratio with those of the Si/Al and TOC/Al ratios. The strong correlation between the Ba/Al and the Ti/Al ratios in the Amirante Passage (Core MD 90929) is related to a southern source of terrigenous material. The various correlations observed between the Ba/Al ratio and the "direct proxies" suggests that the barium enrichment is related to different processes, depending on the paleoceanographic conditions. The distribution of the barium within the different fractions of the sediment may help to determine the origin of barium, and, thus, the paleoceanographic process leading to the barium accumulation. Previous studies have underlined some marked differences in the barium distribution within some sediments located in the same domain, either pelagic (Jacot Des Combes et al., accepted) or coastal upwelling (Ouahdi, 1997a; Jacot Des Combes et al., submitted). In both domains, the barite content in the sediment, that is considered as representative of the biogenic barium content, presents a negative correlation with the terrigenous content. Diagenetic processes, especially through barite dissolution under reducing conditions, may affect the distribution of the barium within the different fractions of the sediments. The changes in the redox conditions may be influenced by the variations of the bulk MAR and/or the TOC content: an increased bulk MAR limiting the time of exchange between the sediment and the bottom water lying above, and an increased TOC content by limiting the dissolved oxygen content in the bottom and pore water during organic matter degradation (Van Os et al., 1991; Von Breymann et al., 1992; Thomson et al., 1993; 1995; De Lange et al., 1994; Van Santvoort et al. 1996). No relation is, however, observed between the Ba/Al ratio and the bulk MAR, or between Ba/Al and TOC both at a regional and individual site scales. The variations of both the TOC and the bulk MAR, and the corresponding changes in the redox conditions do not influence the barium accumulation in the western Indian Ocean. Lastly, no significant trace-metal enrichment, that could indicate reducing diagenetic conditions, is observed in the sites. It may, thus, be concluded that the diagenetic process is not the main control of barium accumulation and storage, suggesting that the different sources of barium and the interrelations between these sources restrain the use of barium as a reliable paleoproductivity proxy under specific conditions only.

Copper, Ni and Zn are known to be sensitive to both changes in redox conditions and surface productivity (Calvert and Pedersen, 1993). In the western Indian Ocean, these abundance of trace metals can be related to surface productivity changes as evidenced by the positive correlations observed between the Cu/Al, Ni/Al, and Zn/Al ratios on one side and the Si/Al ratio

and the $CaCO_3$ content on the other side. On the contrary, negative correlations are observed between the Cu/Al, Ni/Al, and Zn/Al ratios on one side and the TOC content, the bulk MAR and the Ti/Al ratio on the other side, despite the isolated location of Core MD 90929. At an individual site scale, the comparison of the variations of the Cu/Al, Ni/Al, and Zn/Al ratios with those of the "direct proxies" at each site shows no characteristic sedimentation pattern, except for Core MD 90929 where the positive correlation of the Cu/Al, Ni/Al, and Zn/Al ratios with the Ti/Al ratio indicates that the origin of the enrichment of the sediment in Cu, Ni, and Zn is clearly related to the increase of terrigenous inputs. Both cores MD 90929 and 90940 were recovered in the pelagic domain, and the corresponding sites are located in a seemingly homogeneous environment. Marked differences affect, however, these sites, especially the geochemical nature of the terrigenous inputs. The geochemical record, through the normalized ratios permits, thus, to highlight differences in the sedimentary processes occurring in a apparently homogeneous domain.

The redox conditions may strongly influence the message carried by the trace elements, and limit their use as paleoproductivity proxies. The variations of the redox conditions can be estimated at the individual core scale through the variations of the Mn/Al and V/Al ratios. Their opposite behavior may help to precise the conditions of deposition: it is generally considered that the sediment is enriched in Mn under oxic conditions, while it is enriched in V under reducing ones (Calvert and Pedersen, 1993; Thomson et al., 1993; 1995; De Lange et al., 1994; Van Santvoort et al. 1996). In the western Indian Ocean, the situation is not that clear. Core MD 921002 (Gulf of Aden) presents a particular record: its sediment is significantly enriched in both Mn and V. Such an enrichment in both these trace metals may be related to the location of Core MD 921002, under the influence of the outflow from the Red Sea Water (Ouahdi, 1997b). Previous studies have shown that sediments from the Red Sea contains vanadium-enriched magnetites (Jedwab et al., 1989). The presence of such minerals in the sediment of core MD 921002 could be responsible for the high V content recorded at this site. Manganese can be released by hydrothermal vents, and such vents are known to be active in the Red Sea (Clément and Giannesinni, 1998). The southward decrease of the enrichment of the sediment in these trace metals strengthens this hypothesis (Fig. 3m, n). The relative high value of both the Mn/Al and V/Al ratios observed in Core MD 85664 may be related to the depth where this core was recovered (740 m), that is close to the depth where the water mass from the Red Sea flows southward (800-1500 m) (Caulet et al., 1988). The correlations of both these trace elements with

$CaCO_3$, Si/Al and Ti/Al are rather similar, but differences are observed in the response of these trace metals to TOC and bulk MAR variations. As said before, both these "direct proxies" may reflect the redox conditions. The comparison between the values of the Mn/Al and Ti/Al ratios separates the pelagic sites (high Mn/Al ratio) from the others. This observation is consistent with the more reducing conditions that generally occur under upwelling areas and sites with a relatively high bulk MAR. The correlation of the variations of both the Mn/Al and V/Al ratios with the redox conditions are, thus, recognized at a regional scale, but this correlation is disturbed by the inputs of both these trace metals in the Somali Basin from the Red Sea through the Gulf of Aden.

core number	CaCO3	COT	COT/Al	Si/Al	bulk MAR
ODP site 724	biogenic terrigenous	-	-	terrigenous	terrigenous upwelling
MD 85664	biogenic terrigenous	detrital	carbonate	biogenic terrigenous	terrigenous
MD 921002	biogenic terrigenous	detrital biogenic	carbonate opal	terrigenous biogenic	terrigenous biogenic
ODP site 722	biogenic terrigenous	-	-	terrigenous	biogenic terrigenous upwelling
MD 90929	biogenic	-	-	biogenic	carbonate
MD 85682	biogenic terrigenous	biogenic detrital	opal	biogenic terrigenous	upwelling terrigenous biogenic
MD 962073	biogenic terrigenous	biogenic detrital	opal	biogenic terrigenous	upwelling terrigenous biogenic
MD 90940	biogenic	-	-	-	carbonate
MD 85668	biogenic terrigenous	detrital	carbonate	biogenic terrigenous	biogenic terrigenous
MD 85674	biogenic terrigenous	Biogenic detrital	opal carbonate	biogenic terrigenous	terrigenous upwelling biogenic

Table 4: Origin of the main signal carried by $CaCO_3$, TOC, TOC/Al, Si/Al, and Ti/Al in each site.
- : no data available.

The use of the "direct proxies" allows to recognize the main sedimentation patterns in this region of the western Indian Ocean. Despite some exceptions, such as the correlation between Si/Al and TOC/Al in the cores located under the upwelling gyres in the Somali Basin, the behavior of these geochemical proxies is not significantly different from one site to the others. Moreover, for every proxy, no threshold value can be determined and it is, thus, impossible to separate the cores into well-defined groups (terrigenous-influenced, upwelling-influenced, pelagic) with these proxies. Comparison of geochemical markers allows, however, to isolate Core MD 90929 because of its very high Ti content, and ODP site 724 due to its high bulk MAR. The different sources of the "direct proxies" are summarized in Table 4.

Resulting interpretation from such a comparison of the geochemical record, both at regional and individual site scales does not supply very accurate tools to classify the sites. The location of the sites, as well as the studies already realized upon them, were used to cluster the sites into pre-defined groups: the pelagic cores, the terrigenous-influenced sites, and the sites located under high productivity areas. The results of this geochemistry-grounded comparison barely allow distinguishing between these groups. This is related to the absence of threshold values that clearly separate the cores, and to the absence of significant differences of the geochemical behavior at each site. According to these results, it is impossible to accurately define either characteristic limit values nor typical geochemical response for each group of sites. Three sites were considered as being located in the pelagic domain: cores MD 85668, 90929, and 90940. The geochemical interpretation of these sites produces no common and coherent geochemical response. Core MD 85668 is subjected to terrigenous inputs. These inputs are relatively low, but they are significant enough to disturb the pelagic sedimentation (Tribovillard et al. 1996; Jacot Des Combes et al., in press). Sedimentation in Core MD 90929 appears to be influenced by sediments originating from the southern part of the Indian Ocean. These southern inputs are characterized by a strong association between Ti and other trace elements, such as Ba, Cu, Ni, V, and Zn. Core MD 90940 is a true pelagic core, where the terrigenous inputs are neglectible (Jacot Des Combes et al., in press). On the other hand, the geochemical record confirms the differences already observed between the Socotra gyre and the Somali gyre (Ouahdi, 1997a). The Mg/Al and Mg/Ca ratios, that separates the terrigenous-influenced cores from the biogenic-influenced ones, indicates that Core MD 85674, located under the Somali gyre, is in the terrigenous group, while cores MD 85682 and 962073 are in the biogenic one. According to the results obtained on the ten sites, we may conclude that, in this region of the

western Indian Ocean, the sediment material is relatively homogeneous from a lithological point of view, but more subtle processes controlling the sedimentation vary from one site to the other, inducing differences in the geochemical composition of the sediment. The sites located at the limits of the Somali Basin testify of the influence of inputs of sedimentary material from fairly distinct sources.

Conclusions

This study concerns various sites from different oceanic environments from the western Indian Ocean, from 18°N to 6°S. It illustrates that the major and trace element data may provide useful information to characterize the deposition and accumulation processes at each site. However, a wide range of geochemical proxies is necessary to discriminate unambiguously the sites representative of three oceanic environments: truly pelagic, more or less influenced by land-derived supply, and influenced by upwelling systems, because the accumulation pattern of most of them may be influenced by processes, different at each site, and because te oceanic environments are too complex to be monitored by only one element.

The geochemical record in this area mainly results in a transition between the more pelagic cores and the more terrigenous or biogenic cores. Few proxies clearly separate the cores into well defined groups. The Mg/Ca, Mg/Al, and P/Al allow, however, to unambiguously distinguish the terrigenous-influenced sites from the biogenic-influenced ones, both in the pelagic and coastal domains. Apart from these three proxies, the geochemical record does not show threshold values, or particular behavior that may be used to determine the characteristics of the sedimentation in a specific environment (pelagic, terrigenous- or upwelling-influenced).

On the regional scale, the geochemical record is, however, rather homogeneous in the northwestern Indian Ocean, and permits to identify the cores subjected to external sources of material. Core MD 90929 records a southern source of material, Core MD 921002 is subjected to V and Mn input from the Red Sea water, and the ODP sites, located in the Arabian sea are influenced by a specific quartz-rich detrital source.

Within one single group of these ones, the geochemical record varies markedly from one core to one another, even if the sedimentary facies look identical. This means that the geochemical record is a parameter too sensitive, hence too variable, to unravel, alone, the numerous mechanisms affecting a broad region of the oceanic, pelagic environment.

Additionally, the variability of the geochemical record tends to show that it is not possible to envisage even relatively small parts of the western Indian Ocean as homogeneous pelagic units. This should be taken in consideration for ocean-scale modeling.

Due to different processes, e.g. changes in the material supply, rapid decay of marine organic matter or changes in the redox conditions, the sediment response to the surface productivity is difficult to monitor, especially in the coastal areas, where both the biogenic and terrigenous input are involved in the deposition and accumulation. The wide range of geochemical proxies used in this study provides useful information to reconstruct changes in the sediment response, and the association of these geochemical proxies with biologic markers may help to reconstruct the variations in paleoproductivity and paleoceanographic conditions, and, thus, to make the interpretation of the sediment response more accurate.

References

Barton, E.D. and Hill, A.E., 1989. Abyssal flow through the Amirante Trench (Western Indian Ocean). *Deep Sea Res.*, 36: 1121-1126.

Bishop, J.K.B., 1988. The barite-opal-organic carbon association in oceanic particulate matter. *Nature*, 332: 341-343.

Brumsack, H.J., 1980. Geochemistry of Cretaceous black shales from the Atlantic Ocean (DSDP Legs 11, 14, 36 & 41). *Chem. Geol.*, 31: 1-25.

Brumsack, H.J.and Gieskes, J.M., 1983. Interstitial water trace-elements geochemistry of laminated sdiments of the Gulf of California (Mexico). *Mar. Chem.*, 14: 83-97.

Brumsack, H.J., 1986. Geochemistry of Cretaceous black shales (DSDP Leg 41) in comparison to modern upwelling sediments from the Gulf of California. In: C.P. Summerhayes and N.J. Shackelton (Editors), North Atlantic paleoceanography. Geol. Soc. Spec. Publ., 21: 447-462.

Calvert, S.E. and Pedersen, T.F., 1993. Geochemistry of recent oxic and anoxic sediments: Implications for the geological record. *Mar. Geol.*, 113: 67-88.

Caulet, J.P., Debrabant, P. and Fieux, M., 1988. Dynamique des masses d'eau océaniques et sédimentation quaternaire sur la marge d'Afrique de l'est et dans le Bassin de Somalie. Résultats préliminaires de la mission MD 44-INDUSOM du "Marion-Dufresne". C.R.A.S. Paris, Série II, 17:281-288.

Caulet, J.P., Clément, P. and Giannesinni, P.J., 1992. GEOCORES : Inventaire informatisé des roches et sédiments marins conservés au Muséum National d'Histoire Naturelle. *Bull. Mus. natl. Hist. nat.*, 14: 93-136.

Clemens, S.C. and Prell, W.L., 1991. One million year record of summer monsoon winds and continental aridity from the Owen Ridge (site 722) Northwest Arabian Sea. In: Prell W.L. et al. (Editors), Proc. ODP, Sci. Res., 117: 365-368.

Clément, P. and Giannesinni, P.J. 1998. Lessédiments metallifères des fosses Atlantis II, Néréus et Comission I de la Mer Rouge. Campagne MD 29 du Marion Dufresne (1981). Collections Lithothèque marine du Muséum. *Géodiversitas*, 20: 153-228.

Collier, R. and Edmond, J., 1984. The trace element geochemistry of marin biogenic particulate matter. *Progress in Oceanography*, 13: 113-199.

De Lange, G.J., Van Os, B., Pruysers, P.A., Middelburg, J.J., Castadori, D., Van Santvoort P., Muller, P.J., Eggenkamp, H. and Prahl, F.G., 1994. Possible early diagenetic alteration of paleo-proxies. In: Iahn et al. (Editors), Carbon cycling in the glacial ocean: constraints on the ocean role on global change. Quantitative approaches in paleoceanography. NATO ASI Series, serie 1, Global Environment Changes, 17:225-258.

Dean, W.E., Gardner, J.V. and Piper, D.Z., 1997. Inorganic geochemical indicators of glacial-interglacial changes in productivity and anoxia on the California continental margin. *Geochim. Cosmochim. Acta*, 61 (21): 4507-4518.

Dehairs, F., Chesselet, R. and Jedwab, J., 1980. Discrete suspended particles of barite and barium cycle in the open ocean. *Earth Planet. Sci. Lett.*, 49: 528-550.

Dehairs, F., Lambert, C.E., Chesselet, R. and Risler, N., 1987. The biological production of marine suspended barite and the baryum cycle in the Western Mediterranean Sea. *Biogeochemistry*, 4: 119-139.

Dehairs, F., Stroobants, N. and Goeyens, L., 1991. Suspended barite as tracer of biological activity in the Southern Ocean. *Mar. Chem.*, 35: 399-410.

Dymond, J., Suess, E. and Lyle, M., 1992. Barium in deep-sea sediment: A geochemical proxy for paleoproductivity. *Paleoceanography*, 7: 163-181.

Dymond, J., Collier, R., McManus, J., Honjo, S. and Manganini, S., 1997. Can the aluminium and titanium contents of ocean sediments be used to determine the paleoproductivity of the oceans ? *Paleoceanography*, 12: 586-593.

El Foukali H., 1995. Le contrôle paléoclimatique de la sédimentation quaternaire dans le bassin de Somalie (Océan Indien du Nord-Ouest). PhD thesis. Mus. Ntal. Hist. Nat., Paris, 214 p.

Francois, R., Honjo, S., Manganini, S.J. and Ravizza, G.E., 1995. Biogenic barium fluxes to the deep sea: Implications for paleoproductivity reconstruction. *Global Biogeochem. Cycles*, 9: 289-303.

Gingele, F. and Dahmke, A., 1994. Discrete barite particles and barium as tracers of paleoproductivity in south Atlantic sediments. *Paleoceanography*, 9: 151-168.

Goldberg, E.D. and Arrhenius, G.O.S., 1958. Chemistry of Pacific pelagic sediments. *Geochim. Cosmochim. Acta*, 13: 153-212.

Jacot Des Combes, H., Caulet, J.P., and Tribovillard N.P. Pelagic productivity changes in the equatorial area of the NW Indian Ocean during the last 400 kyr. *Mar. Geol.*, in press.

Jacot Des Combes, H., Tribovillard N.P., and Caulet, J.P. Paleoproductivity and paleoceanography changes in the Amirante Passage area (Equatorial Indian Ocean): 200 kyr of lower pelagic productivity. *Bull Soc. Geol. Fr.*, accepted.

Jedwab, J., Blanc, G. and Boulègue, J. 1989. Vanadiferous minerals from the Nereus Deep, Red Sea. *Terra Nova*, 1: 188-194.

Johnson, D.A., Schneider, D.A., Nigrini, C.A., Caulet, J.P. and Kent, D.V. 1989. Pliocene-Pleistocene radiolarian events and magnetostratigraphic calibrations for the tropical Indian Ocean. *Mar. Micropal.*, 14: 33-66.

Johnson, G.C. and Damuth, J.E., 1979. Deep thermohaline flow and current-controlled sedimentation in the Amirante Passage: Western Indian Ocean. *Mar. Geol.*, 33: 1-44.

Jones, B., and Manning, D.A.C., 1994. Comparison of geochemical indices used for the interpretation of paleoredox conditions in ancient mudstones. *Chem. Geol.*, 114: 111-129.

Lea, D.W. and Spero, H.J., 1994. Assessing the reliability of paleochemical tracers: Barium uptake in the shells of planktonic foraminifera. *Paleoceanography*, 9: 445-452.

Leclaire L., 1974. Late Cretaceous and Cenozoic pelagic deposits-Paleoenvironment and paleoceanography of the central western Indian Ocean. In; Simpson, E.S.W. and Schlich, R. (Editors), Proc. ODP, Init. Rep., 25: 481-513.

Lyle, M., Heath, G.R. and Robbins, J.M., 1984. Transport and release of transition elements during early diagenesis: Sequential leaching from MANOP sites M and H. Part I: pH 5 acetic acid leach. *Geochim. Cosmochim. Acta*, 48: 1705-1715.

Martinez, P. 1997. Paléoproductivités du système d'upwellings nord-ouest africain et variations climatiques au cours du Quaternaire terminal. Ph.D thesis, Université de Bordeaux I, 298 pp.

Murray, D.W. and Prell, W.L., 1991. Pliocene to Pleistocene variations in calcium carbonate, organic carbon, and opal on the Owen Ridge, Northern Arabian Sea. In: Prell W.L. et al. (Editors), Proc. ODP, Sci. Res., 117: 343-365.

Ouahdi, R., 1997a. Variations de la productivité au nord-ouest de l'Océan Indien lors des derniers 70 000 ans dans l'upwelling de Socotra et de Somalie: Enregistrements géochimiques. *Bull. Soc. Géol. Fr.*, 168: 93-107.

Ouahdi, R., 1997b. Paléocéanographie et paléoproductivité liées à la mousson indienne dans le bassin de Somalie, le Golfe d'Aden et la Mer Rouge durant les derniers 460 000 ans. PhD Thesis, Mus. Ntal. Hist. Nat. 165 pp.

Paytan, A. and Kastner, M., 1996. Benthic Ba fluxes in the Central Equatorial Pacific, implications for the oceanic Ba cycle. *Earth Planet. Sci. Lett.*, 142: 439-450.

Prell W.L., Niitsuma, N. and LEG ODP 117 Shipboard scientific Party, 1989. Proceedings of the ODP, Initial Reports., 117: 255-319, and 385-419.

Shimmield, G.B., 1992. Can sediment geochemistry record changes in coastal upwelling paleoproductivity ? Evidence from Northwest Africa and the Arabian Sea. In: C.P. Summerhayes et al. (Editors), Upwelling systems: Evolution since the Early Miocene, Geol. Soc. Spec. Publ., 64: 9-46.

Shimmield, G.B. and Mowbrays, R., 1991. The inorganic geochemical record of Northwestern Arabian Sea: A history of productivity variation over the last 4,000 ky from sites 722A and 724. In: Prell W.L. et al. (Editors), Proc. ODP, Sci. Res., 117: 409-429.

Shimmield, G.B., Derrick, S., Mackensen, A., Grobe, H. and Pudsey, C., 1994. The history of barium, biogenic silica and organic carbon accumulation in the Weddel Sea and the Antarctic Ocean during the last 150,000 years. In: R. Iahn et al. (Editors), Carbon cycling in the glacial ocean: constraints on the ocean role in global change. Quantitative approaches in paleoceanography. NATO ASI Series (1): Global environmental changes, 17: 555-574.

Stroobants, N., Dehairs, F., Goeyens, L., Vanderheidjen, N. and Van Grieken, R., 1991. Barite formation in the Southern Ocean water column. *Mar. Chem.*, 35: 411-421.

Thomson, J., Higgs, N.C., Croudace, I.W., Colley, S. and Hydes, D.J., 1993. Redox zonation of elements at an oxic/post-oxic boundary in deep-sea sediments. *Geochim. et Cosmochim. Acta*, 57: 579-595.

Thomson, J., Higgs, N.C., Wilson, T.R.S., Croudace, I.W., De Lange, G.J. and Van Santvoort, P.J.M. , 1995. Redistribution and geochemical behaviour of redox sensitive elements around S1, the most recent eastern Mediterranean sapropel. *Geochim. et Cosmochim. Acta*, 59: 3487-3501.

Torres, M.E., Brumsack, H.J., Bohrman, G. and Emeis, K.C., 1996. Barite fronts in continental margin sediments: a new look at Ba remobilization in the zone of sulfate reduction and formation of heavy barite in diagenetic fronts. *Chem. Geol.*, 127: 125-139.

Tribovillard, N.P., Caulet, J.P., Vergnaud-Grazzini, C., Moureau, N. and Tremblay, P., 1996. Lack of organic matter accumulation on the upwelling-influenced Somalia margin in a glacial-interglacial transition. *Mar. Geol.*, 133: 157-182.

Turekian, K.K. and Wedepohl, K.H., 1961. Distribution of the elements in some major units of the Earth's crust. *Geol. Soc. Am. Bull.*, 72: 175-191.

Van Os, B.J.H., Middelburg, J.J. and De Lange, G.J., 1991. Possible diagenetic mobilization of barium in sapropelic sediment from the eastern Mediterranean. *Mar. Geol.*, 100: 125-136.

Van Santvoort, P.J.M., De Lange, G.J., Thomson, J., Cussen, H., Wilson, T.R.S., Krom, M.D. and Ströhle, K., 1996. Active post-depositional oxidation of the most recent sapropel (S1) in sediments of the eastern Mediterranean sea. *Geochim. et Cosmochim. Acta*, 60: 4007-4024.

Vénec-Peyré, M.T., Caulet, J.P. and Vergnaud-Grazzini, C., 1995. Paleohydrographic changes in the Somali Basin (5°N upwelling and equatorial areas) during the last 160 kyr, based on correspondence analysis of foraminiferal and radiolarian assemblages. *Paleoceanography*, 10: 473-491.

Von Breymann, M.T., Emeis, K.C. and Suess, E., 1992. Water depth and diagenetic constraints on the use of barium as a paleoproductivity indicator. In: C.P. Summerhayes et al. (Editors), Upwelling systems: Evolution since the Early Miocene, Geol. Soc. Spec. Publ., 64: 273-284.

Weedon, G.P. and Shimmield, G.B., 1991. Late pleistocene upwelling and productivity variations in the Northwestern Indian Ocean deduced from spectral analyses of geochemical data from sites 722 and 724. In: W.L. Prell et al. (Editors), Proc. ODP, Sci. Res., 117: 431-440.

Zahn, R. and Pedersen, T.F., 1991. Late Pleistocene evolution of surface and mid-depth hydrography at the Oman Margin: planktonic and benthic isotope records. In: Prell W.L. et al. (Editors), Proc. ODP, Sci. Res., 117: 291-308.

CONCLUSIONS GÉNÉRALES

Une reconstruction des variations de la paléoproductivité dans l'océan Indien occidental durant les derniers 300 000 ans est proposée à partir de l'utilisation conjointe de marqueurs géochimiques et biologiques, appliquée à trois sites du basin de Somalie. Afin de déterminer les variations de la productivité de surface dans l'océan ouvert, deux sites ont été choisis dans le domaine pélagique : l'un sur la ride de Madingley (au nord-est des Seychelles) et le second dans le passage des Amirantes (au sud-ouest des Seychelles). Un autre site, situé dans l'upwelling de Socotra, a été étudié pour reconstruire les variations de la paléoproductivité en domaine d'upwelling. Les résultats obtenus ont été comparés à d'autres données concernant la région afin d'établir une synthèse de l'enregistrement géochimique de la paléoproductivité à l'échelle régionale.

Fiabilité des marqueurs de la paléoproductivité

Les marqueurs géochimiques

Le taux de sédimentation global ou "bulk MAR" est considéré comme un bon indicateur des variations de la paléoproductivité en domaine pélagique. Sur la ride de Madingley comme dans le passage des Amirantes, ses variations sont très bien calquées sur celles marqueurs biologiques comme les index à radiolaires, qui sont des indicateurs de la paléoproductivité de surface. Le lien entre le bulk MAR et la productivité de surface est du à l'absence, ou à l'insignifiance, d'autres sources de matériel sédimentaire, notamment terrigène. Dans les sites plus côtiers, le bulk MAR enregistre aussi bien les variations de la paléoproductivité que celles des apports terrigènes et ne peut plus être utilisé comme un marqueur de la paléoproductivité.

En domaine pélagique, le $CaCO_3$ représente le constituant majeur du sédiment et les flux de $CaCO_3$ peuvent être utilisés comme marqueurs de la paléoproductivité sous condition que la dissolution ne modifie pas le signal. L'ensemble des résultats montre que dans le bassin de Somalie, pour les profondeurs considérées, la dissolution des carbonates n'est pas le principal

facteur contrôlant les variations des teneurs en $CaCO_3$ ni la composition des assemblages planctoniques carbonatés.

Régionalement, le marqueur le plus direct pour estimer la paléoproductivité est l'enrichissement des sédiments en matière organique. Les deux sites pélagiques (ride de Madingley et passage des Amirantes) sont caractérisés cependant par un sédiment très pauvre en matière organique. Dans ces deux sites, les teneurs en COT sont inférieures à la limite de détection de l'appareil (0,02%). La nature très labile de cette matière organique, la productivité de surface relativement faible ainsi que le faible taux de sédimentation amènent à une dégradation complète du contenu organique et à l'absence de COT dans le sédiment. Dans les sites situés plus près des côtes, avec un taux de sédimentation plus important, les teneurs en COT deviennent détectables. Le message porté par l'enrichissement en COT du sédiment n'a donc été étudié en détail que sur le site du tourbillon de Socotra et dans les sites impliqués dans la comparaison à l'échelle régionale. Les palynofaciès réalisés sur certains échantillons provenant de différents sites dans le bassin de Somalie indiquent que la matière organique présente dans les sédiments de cette région a deux origines distinctes. Une fraction du COT est d'origine marine et se présente sous forme de résidus planctoniques identifiables, de scolécodontes et/ou sous forme d'un gel amorphe. Une autre fraction du COT est d'origine terrigène, et composée de débris de plantes supérieures (grains de pollen, cuticules, fragments ligneux). L'importance relative de chacune de ces deux composantes de la matière organique est difficile à déterminer et peut varier significativement d'un échantillon à l'autre, et d'un site à l'autre. L'observation des préparations de palynofaciès peut permettre d'estimer la part de COT terrigène mais, à l'exception de certains sites où la part de l'une des composantes est insignifiante, l'estimation quantitative de la proportion de matière organique marine est hors de portée. Les variations du rapport COT/Al ont donc été utilisées pour reconstruire les variations de la paléoproductivité marine. Leur bonne corrélation avec l'enrichissement en silice dans les sites d'upwelling permet d'utiliser le rapport COT/Al comme un marqueur de la paléoproductivité dans ces environnements particuliers. La matière organique semble également être associée à un cortège d'éléments chimiques (Ba, P, Cu, Ni et Zn). Cette association ne se retrouve pas dans le passage des Amirantes où ces métaux sont liés au cortège terrigène. Sur la ride de Madingley, où les teneurs en COT sont négligeables et où les données sur la silice ne sont pas disponibles, la réponse géochimique à la paléoproductivité semble similaire à celle observée dans l'upwelling de Socotra. Les autres sites étudiés lors de la comparaison à l'échelle

régionale présentent également des associations particulières entre la matière organique et les éléments en traces. On peut toutefois remarquer que les teneurs en COT des sédiments prélevés sous l'upwelling de Somalie-Socotra sont faibles comparées à celles mesurées dans les autres upwellings. Ce faible taux de COT peut être lié au caractère saisonnier de l'upwelling, qui n'est actif que pendant l'été boréal, mais aussi aux conditions de préservation de la matière organique au fond. Les eaux de fond étant oxydantes dans cette région, la dégradation de la matière organique la plus labile va diminuer l'accumulation de COT. Les conditions de préservation de la matière organique vont toutefois varier d'un site à l'autre. L'absence de matière organique dans les sites pélagiques est ainsi due à plusieurs facteurs. Premièrement, la relativement faible productivité de surface, ensuite la nature de cette matière organique, très labile et donc très rapidement dégradée. Enfin, certaines conditions ne favorisent pas la préservation de cette matière organique, comme le faible taux de sédimentation permettant un contact prolongé entre le COT déposé et l'eau de fond. Sous l'upwelling de Socotra, le taux de sédimentation est plus important et limite donc ce contact. D'autre part, une partie de la matière organique déposée à ce site est d'origine terrigène, et est donc plus résistante à la dégradation que la matière organique marine. Les conditions suboxiques principalement observées à ce site pour l'intervalle de temps considéré indiquent cependant que la matière organique déposée à ce site a subi une dégradation partielle.

La bonne corrélation entre le rapport Si/Al et le rapport COT/Al indique que le rapport Si/Al peut être utilisé comme un marqueur de la paléoproductivité. Toutefois, dans d'autres sites, localisés en mer d'Arabie, l'enrichissement en silice semble être lié à l'augmentation des teneurs en quartz du sédiment.

L'emploi du baryum comme marqueur de la productivité doit être manié avec précaution, car il existe de profondes disparités entre les différents processus liés à l'accumulation du baryum dans le sédiment. La répartition du baryum dans les diverses fractions du sédiment est différente dans les trois sites pélagiques pour lesquels ce type de données était disponible. Principalement d'origine biogène sur la ride de Madingley, le baryum est presque exclusivement d'origine terrigène dans le site pélagique du bassin de Somalie et participe des deux dans le passage des Amirantes. Les différents résultats indiquent que l'utilisation du baryum comme marqueur de la paléoproductivité est délicate et que les teneurs en baryum du sédiment total ne sont pas systématiquement liées à la production de surface, même dans le domaine pélagique où les apports terrigènes ne sont pas significatifs. Là encore, l'utilisation de cet élément dans la

reconstruction de la paléoproductivité sera limitée à certains sites. Le phosphore semble être un marqueur plus fiable, puisque dans la plupart des sites où ses teneurs ont été mesurées, les variations du rapport P/Al covarient avec celles des rapports COT/Al et/ou Si/Al.

Le message porté par Cu, Ni, et Zn est également lié à la productivité de surface, mais la relation est moins directe. En effet, d'une part les variations d'abondance de ces trois métaux peuvent être légèrement influencées par les modifications des conditions redox, ce qu'on observe dans l'upwelling de Socotra; d'autre part, la présence de ces éléments chimiques dans ou sur certains minéraux détritiques peut perturber l'enregistrement des variations de la paléoproductivité par ces métaux.

Les marqueurs biologiques

Les marqueurs biologiques utilisés dans cette thèse sont des index à radiolaires (TSRI, ou rad ratio, et URI) basés sur des rapports d'abondance d'espèces, caractéristiques de masses d'eau bien précises (eaux de surface, thermocline, upwelling).

Dans le domaine pélagique, où la colonne d'eau est bien stratifiée, le TSRI (ou rad ratio) est utilisé pour reconstruire les variations de la paléoproductivité de surface. Cet index correspond au rapport de l'abondance des espèces de radiolaires vivant à la profondeur de la thermocline (200 à 500 m) à celle des espèces caractéristiques de la couche de surface (0-100 m). Cet index, bien adapté au milieu pélagique, donne de bons résultats sur la ride de Madingley et dans le passage des Amirantes, où ses variations sont parallèles à celles du taux de sédimentation global. En revanche, cet index n'est pas utilisable en domaine d'upwelling, où la remontée d'eaux semi-profondes vers la surface fait disparaître la thermocline et donc la stratification des eaux de surface et subsurface.

Dans ces environnements d'upwelling, l'index TSRI est remplacé par URI, qui traduit l'importance des espèces de radiolaires caractéristiques de ces zones par rapport au reste des populations. Cet index a déjà été utilisé sur les deux tourbillons de la côte somalienne et les résultats des études précédentes montrent que, si les variations d'URI reflètent celles de l'intensité de l'upwelling de Somalie, il n'en est pas de même pour l'upwelling de Socotra.

D'une manière générale, le point fort de cette étude sur la fiabilité des marqueurs est la mise en évidence de l'absence d'un marqueur universel de la paléoproductivité dans cette région,

qu'il soit de nature géochimique ou biologique. Lorsque l'on compare les résultats obtenus sur les trois sites étudiés à des données précédemment publiées, on peut observer que les conditions locales de dépôt sont prépondérantes par rapport aux changements globaux dans la réponse des sédiments aux variations de la paléoproductivité. Certains marqueurs, tels que l'index TSRI, et les rapports Ba/Al et P/Al, donnent néanmoins de bons résultats et seule l'analyse conjuguée de plusieurs marqueurs géochimiques et biologiques permet de reconstruire d'une manière satisfaisante les variations de la paléoproductivité.

Les apports continentaux

Outre les variations de la paléoproductivité, le sédiment enregistre également les fluctuations des apports terrigènes, notamment grâce aux marqueurs géochimiques comme Al et Ti. Dans le domaine pélagique, les apports terrigènes sont très faibles (Al < ou << 4%) et les vents sont leur principal vecteur. Les variations des apports éoliens dans l'océan Indien du nord-ouest sont estimées par les fluctuations des rapports Ti/Al et Mg/Ca. Le premier rapport traduit l'importance des minéraux lourds dans le sédiment, et donc la force des vents porteurs. Le second traduit l'importance de la dolomite et autres calcaires magnésiens, qui sont d'origine continentale et non marine (zones de sebkhas de la péninsule arabique, voire des domaines plus méridionaux).

Dans les sites pélagiques du bassin de Somalie, on peut observer une bonne corrélation entre ces deux marqueurs, indiquant une source unique, probablement éolienne, du matériel terrigène. La situation se complique à mesure que l'on se rapproche des côtes. Au niveau des sites localisés plus près de la côte somalienne, on observe une différenciation des deux enregistrements, impliquant deux sources différentes de matériel détritique. Dans la plupart des cas, le rapport Mg/Ca augmente plus vite, et de manière plus importante que le rapport Ti/Al. Ceci semble indiquer que l'apport en carbonates détritiques est plus important près des côtes, suggérant que le rapport Mg/Ca correspondrait plutôt à des apports détritiques liés au ruissellement sur les continents, puis aux descentes de matériel le long de la pente continentale, alors que le rapport Ti/Al serait majoritairement lié aux apports éoliens.

La comparaison des relations entre Ti et les autres éléments en traces permet également d'établir le contenu chimique de la fraction terrigène en mettant en évidence les différences chimiques dans le cortège terrigène, qui implique des différences de composition et donc

d'origine. Un cortège détritique particulier, associant Ti, Ba, Cu, Ni et Zn est ainsi mis en évidence dans le passage des Amirantes. Cette association d'éléments en traces n'a pas été observée dans les sédiments des autres sites étudiés, ni dans ceux des sites utilisés lors de la comparaison à l'échelle régionale. Il existe donc une source de matériel détritique différente pour la partie sud du bassin de Somalie qui provient des bassins des Mascareignes, de Madagascar ou de Crozet. Un phénomène comparable est observé dans les sédiments des deux sites de la mer d'Arabie étudiés lors de la comparaison à l'échelle régionale. Ces sites présentent une bonne corrélation entre les rapports Ti/Al et Si/Al qui suggère la présence dans ce sédiment d'une fraction non négligeable de quartz. Cette corrélation n'étant pas observée aux autres sites, cet apport de quartz doit correspondre à une source très localisée aux environs de ces deux sites, et à un vecteur non éolien, limitant "l'enrichissement" en quartz à une zone bien délimitée.

En résumé, les variations des apports terrigènes mettent en évidence des sources de matériel détritique différentes dans l'océan Indien du nord-ouest. La comparaison à l'échelle régionale des sites étudiés montre une relative homogénéité dans la composition du cortège terrigène dans tous les sites du bassin de Somalie. Cette homogénéité de composition est associée à une similitude des sources, ce qui revient à supposer que le matériel terrigène présent dans les sédiments du bassin de Somalie a une source commune. A la périphérie du bassin, les sources changent. Si le site de la ride de Madingley présente un cortège détritique similaire à celui rencontré dans le bassin de Somalie, le site du passage des Amirantes et ceux de la mer d'Arabie présentent des sources différentes de matériel terrigène.

Les conditions de dépôt

L'enregistrement géochimique de la paléoproductivité peut être perturbé par les modifications des conditions redox, qui régissent l'accumulation de certains éléments en trace (Ba, Mn, Mo, P, U, V) par une mise en solution et/ou la précipitation de certains composés. Certains éléments en traces (Mn, Mo, U et V) apparaissent plutôt comme des marqueurs des variations des conditions redox. Les résultats obtenus montrent que Mn et V peuvent être fortement influencés par les apports terrigènes, lorsque les conditions sont oxiques. Les éléments en traces Mo et U semblent donner des résultats plus fiables et plus précis, en particulier dans des environnements où les conditions deviennent plus réductrices.

Ces conditions redox peuvent être influencées par le taux de sédimentation. Toutefois, la comparaison des marqueurs géochimiques à l'échelle régionale montre une bonne corrélation entre les taux de sédimentation et la teneur en COT. Il est donc assez difficile de séparer, à certains sites, l'influence exercée sur les conditions redox par le taux de sédimentation, de celle exercée par la teneur en COT. C'est la raison pour laquelle les variations des conditions redox ont été estimées par l'intermédiaire de marqueurs plus précis, notamment Mn, Mo, U et V.

Le manganèse se dépose principalement dans le sédiment sous forme d'oxydes. Il est donc particulièrement sensible aux changement des conditions redox. L'accumulation et l'enrichissement du sédiment en manganèse sont donc généralement considérés comme indicateurs de conditions oxiques. Le problème soulevé par l'utilisation de ce métal est la possibilité de remise en solution des fronts de dépôt de Mn diagénétique lorsque les conditions redeviennent plus réductrices. Il y a donc un risque de perdre l'information stockée par ces fronts. C'est la raison pour laquelle les variations de l'accumulation de cet élément ont été étudiées conjointement avec celles du V, qui lui, se dépose préférentiellement en conditions réductrices.

La situation devient plus complexe le long de la côte de Somalie où les apports plus importants en matière organique, ainsi que le taux de sédimentation plus élevé, sont susceptibles de provoquer des variations rapides des conditions redox. Les risques de perte d'information liés à l'utilisation du Mn augmentent. D'autre part, lors de la comparaison de l'enregistrement géochimique à l'échelle régionale, une source de Mn et de V, localisée en Mer Rouge et faisant sentir ses effets le long de la côte est-africaine jusqu'à l'équateur est mise en évidence. Il est donc probable que les variations de Mn et de V dans le sédiment soient en partie induites par les variations de l'intensité du courant venant de la mer Rouge. Le site du tourbillon de Socotra se situant sur le trajet de l'eau de la mer Rouge, d'autres marqueurs, comme Mo et U, ont été utilisés pour reconstruire les variations des conditions redox sur ce site.

Les sédiments du tourbillon de Socotra contiennent de la matière organique et le taux de sédimentation enregistré à ce site est relativement important. Ceci peut induire des variations des conditions redox plus importantes que dans le milieu pélagique, et notamment l'occurrence de conditions de dépôt suboxiques à anoxiques. Les sédiments du site du tourbillon de Socotra présentent un léger enrichissement en U, mais pas en Mo, à l'exception de quelques intervalles d'enrichissement du sédiment en Mo, signe de conditions de dépôt anoxiques. Ces intervalles sont rencontrés pendant les stades interglaciaires 7 et 5 et correspondent à des périodes où les

apports en matière organique dans le sédiment étaient importants. Le léger enrichissement en U observé dans les sédiments de ce site durant tout l'intervalle de temps considéré indique que le dépôt s'est effectué sous des conditions légèrement suboxiques. Les alternances entre des périodes anoxiques et des intervalles suboxiques ne semblent toutefois pas perturber de manière significative l'enregistrement géochimique de la paléoproductivité à ce site.

En résumé, l'étude des conditions de dépôt montre que, dans les sites localisés en domaine pélagique, l'accumulation de sédiments s'est déroulée en conditions oxiques. Dans le tourbillon de Socotra, les conditions sont, en revanche, un peu plus réductrices, majoritairement suboxiques, avec quelques périodes anoxiques, probablement liées à un apport supplémentaire de matière organique. La comparaison des variations de conditions de dépôt à l'échelle régionale est rendue délicate par l'utilisation de marqueurs différents à chaque site, Mn et V en milieu pélagique, Mo et U sous l'upwelling de Socotra. Le long de la côte est-africaine, Mn et V ont été utilisés sur d'autres sites, mais les apports de ces métaux depuis la Mer Rouge ont pu provoquer des modifications de l'enregistrement des changements de conditions redox.

Variations de la paléoproductivité

Les principaux résultats de ce travail montrent que les intervalles de forte paléoproductivité relevés à chaque site ne sont pas synchrones sur l'ensemble du bassin de Somalie et des zones adjacentes. En ce qui concerne le domaine pélagique, une forte productivité est enregistrée pendant le stade isotopique interglaciaire 9 (de 340 à 330 ka) ainsi que durant les stades glaciaires 8, 6, 4 et 2 sur la ride de Madingley. En revanche, le site pélagique étudié dans le passage des Amirantes présente des pics de productivité aux transitions entre les stades 12 et 11, 9, 8 et 7, suivis par une période de faible productivité entre 238 et 38 ka. Dans l'upwelling de Socotra, la paléoproductivité a augmenté pendant les stades interglaciaires, principalement à 235 ka, entre 210 et 200 ka, à 170 ka, de 140 à 130 ka, de 110 à 100 ka, et de 50 à 40 ka. Des données préexistantes montrent également des périodes de forte productivité différentes par rapport aux sites de la région étudiés lors de ce travail. Le bassin de Somalie enregistre des périodes de forte accumulation carbonatée, probablement influencée par la productivité de surface pendant les stades isotopiques glaciaires 10 et 6, de 80 à 60 ka, et entre 25 et 5 ka. Dans l'upwelling de Somalie, des périodes de forte productivité sont reconnues durant les stades

isotopiques glaciaires 6 et 2, alors que, plus au nord, en mer d'Arabie la paléoproductivité a été plus forte pendant les stades isotopiques interglaciaires 9, 7, 5, 3 et 1.

Malgré ce manque apparent de synchronisme, certains intervalles de temps relativement larges peuvent être caractérisés par une plus forte paléoproductivité dans plusieurs sites de cette région. En adoptant pour chaque site le marqueur de paléoproductivité apparaissant comme le plus fiable, on peut dresser un tableau d'ensemble montrant les variations de la paléoproductivité à grande échelle pour les derniers 250 000 ans (Fig. 1). La comparaison des différents sites met en évidence des périodes de forte productivité communes à plusieurs sites comme à 235, 170, 140, 85, et 55 ka et aux périodes de transition 3/2 et 2/1. Cette homogénéité n'est toutefois qu'apparente : si les pics de productivité peuvent être communs à plusieurs sites, les périodes de productivité maximale ou minimale sont différentes pour chaque site. Ceci indique que chaque site possède une réponse qui lui est propre et suggère que les fluctuations de paléoproductivité de surface dépendent plus des variations des conditions locales que des changements climatiques globaux.

Il n'est donc pas possible d'établir dans cette région un schéma de variation de la paléoproductivité qui s'applique à un domaine spécifique: le domaine pélagique ou les systèmes d'upwelling. Que ce soit à l'échelle régionale où à une échelle plus grande, incluant des sites localisés dans le même domaine, les enregistrements géochimiques et biologiques de la paléoproductivité indiquent qu'elle a été influencée plus par les conditions locales que par les changements globaux. On peut toutefois remarquer que certains sites (ride de Madingley et upwelling de Socotra) présentent un pic de productivité aux alentours de 170 ka, qui pourrait correspondre au maximum d'insolation correspondant pour l'hémisphère nord. Mais là encore, tous les sites ne présentent pas ce pic et ceux qui sont concernés sont localisés dans des domaines très différents. L'occurrence d'intervalles plus productifs, tant en période glaciaire qu'interglaciaire, ainsi que l'absence de synchronisme entre ces intervalles et les périodes d'insolation maximale, confirment que les conditions locales, et non les changements climatiques globaux, sont responsables de ces variations de la productivité de surface. Tous les sites étant situés aux basses latitudes, on peut donc considérer que les différences d'insolation entre les sites n'ont pas une amplitude suffisante pour être à l'origine de ces disparités. Les variations de paléoproductivité seraient donc le reflet des variations de la circulation des masses d'eau profondes, semi-profondes et de surface dans cette région.

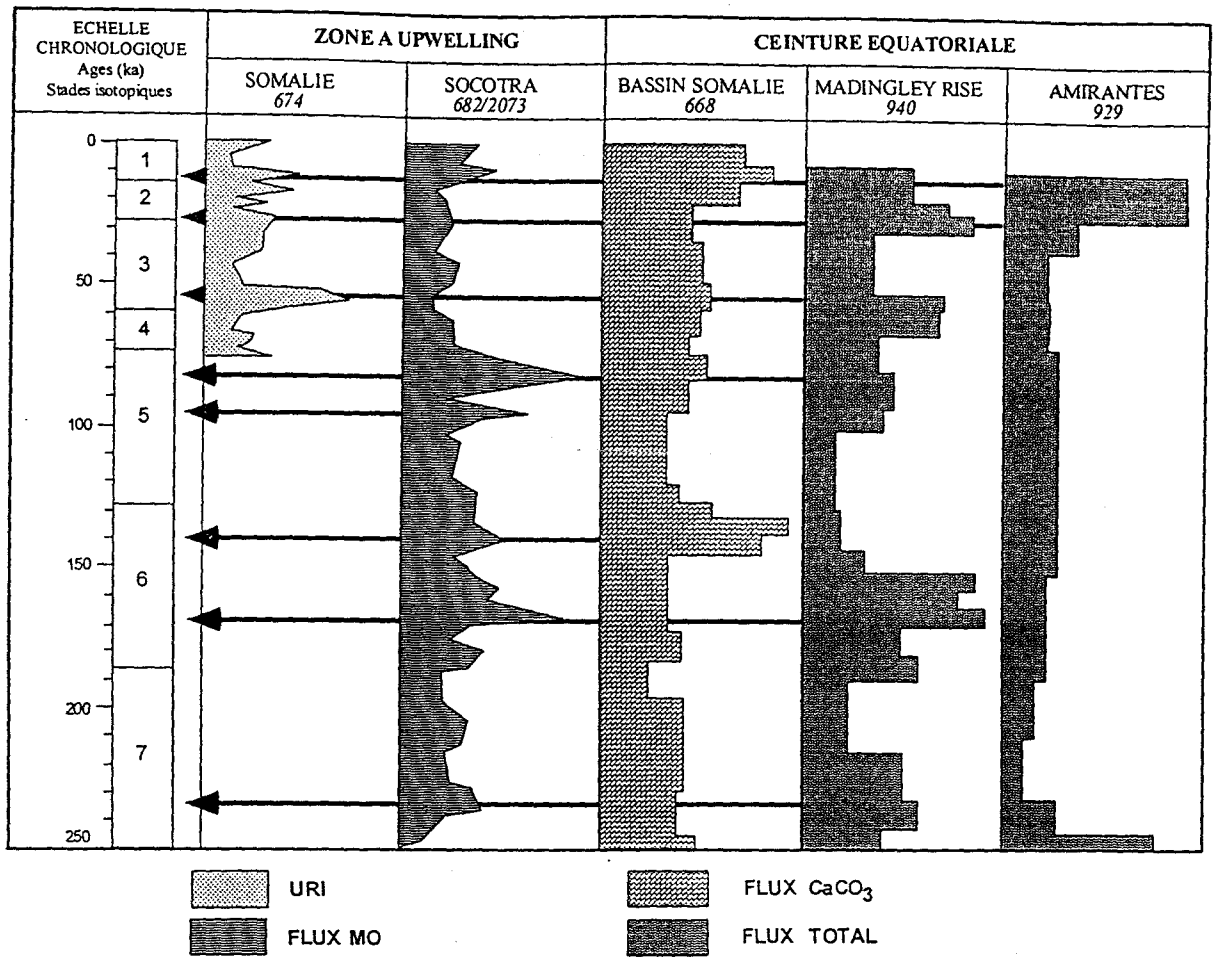

Figure 1. Comparaison des variations de la paléoproductivité dans 5 sites de l'Océan Indien occidental. Pour chaque site, a été choisi le marqueur le plus fiable des variations de la productivité. Les flèches indiquent les intervalles à productivité plus élevée sur un ou plusieurs sites.

Variations paléocéanographiques

L'interprétation des variations de paléoproductivité conduit à des hypothèses nouvelles sur les fluctuations de la distribution des masses d'eau dans l'océan Indien du nord-ouest.

Dans le domaine pélagique, le pic de productivité enregistré sur la ride de Madingley durant le stade 9 (de 340 à 330 ka) peut être expliqué par une moindre remontée vers le nord du contre-courant équatorial. De la même façon, la période de faible productivité enregistrée dans le passage des Amirantes peut être interprétée par un affaiblissement de l'oscillation saisonnière des systèmes de courants de surface entre leur position nord (été) et leur position sud (hiver). Cet affaiblissement résulterait dans le maintien au niveau du site étudié d'un tourbillon oligotrophique, isolé de la circulation équatoriale et, par conséquent, très appauvri en nutriments. Dans le domaine pélagique de l'océan Indien du nord-ouest, la paléoproductivité paraît donc être

sous le contrôle des oscillations des courants et contre-courants équatoriaux. Les variations de ces oscillations peuvent entraîner la mise en place de situations locales particulières aux sites localisés à la limite du système ou d'un de ses éléments, comme les tourbillons oligotrophiques reliant les courants nord- et sud-équatorial au contre-courant équatorial.

Dans l'upwelling de Somalie-Socotra, l'importance de la productivité de surface dépend majoritairement de l'intensité de l'upwelling, lui même contrôlé par la force de la mousson d'été. Les résultats obtenus montrent que l'advection verticale d'eaux de subsurface s'est maintenue pendant les derniers 250 000 ans. Les variations observées entre les tourbillons de Somalie et de Socotra indiquent, toutefois, que des différences hydrologiques existent entre ces deux sites. La structure hydrologique des upwellings crée des structures assez complexes en surface. Les images satellites montrent en effet que les zones où la productivité de surface est importante ne se présentent pas comme un domaine homogène mais comme un ensemble de mini-tourbillons et de filaments où la production de surface est beaucoup plus importante que dans les zones voisines de ces filaments. La position de ces espaces très limités géographiquement peut varier très vite, ce qui peut entraîner des fluctuations considérables dans les apports de matériel vers le fond. Les variations observées entre les deux upwellings peuvent résulter de la position différente des sites par rapport à ces filaments de forte productivité. Une autre hypothèse est liée à la différence des masses d'eau de fond baignant les deux sites, ce qui peut induire des modifications dans l'enregistrement des variations de la productivité et dans la préservation de cet enregistrement. Enfin, les différences dans les courants près du fond, principaux responsables des phénomènes d'advection latérale de matériel sédimentaire peuvent également induire des variations d'enregistrement du signal venu de la surface.

Les variations de la circulation de l'eau intermédiaire vont, dans les deux sites d'upwelling, influencer l'enregistrement des variations de la paléoproductivité plus que les variations elles même. Dans le bassin de Somalie, le processus le plus important aux profondeurs intermédiaires (800-1 500 m) est l'arrivée d'une masse d'eau en provenance de la mer Rouge et de la mer d'Arabie. Cette eau est plus salée et plus pauvre en oxygène que les eaux environnantes, elle va donc modifier les conditions de dépôt et de préservation de la matière organique sur les sites qu'elle baigne. D'autre part, l'étude d'une carotte située dans le golfe d'Aden montre un fort enrichissement en Mn et V qui pourrait être relié à la présence d'oxydes de Mn et de magnétites à V, provenant de la mer Rouge, dans le sédiment. On peut suivre la progression vers le sud de cette masse d'eau grâce aux sites localisés le long de la côte est-

africaine qui présentent une diminution de leurs teneurs en Mn et V vers le sud. Un seul site localisé sur l'équateur, montre des teneurs en Mn et en V très élevées par rapport à d'autres sites voisins. Cette situation peut être expliquée par la profondeur du site (744 m) qui est très proche de la profondeur de la masse d'eau de la mer Rouge et qui est donc plus sensible aux variations induites par cette masse d'eau que les carottes étudiées vers 3 000-4 000 m de profondeur. On peut suivre les variations des apports de cette masse d'eau grâce aux rapports Mn/Al et V/Al dans les sites localisés le long de la côte est-africaine, où ces données sont disponibles.

Le point fort de cette reconstruction paléocéanographique est donc la mise en évidence de la prépondérance des conditions océanographiques locales sur les variations climatiques régionales ou globales, et ce, même en domaine pélagique, réputé homogène. La création de zones géographiques restreintes (où les conditions sont très différentes de celles existant dans les zones voisines) par les variations de la circulation générale, notamment dans la couche de surface, limite la généralisation des effets des variations de circulation à toute un domaine océanique. Les modèles globaux d'évolution de la circulation océanique qui ne prendraient pas en compte les singularités locales ne peuvent, donc, en l'état actuel, fournir de reconstruction convaincante des paléocirculations et de la paléoproductivité.

Perspectives

Les résultats obtenus pendant ce travail ont permis de déterminer les variations de paléoproductivité dans la région du bassin de Somalie, mais également de mettre en évidence la grande hétérogénéité dans l'enregistrement de cette paléoproductivité. Cette hétérogénéité, que l'on retrouve aussi bien dans son origine que dans son enregistrement par les sédiments soulève plusieurs problèmes. La multiplication des marqueurs et leur comparaison, si elle donne de bons résultats, est également un bon indicateur de la complexité du système "production de surface-enregistrement sédimentaire" dans tous les domaines océaniques. Pour obtenir une meilleure estimation de la paléoproductivité et une reconstruction plus fiable de ses variations, il est donc nécessaire d'augmenter le maillage des prélèvements, c'est-à-dire étudier de nombreux sites avec une résolution suffisante pour enregistrer les variations mêmes rapides. La comparaison des résultats obtenus à partir de marqueurs indépendants permettra de mieux comprendre le message

sédimentaire et de reconnaître les différentes sources de perturbation de l'enregistrement de la paléoproductivité dans le sédiment.

Ces données montrent également que les cycles glaciaire-interglaciaire ne sont pas similaires. On ne peut donc pas généraliser la réponse géochimique ou biologique enregistrée pendant l'un de ces cycles à tous les autres. Chaque alternance climatique doit donc être considérée comme étant particulière, voire unique, et étudiée précisément afin d'obtenir une estimation fiable des conditions prévalant durant chaque stade isotopique. Certains événements comme les pics de productivité observés aux environs de 170 ka, et correspondant peut être à l'effet Dole, ont été enregistrés dans certains sites de cette région. Compte tenu de l'importance potentielle de ces évènements dans le cycle du CO_2 atmosphérique et donc dans les variations climatiques, cette période pourrait être étudiée plus précisément et à plus haute résolution, de façon à préciser sa durée, mais également afin de comprendre pourquoi cet événement est enregistré dans certains sites et pas dans d'autres. La même question se pose également pour l'intervalle de forte productivité enregistré à certains sites pendant le stade isotopique interglaciaire 9 (340-330 ka).

ANNEXES

ANNEXE 1 : **Logs lithologiques des carottes étudiées.**

ANNEXE 2 : **Résumés des interventions aux congrès**

ANNEXE 1

Carte Géologie Dépôts M.N.H.N.

SAMPLE : GS 90929 (1)

STATION : 20
Latitude : 6°. 59 S
Longitude : 52°. 03 E
Core Length : 15.35 m
Water Depth : 3070 m

Site: Passage des Amirantes.
Amirantes Passage

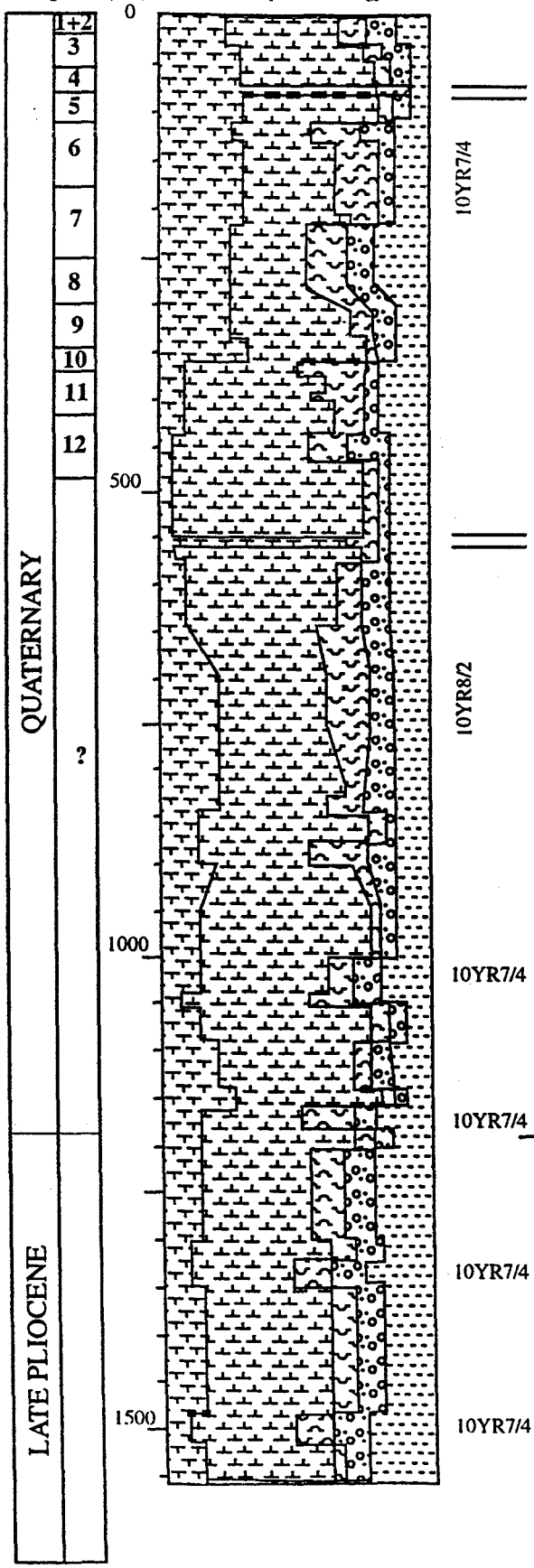

BOUES CALCAIRES beiges (10YR8/2) à brun clair (10YR7/4) avec coccolithes, foraminifères, discoasters (au dessous de 11.8m) et silice biogène (diatomées, radiolaires et spicules d'éponges).

CALCAREOUS OOZE beige (10YR8/2) to light brown (10YR7/4) with nannofossils, foraminifers, discoasters (below 11.8m) and biogenous silica (diatoms, radiolarians, and sponge soicules).

Isotopes Stages after H. Jacot des Combes et al., in press

Core Géologie Depository
M.N.H.N.

SAMPLE : GS 90940

STATION : 27
Latitude : 5°. 20 S
Longitude : 61°. 24 E
Core Length : 32 m
Water Depth : 4020 m

Site: Madingley Rise.
Océan Indien Central

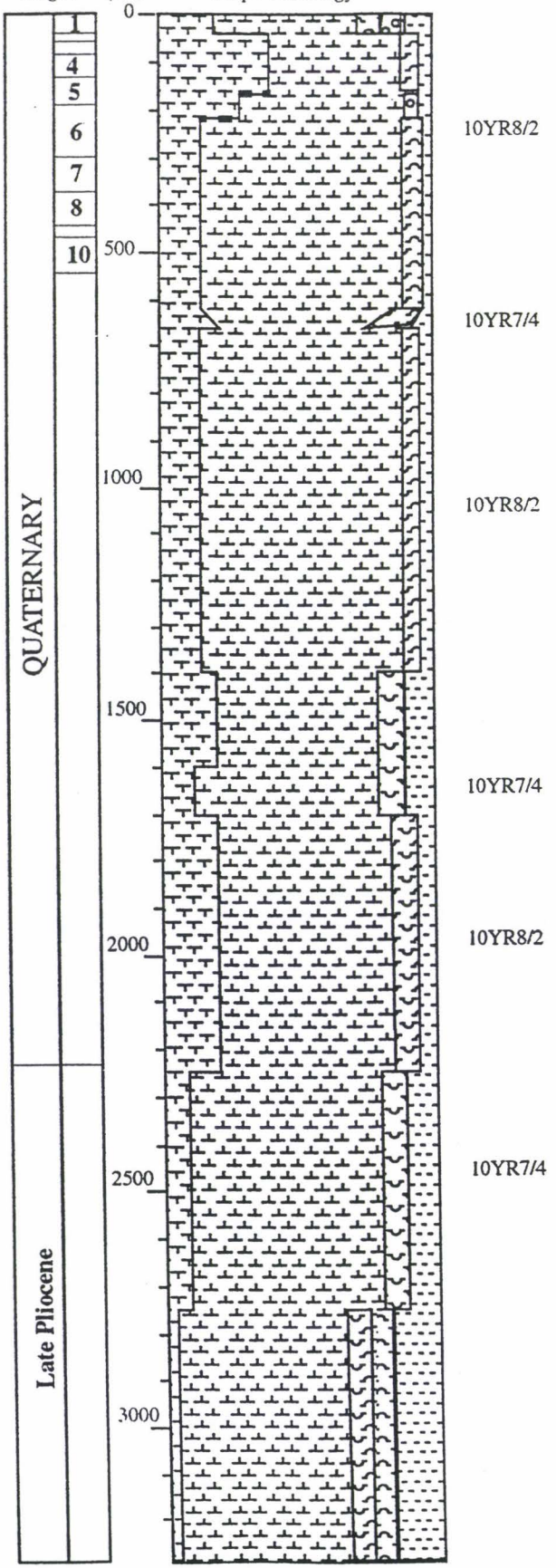

Lithologic description

BOUES CALCAIRES blanches (10YR8/2) à coccolithes et foraminifères.
Présence de cycles illustrés par une succession de lits homogènes, entrecoupés de lits marbrés bruns (10YR5/4) moins riches en nannofossiles et avec plus d'oxydes.

Foraminifer bearing NANNOFOSSIL OOZE white (10YR8/2).
Occurrence of alternating layers of nannofossil ooze and oxyde-rich beds (10YR7/4).

Isotopes Stages after H. Jacot des Combes et al., in press

Core Géologie Depository
M.N.H.N.

SAMPLE : GS 962073

STATION : 27
Latitude : 10°. 592 N
Longitude : 52°. 370 E
Core Length : 33 m
Water Depth : 3141 m

Site: Extrême Nord du Bassin de Somalie.
Pente continentale.
Northern Somali Basin.
Continental slope.

Remarks: même site que GS 85682 et AT 96029.
Same site as GS 85682 and AT 96029.

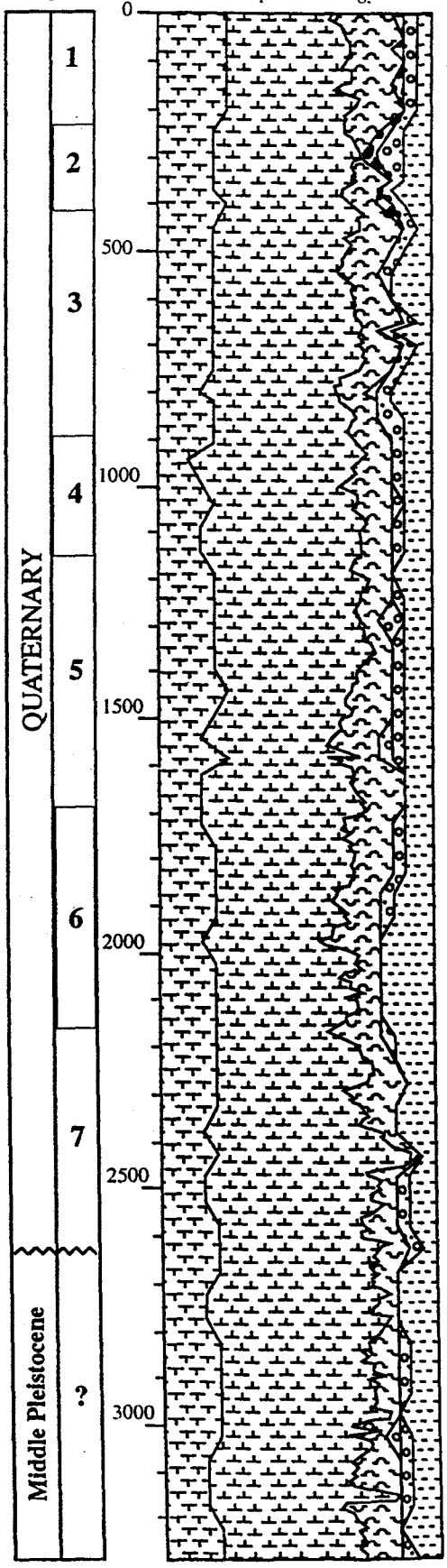

Isotopes Stages after H. Jacot des Combes et al., in press

ANNEXE 2

9ème Congrès de l'European union of geosciences
Strasbourg. 23-27 mars 1997

Monitoring the sedimentary response to the late Pleistocene pelagic productivity and oceanic circulation changes in the northwestern Indian Ocean through barium analyses.

Hélène Jacot Des Combes[1]
(hjdc@geol.u-psud.fr)
Jean-Pierre Caulet[2] (caulet@mnhn.fr)
Nicolas P. Tribovillard[1] (tribovil@geol.u-psud.fr)

1 Laboratoire de géochimie des roches sédimentaires, URA 723,Université de Paris Sud, Bat. 504, 91405 Orsay Cedex
2 Laboratoire de géologie, Museum National d'Histoire Naturelle, URA 723, 43 rue Buffon, 75005 Paris

Late Pleistocene changes in pelagic sedimentation are studied along three piston cores collected on the Madingley Rise (MD 940, 05°33,53'S, 61°40,12'E, 3875 m deep), the Seychelles Plateau (MD 929, 06°59'S, 52°03'E, 3071 m deep) and the Somali Basin (MD 668, 0,010°S, 46,023°E, 4020 m deep). All material is dated using the $\delta^{18}O$ isotopic method, and contents in calcium carbonate, organic carbon, major and minor elements are calculated.

Low terrigenous input, high carbonate content (79%), no organic matter, and a surprisingly high barium fraction (1400 ppm), characterize the pelagic sedimentation on the Madingley Rise. A sequential leach procedure shows that most of barium is deposited as barite and can be used as a paleoproductivity proxy. Mass accumulation rates and major/minor elements fluxes show a marked cyclicity that can be related to climatic events.

Clastic supply from the continent is increasing (3% of Al) in the equatorial Somali Basin core MD 668. Mass accumulation rates and major/minor elements fluxes also show a marked cyclicity that is, however, different from core MD 940. The barium input is related to land-derived clastic supplies (feldspars).

Barium contents in sediments from the Madingley Rise and the equatorial Somali Basin show, however, close temporal variations.

Cross study of these new data helps to build a simplified model of the sedimentary response to pelagic productivity and/or oceanic circulation in the northwestern Indian Ocean during the late Pleistocene.

Terra Nova, 9, Abstract supplement n°1. p. 619.

17ème Réunion des Sciences de la Terre
Brest. 31 mars- 3 avril 1998

La sédimentation pélagique de l'océan indien du NW depuis le Pléistocène supérieur enregistrée par les éléments majeurs et en traces, en relation avec les variations climatiques globales

H. Jacot des Combes* (1), J.P. Caulet (2) & N. Tribovillard (1)

(1) Laboratoire de sédimentologie et géodynamique, Université de Lille I, 59655 Villeneuve d'Ascq Cedex,
(2) Laboratoire de géologie du MNHN, 43 rue Buffon, 75005 Paris, * actuellement à (2)

La sédimentation pélagique du Pléistocène supérieur de l'océan Indien du nord-ouest est étudiée à partir de trois carottes: la carotte MD 90940 (05°33,53'S, 61°40,12'E, 3875 m de fond) située sur la ride de Madingley, la carotte MD 85668 (0,010°S, 46,023°E, 4020 m de fond) dans le bassin de Somalie, et la carotte MD 90929 (06°59'S, 52°03'E, 3071 m de fond) localisée dans le détroit des Amirantes.

La sédimentation pélagique sur la ride de Madingley est différente de celle du bassin de Somalie, particulièrement durant le stade isotopique 9. Pendant cet intervalle, un taux de sédimentation élevé caractérise la carotte MD 90940, alors que le taux de sédimentation de la carotte MD 85668 est faible. L'enregistrement du taux de sédimentation de la carotte MD 90929 peut être divisé en deux parties :

- Depuis le début du stade isotopique 7 (240 ka) jusqu'à l'Actuel, le taux de sédimentation reste stable autour de 0,5 g/cm^2/ka, sauf lors de la transition 2/1 (12 ka).
- Entre 600 ka et la transition 8/7 (245 ka), on observe des variations significatives (de 0,5 g/cm^2/ka à 3,25 g/cm^2/ka). Les forts taux de sédimentation sont principalement observés durant les transitions entre stades isotopiques mais on en enregistre également pendant le stade isotopique 9.

Les attaques chimiques séquentielles réalisées sur les trois carottes montrent une répartition différente du baryum dans les différentes phases du sédiment (carbonates, oxy-hydroxydes de Mn, aluminosilicates et fraction résiduelle).

La comparaison entre les résultats des carottes MD 90929, MD 90940 et MD 85668 permet de déterminer les processus contrôlant la sédimentation pélagique de l'océan Indien du nord-ouest et de modéliser leur évolution depuis le Pléistocène supérieur.

Résumés de la 17ème Réunoin des Sciences de la Terre. p. 134.

15th International Sedimentological Congress
Alicante. 12-17 avril 1998

LATE PLEISTOCENE PELAGIC SEDIMENTATION IN THE NORTHWESTERN INDIAN OCEAN THROUGH MAJOR AND TRACE ELEMENTS, RELATED TO GLOBAL CLIMATIC CHANGES

H. Jacot des Combes* (1), J.P. Caulet (2) & N. Tribovillard (1)

(1) Laboratoire de sedimentologie et geodynamique, U.F.R des Sciences de la terre, Université de Lille I, 59655 Villeneuve d'Ascq Cedex france; (2) Laboratoire de géologie du Museum National d'Histoire Naturelle, 43 rue Buffon, 75005 Paris France, * now at (2)

The late Pleistocene sedimentation in the pelagic domain of the northwestern Indian Ocean is recorded in three cores recovered in this area : core MD 90940 (05°33.53'S, 61°40.12'E, 3875 m deep) located on the Madingley Rise, core MD 85668 (0.010°S, 46.023°E, 4020 m deep) in the Somali Basin, and core MD 90929 (06°59'S, 52°03'E, 3071 m deep) located in the Admirantes Strait.

A previous study (Jacot des Combes et al., 1997) shows that tropical pelagic sedimentation patterns differ between the Madingley Rise and the Somali Basin, especially during the isotope stage 9. During this interglacial interval, high bulk MAR are recorded in core MD 90940, but not in core MD 85668. Sediments of core MD 90929 are studied to provide complementary information on the pelagic sedimentation in this area. This material is dated using the $\delta^{18}O$ isotopic method on the bulk sediment. Contents in calcium carbonate, organic carbon, and major and selected trace elements, especially barium, are measured by ICP-MS.

The bulk MAR record in core MD 90929 can be divided in two sets:

- From the lower part of isotope stage 7 (240 ka) until present, no strong variations are recorded, but at the 2/1 transition (12 ka).
- From 600 ka until the 8/7 transition (245 ka), significant variations can be observed (from 0.5 g/cm^2/ka to 3.25 g/cm^2/ka). The bulk MAR peak values are mostly located within transition intervals, but a single bulk MAR peak value is recorded during isotope stage 9, that is synchronous with the bulk MAR peak value from core MD 90940.

Terrigenous input is higher in core MD 90929 than in core MD 90940 (0.5 to 3 % of Al compared to 0.4 to1.2 % of Al), carbonate content is slightly lower (58 to 84 %) in core MD 90929 than in core MD 90940 (62 to 85 %). The barium content of core MD 90929 is lower (700 to 1800 ppm) than in core MD 90940 (800 to 3200 ppm). A sequential leaching procedure realized on both sites shows a significant difference in the barium distribution within the different fractions of the sediment (carbonate, poorly crystalline ferromanganese oxihydroxides, aluminosilicates and residual fraction).

Comparison of the results from core MD 90929 and core MD 90940 helps to differentiate the major processes controlling the pelagic sedimentation in the northwestern Indian Ocean and to monitor the evolution of these processes during the late Pleistocene.

Reference list :

Jacot des Combes H., Caulet J.P. and Tribovillard N. (1997) Pelagic productivity changes in the equatorial area of the northwestern Indian Ocean through barium analyses during the last 350 ka. Mar. Geol. (submitted).

Abstracts of the 15th International Sedimentological Congress : p. 445

6th International Conference on paleoceanography
Lisbonne. 24-28 août 1998

Monitoring the variations of the activity of the Socotra upwelling system during the last 300 ka

Jacot Des Combes H. (Sédimentologie & Géodynamique, University Lille I, 59655 Villeneuve d'Ascq, France)
Caulet J.P. (Géologie, MNHN), Tribovillard N. (Sedimentologie & Geodynamique, University Lille I), & Vénec-Peyré M.-T. (Paléontologie, MNHN)

Along the eastern coast of Africa, two major gyres are induced by the SW Indian Monsoon : the Somalian gyre, at 5°N, and the Socotra gyre at 10°N. Despite their belonging to the same monsoonal system, previous studies (Ouahdi, 1997) have shown that the intervals of high upwelling activity in the Somalian gyre do not correspond to those in the Socotra gyre.for the last 72 ka Supplementary data show that micropaleontological, mineralogical and chemical records from sediments of both areas are very different, indicating that the origin of the sedimentary acumulation under the Socotra upwelling system are more biogenic and less terrigenous that under the Somalian gyre. The combined lithological ($CaCO_3$, clays and quartz contents, and MARs) geochemical (Si, Al, Fe, K, Mg, Ba, P, Ti, Mn, V, Cu, and Ni contents, and MARs) and biogenic (planktonic and benthic foraminifers and radiolarians) records allow to reconstruct the activity of the Socotra upwelling system, and the associated paleoceanographic changes during the last 300 ka.

Abstracts of the ICP VI. p. 134

8th International Goldschmidt
Toulouse. 30 août – 3 septembre 1998

The message of the geochemical proxies in upper Quaternary sediments of the nortwestern Indian Ocean and the Gulf of Aden: a heterogeneous record

Jacot Des Combes Hélène (1), Tribovillard Nicolas (1), and Caulet Jean Pierre (2)

(1) Laboratoire de Sédimentologie et Géodynamique, UFR des Sciences de la terre, Université de Lille 1, 59655 Villeneuve d'Ascq, France.
(2) Laboratoire de Géologie, Muséum National d'Histoire Naturelle, 43 rue Buffon, 75005 Paris, France.

The inorganic geochemical proxies are a very useful tool to reconstruct the variations of paleoceanographic conditions, especially the changes in the surface paleoproductivity, or the changes in the redox conditions. Many of the trace metals are, however, related to different processes. Barium, for example, can have a terrigenous and a biogenic origin, and, as barite, is sensible to the variations in the redox conditions.

The behavior of a wide range of trace metals was studied upon the sediment of seven cores located in the northwestern Indian Ocean and the Gulf of Aden. These cores are very different following the depth where they were recovered (from 774 m to 4020 m), the importance of the terrigenous input (from less than 1% to more than 8% of Al), and the oceanic domain they belong to: pelagic realm, coastal area, and upwelling system.

In this region of the Indian Ocean, the trace elements exhibit a heterogeneous behavior with strong differences. These differences occur between the different subdomains, but also within a specific domain, e.g. the pelagic realm or the upwelling system. The data do not permit to distinguish one subdomains from the others, and limit the establishment of a model of the trace metals behavior in the northwestern Indian Ocean. Preliminary results show that the variations of the contents of the trace elements partly originate in the terrigenous fraction are strongly influenced by the variations of this fraction, so that their variations related to the other possible source of the element are overwhelmed.

Mineralogical Magazine, Vol 62A, part 2. P. 698.